IN THE UNITED STATES PATENT AND TRADEMARK OFFICE

In re application of:)	Examiner: Chernyshev, Olga
)	
ASHKENAZI, et al.)	Art Unit: 1646
)	
Application Serial No. 09/665,350)	Confirmation No: 8200
)	
Filed: September 18, 2000)	Attorney's Docket No. 39780-1618 P2C1
)	
For: SECRETED AND TRANSMEMBRANE)	Customer No. 35489
POLYPEPTIDES AND NUCLEIC)	
ACIDS ENCODING THE SAME)	

EXPRESS MAIL LABEL NO. : <u>EL 976 551 895 US</u>
DATE MAILED: **March 15, 2006**

ON APPEAL TO THE BOARD OF PATENT APPEALS AND INTERFERENCES
APPELLANTS' BRIEF

MAIL STOP APPEAL BRIEF - PATENTS
Commissioner for Patents
P.O. Box 1450
Alexandria, Virginia 22313-1450

Dear Sir:

This Appeal Brief, filed in connection with the above captioned patent application, is responsive to the Final Office Action mailed on July 23, 2005. A Notice of Appeal was filed herein on September 15, 2005. A request for a four-month extension of time is requested herewith. Appellants hereby appeal to the Board of Patent Appeals and Interferences from the final rejection in this case.

The following constitutes the Appellants' Brief on Appeal.

I. REAL PARTY IN INTEREST

The real party in interest is Genentech, Inc., South San Francisco, California, by an assignment of the parent application, U.S. Patent Application Serial No. 09/665,350 recorded July 9, 2001, at Reel 011964 and Frame 0181.

II. RELATED APPEALS AND INTERFERENCES

The claims pending in the current application are directed to a polypeptide referred to herein as "PRO187." There exists a related patent application, U.S. Patent Application Serial No. 09/906,838, filed July 16, 2001 (containing claims directed to nucleic acids encoding PRO187 polypeptides) that is **allowed** and for which, the issue fee was paid on December 9, 2005. In addition, there are two related pending applications that rely on "Assay 9: inhibition of endothelial cell proliferation for patentable utility; they are: U.S. Patent Application Serial No. 11/050,559 filed February 2, 2005 (containing claims directed to nucleic acids encoding PRO187 polypeptides) and U.S. Patent Application Serial No. 11/050,154 filed February 2, 2005 (containing claims directed to PRO187 polypeptides).

III. STATUS OF CLAIMS

Claims 39-46 and 49-51 are in this application.

Claims 1-38 and 47-48 have been canceled.

Claims 39-46 and 49-51 stand rejected and Appellants appeal the rejection of these claims.

A copy of the rejected claims in the present Appeal is provided as Appendix A.

IV. STATUS OF AMENDMENTS

There were no amendments submitted after the final rejection of June 15, 2005. All previous amendments have been entered.

V. SUMMARY OF CLAIMED SUBJECT MATTER

The invention claimed in the present application is related to an isolated polypeptide comprising the amino acid sequence of the polypeptide of SEQ ID NO: 23, referred to in the present application as "PRO187." The PRO187 gene was shown for the first time in the present application to be significantly amplified in human lung and colon cancers as compared to

normal, non-cancerous human tissue controls (Example 92). This feature is specifically recited in Claim 44, and carried by all claims dependent from Claim 44. In addition, the invention also claims the amino acid sequence of the polypeptide of SEQ ID NO: 23, lacking its associated signal-peptide; or the amino acid sequence of the polypeptide encoded by the full-length coding sequence of the cDNA deposited under ATCC accession number 209375 (Claims 44-46 and 49). The invention is further directed to polypeptides having at least 80% to 99% amino acid sequence identity to the amino acid sequence of the polypeptide of SEQ ID NO: 23; the amino acid sequence of the polypeptide of SEQ ID NO: 23, lacking its associated signal peptide; or the amino acid sequence of the polypeptide encoded by the full-length coding sequence of the cDNA deposited under ATCC accession number 209375, wherein the nucleic acid encoding said polypeptide is amplified in lung or colon tumor (Claims 39-46 and 49-51). The invention is further directed to a chimeric polypeptide comprising one of the above polypeptides fused to a heterologous polypeptide (Claim 50), and to a chimeric polypeptide wherein the heterologous polypeptide is an epitope tag or an Fc region of an immunoglobulin (Claim 51). PRO polypeptide variants having at least about 80-99% amino acid sequence identity with a full length PRO polypeptide sequence, or a PRO polypeptide sequence lacking the signal peptide are generally described in the specification at, for example, page 112, line 37 onwards, and percent amino acid sequence identity determination is generally described at least at, for example, page 67-70, line 67 onwards.

The preparation of chimeric PRO polypeptides (Claims 50 and 51), including those wherein the heterologous polypeptide is an epitope tag or an Fc region of an immunoglobulin, is set forth in the specification at page 74, lines 23 to page 75, line 5. Examples 53-56, pages 192-199, describe the expression of PRO polypeptides in various host cells, including *E. coli*, mammalian cells, yeast and Baculovirus-infected insect cells.

The amino acid sequence of the native "PRO187" polypeptide and the nucleic acid sequence encoding this polypeptide (referred to in the present application as "DNA27864-1155" or ATCC 209375) are shown in the present specification as SEQ ID NOs: 23 and 22, respectively, and in Figures 11 and 10, described on pages 59, lines 7-10. The full-length PRO187 polypeptide having the amino acid sequence of SEQ ID NO: 23 is described in the specification at, for example, on pages 5-6 and page 100 and the isolation of cDNA clones

encoding PRO187 of SEQ ID NO: 23 is described in Example 5, page 150-151 of the specification. The specification discloses that the PRO187 polypeptide possess 74% amino acid sequence similarity to human fibroblast growth factor-8 (androgen-induced growth factor (see, for example, page 151, lines 6-8.

Finally, Example 92, in the specification at page 222, line 26, to page 235, line 3, sets forth a 'Gene Amplification assay' which shows that the PRO187 gene is amplified in the genome of certain human lung and colon cancers (see Table 9, pages 230-234). The profiles of various primary lung and colon tumors used for screening the PRO polypeptide compounds of the invention in the gene amplification assay are summarized on Table 8, page 227 of the specification.

VI.   GROUNDS OF REJECTION TO BE REVIEWED ON APPEAL

1.   Whether Claims 39-46 and 49-51 satisfy the utility/ enablement requirement under 35 U.S.C. §§101/112, first paragraph.

2.   Whether Claims 39-46 and 49-51 satisfy the written description requirement under 35 U.S.C. §112, first paragraph.

VII.   ARGUMENTS

Summary of the Arguments

Issue 1: Utility/ Enablement

Patentable utility requires an assertion of specific, substantial and credible utility in the application for patent, or a well-recognized utility. The evidentiary standard to be used in setting forth a rejection is a preponderance of the totality of the evidence under consideration. Thus, to overcome the presumption of truth that an assertion of utility by the Appellant enjoys, the Examiner must establish that it is more likely than not that one of ordinary skill in the art would doubt the truth of the statement of utility. Only after the Examiner has made a proper *prima facie* showing of lack of utility, does the burden of rebuttal shift to the Appellant.

Appellants rely upon the gene amplification data of the PRO187 gene for patentable utility of the PRO187 polypeptides. This data is clearly disclosed in the instant specification in

Example 92 which discloses that the gene encoding PRO187 showed <u>significant</u> amplification, ranging from **3.182 to 16.564-fold amplification in 6 primary lung tumors** and **2.014 to 11.794-fold amplification in 10 primary colon tumors**. Therefore, such a gene is <u>useful as a marker for the diagnosis of lung and colon cancer</u>, and for monitoring cancer development and/or for measuring the efficacy of cancer therapy.

Appellants have also submitted, with their Response filed June 6, 2003, the Declaration of Dr. Audrey Goddard, which explains that a gene identified as being amplified at least 2-fold by the disclosed gene amplification assay in a tumor sample relative to a normal sample is <u>useful as a marker for the diagnosis of cancer</u>, for monitoring cancer development and/or for measuring the efficacy of cancer therapy. Therefore, one of ordinary skill would find it credible that the claimed PRO187 polypeptides, and therefore their antibodies have utility <u>as markers for the diagnosis of lung or colon tumors</u>.

In addition, Appellants have submitted ample evidence to show that, in general, if a gene is amplified in cancer, it is more likely than not that the encoded protein will be expressed at an elevated level. First, the articles by Orntoft *et al.*, Hyman *et al.*, and Pollack *et al.* (made of record in Appellants' Response filed October 8, 2004) collectively teach that <u>in general, gene amplification increases mRNA expression</u>. Second, the Declaration of Dr. Paul Polakis (made of record in Appellants' Response filed October 8, 2004), principal investigator of the Tumor Antigen Project of Genentech, Inc., the assignee of the present application, shows that, <u>in general, there is a correlation between mRNA levels and polypeptide levels</u>.

Appellants further submit that even if there were no correlation between gene amplification and increased mRNA/protein expression, (which Appellants expressly do <u>not</u> concede), a polypeptide encoded by a gene that is amplified in cancer would <u>still</u> have a specific, substantial, and credible utility. Appellants submit that, as evidenced by the Ashkenazi Declaration and the teachings of Hanna and Mornin (both made of record in Appellants' Response filed October 8, 2004), simultaneous testing of gene amplification and gene product over-expression enables <u>more accurate tumor classification</u>, even if the gene-product, the protein, is not over-expressed. This leads to better determination of a suitable therapy for the tumor, as demonstrated by a <u>real-world example</u> of the breast cancer marker HER-2/neu.

Appellants further note that the sale of gene expression chips to measure mRNA levels is a highly successful business, with a company such as Affymetrix recording 168.3 million dollars in sales of their GeneChip arrays in 2004. Clearly, the research community believes that the information obtained from these chips is useful (*i.e.,* that it is more likely than not informative of the protein level).

Taken together, although there are some examples in the scientific art that do not fit within the central dogma of molecular biology that there is a correlation between DNA, mRNA, and polypeptide levels, these instances are <u>exceptions rather than the rule</u>. <u>In the majority of amplified genes</u>, as exemplified by Haynes *et al.,* Orntoft *et al.,* Hyman *et al.,* Pollack *et al.,* and the Polakis Declaration, the teachings in the art overwhelmingly show that <u>gene amplification influences gene expression at the mRNA and protein levels</u>. Therefore, one of skill in the art would reasonably expect in this instance, based on the amplification data for the PRO187 gene, that the PRO187 polypeptide is concomitantly overexpressed. Thus, the claimed PRO187 polypeptides have utility in the diagnosis of cancer.

However, the Examiner maintains, in the Final Office Action mailed June 23, 2005, that amplification of the PRO187 polynucleotide does not impart a specific, substantial, and credible utility to the PRO187 antibody since, "gene amplification of polynucleotides encoding PRO187....is not predictive of increased amounts of polynucleotide of SEQ ID NO: 23, and, therefore, the polypeptide of SEQ ID NO: 23 could not be used as a marker for lung and colon cancer without further and significant amount of experimentation" (page 3, line 6). Appellants submit, as discussed below, that a *prima facie* case for lack of utility has not been established based on the Examiner's rejections.

Accordingly, Appellants submit that when the proper legal standard is applied, one should reach the conclusion that the present application discloses at least one patentable utility for the claimed PRO187 polypeptides and their antibodies in the diagnosis of cancer. Based on such a utility, one of skill in the art would know exactly how to use the claimed polypeptides for diagnosis of cancer, without any undue experimentation. The specification provides ample guidance to allow the skilled artisan, including a detailed protocol for the gene amplification assay, and detailed guidance as to how to identify and make polypeptides of PRO187 (SEQ ID NO: 23) and detailed guidance on how to make and use antibodies to PRO187 (SEQ ID NO: 23).

Accordingly, one of ordinary skill in the art would understand how to make and use the recited antibodies without any undue experimentation.

Issue 2: Written Description

Claims 39-46 and 49-51 stand rejected under 35 U.S.C. §112, first paragraph, allegedly "as containing subject matter which was not described in the specification in such a way as to reasonably convey to one skilled in the relevant art that the inventor(s), at the time the application was filed, had possession of the claimed invention.." (Page 5 of the Final Office Action mailed June 23, 2005).

The factors to be considered in evidencing possession of a claimed genus include "disclosure of complete or partial structure, physical and/or chemical properties, functional characteristics, structure/function correlation, methods of making the claimed product, or any combination thereof." Current applicable case law holds that biological sequences are not adequately described solely by a description of their desired functional activities. It is, however, well established that a combination of functional and structural features suffices to describe a claimed genus, as discussed in the PTO's own Written Description Guidelines, and as set forth in *Enzo Biochem., Inc. v. Genprobe, Inc.* Appellants note that the claims recite structural features, namely, 80% sequence identity to SEQ ID NO: 23, which are common to the genus. The genus of claimed polypeptides is further defined by having a specific functional activity for the encoding nucleic acids, namely, that the encoding nucleic acid is amplified in lung tumors. The specification provides detailed guidance as to how to identify the recited variants of SEQ ID NO: 23, including methods for determining percent identity between two amino acid sequences, as well as listings of exemplary and preferred sequence substitutions, as well as detailed protocols for determining whether a gene encoding a variant PRO187 protein is amplified in lung tumor. Thus one of skill in the art could easily identify whether a variant PRO187 sequence falls within the parameters of the claimed invention.

Accordingly, a description of the claimed genus has been achieved by the recitation of both structural and functional characteristics.

These arguments are all discussed in further detail below under the appropriate headings.

Response to Rejections

ISSUE 1. Claims 39-46 and 49-51 are supported by a credible, specific and substantial asserted utility, and thus meet the utility requirement of 35 U.S.C. §§101/112, first paragraph

The sole basis for the Examiner's rejection of Claims 39-46 and 49-51 under this section is that the data presented in Example 92 of the present specification is allegedly insufficient under the present legal standards to establish a patentable utility under 35 U.S.C. §101 for the presently claimed subject matter.

Claims 39-46 and 49-51 stand further rejected under 35 U.S.C. §112, first paragraph, allegedly "since the claimed invention is not supported by either a specific and substantial asserted utility or a well established utility for the reasons set forth above, one skilled in the art clearly would not know how to use the claimed invention."

Appellants strongly disagree and, therefore, respectfully traverse the rejection.

A.   The Legal Standard For Utility Under 35 U.S.C. §101

According to 35 U.S.C. §101:

Whoever invents or discovers any new and *useful* process, machine, manufacture,
or composition of matter, or any new and *useful* improvement thereof, may obtain
a patent therefor, subject to the conditions and requirements of this title.
(Emphasis added).

In interpreting the utility requirement, in *Brenner v. Manson*,[1] the Supreme Court held that the *quid pro quo* contemplated by the U.S. Constitution between the public interest and the interest of the inventors required that a patent Appellant disclose a "substantial utility" for his or her invention, *i.e.*, a utility "where specific benefit exists in currently available form."[2] The Court concluded that "a patent is not a hunting license. It is not a reward for the search, but compensation for its successful conclusion. A patent system must be related to the world of commerce rather than the realm of philosophy."[3]

---

[1] *Brenner v. Manson*, 383 U.S. 519, 148 U.S.P.Q. (BNA) 689 (1966).

[2] *Id.* at 534, 148 U.S.P.Q. (BNA) at 695.

[3] *Id.* at 536, 148 U.S.P.Q. (BNA) at 696.

Later, in *Nelson v. Bowler*,[4] the C.C.P.A. acknowledged that tests evidencing pharmacological activity of a compound may establish practical utility, even though they may not establish a specific therapeutic use. The Court held that "since it is crucial to provide researchers with an incentive to disclose pharmaceutical activities in as many compounds as possible, we conclude adequate proof of any such activity constitutes a showing of practical utility."[5]

In *Cross v. Iizuka*,[6] the C.A.F.C. reaffirmed *Nelson*, and added that *in vitro* results might be sufficient to support practical utility, explaining that "*in vitro* testing, in general, is relatively less complex, less time consuming, and less expensive than *in vivo* testing. Moreover, *in vitro* results with the particular pharmacological activity are generally predictive of *in vivo* test results, i.e. there is a reasonable correlation there between."[7] The Court perceived, "No insurmountable difficulty" in finding that, under appropriate circumstances, "*in vitro* testing, may establish a practical utility."[8]

The case law has also clearly established that Appellants' statements of utility are usually sufficient, unless such statement of utility is unbelievable on its face.[9] The PTO has the initial burden to prove that Appellants' claims of usefulness are not believable on their face.[10] In general, an Appellant's assertion of utility creates a presumption of utility that will be sufficient

---

[4] *Nelson v. Bowler*, 626 F.2d 853, 206 U.S.P.Q. (BNA) 881 (C.C.P.A. 1980).

[5] *Id.* at 856, 206 U.S.P.Q. (BNA) at 883.

[6] *Cross v. Iizuka*, 753 F.2d 1047, 224 U.S.P.Q. (BNA) 739 (Fed. Cir. 1985).

[7] *Id.* at 1050, 224 U.S.P.Q. (BNA) at 747.

[8] *Id.*

[9] *In re Gazave*, 379 F.2d 973, 154 U.S.P.Q. (BNA) 92 (C.C.P.A. 1967).

[10] *Ibid.*

to satisfy the utility requirement of 35 U.S.C. §101, "unless there is a reason for one skilled in the art to question the objective truth of the statement of utility or its scope."[11],[12]

Compliance with 35 U.S.C. §101 is a question of fact.[13] The evidentiary standard to be used throughout *ex parte* examination in setting forth a rejection is a preponderance of the totality of the evidence under consideration.[14] Thus, to overcome the presumption of truth that an assertion of utility by the Appellant enjoys, the Examiner must establish that it is more likely than not that one of ordinary skill in the art would doubt the truth of the statement of utility. Only after the Examiner made a proper *prima facie* showing of lack of utility, does the burden of rebuttal shift to the Appellant. The issue will then be decided on the totality of evidence.

The well established case law is clearly reflected in the Utility Examination Guidelines ("Utility Guidelines"),[15] which acknowledge that an invention complies with the utility requirement of 35 U.S.C. §101, if it has at least one asserted "specific, substantial, and credible utility" or a "well-established utility." Under the Utility Guidelines, a utility is "specific" when it is particular to the subject matter claimed. For example, it is generally not enough to state that a nucleic acid is useful as a diagnostic without also identifying the conditions that are to be diagnosed.

In explaining the "substantial utility" standard, M.P.E.P. §2107.01 cautions, however, that Office personnel must be careful not to interpret the phrase "immediate benefit to the public" or similar formulations used in certain court decisions to mean that products or services based on the claimed invention must be "currently available" to the public in order to satisfy the

---

[11] *In re Langer*, 503 F.2d 1380,1391, 183 U.S.P.Q. (BNA) 288, 297 (C.C.P.A. 1974).

[12] *See also In re Jolles*, 628 F.2d 1322, 206 USPQ 885 (C.C.P.A. 1980); *In re Irons*, 340 F.2d 974, 144 USPQ 351 (1965); *In re Sichert*, 566 F.2d 1154, 1159, 196 USPQ 209, 212-13 (C.C.P.A. 1977).

[13] *Raytheon v. Roper*, 724 F.2d 951, 956, 220 U.S.P.Q. (BNA) 592, 596 (Fed. Cir. 1983) *cert. denied*, 469 US 835 (1984).

[14] *In re Oetiker*, 977 F.2d 1443, 1445, 24 U.S.P.Q.2d (BNA) 1443, 1444 (Fed. Cir. 1992).

[15] 66 Fed. Reg. 1092 (2001).

utility requirement. "Rather, any reasonable use that an applicant has identified for the invention that can be viewed as providing a public benefit should be accepted as sufficient, at least with regard to defining a 'substantial' utility."[16] Indeed, the Guidelines for Examination of Applications for Compliance With the Utility Requirement,[17] gives the following instruction to patent examiners: "If the Appellant has asserted that the claimed invention is useful for any particular practical purpose . . . and the assertion would be considered credible by a person of ordinary skill in the art, do not impose a rejection based on lack of utility."

B.   Proper Application of the Legal Standard

Appellants respectfully submit that the data presented in Example 92 starting on page 222 of the specification of the specification and the cumulative evidence of record, which underlies the current dispute, indeed support a "specific, substantial and credible" asserted utility for the presently claimed invention.

Patentable utility for the PRO187 polypeptides is based upon the gene amplification data for the gene encoding the PRO187 polypeptide. Example 92 describes the results obtained using a very well-known and routinely employed polymerase chain reaction (PCR)-based assay, the TaqMan™ PCR assay, also referred to herein as the gene amplification assay. This assay allows one to quantitatively measure the level of gene amplification in a given sample, say, a tumor extract, or a cell line. It was well known in the art at the time the invention was made that gene amplification is an essential mechanism for oncogene activation. Appellants isolated genomic DNA from a variety of primary cancers and cancer cell lines that are listed in Table 9 (page 222 onwards of the specification), including primary lung and colon cancers of the type and stage indicated in Table 8 (page 227). The tumor samples were tested in triplicates with Taqman™ primers and with internal controls, beta-actin and GADPH in order to quantitatively compare DNA levels between samples (page 229). As a negative control, DNA was isolated from the cells of ten normal healthy individuals, which was pooled and used as a control and also, no-template controls (page 229, lines 28-29). The results of TaqMan™ PCR are reported in ΔCt

---

[16] M.P.E.P. §2107.01.

[17] M.P.E.P. §2107 II (B)(1).

-11-

units, as explained in the passage bridging pages 222 to 223, last line onwards. One unit corresponds to one PCR cycle or approximately a 2-fold amplification, relative to control, two units correspond to 4-fold, 3 units to 8-fold amplification and so on. Using this PCR-based assay, Appellants showed that the gene encoding for PRO187 was amplified, that is, it showed approximately ΔCt units for lung tumors which corresponds to $2^{1.67}$-$2^{4.05}$- fold amplification in lung, or **3.182 to 16.564-fold amplification in 6 primary lung tumors** and $2^{1.01}$-$2^{3.56}$-fold amplification or **2.014 to 11.794-fold amplification in 10 primary colon tumors**.

In support of their showing that these gene amplification values are significant, Appellants submitted, in their Response filed June 6, 2003, a Declaration by Dr. Audrey Goddard. Appellants particularly draw the Board's attention to page 3 of the Goddard Declaration which clearly states that:

> It is further my considered scientific opinion that an at least **2-fold increase** in gene copy number in a tumor tissue sample relative to a normal (*i.e.,* non-tumor) sample is significant and useful in that the detected increase in gene copy number in the tumor sample relative to the normal sample serves as a basis for using relative gene copy number as quantitated by the TaqMan PCR technique as a diagnostic marker for the presence or absence of tumor in a tissue sample of unknown pathology. Accordingly, a gene identified as being amplified at least 2-fold by the quantitative TaqMan PCR assay in a tumor sample relative to a normal sample is **useful as a marker for the diagnosis of cancer**, for monitoring cancer development and/or for measuring the efficacy of cancer therapy. (Emphasis added).

Further, Example 92 in the specification further discloses, "Amplification is associated with overexpression of the gene product, indicating that <u>the polypeptides are useful targets for therapeutic intervention in certain cancers</u> such as colon, lung, breast and other cancers and diagnostic determination of the presence of those cancers" (emphasis added). Accordingly, the **3.182 to 16.564-fold amplification in 6 primary lung tumors** and **2.014 to 11.794-fold amplification in 10 primary colon tumors** would be considered <u>significant and credible</u> by one skilled in the art, based upon the facts disclosed in the Goddard Declaration.

However, Appellants note that the Examiner maintains the position in the Office Action, especially on page 4, line 3 onwards of the Final Office Action mailed on June 23, 2005, that:

> "gene amplification of polynucleotides encoding PRO187 of SEQ ID NO: 2 in primary samples of lung and colon cancer, as indicated in Table 9 on pages 230-234 of the instant specification, is not predictive of increased amounts of

On Appeal to the Board of Patent Appeals and Interferences
Appellants' Brief
Application Serial No. 09/665,350
Attorney's Docket No. 39780-1618 P2C1

polypeptide of SEQ ID NO: 2 and therefore, the polypeptide of SEQ ID NO: 2 could not be used as a marker for lung and colon cancer without further and significant amount of experimentation."

But Appellants have submitted ample evidence (submitted with Appellants' Response October 8, 2004) to show that, in general, if a gene is amplified in cancer, it is more likely than not that the encoded protein will be expressed at an elevated level as well. Appellants respectfully remind the Examiner that the evidentiary standard to be used throughout *ex parte* examination of a patent application is a preponderance of the **totality of the evidence under consideration**. Thus, to overcome the presumption of truth that an assertion of utility by the applicant enjoys, the Examiner must establish that it is <u>more likely than not</u> that one of ordinary skill in the art would doubt the truth of the statement of utility. Only after the Examiner has made a proper *prima facie* showing of lack of utility, does the burden of rebuttal shift to the Appellant.

First, the articles by Orntoft *et al.*, Hyman *et al.*, and Pollack *et al.* collectively teach that <u>in general, gene amplification increases mRNA expression</u>. Appellants submit that these and numerous other articles show that generally, if a gene is amplified in cancer, it is more likely than not that the mRNA transcript will be expressed at an elevated level. For example, Orntoft *et al.* studied transcript levels of 5600 genes in malignant bladder cancers, many of which were linked to the gain or loss of chromosomal material using an array-based method. Orntoft *et al.* showed that there was a gene dosage effect and taught that "in general (18 of 23 cases) chromosomal areas with more than 2-fold gain of DNA showed a corresponding increase in mRNA transcripts" (see column 1, abstract). In addition, Hyman *et al.* showed, using CGH analysis and cDNA microarrays which compared DNA copy numbers and mRNA expression of over 12,000 genes in breast cancer tumors and cell lines, that there was "evidence of a prominent global influence of copy number changes on gene expression levels." (See page 6244, column 1, last paragraph). Additional supportive teachings were also provided by Pollack *et al.,* who studied a series of primary human breast tumors and showed that "...62% of highly amplified genes show moderately or highly elevated expression, and DNA copy number influences gene expression across a wide range of DNA copy number alterations (deletion, low-, mid- and high-level amplification), and that on average, a 2-fold change in DNA copy number is associated

with a corresponding 1.5-fold change in mRNA levels." Thus, these articles collectively teach that <u>in general, gene amplification increases mRNA expression</u>.

In addition, in their Response filed October 8, 2004, Appellants submitted a Declaration by Dr. Polakis, principal investigator of the Tumor Antigen Project of Genentech, Inc., the assignee of the present application, to show that <u>mRNA expression correlates well with protein levels, in general.</u> As Dr. Polakis explains, the primary focus of the microarray project was to identify tumor cell markers useful as targets for both the diagnosis and treatment of cancer in humans. The scientists working on the project extensively rely on results of microarray experiments in their effort to identify such markers. As Dr. Polakis explains, using microarray analysis, Genentech scientists have identified approximately 20 gene transcripts (mRNAs) that are present in human tumor cells at significantly higher levels than in corresponding normal human cells. To the date of the Declaration, they have generated antibodies that bind to about 30 of the tumor antigen proteins expressed from these differentially expressed gene transcripts and have used these antibodies to quantitatively determine the level of production of these tumor antigen proteins in both human cancer cells and corresponding normal cells. Having compared the levels of mRNA and protein in both the tumor and normal cells analyzed, they found a very good correlation between mRNA and corresponding protein levels. Specifically, in approximately 80% of their observations they have found that increases in the level of a particular mRNA correlates with changes in the level of protein expressed from that mRNA. While the proper legal standard is to show that the existence of correlation between mRNA and polypeptide levels is more likely than not, in approximately <u>80% of the cases</u>, the researchers found that <u>increases in the level of a particular mRNA correlated with changes in the level of protein expressed from that mRNA when human tumor cells are compared with their corresponding normal cells</u>, which greatly exceeds this legal standard. Based on these experimental data and his vast scientific experience of more than 2 years, Dr. Polakis states that, for human genes, increased mRNA levels typically correlate with an increase in abundance of the encoded protein. He further confirms that "it remains a central dogma in molecular biology that increased mRNA levels are predictive of corresponding increased levels of the encoded protein." Therefore, Dr. Polakis' research, which is referenced in his Declaration, shows that, <u>in general, there is a correlation between increased mRNA and polypeptide levels</u>.

Appellants further note that the sale of gene expression chips to measure mRNA levels is a highly successful business, with a company such as Affymetrix recording 168.3 million dollars in sales of their GeneChip® arrays in 2004. Clearly, the research community believe that the information obtained from these chips is useful (*i.e.*, that it is more likely than not that the results are informative of protein levels).

Therefore, <u>in the majority of amplified genes</u>, the teachings in the art, overwhelmingly show that gene amplification influences gene expression at the mRNA and protein levels. Therefore, it is "more likely than not" for amplified genes to have increased mRNA and protein levels, in general.

However, in the Final Office Action, the Examiner alleges based on the teachings of Orntoft *et al.*, Hyman *et al.* and Pollack *et al.* that:

"(1) the references are mostly limited to the analysis of correlation between increased copy of DNA and corresponding amount of mRNA, which is not relevant in the instant case to support the correlation between DNA and protein levels; (page 3 of the Final Office Action);

(2) the references explain that when a copy of DNA is amplified less than 2-fold, which is only 3 out of 13 cases of lung cancer samples and zero out of 6 cases of colon cancer samples in the instant case of polypeptide of SEQ ID NO: 2 (see Table 9), (they) are considered at the border of detection (see page 3-4 of the Final Office Action);

(3) the references clearly caution regarding limitations of gene expression pattern analysis, despite this progress of classification, the molecular mechanisms underlying gene expression patterns in cancer have remained elusive, and the utility of gene expression profiling in the identification of specific therapeutic targets remain limited (page 4 of the Final Office action)." The Examiner adds that "even if (we) assume that the increase of DNA copy correlates with the increase of the amount of corresponding protein, there appears to be no evidence or scientific reasoning presented to conclude that such increase is **directly proportional** to the amount of number of copies of DNA" (emphasis added- page 4, line 11-13 of the Final Office Action).

Appellants strongly disagree with each of the points for the reasons discussed below. On the whole, the rejections made by the Examiner are based either on erroneous conclusions due to a misinterpretation of the gene amplification data, or on standards other than the utility standard.

-15-

Regarding point (1), Appellants submit that the Examiner is mischaracterizing the Appellants' reason for presenting the Orntoft *et al.*, Hyman *et al.* and Pollack *et al.* references. Appellants respectfully submit that these articles were presented to support the correlation between gene amplification and mRNA levels, while Dr. Polakis' Declaration was presented to support the correlation between mRNA levels and polypeptide levels. Appellants have clearly explained this throughout prosecution. Therefore, the Examiner's rejection based on the irrelevance of the Orntoft *et al.*, Hyman *et al.* and Pollack *et al.* references in showing the correlation between "DNA and protein levels" is an inappropriate characterization of the reasoning behind the presentation of the evidence by the Appellant.

Further, the remarks made by the Examiner in point number (2) regarding "the copy of DNA being amplified less than 2-fold" is entirely incorrect. The Examiner seems to confuse the ΔCt units disclosed in Table 9 of the instant specification with "fold amplification". The observed fold- amplification values for PRO187 and methods to calculate them have been discussed in detail in the specification (Example 92) and above. That is, the fold-amplification for PRO187 was **3.182 to 16.564-fold amplification in 6 primary lung tumors** and **2.014 to 11.794-fold amplification in 10 primary colon tumors** which are <u>well above</u> the 2-fold levels erroneously cited by the Examiner. Therefore, any conclusion drawn by the Examiner based on such an error would also be incorrect.

Lastly, the points raised in item (3) cited above, namely that "the <u>molecular mechanisms underlying the gene expression patterns</u> in cancer have remained elusive," (emphasis added) is also <u>not</u> a proper basis for a utility rejection. The Examiner's general contention in this rejection seems to be the <u>underlying mechanism</u> of the PRO187 protein in causing cancer rather than the positive result in the gene amplification assay. Appellants respectfully submit that the mechanism of action need not be understood for attaining utility. In fact, as stated by the Federal Circuit, "it is not a requirement of patentability that an inventor correctly set forth, or even know, how or why the invention works." *In re Cortwright*, 165 F.2d 1353, 1359 (Fed. Cir. 1999). The Federal Circuit has also stated that "[a]n invention need not be the best or only way to accomplish a certain result, and it need only be useful to some extent and in certain applications: "[T]he fact that an invention has only limited utility and is not operable in certain applications is not grounds for finding lack of utility." *Envirotech Corp. v. Al George, Inc.* 730 F.2d 753,762,

221 USPQ 473,480 (Fed. Cir. 1984)." Thus, Appellants submit that such a concern is misplaced, and cannot properly form the basis of utility rejections of the present claims.

On the other hand, Appellants wholly acknowledge that the issue in this instance is the standard of proof required for Appellants to demonstrate the correlation between increased DNA levels, mRNA levels and protein levels. Based on the Utility Guidelines set by the PTO, this standard is <u>more likely than not</u>. It is <u>not absolute certainty</u>. Therefore, the Examiner's requirement for "evidence or scientific reasoning presented to conclude that **such increase is directly proportional to the amount of number of copies of DNA**" is not required to meet the "utility" standard of the Patent Statute for PRO187. Instead, Appellants' showing that gene amplification DNA results are well- correlated with mRNA and protein overexpression <u>in general</u> and therefore, it is more likely than not that, for PRO187, <u>as for most other genes</u>, gene amplification is correlated with mRNA and protein overexpression, sufficiently meets the "utility" standard set by the PTO.

Further, based on the asserted utility for PRO187 in the diagnosis of selected lung and colon cancers, the reduction to practice of the instantly claimed protein sequence of SEQ ID NO: 23 in the present application (also see page 5-6, page 36, page 100), the disclosure of the step-by-step protocol for the preparation, isolation and detection of monoclonal, polyclonal and other types of antibodies against the PRO187 protein in the specification (monoclonal and polyclonal antibodies at page 139, line 32, to page 141, line 13; humanized antibodies at page 141, line 15, to page 142, line 16; antibody fragments at page 143, line 8 onwards; labeled antibodies at pages 144-145, line 16 onwards and page 146, line 33 to page 147, line 6) and the disclosure of the gene amplification assay in Example 92, the skilled artisan would know exactly how to <u>make and use</u> the claimed antibodies for the diagnosis of lung and colon cancers. Appellants submit that based on the detailed information presented in the specification and the advanced state of the art in oncology, the skilled artisan would have found such testing routine and <u>not</u> 'undue.'

Therefore, since the instantly claimed invention <u>is</u> supported by either a credible, specific and substantial asserted utility or a well-established utility, and since the present specification clearly teaches one skilled in the art "how to make and use" the claimed invention without undue

experimentation, Appellants respectfully request reconsideration and reversal of this outstanding rejections under 35 U.S.C. §101 and §112, First Paragraph to Claims 39-46 and 49-51.

ISSUE 2: Claims 39-46 and 49-51 satisfy the written description requirement of 35 U.S.C. §112, First Paragraph

Claims 39-46 and 49-51 stand rejected under 35 U.S.C. §112, first paragraph, as allegedly containing "subject matter which was not described in the specification in such a way as to reasonably convey to one skilled in the relevant art that the inventor(s), at the time the application was filed, had possession of the claimed invention." Appellants respectfully disagree.

A. The Legal Test for Written Description

The well-established test for sufficiency of support under the written description requirement of 35 U.S.C. §112, first paragraph is "whether the disclosure of the application as originally filed reasonably conveys to the artisan that the inventor had possession at that time of the later claimed subject matter, rather than the presence or absence of literal support in the specification for the claim language."[18],[19] The adequacy of written description support is a factual issue and is to be determined on a case-by-case basis.[20] The factual determination in a written description analysis depends on the nature of the invention and the amount of knowledge imparted to those skilled in the art by the disclosure.[21],[22]

---

[18] *In re Kaslow*, 707 F.2d 1366, 1374, 212 USPQ 1089, 1096 (Fed. Cir. 1983).

[19] *See also Vas-Cath, Inc. v. Mahurkar*, 935 F.2d at 1563, 19 USPQ2d at 1116 (Fed. Cir. 1991).

[20] *See e.g., Vas-Cath*, 935 F.2d at 1563; 19 USPQ2d at 1116.

[21] *Union Oil v. Atlantic Richfield Co.*, 208 F.2d 989, 996 (Fed. Cir. 2000).

[22] *See also M.P.E.P.* §2163 II(A).

In *Environmental Designs, Ltd. v. Union Oil Co.,*[23] the Federal Circuit held, "Factors that may be considered in determining level of ordinary skill in the art include: (1) the educational level of the inventor; (2) type of problems encountered in the art; (3) prior art solutions to those problems; (4) rapidity with which innovations are made; (5) sophistication of the technology; and (6) educational level of active workers in the field."[24] Further, the "hypothetical 'person having ordinary skill in the art' to which the claimed subject matter pertains would, of necessity have the <u>capability of understanding the scientific and engineering principles applicable to the pertinent art.</u>"[25],[26]

B. The Disclosure Provides Sufficient Written Description for the Claimed Invention

Applicants claim those **native peptide sequences** with 80-99% homology to SEQ ID NO: 23 <u>and</u> wherein the nucleic acid encoding said polypeptide is amplified in lung or colon tumors. Applicants submit that the instant specification evidences the actual reduction to practice of a full-length PRO187 polypeptide of SEQ ID NO: 23, with or without its signal sequence. Thus, the genus of **native polypeptide sequences** with at least 80% sequence identity to SEQ ID NO: 23, and which possess the functional property "wherein the nucleic acid encoding said polypeptide is amplified in lung or colon tumors" would meet the requirement of 35 U.S.C. §112, first paragraph, as providing adequate written description.

In fact, Applicants point out that the Specification describes methods for the determination of percent identity between two amino acid sequence. The Specification further describes methods for one of ordinary skill in the art to *identify* peptide sequences having at least 80% identity to SEQ ID NO: 23 'wherein the nucleic acid encoding said polypeptide is amplified in lung or colon tumors' by testing the nucleic acids encoding these variants in the gene

---

[23] 713 F.2d 693, 696, 218 USPQ 865, 868 (Fed. Cir. 1983), *cert. denied,* 464 U.S. 1043 (1984).

[24] *See also* M.P.E.P. §2141.03.

[25] *Ex parte Hiyamizu,* 10 USPQ2d 1393, 1394 (Bd. Pat. App. & Inter. 1988) (emphasis added).

[26] *See also* M.P.E.P. §2141.03.

amplification assay which is well-described in Example 90 of the instant specification. The specification further provides detailed guidance as to changes that may be made to a PRO polypeptide without adversely affecting its activity (page 112, line 37 to page 117, line 8). This guidance includes a listing of exemplary and preferred substitutions for each of the twenty naturally occurring amino acids (Table 6, page 114). Accordingly, one of skill in the art could identify whether the variant PRO187 sequence falls within the parameters of the claimed invention. Once such an amino acid sequence was identified, the specification sets forth methods for making the amino acid sequences (see page 113, line 18 to page 115, line 8) and methods of preparing the PRO polypeptides (see Examples 53-56).

One of skill in the art could readily test these variant native polypeptide sequences to determine whether its encoding nucleic acid is amplified in lung or colon tumors based on the step-by-step methods set forth throughout the specification and in Example 90. There is no need to provide a description of the conserved regions of the polypeptide. Neither is there a need to correlate structure- to- function for the instantly claimed peptides or to identify specific sites at which variability is tolerated. The rejection based on difficulty in structure-function prediction in the art is irrelevant here, since Applicants are not predicting function of the variant native polypeptide sequences of SEQ ID NO: 23. Instead, Applicants claim those peptides with these prerequisites: 1) 80-99% homology to SEQ ID NO: 23 and 2) which demonstrate a well-defined function, namely, whose encoding nucleic acids are amplified in the gene amplification assay.

Appellants further submit that the specification provides ample written support for detecting and quantifying amplification of such nucleic acids in several tumors and/or cell lines as described in Example 92. Example 92 of the present application provides step-by-step guidelines and protocols for the gene amplification assay. By following this disclosure, one skilled in the art would know that it is easy to test whether a gene encoding a variant PRO187 protein is amplified in lung or colon tumors by the methods set forth in Example 92.

More recently, in *Enzo Biochem., Inc. v. Genprobe, Inc.* 296 F.3d 1316 (Fed. Cir. 2002), the court adopted the standard that "the written description requirement can be met by 'showing that the invention is complete by disclosure of sufficiently detailed, relevant identifying characteristics, . . . *i.e.,* complete or partial structure, other physical and/or chemical properties, functional characteristics when coupled with a known or disclosed correlation between function

-20-

and structure, or some combination of such characteristics." *Id.* at 1324. While the invention in *Enzo* was still a DNA, the holding has been treated as being applicable to proteins as well. Indeed, the court adopted the standard from the USPTO's Written Description Examination Guidelines, which apply to both proteins and nucleic acids.

Accordingly, current applicable case law holds that biological sequences are not adequately described **solely** by a description of their desired functional activities. The instant claims meet the standard set by the *Enzo* court in that the claimed sequences are defined not only by functional properties, but also by structural limitations. It is well established that a **combination** of functional and structural features may suffice to describe a claimed genus. "An applicant may also show that an invention is complete by disclosure of sufficiently detailed, relevant identifying characteristics which provide evidence that applicant was in possession of the claimed invention, i.e., complete or partial structure, other physical and/or chemical properties, functional characteristics when coupled with a known or disclosed correlation between function and structure, or some combination of such characteristics."[27] Thus, the genus of polypeptides with at least 80-99% sequence identity to SEQ ID NO: 23, which possess the functional property of having a nucleic acid which is amplified in lung tumor would meet the requirement of 35 U.S.C. §112, first paragraph, as providing adequate written description. Accordingly, one skilled in the art would have known that Appellants had knowledge and possessed the claimed polypeptides with 80-99% sequence identity to SEQ ID NO: 23 whose encoding nucleic acids were amplified in lung tumors. The recited property of amplification of the encoding gene adds to the characterization of the claimed polypeptide sequences in a manner that one of skill in the art could readily assess and understand.

As discussed above, Appellants have recited structural features, namely, 80% sequence identity to SEQ ID NO: 23, which are common to the genus. Appellants have also provided guidance as to how to make the recited variants of SEQ ID NO: 23, including listings of exemplary and preferred sequence substitutions. The genus of claimed polypeptides is further

---

[27] M.P.E.P. §2163 II(A)(3)(a)

defined by having a specific functional activity for the encoding nucleic acids. Accordingly, a description of the claimed genus has been achieved.

For the above reasons, the specification provides adequate written description for polypeptides having at least 80% identity to SEQ ID NO: 23 wherein the nucleic acid encoding the polypeptide is amplified in lung tumor. Accordingly, Appellants respectfully request reconsideration and reversal of the written description rejection of Claims 39-46 and 49-51 under 35 U.S.C. §112, first paragraph.

Accordingly, this rejection under §112, first paragraph should be withdrawn.

CONCLUSION

For the reasons given above, Appellants submit that present specification clearly describes, details and provides a patentable utility for the claimed invention. Moreover, it is respectfully submitted that based upon this disclosed patentable utility, the present specification clearly teaches "how to use" the presently claimed polypeptide. As such, Appellants respectfully request reconsideration and reversal of the outstanding rejection of Claims 39-46 and 49-51.

The Commissioner is authorized to charge any fees which may be required, including extension fees, or credit any overpayment to Deposit Account No. **08-1641** (referencing Attorney's Docket No. **39780-1618P2C1**).

Respectfully submitted,

(Panpan Gao 43,626)
on behalf of
Daphne Reddy

Date: March 15, 2006

Daphne Reddy
Reg. No. 53,507

HELLER EHRMAN LLP
275 Middlefield Road
Menlo Park, California 94025-3506
Telephone: (650) 324-7000
Facsimile: (650) 324-0638

IX. CLAIMS APPENDIX

Claims on Appeal

39.   An isolated native sequence polypeptide having at least 80% amino acid sequence identity to:

(a)   the amino acid sequence of the polypeptide of SEQ ID NO: 23;

(b)   the amino acid sequence of the polypeptide of SEQ ID NO: 23, lacking its associated signal peptide; or

(c)   the amino acid sequence of the polypeptide encoded by the full-length coding sequence of the cDNA deposited under ATCC accession number 209375,

wherein the nucleic acid encoding said polypeptide is amplified in lung or colon tumors.

40.   The isolated native sequence polypeptide of claim 39 having at least 85% amino acid sequence identity to:

(a)   the amino acid sequence of the polypeptide of SEQ ID NO: 23;

(b)   the amino acid sequence of the polypeptide of SEQ ID NO: 23, lacking its associated signal peptide; or

(c)   the amino acid sequence of the polypeptide encoded by the full-length coding sequence of the cDNA deposited under ATCC accession number 209375,

wherein the nucleic acid encoding said polypeptide is amplified in lung or colon tumors.

41.   The isolated native sequence polypeptide of claim 39 having at least 90% amino acid sequence identity to:

(a)   the amino acid sequence of the polypeptide of SEQ ID NO: 23;

(b)   the amino acid sequence of the polypeptide of SEQ ID NO: 23, lacking its associated signal peptide; or

(c)   the amino acid sequence of the polypeptide encoded by the full-length coding sequence of the cDNA deposited under ATCC accession number 209375,

wherein the nucleic acid encoding said polypeptide is amplified in lung or colon

tumors.

42.   The isolated native sequence polypeptide of claim 39 having at least 95% amino

acid sequence identity to:

(a)   the amino acid sequence of the polypeptide of SEQ ID NO: 23;

(b)   the amino acid sequence of the polypeptide of SEQ ID NO: 23, lacking its

associated signal peptide; or

(c)   the amino acid sequence of the polypeptide encoded by the full-length coding

sequence of the cDNA deposited under ATCC accession number 209375,

wherein the nucleic acid encoding said polypeptide is amplified in lung or colon tumors.

43.   The isolated native sequence polypeptide of claim 39 having at least 99% amino

acid sequence identity to:

(a)   the amino acid sequence of the polypeptide of SEQ ID NO: 23;

(b)   the amino acid sequence of the polypeptide of SEQ ID NO: 23, lacking its

associated signal peptide; or

(c)   the amino acid sequence of the polypeptide encoded by the full-length coding

sequence of the cDNA deposited under ATCC accession number 209375,

wherein the nucleic acid encoding said polypeptide is amplified in lung or colon tumors.

44.   An isolated polypeptide comprising:

(a)   the amino acid sequence of the polypeptide of SEQ ID NO: 23;

(b)   the amino acid sequence of the polypeptide of SEQ ID NO: 23, lacking its

associated signal peptide; or,

(c)   the amino acid sequence of the polypeptide encoded by the full-length coding

sequence of the cDNA deposited under ATCC accession number 209375.

45.   The isolated polypeptide of Claim 44 comprising the amino acid sequence of the

polypeptide of SEQ ID NO: 23.

46.   The isolated polypeptide of Claim 44 comprising the amino acid sequence of the polypeptide of SEQ ID NO: 23, lacking its associated signal peptide.

49.   The isolated polypeptide of Claim 44 comprising the amino acid sequence of the polypeptide encoded by the full-length coding sequence of the cDNA deposited under ATCC accession number 209375.

50.   A chimeric polypeptide comprising a polypeptide according to Claim 44 fused to a heterologous polypeptide.

51.   The chimeric polypeptide of Claim 50, wherein said heterologous polypeptide is an epitope tag or an Fc region of an immunoglobulin.

X.   EVIDENCE APPENDIX

1.   Declaration of Audrey Goddard, Ph.D. under 35 C.F.R. §1.132, with attached Exhibits A-G:

    A.   Curriculum Vitae of Audrey D. Goddard, Ph.D.
    B.   Higuchi, R. et al., "Simultaneous amplification and detection of specific DNA sequences," *Biotechnology* **10**:413-417 (1992).
    C.   Livak, K.J., et al., "Oligonucleotides with fluorescent dyes at opposite ends provide a quenched probe system useful for detecting PCR product and nucleic acid hybridization," *PCR Methods Appl.* **4**:357-362 (1995).
    D.   Heid, C.A. et al., "Real time quantitative PCR," *Genome Res.* **6**:986-994 (1996).
    E.   Pennica, D. et al., "WISP genes are members of the connective tissue growth factor family that are up-regulated in Wnt-1-transformed cells and aberrantly expressed in human colon tumors," *Proc. Natl. Acad. Sci. USA* **95**:14717-14722 (1998).
    F.   Pitti, R.M. et al., "Genomic amplification of a decoy receptor for Fas ligand in lung and colon cancer," *Nature* **396**:699-703 (1998).
    G.   Bieche, I. et al., "Novel approach to quantitative polymerase chain reaction using real-time detection: Application to the detection of gene amplification in breast cancer," *Int. J. Cancer* **78**:661-666 (1998).

2.   Declaration of Paul Polakis, Ph.D. under 35 C.F.R. §1.132.

3.   Declaration of Avi Ashkenazi, Ph.D. under 35 C.F.R. §1.132, with attached Exhibit A (Curriculum Vitae).

4.   Orntoft, T.F., et al., "Genome-wide Study of Gene Copy Numbers, Transcripts, and Protein Levels in Pairs of Non-Invasive and Invasive Human Transitional Cell Carcinomas," *Molecular & Cellular Proteomics* **1**:37-45 (2002).

5.   Hyman, E., et al., "Impact of DNA Amplification on Gene Expression Patterns in Breast Cancer," *Cancer Research* **62**:6240-6245 (2002).

6.   Pollack, J.R., et al., "Microarray Analysis Reveals a Major Direct Role of DNA Copy Number Alteration in the Transcriptional Program of Human Breast Tumors," *Proc. Natl. Acad. Sci. USA* **99**:12963-12968 (2002).

7.   Hanna et al., "HER-2/neu Breast Cancer Predictive Testing," Pathology Associates Medical Laboratories (1999).

Item 1 was submitted with the Appellants' Response filed on June 6, 2003 and was considered by the Examiner as indicated in the Final Office Action dated November 25, 2003.

Items 2-7 were submitted with the Appellants' Response filed on October 8, 2004 and was considered by the Examiner as indicated in the Office Action dated December 9, 2004.

XI. RELATED PROCEEDINGS APPENDIX

None- no decision rendered by a Court or the Board in any related proceedings identified above.

IN THE UNITED STATES PATENT AND TRADEMARK OFFICE

In re Application of: Ashkenazi et al.	Group Art Unit: 1647
Serial No.: 09/903,925	Examiner: Fozia Hamid
Filed: July 11, 2001	**CERTIFICATE OF MAILING** I hereby certify that this correspondence is being deposited with the United States Postal Service with sufficient postage as first class mail in an envelope addressed to: Assistant Commissioner of Patents, Washington, D.C. 20231 on Date
For: SECRETED AND TRANSMEMBRANE POLYPEPTIDES AND NUCLEIC ACIDS	

DECLARATION OF AUDREY D. GODDARD, Ph.D UNDER 37 C.F.R. § 1.132

Assistant Commissioner of Patents
Washington, D.C. 20231

Sir:

I, Audrey D. Goddard, Ph.D. do hereby declare and say as follows:

1.   I am a Senior Clinical Scientist at the Experimental Medicine/BioOncology, Medical Affairs Department of Genentech, Inc., South San Francisco, California 94080.

2.   Between 1993 and 2001, I headed the DNA Sequencing Laboratory at the Molecular Biology Department of Genentech, Inc. During this time, my responsibilities included the identification and characterization of genes contributing to the oncogenic process, and determination of the chromosomal localization of novel genes.

3.   My scientific Curriculum Vitae, including my list of publications, is attached to and forms part of this Declaration (Exhibit A).

4.   I am familiar with a variety of techniques known in the art for detecting and quantifying the amplification of oncogenes in cancer, including the quantitative TaqMan PCR (i.e., "gene amplification") assay described in the above captioned patent application.

5.   The TaqMan PCR assay is described, for example, in the following scientific publications: Higuchi *et al.*, Biotechnology 10:413-417 (1992) (Exhibit B); Livak *et al.*, PCR Methods Appl., 4:357-362 (1995) (Exhibit C) and Heid *et al.*, Genome Res. 6:986-994 (1996) (Exhibit D). Briefly, the assay is based on the principle that successful PCR yields a fluorescent signal due to Taq DNA polymerase-mediated exonuclease digestion of a fluorescently labeled oligonucleotide that is homologous to a sequence between two PCR primers. The extent of digestion depends directly on the amount of PCR, and can be quantified accurately by measuring the increment in fluorescence that results from decreased energy transfer. This is an extremely sensitive technique, which allows detection in the exponential phase of the PCR reaction and, as a result, leads to accurate determination of gene copy number.

6.   The quantitative fluorescent TaqMan PCR assay has been extensively and successfully used to characterize genes involved in cancer development and progression. Amplification of protooncogenes has been studied in a variety of human tumors, and is widely considered as having etiological, diagnostic and prognostic significance. This use of the quantitative TaqMan PCR assay is exemplified by the following scientific publications: Pennica *et al.*, Proc. Natl. Acad. Sci. USA 95(25):14717-14722 (1998) (Exhibit E); Pitti *et al.*, Nature 396(6712):699-703 (1998) (Exhibit F) and Bieche *et al.*, Int. J. Cancer 78:661-666 (1998) (Exhibit G), the first two of which I am co-author. In particular, Pennica *et al.* have used the quantitative TaqMan PCR assay to study relative gene amplification of WISP and c-myc in various cell lines, colorectal tumors and normal mucosa. Pitti *et al.* studied the genomic amplification of a decoy receptor for Fas ligand in lung and colon cancer, using the quantitative TaqMan PCR assay. Bieche *et al.* used the assay to study gene amplification in breast cancer.

7.   It is my personal experience that the quantitative TaqMan PCR technique is technically sensitive enough to detect at least a 2-fold increase in gene copy number relative to control. It is further my considered scientific opinion that an at least 2-fold increase in gene copy number in a tumor tissue sample relative to a normal (i.e., non-tumor) sample is significant and useful in that the detected increase in gene copy number in the tumor sample relative to the normal sample serves as a basis for using relative gene copy number as quantitated by the TaqMan PCR technique as a diagnostic marker for the presence or absence of tumor in a tissue sample of unknown · pathology. Accordingly, a gene identified as being amplified at least 2-fold by the quantitative TaqMan PCR assay in a tumor sample relative to a normal sample is useful as a marker for the diagnosis of cancer, for monitoring cancer development and/or for measuring the efficacy of cancer therapy.

8.   I declare further that all statements made herein of my own knowledge are true and that all statements made on information and belief are believed to be true. I declare that these statements were made with the knowledge that willful false statements and the like so made are punishable by fine or imprisonment, or both, under Section 1001 of Title 18 of the United States Code, and that such willful false statements may jeopardize the validity of the application or any patent issuing thereon.

Jan. 16, 2003

Date

Audrey Goddard

Audrey D. Goddard, Ph.D.

AUDREY D. GODDARD, Ph.D.

Genentech, Inc.
1 DNA Way
South San Francisco, CA, 94080
650.225.6429
goddarda@gene.com

110 Congo St.
San Francisco, CA, 94131
415.841.9154
415.819.2247 (mobile)
agoddard@pacbell.net

PROFESSIONAL EXPERIENCE

Genentech, Inc.   **1993-present**
South San Francisco, CA

2001 - present   Senior Clinical Scientist
Experimental Medicine / BioOncology, Medical Affairs

Responsibilities:
- *Companion diagnostic oncology products*
- *Acquisition of clinical samples from Genentech's clinical trials for translational research*
- *Translational research using clinical specimen and data for drug development and diagnostics*
- *Member of Development Science Review Committee, Diagnostic Oversight Team, 21 CFR Part 11 Subteam*

Interests:
- *Ethical and legal implications of experiments with clinical specimens and data*
- *Application of pharmacogenomics in clinical trials*

1998 - 2001   Senior Scientist
Head of the DNA Sequencing Laboratory, Molecular Biology Department, Research

Responsibilities:
- *Management of a laboratory of up to nineteen –including postdoctoral fellow, associate scientist, senior research associate and research assistants/associate levels*
- *Management of a $750K budget*
- *DNA sequencing core facility supporting a 350+ person research facility.*
- *DNA sequencing for high throughput gene discovery, - ESTs, cDNAs, and constructs*
- *Genomic sequence analysis and gene identification*
- *DNA sequence and primary protein analysis*

Research:
- *Chromosomal localization of novel genes*
- *Identification and characterization of genes contributing to the oncogenic process*
- *Identification and characterization of genes contributing to inflammatory diseases*
- *Design and development of schemes for high throughput genomic DNA sequence analysis*
- *Candidate gene prediction and evaluation*

1993 - 1998   Scientist
Head of the DNA Sequencing Laboratory, Molecular Biology Department, Research

Responsibilities
- *DNA sequencing core facility supporting a 350+ person research facility*
- *Assumed responsibility for a pre-existing team of five technicians and expanded the group into fifteen, introducing a level of middle management and additional areas of research*
- *Participated in the development of the basic plan for high throughput secreted protein discovery program – sequencing strategies, data analysis and tracking, database design*
- *High throughput EST and cDNA sequencing for new gene identification.*
- *Design and implementation of analysis tools required for high throughput gene identification.*
- *Chromosomal localization of genes encoding novel secreted proteins.*

Research:
- *Genomic sequence scanning for new gene discovery.*
- *Development of signal peptide selection methods.*
- *Evaluation of candidate disease genes.*
- *Growth hormone receptor gene SNPs in children with Idiopathic short stature*

Imperial Cancer Research Fund   **1989-1992**
London, UK with Dr. Ellen Solomon

6/89 –12/92 Postdoctoral Fellow
- Cloning and characterization of the genes fused at the acute promyelocytic leukemia translocation breakpoints on chromosomes 17 and 15.
- Prepared a successfully funded European Union multi-center grant application

McMaster University   **1983**
Hamilton, Ontario, Canada with Dr. G. D. Sweeney

5/83 – 8/83: NSERC Summer Student
- *In vitro* metabolism of β-naphthoflavone in C57Bl/6J and DBA mice

EDUCATION

Ph.D.
"Phenotypic and genotypic effects of mutations in the human retinoblastoma gene."
Supervisor: Dr. R. A. Phillips

University of Toronto
Toronto, Ontario, Canada.   1989
Department of Medical
Biophysics.

Honours B.Sc
"The *in vitro* metabolism of the cytochrome P-448 inducer β-naphthoflavone in C57BL/6J mice."
Supervisor: Dr. G. D. Sweeney

McMaster University,
Hamilton, Ontario, Canada.   1983
Department of Biochemistry

ACADEMIC AWARDS

Imperial Cancer Research Fund Postdoctoral Fellowship	1989-1992
Medical Research Council Studentship	1983-1988
NSERC Undergraduate Summer Research Award	1983
Society of Chemical Industry Merit Award (Hons. Biochem.)	1983
Dr. Harry Lyman Hooker Scholarship	1981-1983
J.L.W. Gill Scholarship	1981-1982
Business and Professional Women's Club Scholarship	1980-1981
Wyerhauser Foundation Scholarship	1979-1980

INVITED PRESENTATIONS

Genentech's gene discovery pipeline: High throughput identification, cloning and characterization of novel genes. Functional Genomics: From Genome to Function, Litchfield Park, AZ, USA. October 2000

High throughput identification, cloning and characterization of novel genes. G2K:Back to Science, Advances in Genome Biology and Technology I. Marco Island, FL, USA. February 2000

Quality control in DNA Sequencing: The use of Phred and Phrap. Bay Area Sequencing Users Meeting, Berkeley, CA, USA. April 1999

High throughput secreted protein identification and cloning. Tenth International Genome Sequencing and Analysis Conference, Miami, FL, USA. September 1998

The evolution of DNA sequencing: The Genentech perspective. Bay Area Sequencing Users Meeting, Berkeley, CA, USA. May 1998

Partial Growth Hormone Insensitivity: The role of GH-receptor mutations in Idiopathic Short Stature. Tenth Annual National Cooperative Growth Study Investigators Meeting, San Francisco, CA, USA. October, 1996

Growth hormone (GH) receptor defects are present in selected children with non-GH-deficient short stature: A molecular basis for partial GH-insensitivity. 76th Annual Meeting of The Endocrine Society, Anaheim, CA, USA. June 1994

A previously uncharacterized gene, myl, is fused to the retinoic acid receptor alpha gene in acute promyelocytic leukemia. XV International Association for Comparative Research on Leukemia and Related Disease, Padua, Italy. October 1991

PATENTS

Goddard A, Godowski PJ, Gurney AL. NL2 Tie ligand homologue polypeptide. Patent Number: 6,455,496. Date of Patent: Sept. 24, 2002.

Goddard A, Godowski PJ and Gurney AL. NL3 Tie ligand homologue nucleic acids. Patent Number: 6,426,218. Date of Patent: July 30, 2002.

Godowski P, Gurney A, Hillan KJ, Botstein D, **Goddard A**, Roy M, Ferrara N, Tumas D, Schwall R. NL4 Tie ligand homologue nucleic acid. Patent Number: 6,4137,770. Date of Patent: July 2, 2002.

Ashkenazi A, Fong S, **Goddard A**, Gurney AL, Napier MA, Tumas D, Wood WI. Nucleic acid encoding A-33 related antigen poly peptides. Patent Number: 6,410,708. Date of Patent:: Jun. 25, 2002.

Botstein DA, Cohen RL, **Goddard AD**, Gurney AL, Hillan .KJ, Lawrence DA, Levine AJ, Pennica D, Roy MA and Wood WI. WISP polypeptides and nucleic acids encoding same. Patent Number: 6,387,657. Date of Patent: May 14, 2002.

Goddard A, Godowski PJ and Gurney AL. Tie ligands. Patent Number: 6,372,491. Date of Patent: April 16, 2002.

Godowski PJ, Gurney AL, **Goddard A** and Hillan K. TIE ligand homologue antibody. Patent Number: 6,350,450. Date of Patent: Feb. 26, 2002.

Fong S, Ferrara N, **Goddard A**, Godowski PJ, Gurney AL, Hillan K and Williams PM. Tie receptor tyrosine kinase ligand homologues. Patent Number: 6,348,351. Date of Patent: Feb. 19, 2002.

Goddard A, Godowski PJ and Gurney AL. Ligand homologues. Patent Number: 6,348,350. Date of Patent: Feb. 19, 2002.

Attie KM, Carlsson LMS, Gesundheit N and **Goddard A**. Treatment of partial growth hormone insensitivity syndrome. Patent Number: 6,207,640. Date of Patent: March 27, 2001.

Fong S, Ferrara N, **Goddard A**, Godowski PJ, Gurney AL, Hillan K and Williams PM. Nucleic acids encoding NL-3. Patent Number: 6,074,873. Date of Patent: June 13, 2000

Attie K, Carlsson LMS, Gesunheit N and **Goddard A**. Treatment of partial growth hormone insensitivity syndrome. Patent Number: 5,824,642. Date of Patent: October 20, 1998

Attie K, Carlsson LMS, Gesunheit N and **Goddard A**. Treatment of partial growth hormone insensitivity syndrome. Patent Number: 5,646,113. Date of Patent: July 8, 1997

Multiple additional provisional applications filed

PUBLICATIONS

Seshasayee D, Dowd P, Gu Q, Erickson S, **Goddard AD** Comparative sequence analysis of the *HER2* locus in mouse and man. Manuscript in preparation.

Abuzzahab MJ, **Goddard A**, Grigorescu F, Lautier C, Smith RJ and Chernausek SD. Human IGF-1 receptor mutations resulting in pre- and post-natal growth retardation. Manuscript in preparation.

Aggarwal S, Xie, M-H, Foster J, Frantz G, Stinson J, Corpuz RT, Simmons L, Hillan K, Yansura DG, Vandlen RL, **Goddard AD** and Gurney AL. FHFR, a novel receptor for the fibroblast growth factors. Manuscript submitted.

Adams SH, Chui C, Schilbach SL, Yu XX, **Goddard AD**, Grimaldi JC, Lee J, Dowd P, Colman S., Lewin DA. (2001) BFIT, a unique acyl-CoA thioesterase induced in thermogenic brown adipose tissue: Cloning, organization of the human gene, and assessment of a potential link to obesity. *Biochemical Journal* **360**: 135-142.

Lee J. Ho WH. Maruoka M. Corpuz RT. Baldwin DT. Foster JS. **Goddard AD**. Yansura DG. Vandlen RL. Wood WI. Gurney AL. (2001) IL-17E, a novel proinflammatory ligand for the IL-17 receptor homolog IL-17Rh1. *Journal of Biological Chemistry* **276**(2): 1660-1664.

Xie M-H, Aggarwal S, Ho W-H, Foster J, Zhang Z, Stinson J, Wood WI, **Goddard AD** and Gurney AL. (2000) Interleukin (IL)-22, a novel human cytokine that signals through the interferon-receptor related proteins CRF2-4 and IL-22R. *Journal of Biological Chemistry* **275**: 31335-31339.

Weiss GA, Watanabe CK, Zhong A, **Goddard A** and Sidhu SS. (2000) Rapid mapping of protein functional epitopes by combinatorial alanine scanning. *Proc. Natl. Acad. Sci. USA* **97**: 8950-8954.

Guo S, Yamaguchi Y, Schilbach S, Wada T.;Lee J, **Goddard A**, French D , Handa H, Rosenthal A. (2000) A regulator of transcriptional elongation controls vertebrate neuronal development. *Nature* **408**: 366-369.

Yan M, Wang L-C, Hymowitz SG, Schilbach S, Lee J, **Goddard A**, de Vos AM, Gao WQ, Dixit VM. (2000) Two-amino acid molecular switch in an epithelial morphogen that regulates binding to two distinct receptors. *Science* **290**: 523-527.

Sehl PD, Tai JTN, Hillan KJ, Brown LA, **Goddard A**, Yang R, Jin H and Lowe DG. (2000) Application of cDNA microarrays in determining molecular phenotype in cardiac growth, development, and response to injury. *Circulation* **101**: 1990-1999.

Guo S, Brush J, Teraoka H, **Goddard A**, Wilson SW, Mullins MC and Rosenthal A. (1999) Development of noradrenergic neurons in the zebrafish hindbrain requires BMP, FGF8, and the homeodomain protein soulless/Phox2A. *Neuron* **24**: 555-566.

Stone D, Murone, M, Luoh, S, Ye W, Armanini P, Gurney A, Phillips HS, Brush, J, **Goddard A**, de Sauvage FJ and Rosenthal A. (1999) Characterization of the human suppressor of fused; a negative regulator of the zinc-finger transcription factor Gli. *J. Cell Sci.* **112**: 4437-4448.

Xie M-H, Holcomb I, Deuel B, Dowd P, Huang A, Vagts A, Foster J, Liang J, Brush J, Gu Q, Hillan K, **Goddard A** and Gurney, A.L. (1999) FGF-19, a novel fibroblast growth factor with unique specificity for FGFR4. *Cytokine* **11**: 729-735.

Yan M, Lee J, Schilbach S, **Goddard A** and Dixit V. (1999) mE10, a novel caspase recruitment domain-containing proapoptotic molecule. *J. Biol. Chem.* **274**(15): 10287-10292.

Gurney AL, Marsters SA, Huang RM, Pitti RM, Mark DT, Baldwin DT, Gray AM, Dowd P, Brush J, Heldens S, Schow P, **Goddard AD**, Wood WI, Baker KP, Godowski PJ and Ashkenazi A. (1999) Identification of a new member of the tumor necrosis factor family and its receptor, a human ortholog of mouse GITR. *Current Biology* **9**(4): 215-218.

Ridgway JBB, Ng E, Kern JA ,Lee J, Brush J, **Goddard A** and Carter P. (1999) Identification of a human anti-CD55 single-chain Fv by subtractive panning of a phage library using tumor and nontumor cell lines. *Cancer Research* **59**: 2718-2723.

Pitti RM, Marsters SA, Lawrence DA, Roy M, Kischkel FC, Dowd P, Huang A, Donahue CJ, Sherwood SW, Baldwin DT, Godowski PJ, Wood WI, Gurney AL, Hillan KJ, Cohen RL, **Goddard AD**, Botstein D and Ashkenazi A. (1998) Genomic amplification of a decoy receptor for Fas ligand in lung and colon cancer. *Nature* **396**(6712): 699-703.

Pennica D, Swanson TA, Welsh JW, Roy MA, Lawrence DA, Lee J, Brush J, Taneyhill LA, Deuel B, Lew M, Watanabe C, Cohen RL, Melhem MF, Finley GG, Quirke P, **Goddard AD**, Hillan KJ, Gurney AL, Botstein D and Levine AJ. (1998) WISP genes are members of the connective tissue growth factor family that are up-regulated in wnt-1-transformed cells and aberrantly expressed in human colon tumors. *Proc. Natl. Acad. Sci. USA.* **95**(25): 14717-14722.

Yang RB, Mark MR, Gray A, Huang A, Xie MH, Zhang M, **Goddard A**, Wood WI, Gurney AL and Godowski PJ. (1998) Toll-like receptor-2 mediates lipopolysaccharide-induced cellular signalling. *Nature* **395**(6699): 284-288.

Merchant AM, Zhu Z, Yuan JQ, **Goddard A**, Adams CW, Presta LG and Carter P. (1998) An efficient route to human bispecific IgG. *Nature Biotechnology* **16**(7): 677-681.

Marsters SA, Sheridan JP, Pitti RM, Brush J, **Goddard A** and Ashkenazi A. (1998) Identification of a ligand for the death-domain-containing receptor Apo3. *Current Biology* **8**(9): 525-528.

Xie J, Murone M, Luoh SM, Ryan A, Gu Q, Zhang C, Bonifas JM, Lam CW, Hynes M, **Goddard A**, Rosenthal A, Epstein EH Jr. and de Sauvage FJ. (1998) Activating Smoothened mutations in sporadic basal-cell carcinoma. *Nature.* **391**(6662): 90-92.

Marsters SA, Sheridan JP, Pitti RM, Huang A, Skubatch M, Baldwin D, Yuan J, Gurney A, **Goddard AD**, Godowski P and Ashkenazi A. (1997) A novel receptor for Apo2L/TRAIL contains a truncated death domain. *Current Biology.* **7**(12): 1003-1006.

Hynes M, Stone DM, Dowd M, Pitts-Meek S, **Goddard A**, Gurney A and Rosenthal A. (1997) Control of cell pattern in the neural tube by the zinc finger transcription factor *Gli-1. Neuron* **19**: 15–26.

Sheridan JP, Marsters SA, Pitti RM, Gurney A., Skubatch M, Baldwin D, Ramakrishnan L, Gray CL, Baker K, Wood WI, **Goddard AD**, Godowski P, and Ashkenazi A. (1997) Control of TRAIL-Induced Apoptosis by a Family of Signaling and Decoy Receptors. *Science* **277** (5327): 818-821.

Goddard AD, Dowd P, Chernausek S, Geffner M, Gertner J, Hintz R, Hopwood N, Kaplan S, Plotnick L, Rogol A, Rosenfield R, Saenger P, Mauras N, Hershkopf R, Angulo M and Attie, K. (1997) Partial growth hormone insensitivity: The role of growth hormone receptor mutations in idiopathic short stature. *J. Pediatr.* **131**: S51-55.

Klein RD, Sherman D, Ho WH, Stone D, Bennett GL, Moffat B, Vandlen R, Simmons L, Gu Q, Hongo JA, Devaux B, Poulsen K, Armanini M, Nozaki C, Asai N, **Goddard A**, Phillips H, Henderson CE, Takahashi M and Rosenthal A. (1997) A GPI-linked protein that interacts with Ret to form a candidate neurturin receptor. *Nature.* **387**(6634): 717-21.

Stone DM, Hynes M, Armanini M, Swanson TA, Gu Q, Johnson RL, Scott MP, Pennica D, **Goddard A**, Phillips H, Noll M, Hooper JE, de Sauvage F and Rosenthal A. (1996) The tumour-suppressor gene patched encodes a candidate receptor for Sonic hedgehog. *Nature* **384**(6605): 129-34.

Marsters SA, Sheridan JP, Donahue CJ, Pitti RM, Gray CL, **Goddard AD**, Bauer KD and Ashkenazi A. (1996) Apo-3, a new member of the tumor necrosis factor receptor family, contains a death domain and activates apoptosis and NF-kappa β. *Current Biology* **6**(12): 1669-76.

Rothe M, Xiong J, Shu HB, Williamson K, **Goddard A** and Goeddel DV. (1996) I-TRAF is a novel TRAF-interacting protein that regulates TRAF-mediated signal transduction. *Proc. Natl. Acad. Sci. USA* **93**: 8241-8246.

Yang M, Luoh SM, **Goddard A**, Reilly D, Henzel W and Bass S. (1996) The bglX gene located at 47.8 min on the Escherichia coli chromosome encodes a periplasmic beta-glucosidase. *Microbiology* **142**: 1659-65.

Goddard AD and Black DM. (1996) Familial Cancer in <u>Molecular Endocrinology of Cancer.</u> Waxman, J. Ed. Cambridge University Press, Cambridge UK, pp.187-215.

Treanor JJS, Goodman L, de Sauvage F, Stone DM, Poulson KT, Beck CD, Gray C, Armanini MP, Pollocks RA, Hefti F, Phillips HS, **Goddard A**, Moore MW, Buj-Bello A, Davis AM, Asai N, Takahashi M, Vandlen R, Henderson CE and Rosenthal A. (1996) Characterization of a receptor for GDNF. *Nature* **382**: 80-83.

Klein RD, Gu Q, **Goddard A** and Rosenthal A. (1996) Selection for genes encoding secreted proteins and receptors. *Proc. Natl. Acad. Sci. USA* **93**: 7108-7113.

Winslow JW, Moran P, Valverde J, Shih A, Yuan JQ, Wong SC, Tsai SP, **Goddard A**, Henzel WJ, Hefti F and Caras I. (1995) Cloning of AL-1, a ligand for an Eph-related tyrosine kinase receptor involved in axon bundle formation. *Neuron* **14**: 973-981.

Bennett BD, Zeigler FC, Gu Q, Fendly B, **Goddard AD**, Gillett N and Matthews W. (1995) Molecular cloning of a ligand for the EPH-related receptor protein-tyrosine kinase Htk. *Proc. Natl. Acad. Sci. USA* **92**: 1866-1870.

Huang X, Yuang J, **Goddard A**, Foulis A, James RF, Lernmark A, Pujol-Borrell R, Rabinovitch A, Somoza N and Stewart TA. (1995) Interferon expression in the pancreases of patients with type I diabetes. *Diabetes* **44**: 658-664.

Goddard AD, Yuan JQ, Fairbairn L, Dexter M, Borrow J, Kozak C and Solomon E. (1995) Cloning of the murine homolog of the leukemia-associated PML gene. *Mammalian Genome* **6**: 732-737.

Goddard AD, Covello R, Luoh SM, Clackson T, Attie KM, Gesundheit N, Rundle AC, Wells JA, Carlsson LMTI and The Growth Hormone Insensitivity Study Group. (1995) Mutations of the growth hormone receptor in children with idiopathic short stature. *N. Engl. J. Med.* **333**: 1093-1098.

Kuo SS, Moran P, Gripp J, Armanini M, Phillips HS, **Goddard A** and Caras IW. (1994) Identification and characterization of Batk, a predominantly brain-specific non-receptor protein tyrosine kinase related to Csk. *J. Neurosci. Res.* **38**: 705-715.

Mark MR, Scadden DT, Wang Z, Gu Q, **Goddard A** and Godowski PJ. (1994) Rse, a novel receptor-type tyrosine kinase with homology to Axl/Ufo, is expressed at high levels in the brain. *Journal of Biological Chemistry* **269**: 10720-10728.

Borrow J, Shipley J, Howe K, Kiely F, **Goddard A**, Sheer D, Srivastava A, Antony AC, Fioretos T, Mitelman F and Solomon E. (1994) Molecular analysis of simple variant translocations in acute promyelocytic leukemia. *Genes Chromosomes Cancer* **9**: 234-243.

Goddard AD and Solomon E. (1993) Genetics of Cancer. *Adv. Hum. Genet.* **21**: 321-376.

Borrow J, **Goddard AD**, Gibbons B, Katz F, Swirsky D, Fioretos T, Dube I, Winfield DA, Kingston J, Hagemeijer A, Rees JKH, Lister AT and Solomon E. (1992) Diagnosis of acute promyelocytic leukemia by RT-PCR: Detection of *PML-RARA* and *RARA-PML* fusion transcripts. *Br. J. Haematol.* **82**: 529-540.

Goddard AD, Borrow J and Solomon E. (1992) A previously uncharacterized gene, PML, is fused to the retinoic acid receptor alpha gene in acute promyelocytic leukemia. *Leukemia* **6 Suppl 3**: 117S–119S.

Zhu X, Dunn JM, **Goddard AD**, Squire JA, Becker A, Phillips RA and Gallie BL. (1992) Mechanisms of loss of heterozygosity in retinoblastoma. *Cytogenet. Cell. Genet.* **59**: 248-252.

Foulkes W, **Goddard A.** and Patel K. (1991) Retinoblastoma linked with Seascale [letter]. *British Med. J.* **302**: 409.

Goddard AD, Borrow J, Freemont PS and Solomon E. (1991) Characterization of a novel zinc finger gene disrupted by the t(15;17) in acute promyelocytic leukemia. *Science* **254**: 1371-1374.

Solomon E, Borrow J and **Goddard AD**. (1991) Chromosomal aberrations in cancer. *Science* **254**: 1153-1160.

Pajunen L, Jones TA, **Goddard A**, Sheer D, Solomon E, Pihlajaniemi T and Kivirikko KI. (1991) Regional assignment of the human gene coding for a multifunctional peptide (P4HB) acting as the β–subunit of prolyl-4-hydroxylase and the enzyme protein disulfide isomerase to 17q25. *Cytogenet. Cell. Genet.* **56**: 165-168.

Borrow J, Black DM, **Goddard AD**, Yagle MK, Frischauf A.-M and Solomon E. (1991) Construction and regional localization of a *Not*I linking library from human chromosome 17q. *Genomics* **10**: 477–480.

Borrow J, **Goddard AD**, Sheer D and Solomon E. (1990) Molecular analysis of acute promyelocytic leukemia breakpoint cluster region on chromosome 17. *Science* **249**: 1577-1580.

Myers JC, Jones TA, Pohjolainen E-R, Kadri AS, **Goddard AD**, Sheer D, Solomon E and Pihlajaniemi T. (1990) Molecular cloning of 5(IV) collagen and assignment of the gene to the region of the region of the X-chromosome containing the Alport Syndrome locus. *Am. J. Hum. Genet.* **46**: 1024-1033.

Gallie BL, Squire JA, **Goddard A**, Dunn JM, Canton M, Hinton D, Zhu X and Phillips RA. (1990) Mechanisms of oncogenesis in retinoblastoma. *Lab. Invest.* **62**: 394-408.

Goddard AD, Phillips RA, Greger V, Passarge E, Hopping W, Gallie BL and Horsthemke B. (1990) Use of the RB1 cDNA as a diagnostic probe in retinoblastoma families. *Clinical Genetics* **37**: 117-126.

Zhu XP, Dunn JM, Phillips RA, **Goddard AD**, Paton KE, Becker A and Gallie BL. (1989) Germline, but not somatic, mutations of the RB1 gene preferentially involve the paternal allele. *Nature* **340**: 312-314.

Gallie BL, Dunn JM, **Goddard A**, Becker A and Phillips RA. (1988) Identification of mutations in the putative retinoblastoma gene. In <u>Molecular Biology of The Eye: Genes, Vision and Ocular Disease</u>. UCLA Symposia on Molecular and Cellular Biology, New Series, Volume 88. J. Piatigorsky, T. Shinohara and P.S. Zelenka, Eds. Alan R. Liss, Inc., New York, 1988, pp. 427-436.

Goddard AD, Balakier H, Canton M, Dunn J, Squire J, Reyes E, Becker A, Phillips RA and Gallie BL. (1988) Infrequent genomic rearrangement and normal expression of the putative RB1 gene in retinoblastoma tumors. *Mol. Cell. Biol.* **8**: 2082-2088.

Squire J, Dunn J, **Goddard A**, Hoffman T, Musarella M, Willard HF, Becker AJ, Gallie BL and Phillips RA. (1986) Cloning of the esterase D gene: A polymorphic gene probe closely linked to the retinoblastoma locus on chromosome 13. *Proc. Natl. Acad. Sci.* USA **83**: 6573-6577.

Squire J, **Goddard AD**, Canton M, Becker A, Phillips RA and Gallie BL (1986) Tumour induction by the retinoblastoma mutation is independent of N-*myc* expression. *Nature* **322**: 555-557.

Goddard AD, Heddle JA, Gallie BL and Phillips RA. (1985) Radiation sensitivity of fibroblasts of bilateral retinoblastoma patients as determined by micronucleus induction *in vitro. Mutation Research* **152**: 31-38.

rotoxin fusion
Sci. USA 85,

dmann, T. A.,
. immunotoxin
to *Pseudomonas*

ngham, M. C.,
iod of cloning
in *coli* as single.
1066-1070.

schberg, D. L.
iour effects of
.toposide phos-

-, C., Deleide,
,penetoa, A. A.
.tc-targeted by
:) 184-1189.
tcd, Vol. 2, p.

?, and Stevens,
; with anti-viral
). Biochem. J.

A. L., Carnicelli,
id properties of
osidase activity.

:rization of the
abito cukaryotic
528.

'urification and
itata americana
hem. Biophys.

1982. Purifica-
of the antiviral
'okeweed). Bio-

L Dodecandrin,
dodecandm. Bio-

icw inhibitor of
iem. 255:6947-

Abbondanza, A.,
ribozome-inacti-
(white bryony).

-synthesis inhib-
; Lett. 153:209-

S. Isolation and
inhibitory pro-
;hem. 52:1223-

o, L., Sperti, S.
vitro by proteins
clon). Biochem.

nza, A., Centri,
Purification and
ith RNA N-gly-
ation from the
Acta. 993:287-

Guillemot, J. C.,
1988. Trichoki-
of *Trichoma nthes*
.8.

itors of animal
Biophys. Acta

roperties of the
'otcin inhibiting

of abrin: a toxic
ferent biological
ur. J. Biochem.

Franz, H. 1980.
Viscum album L.

i. and Stirpe, F.
of modeccin, the

:., Brown, A. N.,
s of volkensin, a
:14689-14995.
nd properties of
nistry 18:2615-

RESEARCH/

SIMULTANEOUS AMPLIFICATION AND DETECTION OF SPECIFIC DNA SEQUENCES

Russell Higuchi*, Gavin Dollinger[1], P. Sean Walsh and Robert Griffith

Roche Molecular Systems, Inc., 1400 53rd St., Emeryville, CA 94608. [1]Chiron Corporation, 1400 53rd St., Emeryville, CA 94608. *Corresponding author.

We have enhanced the polymerase chain reaction (PCR)[1] such that specific DNA sequences can be detected without opening the reaction tube. This enhancement requires the addition of ethidium bromide (EtBr) to a PCR. Since the fluorescence of EtBr increases in the presence of double-stranded (ds) DNA an increase in fluorescence in such a PCR indicates a positive amplification, which can be easily monitored externally. In fact, amplification can be continuously monitored in order to follow its progress. The ability to simultaneously amplify specific DNA sequences and detect the product of the amplification both simplifies and improves PCR and may facilitate its automation and more widespread use in the clinic or in other situations requiring high sample throughput.

Although the potential benefits of PCR[1] to clinical diagnostics are well known[2,3], it is still not widely used in this setting, even though it is four years since thermostable DNA polymerases[4] made PCR practical. Some of the reasons for its slow acceptance are high cost, lack of automation of pre- and post-PCR processing steps, and false positive results from carryover-contamination. The first two points are related in that labor is the largest contributor to cost at the present stage of PCR development. Most current assays require some form of "downstream" processing once thermocycling is done in order to determine whether the target DNA sequence was present and has amplified. These include DNA hybridization[5,6], gel electrophoresis with or without use of restriction digestion[7,8], HPLC[9], or capillary electrophoresis[10]. These methods are labor-intense, have low throughput, and are difficult to automate. The third point is also closely related to downstream processing. The handling of the PCR product in these downstream processes increases the chances that amplified DNA will spread through the typing lab, resulting in a risk of

"carryover" false positives in subsequent testing[11].

These downstream processing steps would be eliminated if specific amplification and detection of amplified DNA took place simultaneously within an unopened reaction vessel. Assays in which such different processes take place without the need to separate reaction components have been termed "homogeneous". No truly homogeneous PCR assay has been demonstrated to date, although progress towards this end has been reported. Chehab, et al.[12], developed a PCR product detection scheme using fluorescent primers that resulted in a fluorescent PCR product. Allele-specific primers, each with different fluorescent tags, were used to indicate the genotype of the DNA. However, the unincorporated primers must still be removed in a downstream process in order to visualize the result. Recently, Holland, et al.[13], developed an assay in which the endogenous 5' exonuclease assay of *Taq* DNA polymerase was exploited to cleave a labeled oligonucleotide probe. The probe would only cleave if PCR amplification had produced its complementary sequence. In order to detect the cleavage products, however, a subsequent process is again needed.

We have developed a truly homogeneous assay for PCR and PCR product detection based upon the greatly increased fluorescence that ethidium bromide and other DNA binding dyes exhibit when they are bound to ds-DNA[14-16]. As outlined in Figure 1, a prototypic PCR

FIGURE 1 Principle of simultaneous amplification and detection of PCR product. The components of a PCR containing EtBr that are fluorescent are listed—EtBr itself, EtBr bound to either ssDNA or dsDNA. There is a large fluorescence enhancement when EtBr is bound to DNA and binding is greatly enhanced when DNA is double-stranded. After sufficient (n) cycles of PCR, the net increase in dsDNA results in additional EtBr binding, and a net increase in total fluorescence.

0 1/16 1/8 1/4 1/2 1 2 4 8 µg/ml EtBr

← expected product

← 'primer-dimer'

FIGURE 2 Gel electrophoresis of PCR amplification products of the human, nuclear gene, HLA DQα, made in the presence of increasing amounts of EtBr (up to 8 µg/ml). The presence of EtBr has no obvious effect on the yield or specificity of amplification.
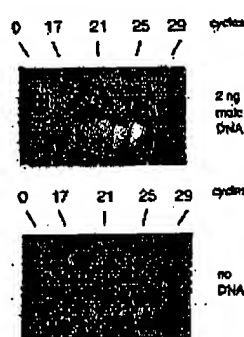
A.

B.

0 17 21 25 29 cycles

2 ng male DNA

0 17 21 25 29 cycles

no DNA

FIGURE 3 (A) Fluorescence measurements from PCRs that contain 0.5 µg/ml EtBr and that are specific for Y-chromosome repeat sequences. Five replicate PCRs were begun containing each of the DNAs specified. At each indicated cycle, one of the five replicate PCRs for each DNA was removed from thermocyding and its fluorescence measured. Units of fluorescence are arbitrary. (B) UV photography of PCR tubes (0.5 ml Eppendorf-style, polypropylene micro-centrifuge tubes) containing reactions, those starting from 2 ng male DNA and control reactions without any DNA, from (A).

begins with primers that are single-stranded DNA (ssDNA), dNTPs, and DNA polymerase. An amount of dsDNA containing the target sequence (target DNA) is also typically present. This amount can vary, depending on the application, from single-cell amounts of DNA[17] to micrograms per PCR[18]. If EtBr is present, the reagents that will fluoresce, in order of increasing fluorescence, are free EtBr itself, and EtBr bound to the single-stranded DNA primers and to the double-stranded target DNA (by its intercalation between the stacked bases of the DNA double-helix). After the first denaturation cycle, target DNA will be largely single-stranded. After a PCR is completed, the most significant change is the increase in the amount of dsDNA (the PCR product itself) of up to several micrograms. Formerly free EtBr is bound to the additional dsDNA, resulting in an increase in fluorescence. There is also some decrease in the amount of ssDNA primer, but because the binding of EtBr to ssDNA is much less than to dsDNA, the effect of this change on the total fluorescence of the sample is small. The fluorescence increase can be measured by directing excitation illumination through the walls of the amplification vessel

before and after, or even continuously during, thermocycling.

RESULTS

PCR in the presence of EtBr. In order to assess the affect of EtBr in PCR, amplifications of the human HLA DQα gene[19] were performed with the dye present at concentrations from 0.06 to 8.0 µg/ml (a typical concentration of EtBr used in staining of nucleic acids following gel electrophoresis is 0.5 µg/ml). As shown in Figure 2, gel electrophoresis revealed little or no difference in the yield or quality of the amplification product whether EtBr was absent or present at any of these concentrations, indicating that EtBr does not inhibit PCR.

Detection of human Y-chromosome specific sequences. Sequence-specific, fluorescence enhancement of EtBr as a result of PCR was demonstrated in a series of amplifications containing 0.5 µg/ml EtBr and primers specific to repeat DNA sequences found on the human Y-chromosome[20]. These PCRs initially contained either 60 ng male, 60 ng female, 2 ng male human or no DNA. Five replicate PCRs were begun for each DNA. After 0, 17, 21, 24 and 29 cycles of thermocycling, a PCR for each DNA was removed from the thermocycler, and its fluorescence measured in a spectrofluorometer and plotted vs. amplification cycle number (Fig. 3A). The shape of this curve reflects the fact that by the time an increase in fluorescence can be detected, the increase in DNA is becoming linear and not exponential with cycle number. As shown, the fluorescence increased about three-fold over the background fluorescence for the PCRs containing human male DNA, but did not significantly increase for negative control PCRs, which contained either no DNA or human female DNA. The more male DNA present to begin with—60 ng versus 2 ng—the fewer cycles were needed to give a detectable increase in fluorescence. Gel electrophoresis on the products of these amplifications showed that DNA fragments of the expected size were made in the male DNA containing reactions and that little DNA synthesis took place in the control samples.

In addition, the increase in fluorescence was visualized by simply laying the completed, unopened PCRs on a UV transilluminator and photographing them through a red filter. This is shown in figure 3B for the reactions that began with 2 ng male DNA and those with no DNA.

Detection of specific alleles of the human β-globin gene. In order to demonstrate that this approach has adequate specificity to allow genetic screening, a detection of the sickle-cell anemia mutation was performed. Figure 4 shows the fluorescence from completed amplifications containing EtBr (0.5 µg/ml) as detected by photography of the reaction tubes on a UV transilluminator. These reactions were performed using primers specific for either the wild-type or sickle-cell mutation of the human β-globin gene[21]. The specificity for each allele is imparted by placing the sickle-mutation site at the terminal 3' nucleotide of one primer. By using an appropriate primer annealing temperature, primer extension—and thus amplification—can take place only if the 3' nucleotide of the primer is complementary to the β-globin allele present[21,22].

Each pair of amplifications shown in Figure 4 consists of a reaction with either the wild-type allele specific (left tube) or sickle-allele specific (right tube) primers. Three different DNAs were typed: DNA from a homozygous, wild-type β-globin individual (AA); from a heterozygous sickle β-globin individual (AS); and from a homozygous sickle β-globin individual (SS). Each DNA (50 ng genomic DNA to start each PCR) was analyzed in triplicate (3 pairs

of reactions each). The DNA type was reflected in the relative fluorescence intensities in each pair of completed amplifications. There was a significant increase in fluorescence only where a β-globin allele DNA matched the primer set. When measured on a spectrofluorometer (data not shown), this fluorescence was about three times that present in a PCR where both β-globin alleles were mismatched to the primer set. Gel electrophoresis (not shown) established that this increase in fluorescence was due to the synthesis of nearly a microgram of a DNA fragment of the expected size for β-globin. There was little synthesis of dsDNA in reactions in which the allele-specific primer was mismatched to both alleles.

Continuous monitoring of a PCR. Using a fiber optic device, it is possible to direct excitation illumination from a spectrofluorometer to a PCR undergoing thermocycling and to return its fluorescence to the spectrofluorometer. The fluorescence readout of such an arrangement, directed at an EtBr-containing amplification of Y-chromosome specific sequences from 25 ng of human male DNA, is shown in Figure 5. The readout from a control PCR with no target DNA is also shown. Thirty cycles of PCR were monitored for each.

The fluorescence trace as a function of time clearly shows the effect of the thermocycling. Fluorescence intensity rises and falls inversely with temperature. The fluorescence intensity is minimum at the denaturation temperature (94°C) and maximum at the annealing/extension temperature (50°C). In the negative-control PCR, these fluorescence maxima and minima do not change significantly over the thirty thermocycles, indicating that there is little dsDNA synthesis without the appropriate target DNA, and there is little if any bleaching of EtBr during the continuous illumination of the sample.

In the PCR containing male DNA, the fluorescence maxima at the annealing/extension temperature begin to increase at about 4000 seconds of thermocycling, and continue to increase with time, indicating that dsDNA is being produced at a detectable level. Note that the fluorescence minima at the denaturation temperature do not significantly increase, presumably because at this temperature there is no dsDNA for EtBr to bind. Thus the course of the amplification is followed by tracking the fluorescence increase at the annealing temperature. Analysis of the products of these two amplifications by gel electrophoresis showed a DNA fragment of the expected size for the male DNA containing sample and no detectable DNA synthesis for the control sample.

DISCUSSION

Downstream processes such as hybridization to a sequence-specific probe can enhance the specificity of DNA detection by PCR. The elimination of these processes means that the specificity of this homogeneous assay depends solely on that of PCR. In the case of sickle-cell disease, we have shown that PCR alone has sufficient DNA sequence specificity to permit genetic screening. Using appropriate amplification conditions, there is little non-specific production of dsDNA in the absence of the appropriate target allele.

The specificity required to detect pathogens can be more or less than that required to do genetic screening, depending on the number of pathogens in the sample and the amount of other DNA that must be taken with the sample. A difficult target is HIV, which requires detection of a viral genome that can be at the level of a few copies per thousands of host cells[6]. Compared with genetic screening, which is performed on cells containing at least one copy of the target sequence, HIV detection requires both more specificity and the input of more total

Homozygous
AA

Heterozygous
AS

Homozygous
SS

FIGURE 4 UV photography of PCR tubes containing amplifications using EtBr that are specific to wild-type (A) or sickle (S) alleles of the human β-globin gene. The left of each pair of tubes contains allele-specific primers to the wild-type alleles, the right tube primers to the sickle allele. The photograph was taken after 30 cycles of PCR, and the input DNAs and the alleles they contain are indicated. Fifty ng of DNA was used to begin PCR. Typing was done in triplicate (3 pairs of PCRs) for each input DNA.

FIGURE 5 Continuous, real-time monitoring of a PCR. A fiber optic was used to carry excitation light to a PCR in progress and also emitted light back to a fluorometer (see Experimental Protocol). Amplification using human male-DNA specific primers in a PCR starting with 20 ng of human male DNA (top), or in a control PCR without DNA (bottom), were monitored. Thirty cycles of PCR were followed for each. The temperature cycled between 94°C (denaturation) and 50°C (annealing and extension). Note in the male DNA PCR, the cycle (time) dependent increase in fluorescence at the annealing/extension temperature.

DNA—up to microgram amounts—in order to have sufficient numbers of target sequences. This large amount of starting DNA in an amplification significantly increases the background fluorescence over which any additional fluorescence produced by PCR must be detected. An additional complication that occurs with targets in low copy-number is the formation of the "primer-dimer" artifact. This is the result of the extension of one primer using the other primer as a template. Although this occurs infrequently, once it occurs the extension product is a substrate for PCR amplification, and can compete with true PCR targets if those targets are rare. The primer-dimer product is of course dsDNA and thus is a potential source of false signal in this homogeneous assay.

To increase PCR specificity and reduce the effect of primer-dimer amplification, we are investigating a number of approaches, including the use of nested-primer amplifications that take place in a single tube[8], and the "hot-start", in which nonspecific amplification is reduced by raising the temperature of the reaction before DNA synthesis begins[23]. Preliminary results using these approaches suggest that primer-dimer is effectively reduced and it is possible to detect the increase in EtBr fluorescence in a PCR instigated by a single HIV genome in a background of 10^5 cells. With larger numbers of cells, the background fluorescence contributed by genomic DNA becomes problematic. To reduce this background, it may be possible to use sequence-specific DNA-binding dyes that can be made to preferentially bind PCR product over genomic DNA by incorporating the dye-binding DNA sequence into the PCR product through a 5' "add-on" to the oligonucleotide primer[24].

We have shown that the detection of fluorescence generated by an EtBr-containing PCR is straightforward, both once PCR is completed and continuously during thermocycling. The ease with which automation of specific DNA detection can be accomplished is the most promising aspect of this assay. The fluorescence analysis of completed PCRs is already possible with existing instrumentation in 96-well format[25]. In this format, the fluorescence in each PCR can be quantitated before, after, and even at selected points during thermocycling by moving the rack of PCRs to a 96-microwell plate fluorescence reader[26].

The instrumentation necessary to continuously monitor multiple PCRs simultaneously is also simple in principle. A direct extension of the apparatus used here is to have multiple fiberoptics transmit the excitation light and fluorescent emissions to and from multiple PCRs. The ability to monitor multiple PCRs continuously may allow quantitation of target DNA copy number. Figure 3 shows that the larger the amount of starting target DNA, the sooner during PCR a fluorescence increase is detected. Preliminary experiments (Higuchi and Dollinger, manuscript in preparation) with continuous monitoring have shown a sensitivity to two-fold differences in initial target DNA concentration.

Conversely, if the number of target molecules is known—as it can be in genetic screening—continuous monitoring may provide a means of detecting false positive and false negative results. With a known number of target molecules, a true positive would exhibit detectable fluorescence by a predictable number of cycles of PCR. Increases in fluorescence detected before or after that cycle would indicate potential artifacts. False negative results due to, for example, inhibition of DNA polymerase, may be detected by including within each PCR an inefficiently amplifying marker. This marker results in a fluorescence increase only after a large number of cycles—many more than are necessary to detect a true

positive. If a sample fails to have a fluorescence increase after this many cycles, inhibition may be suspected. Since, in this assay, conclusions are drawn based on the presence or absence of fluorescence signal alone, such controls may be important. In any event, before any test based on this principle is ready for the clinic, an assessment of its false positive/false negative rates will need to be obtained using a large number of known samples.

In summary, the inclusion in PCR of dyes whose fluorescence is enhanced upon binding dsDNA makes it possible to detect specific DNA amplification from outside the PCR tube. In the future, instruments based upon this principle may facilitate the more widespread use of PCR in applications that demand the high throughput of samples.

EXPERIMENTAL PROTOCOL

Human HLA-DQα gene amplifications containing EtBr. PCRs were set up in 100 µl volumes containing 10 mM Tris-HCl, pH 8.3; 50 mM KCl; 4 mM MgCl$_2$; 2.5 units of *Taq* DNA polymerase (Perkin-Elmer Cetus, Norwalk, CT); 20 pmole each of human HLA-DQα gene specific oligonucleotide primers (GH26 and GH27[19] and approximately 10^9 copies of DQα PCR product diluted from a previous reaction. Ethidium bromide (EtBr; Sigma) was used at the concentrations indicated in Figure 2. Thermocycling proceeded for 20 cycles in a model 480 thermocycler (Perkin-Elmer Cetus, Norwalk, CT) using a "step-cycle" program of 94°C for 1 min. denaturation and 60°C for 30 sec. annealing and 72°C for 30 sec. extension.

Y-chromosome specific PCR. PCRs (100 µl total reaction volume) containing 0.5 µg/ml EtBr were prepared as described for HLA-DQα, except with different primers and target DNAs. These PCRs contained 15 pmole each male DNA-specific primers Y1.1 and Y1.2[20], and either 60 ng male, 60 ng female, 2 ng male, or no human DNA. Thermocycling was 94°C for 1 min. and 60°C for 1 min using a "step-cycle" program. The number of cycles for a sample were as indicated in Figure 3. Fluorescence measurement is described below.

Allele-specific, human β-globin gene PCR. Amplifications of 100 µl volume using 0.5 µg/ml of EtBr were prepared as described for HLA-DQα above except with different primers and target DNAs. These PCRs contained either primer pair HGP2/Hβ14A (wild-type globin specific primers) or HGP2/Hβ14S (sickle-globin specific primers) at 10 pmole each primer per PCR. These primers were developed by Wu et al.[21]. Three different target DNAs were used in separate amplifications—50 ng each of human DNA that was homozygous for the sickle trait (SS), DNA that was heterozygous for the sickle trait (AS), or DNA that was homozygous for the w.t. globin (AA). Thermocycling was for 30 cycles at 94°C for 1 min. and 55°C for 1 min. using a "step-cycle" program. An annealing temperature of 55°C had been shown by Wu et al.[21] to provide allele-specific amplification. Completed PCRs were photographed through a red filter (Wratten 23A) after placing the reaction tubes atop a model TM-36 transilluminator (UV-products San Gabriel, CA).

Fluorescence measurement. Fluorescence measurements were made on PCRs containing EtBr in a Fluorolog-2 fluorometer (SPEX, Edison, NJ). Excitation was at the 500 nm band with about 2 nm bandwidth with a GG 435 nm cut-off filter (Melles Grist, Inc., Irvine, CA) to exclude second-order light. Emitted light was detected at 570 nm with a bandwidth of about 7 nm. An OG 530 nm cut-off filter was used to remove the excitation light.

Continuous fluorescence monitoring of PCR. Continuous monitoring of a PCR in progress was accomplished using the spectrofluorometer and settings described above as well as a fiberoptic accessory (SPEX cat. no. 1950) to both send excitation light to, and receive emitted light from, a PCR placed in a well of a model 480 thermocycler (Perkin-Elmer Cetus). The probe end of the fiberoptic cable was attached with "5 minute-epoxy" to the open top of a PCR tube (a 0.5 ml polypropylene centrifuge tube with its cap removed) effectively sealing it. The exposed top of the PCR tube and the end of the fiberoptic cable were shielded from room light and the room lights were kept dimmed during each run. The monitored PCR was an amplification of Y-chromosome-specific repeat sequences as described above, except using an annealing/extension temperature of 50°C. The reaction was covered with mineral oil (2 drops) to prevent evaporation. Thermocycling and fluorescence measurement were started simultaneously. A time-base scan with a 10 second integration time

was used and the emission signal was ratioed to the excitation signal to control for changes in light-source intensity. Data were collected using the dm3000f, version 2.5 (SPEX) data system.

Acknowledgments

We thank Bob Jones for help with the spectrofluormetric measurements and Heatherbell Fong for editing this manuscript.

References

1. Mullis, K., Faloona, F., Scharf, S., Saiki, R., Horn, G. and Erlich, H. 1986. Specific enzymatic amplification of DNA in vitro: The polymerase chain reaction. CSHSQB 51:263-273.
2. White, T. J., Arnheim, N. and Erlich, H. A. 1989. The polymerase chain reaction. Trends Genet. 5:185-189.
3. Erlich, H. A., Gelfand, D. and Sninsky, J. J. 1991. Recent advances in the polymerase chain reaction. Science 252:1643-1651.
4. Saiki, R. K., Gelfand, D. H., Stoffel, S., Scharf, S. J., Higuchi, R., Horn, G. T., Mullis, K. B. and Erlich, H. A. 1988. Primer-directed enzymatic amplification of DNA with a thermostable DNA polymerase. Science 239:487-491.
5. Saiki, R. K., Walsh, P. S., Levenson, C. H. and Erlich, H. A. 1989. Genetic analysis of amplified DNA with immobilized sequence-specific oligonucleotide probes. Proc. Natl. Acad. Sci. USA 86:6230-6234.
6. Kwok, S. Y., Mack, D. H., Mullis, K. B., Poiesz, B. J., Ehrlich, G. D., Blair, D. and Friedman-Kien, A. S. 1987. Identification of human immunodeficiency virus sequences by using in vitro enzymatic amplification and oligomer cleavage detection. J. Virol. 61:1690-1694.
7. Chehab, F. F., Doherty, M., Cai, S. P., Kan, Y. W., Cooper, S. and Rubin, E. M. 1987. Detection of sickle cell anemia and thalassemia. Nature 329:293-294.
8. Horn, G. T., Richards, B. and Klinger, K. W. 1989. Amplification of a highly polymorphic VNTR segment by the polymerase chain reaction. Nuc. Acids Res. 16:2140.
9. Katz, E. D. and Dong, M. W. 1990. Rapid analysis and purification of polymerase chain reaction products by high-performance liquid chromatography. Biotechniques 8:546-555.
10. Heiger, D. N., Cohen, A. S. and Karger, B. L. 1990. Separation of DNA restriction fragments by high performance capillary electrophoresis with low and zero crosslinked polyacrylamide using continuous and pulsed electric fields. J. Chromatogr. 516:33-48.
11. Kwok, S. Y. and Higuchi, R. G. 1989. Avoiding false positives with PCR. Nature 339:237-238.
12. Chehab, F. F. and Kan, Y. W. 1989. Detection of specific DNA sequences by fluorescence amplification: a color complementation assay. Proc. Natl. Acad. Sci. USA 86:9178-9182.
13. Holland, P. M., Abramson, R. D., Watson, R. and Gelfand, D. H.

14. Markovits, J., Roques, B. P. and Le Pecq, J. B. 1979. Ethidium dimer: a new reagent for the fluorimetric determination of nucleic acids. Anal. Biochem. 94:259-264.
15. Kapuscinski, J. and Szer, W. 1979. Interactions of 4',6-diamidine-2-phenylindole with synthetic polynucleotides. Nuc. Acids Res. 6:3519-3534.
16. Searle, M. S. and Embrey, K. J. 1990. Sequence-specific interaction of Hoescht 33258 with the minor groove of an adenine-tract DNA duplex studied in solution by ¹H NMR spectroscopy. Nuc. Acids Res. 18:3753-3762.
17. Li, H. H., Gyllensten, U. B., Cui, X. F., Saiki, R. K., Erlich, H. A. and Arnheim, N. 1988. Amplification and analysis of DNA sequences in single human sperm and diploid cells. Nature 335:414-417.
18. Abbott, M. A., Poiesz, B. J., Byrne, B. C., Kwok, S. Y., Sninsky, J. J. and Erlich, H. A. 1988. Enzymatic gene amplification: qualitative and quantitative methods for detecting proviral DNA amplified in vitro. J. Infect. Dis. 158:1158.
19. Saiki, R. K., Bugawan, T. L., Horn, G. T., Mullis, K. B. and Erlich, H. A. 1986. Analysis of enzymatically amplified β-globin and HLA-DQα DNA with allele-specific oligonucleotide probes. Nature 324:163-166.
20. Kogan, S. C., Doherty, M. and Gitschier, J. 1987. An improved method for prenatal diagnosis of genetic disease by analysis of amplified DNA sequences. N. Engl. J. Med. 317:985-990.
21. Wu, D. Y., Ugozzoli, L., Pal, B. K. and Wallace, R. B. 1989. Allele-specific enzymatic amplification of β-globin genomic DNA for diagnosis of sickle cell anemia. Proc. Natl. Acad. Sci. USA 85:2757-2760.
22. Kwok, S., Kellogg, D. E., McKinney, N., Spasic, D., Goda, L., Levenson, C. and Sninsky, J. J. 1990. Effects of primer-template mismatches on the polymerase chain reaction: Human immunodeficiency virus type 1 model studies. Nuc. Acids Res. 18:999-1005.
23. Chou, Q., Russell, M., Birch, D., Raymond, J. and Bloch, W. 1992. Prevention of pre-PCR mis-priming and primer dimerization improves low-copy-number amplifications. Submitted.
24. Higuchi, R. 1989. Using PCR to engineer DNA, p. 61-70. In: PCR Technology. H. A. Erlich (Ed.). Stockton Press, New York, N.Y.
25. Haff, L., Atwood, J. G., DiCesare, J., Katz, E., Picozza, E., Williams, J. F. and Woudenberg, T. 1991. A high-performance system for automation of the polymerase chain reaction. Biotechniques 10:102-105, 106-112.
26. Turoosa, N. and Kahan, L. 1989. Fluorescent EIA screening of monoclonal antibodies to cell surface antigens. J. Immun. Meth. 116:59-63.

GENENTECH, INC.
1 DNA Way
South San Francisco, CA 94080 USA
Phone: (650) 225-1000

FAX: (650) 952-9881

FACSIMILE TRANSMITTAL

Date: 19 July 2004

To: **Anna Barry**
Heller Ehrman

Re: Higuchi reference

Fax No: 324 - 6638

From: Patty Tobin, Assistant to Elizabeth M. Barnes, Ph.D.
Genentech, Inc. Legal Department

Number of Pages including this cover sheet: 6

RESEARCH/

SIMULTANEOUS AMPLIFICATION AND DETECTION OF SPECIFIC DNA SEQUENCES

Russell Higuchi*, Gavin Dollinger[1], P. Sean Walsh and Robert Griffith

Roche Molecular Systems, Inc., 1400 53rd St., Emeryville, CA 94608. [1]Chiron Corporation, 1400 53rd St., Emeryville, CA 94608. *Corresponding author.

We have enhanced the polymerase chain reaction (PCR) such that specific DNA sequences can be detected without opening the reaction tube. This enhancement requires the addition of ethidium bromide (EtBr) to a PCR. Since the fluorescence of EtBr increases in the presence of double-stranded (ds) DNA an increase in fluorescence in such a PCR indicates a positive amplification, which can be easily monitored externally. In fact, amplification can be continuously monitored in order to follow its progress. The ability to simultaneously amplify specific DNA sequences and detect the product of the amplification both simplifies and improves PCR and may facilitate its automation and more widespread use in the clinic or in other situations requiring high sample through-put.

Although the potential benefits of PCR[1] to clinical diagnostics are well known[2,3], it is still not widely used in this setting, even though it is four years since thermostable DNA polymerases[4] made PCR practical. Some of the reasons for its slow acceptance are high cost, lack of automation of pre- and post-PCR processing steps, and false positive results from carryover-contamination. The first two points are related in that labor is the largest contributor to cost at the present stage of PCR development. Most current assays require some form of "downstream" processing once thermocycling is done in order to determine whether the target DNA sequence was present and has amplified. These include DNA hybridization[5,6], gel electrophoresis with or without use of restriction digestion[7,8], HPLC[9], or capillary electrophoresis[10]. These methods are labor-intense, have low throughput, and are difficult to automate. The third point is also closely related to downstream processing. The handling of the PCR product in these downstream processes increases the chances that amplified DNA will spread through the typing lab, resulting in a risk of

"carryover" false positives in subsequent testing[11].

These downstream processing steps would be eliminated if specific amplification and detection of amplified DNA took place simultaneously within an unopened reaction vessel. Assays in which such different processes take place without the need to separate reaction components have been termed "homogeneous". No truly homogeneous PCR assay has been demonstrated to date, although progress towards this end has been reported. Chehab, et al.[12], developed a PCR product detection scheme using fluorescent primers that resulted in a fluorescent PCR product. Allele-specific primers, each with different fluorescent tags, were used to indicate the genotype of the DNA. However, the unincorporated primers must still be removed in a downstream process in order to visualize the result. Recently, Holland, et al.[13], developed an assay in which the endogenous 5' exonuclease assay of Taq DNA polymerase was exploited to cleave a labeled oligonucleotide probe. The probe would only cleave if PCR amplification had produced its complementary sequence. In order to detect the cleavage products, however, a subsequent process is again needed.

We have developed a truly homogeneous assay for PCR and PCR product detection based upon the greatly increased fluorescence that ethidium bromide and other DNA binding dyes exhibit when they are bound to ds-DNA[14–16]. As outlined in Figure 1, a prototypic PCR
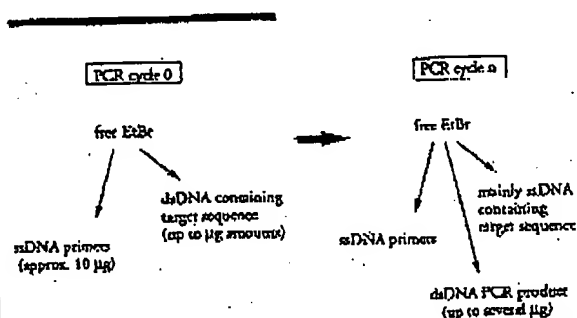

FIGURE 1 Principle of simultaneous amplification and detection of PCR product. The components of a PCR containing EtBr that are fluorescent are listed—EtBr itself, EtBr bound to either ssDNA or dsDNA. There is a large fluorescence enhancement when EtBr is bound to DNA and binding is greatly enhanced when DNA is double-stranded. After sufficient (n) cycles of PCR, the net increase in dsDNA results in additional EtBr binding, and a net increase in total fluorescence.
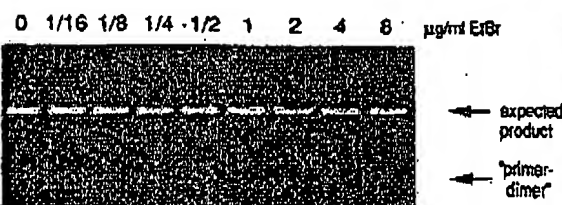
0   1/16 1/8 1/4 1/2   1   2   4   8   µg/ml EtBr

→ expected product

→ 'primer-dimer'

FIGURE 2 Gel electrophoresis of PCR amplification products of the human, nuclear gene, HLA DQα, made in the presence of increasing amounts of EtBr (up to 8 µg/ml). The presence of EtBr has no obvious effect on the yield or specificity of amplification.
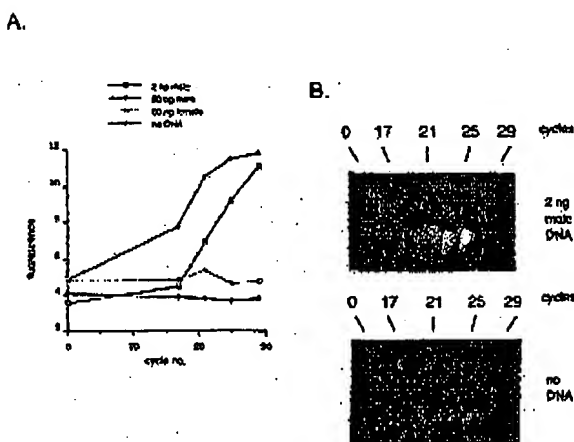
A.

B.

0   17   21   25   29   cycles

2 ng male DNA

0   17   21   25   29   cycles

no DNA

FIGURE 3 (A) Fluorescence measurements from PCRs that contain 0.5 µg/ml EtBr and that are specific for Y-chromosome repeat sequences. Five replicate PCRs were begun containing each of the DNAs specified. At each indicated cycle, one of the five replicate PCRs for each DNA was removed from thermocycling and its fluorescence measured. Units of fluorescence are arbitrary. (B) UV photography of PCR tubes (0.5 ml Eppendorf-style, polypropylene micro-centrifuge tubes) containing reactions, those starting from 2 ng male DNA and control reactions without any DNA, from (A).

begins with primers that are single-stranded DNA (ssDNA), dNTPs, and DNA polymerase. An amount of dsDNA containing the target sequence (target DNA) is also typically present. This amount can vary, depending on the application, from single-cell amounts of DNA[17] to micrograms per PCR[18]. If EtBr is present, the reagents that will fluoresce, in order of increasing fluorescence, are free EtBr itself, and EtBr bound to the single-stranded DNA primers and to the double-stranded target DNA (by its intercalation between the stacked bases of the DNA double-helix). After the first denaturation cycle, target DNA will be largely single-stranded. After a PCR is completed, the most significant change is the increase in the amount of dsDNA (the PCR product itself) of up to several micrograms. Formerly free EtBr is bound to the additional dsDNA, resulting in an increase in fluorescence. There is also some decrease in the amount of ssDNA primer, but because the binding of EtBr to ssDNA is much less than to dsDNA, the effect of this change on the total fluorescence of the sample is small. The fluorescence increase can be measured by directing excitation illumination through the walls of the amplification vessel

before and after, or even continuously during, thermocycling.

RESULTS

PCR in the presence of EtBr. In order to assess the affect of EtBr in PCR, amplifications of the human HLA DQα gene[19] were performed with the dye present at concentrations from 0.06 to 8.0 µg/ml (a typical concentration of EtBr used in staining of nucleic acids following gel electrophoresis is 0.5 µg/ml). As shown in Figure 2, gel electrophoresis revealed little or no difference in the yield or quality of the amplification product whether EtBr was absent or present at any of these concentrations, indicating that EtBr does not inhibit PCR.

Detection of human Y-chromosome specific sequences. Sequence-specific, fluorescence enhancement of EtBr as a result of PCR was demonstrated in a series of amplifications containing 0.5 µg/ml EtBr and primers specific to repeat DNA sequences found on the human Y-chromosome[20]. These PCRs initially contained either 60 ng male, 60 ng female, 2 ng male human or no DNA. Five replicate PCRs were begun for each DNA. After 0, 17, 21, 24 and 29 cycles of thermocycling, a PCR for each DNA was removed from the thermocycler, and its fluorescence measured in a spectrofluorometer and plotted vs. amplification cycle number (Fig. 3A). The shape of this curve reflects the fact that by the time an increase in fluorescence can be detected, the increase in DNA is becoming linear and not exponential with cycle number. As shown, the fluorescence increased about three-fold over the background fluorescence for the PCRs containing human male DNA, but did not significantly increase for negative control PCRs, which contained either no DNA or human female DNA. The more male DNA present to begin with—60 ng versus 2 ng—the fewer cycles were needed to give a detectable increase in fluorescence. Gel electrophoresis on the products of these amplifications showed that DNA fragments of the expected size were made in the male DNA containing reactions and that little DNA synthesis took place in the control samples.

In addition, the increase in fluorescence was visualized by simply laying the completed, unopened PCRs on a UV transilluminator and photographing them through a red filter. This is shown in figure 3B for the reactions that began with 2 ng male DNA and those with no DNA.

Detection of specific alleles of the human β-globin gene. In order to demonstrate that this approach has adequate specificity to allow genetic screening, a detection of the sickle-cell anemia mutation was performed. Figure 4 shows the fluorescence from completed amplifications containing EtBr (0.5 µg/ml) as detected by photography of the reaction tubes on a UV transilluminator. These reactions were performed using primers specific for either the wild-type or sickle-cell mutation of the human β-globin gene[21]. The specificity for each allele is imparted by placing the sickle-mutation site at the terminal 3' nucleotide of one primer. By using an appropriate primer annealing temperature, primer extension—and thus amplification—can take place only if the 3' nucleotide of the primer is complementary to the β-globin allele present[21,22].

Each pair of amplifications shown in Figure 4 consists of a reaction with either the wild-type allele specific (left tube) or sickle-allele specific (right tube) primers. Three different DNAs were typed: DNA from a homozygous, wild-type β-globin individual (AA); from a heterozygous sickle β-globin individual (AS); and from a homozygous sickle β-globin individual (SS). Each DNA (50 ng genomic DNA to start each PCR) was analyzed in triplicate (3 pairs

of reactions each). The DNA type was reflected in the relative fluorescence intensities in each pair of completed amplifications. There was a significant increase in fluorescence only where a β-globin allele DNA matched the primer set. When measured on a spectrofluorometer (data not shown), this fluorescence was about three times that present in a PCR where both β-globin alleles were mismatched to the primer set. Gel electrophoresis (not shown) established that this increase in fluorescence was due to the synthesis of nearly a microgram of a DNA fragment of the expected size for β-globin. There was little synthesis of dsDNA in reactions in which the allele-specific primer was mismatched to both alleles.

Continuous monitoring of a PCR. Using a fiber optic device, it is possible to direct excitation illumination from a spectrofluorometer to a PCR undergoing thermocycling and to return its fluorescence to the spectrofluorometer. The fluorescence readout of such an arrangement, directed at an EtBr-containing amplification of Y-chromosome specific sequences from 25 ng of human male DNA, is shown in Figure 5. The readout from a control PCR with no target DNA is also shown. Thirty cycles of PCR were monitored for each.

The fluorescence trace as a function of time clearly shows the effect of the thermocycling. Fluorescence intensity rises and falls inversely with temperature. The fluorescence intensity is minimum at the denaturation temperature (94°C) and maximum at the annealing/extension temperature (50°C). In the negative-control PCR, these fluorescence maxima and minima do not change significantly over the thirty thermocycles, indicating that there is little dsDNA synthesis without the appropriate target DNA, and there is little if any bleaching of EtBr during the continuous illumination of the sample.

In the PCR containing male DNA, the fluorescence maxima at the annealing/extension temperature begin to increase at about 4000 seconds of thermocycling, and continue to increase with time, indicating that dsDNA is being produced at a detectable level. Note that the fluorescence minima at the denaturation temperature do not significantly increase, presumably because at this temperature there is no dsDNA for EtBr to bind. Thus the course of the amplification is followed by tracking the fluorescence increase at the annealing temperature. Analysis of the products of these two amplifications by gel electrophoresis showed a DNA fragment of the expected size for the male DNA containing sample and no detectable DNA synthesis for the control sample.

DISCUSSION

Downstream processes such as hybridization to a sequence-specific probe can enhance the specificity of DNA detection by PCR. The elimination of these processes means that the specificity of this homogeneous assay depends solely on that of PCR. In the case of sickle-cell disease, we have shown that PCR alone has sufficient DNA sequence specificity to permit genetic screening. Using appropriate amplification conditions, there is little non-specific production of dsDNA in the absence of the appropriate target allele.

The specificity required to detect pathogens can be more or less than that required to do genetic screening, depending on the number of pathogens in the sample and the amount of other DNA that must be taken with the sample. A difficult target is HIV, which requires detection of a viral genome that can be at the level of a few copies per thousands of host cells[6]. Compared with genetic screening, which is performed on cells containing at least one copy of the target sequence, HIV detection requires both more specificity and the input of more total
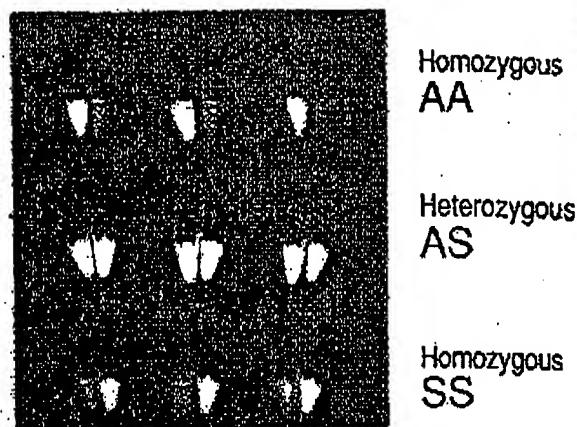

Homozygous
AA

Heterozygous
AS

Homozygous
SS

FIGURE 4 UV photography of PCR tubes containing amplifications using EtBr that are specific to wild-type (A) or sickle (S) alleles of the human β-globin gene. The left of each pair of tubes contains allele-specific primers to the wild-type alleles, the right tube primers to the sickle allele. The photograph was taken after 30 cycles of PCR, and the input DNAs and the alleles they contain are indicated. Fifty ng of DNA was used to begin PCR. Typing was done in triplicate (3 pairs of PCRs) for each input DNA.
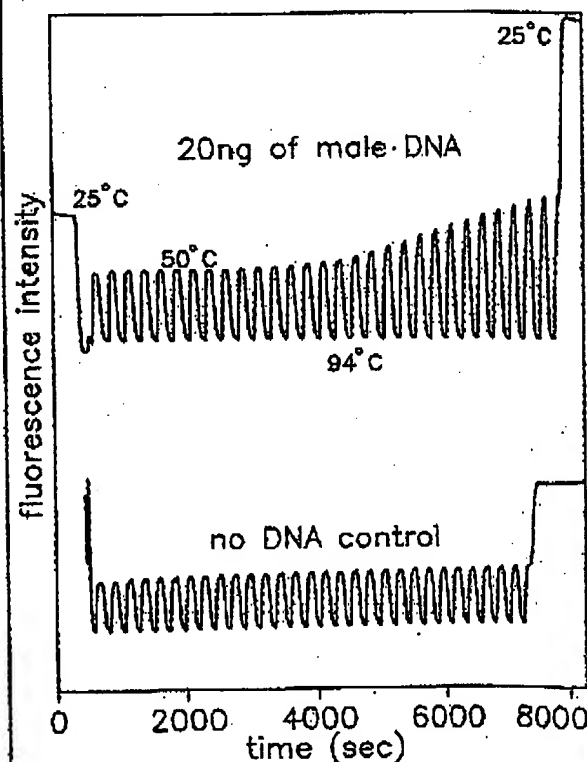

FIGURE 5 Continuous, real-time monitoring of a PCR. A fiber optic was used to carry excitation light to a PCR in progress and also emitted light back to a fluorometer (see Experimental Protocol). Amplification using human male-DNA specific primers in a PCR starting with 20 ng of human male DNA (top), or in a control PCR without DNA (bottom), were monitored. Thirty cycles of PCR were followed for each. The temperature cycled between 94°C (denaturation) and 50°C (annealing and extension). Note in the male DNA PCR, the cycle (time) dependent increase in fluorescence at the annealing/extension temperature.

DNA—up to microgram amounts—in order to have sufficient numbers of target sequences. This large amount of starting DNA in an amplification significantly increases the background fluorescence over which any additional fluorescence produced by PCR must be detected. An additional complication that occurs with targets in low copy-number is the formation of the "primer-dimer" artifact. This is the result of the extension of one primer using the other primer as a template. Although this occurs infrequently, once it occurs the extension product is a substrate for PCR amplification, and can compete with true PCR targets if those targets are rare. The primer-dimer product is of course dsDNA and thus is a potential source of false signal in this homogeneous assay.

To increase PCR specificity and reduce the effect of primer-dimer amplification, we are investigating a number of approaches, including the use of nested-primer amplifications that take place in a single tube[8], and the "hot-start", in which nonspecific amplification is reduced by raising the temperature of the reaction before DNA synthesis begins[23]. Preliminary results using these approaches suggest that primer-dimer is effectively reduced and it is possible to detect the increase in EtBr fluorescence in a PCR instigated by a single HIV genome in a background of 10^5 cells. With larger numbers of cells, the background fluorescence contributed by genomic DNA becomes problematic. To reduce this background, it may be possible to use sequence-specific DNA-binding dyes that can be made to preferentially bind PCR product over genomic DNA by incorporating the dye-binding DNA sequence into the PCR product through a 5' "add-on" to the oligonucleotide primer[24].

We have shown that the detection of fluorescence generated by an EtBr-containing PCR is straightforward, both once PCR is completed and continuously during thermocycling. The ease with which automation of specific DNA detection can be accomplished is the most promising aspect of this assay. The fluorescence analysis of completed PCRs is already possible with existing instrumentation in 96-well format[25]. In this format, the fluorescence in each PCR can be quantitated before, after, and even at selected points during thermocycling by moving the rack of PCRs to a 96-microwell plate fluorescence reader[26].

The instrumentation necessary to continuously monitor multiple PCRs simultaneously is also simple in principle. A direct extension of the apparatus used here is to have multiple fiberoptics transmit the excitation light and fluorescent emissions to and from multiple PCRs. The ability to monitor multiple PCRs continuously may allow quantitation of target DNA copy number. Figure 5 shows that the larger the amount of starting target DNA, the sooner during PCR a fluorescence increase is detected. Preliminary experiments (Higuchi and Dollinger, manuscript in preparation) with continuous monitoring have shown a sensitivity to two-fold differences in initial target DNA concentration.

Conversely, if the number of target molecules is known—as it can be in genetic screening—continuous monitoring may provide a means of detecting false positive and false negative results. With a known number of target molecules, a true positive would exhibit detectable fluorescence by a predictable number of cycles of PCR. Increases in fluorescence detected before or after that cycle would indicate potential artifacts. False negative results due to, for example, inhibition of DNA polymerase, may be detected by including within each PCR an inefficiently amplifying marker. This marker results in a fluorescence increase only after a large number of cycles—many more than are necessary to detect a true

positive. If a sample fails to have a fluorescence increase after this many cycles, inhibition may be suspected. Since, in this assay, conclusions are drawn based on the presence or absence of fluorescence signal alone, such controls may be important. In any event, before any test based on this principle is ready for the clinic, an assessment of its false positive/false negative rates will need to be obtained using a large number of known samples.

In summary, the inclusion in PCR of dyes whose fluorescence is enhanced upon binding dsDNA makes it possible to detect specific DNA amplification from outside the PCR tube. In the future, instruments based upon this principle may facilitate the more widespread use of PCR in applications that demand the high throughput of samples.

EXPERIMENTAL PROTOCOL

Human HLA-DQα gene amplifications containing EtBr. PCRs were set up in 100 µl volumes containing 10 mM Tris-HCl, pH 8.3; 50 mM KCl; 4 mM MgCl₂; 2.5 units of *Taq* DNA polymerase (Perkin-Elmer Cetus, Norwalk, CT); 20 pmole each of human HLA-DQα gene specific oligonucleotide primers (GH26 and GH27[19] and approximately 10^7 copies of DQα PCR product diluted from a previous reaction. Ethidium bromide (EtBr; Sigma) was used at the concentrations indicated in Figure 2. Thermocycling proceeded for 20 cycles in a model 480 thermocycler (Perkin-Elmer Cetus, Norwalk, CT) using a "step-cycle" program of 94°C for 1 min. denaturation and 60°C for 30 sec. annealing and 72°C for 30 sec. extension.

Y-chromosome specific PCR. PCRs (100 µl total reaction volume) containing 0.5 µg/ml EtBr were prepared as described for HLA-DQα, except with different primers and target DNAs. These PCRs contained 15 pmole each male DNA-specific primers Y1.1 and Y1.2[20], and either 60 ng male, 60 ng female, 2 ng male, or no human DNA. Thermocycling was 94°C for 1 min. and 60°C for 1 min using a "step-cycle" program. The number of cycles for a sample were as indicated in Figure 3. Fluorescence measurement is described below.

Allele-specific, human β-globin gene PCR. Amplifications of 100 µl volume using 0.5 µg/ml of EtBr were prepared as described for HLA-DQα above except with different primers and target DNAs. These PCRs contained either primer pair HGP2/Hβ14A (wild-type globin specific primers) or HGP2/Hβ14S (sickle-globin specific primers) at 10 pmole each primer per PCR. These primers were developed by Wu et al[21]. Three different target DNAs were used in separate amplifications—50 ng each of human DNA that was homozygous for the sickle trait (SS), DNA that was heterozygous for the sickle trait (AS), or DNA that was homozygous for the w.t. globin (AA). Thermocycling was for 30 cycles at 94°C for 1 min. and 55°C for 1 min. using a "step-cycle" program. An annealing temperature of 55°C had been shown by Wu et al[21] to provide allele-specific amplification. Completed PCRs were photographed through a red filter (Wratten 23A) after placing the reaction tubes atop a model TM-36 transilluminator (UV-products San Gabriel, CA).

Fluorescence measurement. Fluorescence measurements were made on PCRs containing EtBr in a Fluorolog-2 fluorometer (SPEX, Edison, NJ). Excitation was at the 500 nm band with about 2 nm bandwidth with a GG 435 nm cut-off filter (Melles Griot, Inc., Irvine, CA) to exclude second-order light. Emitted light was detected at 570 nm with a bandwidth of about 7 nm. An OG 530 nm cut-off filter was used to remove the excitation light.

Continuous fluorescence monitoring of PCR. Continuous monitoring of a PCR in progress was accomplished using the spectrofluorometer and settings described above as well as a fiberoptic accessory (SPEX cat. no. 1950) to both send excitation light to, and receive emitted light from, a PCR placed in a well of a model 480 thermocycler (Perkin-Elmer Cetus). The probe end of the fiberoptic cable was attached with "5 minute-epoxy" to the open top of a PCR tube (a 0.5 ml polypropylene centrifuge tube with its cap removed) effectively sealing it. The exposed top of the PCR tube and the end of the fiberoptic cable were shielded from room light and the room lights were kept dimmed during each run. The monitored PCR was an amplification of Y-chromosome-specific repeat sequences as described above, except using an annealing/extension temperature of 50°C. The reaction was covered with mineral oil (2 drops) to prevent evaporation. Thermocycling and fluorescence measurement were started simultaneously. A time-base scan with a 10 second integration time

was used and the emission signal was ratioed to the excitation signal to control for changes in light-source intensity. Data were collected using the dm3000f, version 2.5 (SPEX) data system.

Acknowledgments

We thank Bob Jones for help with the spectrofluorimetric measurements and Heatherbell Fong for editing this manuscript.
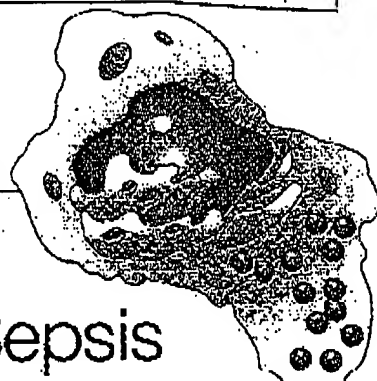
References

1. Mullis, K., Faloona, F., Scharf, S., Saiki, R., Horn, G. and Erlich, H. 1986. Specific enzymatic amplification of DNA in vitro: The polymerase chain reaction. CSHSQB 51:263–273.
2. White, T. J., Arnheim, N. and Erlich, H. A. 1989. The polymerase chain reaction. Trends Genet. 5:185–189.
3. Erlich, H. A., Gelfand, D. and Sninsky, J. J. 1991. Recent advances in the polymerase chain reaction. Science 252:1643–1651.
4. Saiki, R. K., Gelfand, D. H., Stoffel, S., Scharf, S. J., Higuchi, R., Horn, G. T., Mullis, K. B. and Erlich, H. A. 1988. Primer-directed enzymatic amplification of DNA with a thermostable DNA polymerase. Science 239:487–491.
5. Saiki, R. K., Walsh, P. S., Levenson, C. H. and Erlich, H. A. 1989. Genetic analysis of amplified DNA with immobilized sequence-specific oligonucleotide probes. Proc. Natl. Acad. Sci. USA 86:6230–6234.
6. Kwok, S. Y., Mack, D. H., Mullis, K. B., Poiesz, B. J., Ehrlich, G. D., Blair, D. and Friedman-Kien, A. S. 1987. Identification of human immunodeficiency virus sequences by using in vitro enzymatic amplification and oligomer cleavage detection. J. Virol. 61:1690–1694.
7. Chehab, F. F., Doherty, M., Cai, S. P., Kan, Y. W., Cooper, S. and Rubin, E. M. 1987. Detection of sickle cell anemia and thalassemias. Nature 329:293–294.
8. Horn, G. T., Richards, B. and Klinger, K. W. 1989. Amplification of a highly polymorphic VNTR segment by the polymerase chain reaction. Nuc. Acids Res. 16:2140.
9. Katz, E. D. and Dong, M. W. 1990. Rapid analysis and purification of polymerase chain reaction products by high-performance liquid chromatography. Biotechniques 8:546–555.
10. Heiger, D. N., Cohen, A. S. and Karger, B. L. 1990. Separation of DNA restriction fragments by high performance capillary electrophoresis with low and zero crosslinked polyacrylamide using continuous and pulsed electric fields. J. Chromatogr. 516:33–48.
11. Kwok, S. Y. and Higuchi, R. G. 1989. Avoiding false positives with PCR. Nature 339;237–238.
12. Chehab, F. F. and Kan, Y. W. 1989. Detection of specific DNA sequences by fluorescence amplification: a color complementation assay. Proc. Natl. Acad. Sci. USA 86:9178–9182.
13. Holland, P. M., Abramson, R. D., Watson, R. and Gelfand, D. H.
14. 1991. Detection of specific polymerase chain reaction product by utilizing the 5' to 3' exonuclease activity of Thermus aquaticus DNA polymerase. Proc. Natl. Acad. Sci. USA 88:7276–7280.
14. Markovits, J., Roques, B. P. and Le Pecq, J. B. 1979. Ethidium dimer: a new reagent for the fluorimetric determination of nucleic acids. Anal. Biochem. 94:259–264.
15. Kapuscinski, J. and Szer, W. 1979. Interactions of 4',6-diamidine-2-phenylindole with synthetic polynucleotides. Nuc. Acids Res. 6:3519–3534.
16. Searle, M. S. and Embrey, K. J. 1990. Sequence-specific interaction of Hoechst 33258 with the minor groove of an adenine-tract DNA duplex studied in solution by ¹H NMR spectroscopy. Nuc. Acids Res. 18:3753–3762.
17. Li, H. H., Gyllensten, U. B., Cui, X. F., Saiki, R. K., Erlich, H. A. and Arnheim, N. 1988. Amplification and analysis of DNA sequences in single human sperm and diploid cells. Nature 335:414–417.
18. Abbott, M. A., Poiesz, B. J., Byrne, B. C., Kwok, S. Y., Sninsky, J. J. and Erlich, H. A. 1988. Enzymatic gene amplification: qualitative and quantitative methods for detecting proviral DNA amplified in vitro. J. Infect. Dis. 158:1158.
19. Saiki, R. K., Bugawan, T. L., Horn, G. T., Mullis, K. B. and Erlich, H. A. 1986. Analysis of enzymatically amplified β-globin and HLA-DQα DNA with allele-specific oligonucleotide probes. Nature 324:163–166.
20. Kogan, S. C., Doherty, M. and Gitschier, J. 1987. An improved method for prenatal diagnosis of genetic disease by analysis of amplified DNA sequences. N. Engl. J. Med. 317:985–990.
21. Wu, D. Y., Ugozzoli, L., Pal, B. K. and Wallace, R. B. 1989. Allele-specific enzymatic amplification of β-globin genomic DNA for diagnosis of sickle cell anemia. Proc. Natl. Acad. Sci. USA 86:2757–2760.
22. Kwok, S., Kellogg, D. E., McKinney, N., Spasic, D., Goda, L., Levenson, C. and Sninsky, J. J. 1990. Effects of primer-template mismatches on the polymerase chain reaction: Human immunodeficiency virus type 1 model studies. Nuc. Acids Res. 18:999–1005.
23. Chou, Q., Russell, M., Birch, D., Raymond, J. and Bloch, W. 1992. Prevention of pre-PCR mis-priming and primer dimerization improves low-copy-number amplifications: Submitted.
24. Higuchi, R. 1989. Using PCR to engineer DNA. p. 61–70. In: PCR Technology. H. A. Erlich (Ed.). Stockton Press, New York, N.Y.
25. Haff, L., Atwood, J. G., DiCesare, J., Katz, E., Picozza, E., Williams, J. F. and Woudenberg, T. 1991. A high-performance system for automation of the polymerase chain reaction. Biotechniques 10:102–103, 106–112.
26. Tumosa, N. and Kahm, L. 1989. Fluorescent EIA screening of monoclonal antibodies to cell surface antigens. J. Immun. Meth. 116:59–63.

IIIIResearch

Oligonucleotides with Fluorescent Dyes at Opposite Ends Provide a Quenched Probe System Useful for Detecting PCR Product and Nucleic Acid Hybridization

Kenneth J. Livak, Susan J.A. Flood, Jeffrey Marmaro, William Giusti, and Karin Deetz

Perkin-Elmer, Applied Biosystems Division, Foster City, California 94404

The 5' nuclease PCR assay detects the accumulation of specific PCR product by hybridization and cleavage of a double-labeled fluorogenic probe during the amplification reaction. The probe is an oligonucleotide with both a reporter fluorescent dye and a quencher dye attached. An increase in reporter fluorescence intensity indicates that the probe has hybridized to the target PCR product and has been cleaved by the 5'→3' nucleolytic activity of *Taq* DNA polymerase. In this study, probes with the quencher dye attached to an internal nucleotide were compared with probes with the quencher dye attached to the 3'-end nucleotide. In all cases, the reporter dye was attached to the 5' end. All intact probes showed quenching of the reporter fluorescence. In general, probes with the quencher dye attached to the 3'-end nucleotide exhibited a larger signal in the 5' nuclease PCR assay than the internally labeled probes. It is proposed that the larger signal is caused by increased likelihood of cleavage by *Taq* DNA polymerase when the probe is hybridized to a template strand during PCR. Probes with the quencher dye attached to the 3'-end nucleotide also exhibited an increase in reporter fluorescence intensity when hybridized to a complementary strand. Thus, oligonucleotides with reporter and quencher dyes attached at opposite ends can be used as homogeneous hybridization probes.

A homogeneous assay for detecting the accumulation of specific PCR product that uses a double-labeled fluorogenic probe was described by Lee et al.[1] The assay exploits the 5'→3' nucleolytic activity of *Taq* DNA polymerase[2,3] and is diagramed in Figure 1. The fluorogenic probe consists of an oligonucleotide with a reporter fluorescent dye, such as a fluorescein, attached to the 5' end; and a quencher dye, such as a rhodamine, attached internally. When the fluorescein is excited by irradiation, its fluorescent emission will be quenched if the rhodamine is close enough to be excited through the process of fluorescence energy transfer (FET).[4,5] During PCR, if the probe is hybridized to a template strand, *Taq* DNA polymerase will cleave the probe because of its inherent 5'→3' nucleolytic activity. If the cleavage occurs between the fluorescein and rhodamine dyes, it causes an increase in fluorescein fluorescence intensity because the fluorescein is no longer quenched. The increase in fluorescein fluorescence intensity indicates that the probe-specific PCR product has been generated. Thus, FET between a reporter dye and a quencher dye is critical to the performance of the probe in the 5' nuclease PCR assay.

Quenching is completely dependent on the physical proximity of the two dyes.[6] Because of this, it has been assumed that the quencher dye must be attached near the 5' end. Surprisingly, we have found that attaching a rhodamine dye at the 3' end of a probe still provides adequate quenching for the probe to perform in the 5' nuclease

PCR assay. Furthermore, cleavage of this type of probe is not required to achieve some reduction in quenching. Oligonucleotides with a reporter dye on the 5' end and a quencher dye on the 3' end exhibit a much higher reporter fluorescence when double-stranded as compared with single-stranded. This should make it possible to use this type of double-labeled probe for homogeneous detection of nucleic acid hybridization.

## MATERIALS AND METHODS

Oligonucleotides

Table 1 shows the nucleotide sequence of the oligonucleotides used in this study. Linker arm nucleotide (LAN) phosphoramidite was obtained from Glen Research. The standard DNA phosphoramidites, 6-carboxyfluorescein (6-FAM) phosphoramidite, 6-carboxytetramethylrhodamine succinimidyl ester (TAMRA NHS ester), and Phosphalink for attaching a 3'-blocking phosphate, were obtained from Perkin-Elmer, Applied Biosystems Division. Oligonucleotide synthesis was performed using an ABI model 394 DNA synthesizer (Applied Biosystems). Primer and complement oligonucleotides were purified using Oligo Purification Cartridges (Applied Biosystems). Double-labeled probes were synthesized with 6-FAM-labeled phosphoramidite at the 5' end, LAN replacing one of the T's in the sequence, and Phosphalink at the 3' end. Following deprotection and ethanol precipitation, TAMRA NHS ester was coupled to the LAN-containing oligonucleotide in 250
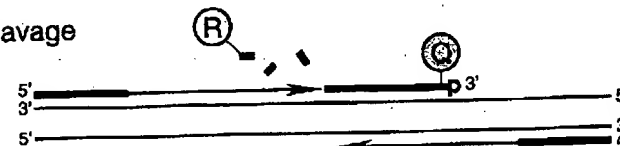
Research

Polymerization
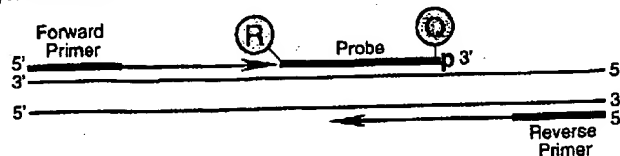
Strand displacement
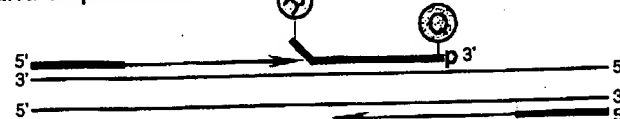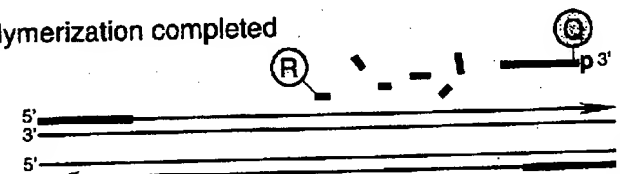
Cleavage

Polymerization completed

FIGURE 1 Diagram of 5' nuclease assay. Stepwise representation of the 5' → 3' nucleolytic activity of *Taq* DNA polymerase acting on a fluorogenic probe during one extension phase of PCR.

mM Na-bicarbonate buffer (pH 9.0) at room temperature. Unreacted dye was removed by passage over a PD-10 Sephadex column. Finally, the double-labeled probe was purified by preparative high-performance liquid chromatography (HPLC) using an Aquapore C_8 220×4.6-mm column with 7-μm particle size. The column was developed with a 24-min linear gradient of 8–20% acetonitrile in 0.1 M TEAA (triethylamine acetate). Probes are named by designating the sequence from Table 1 and the position of the LAN–TAMRA moiety. For example, probe A1-7 has sequence A1 with LAN–TAMRA at nucleotide position 7 from the 5' end.

PCR Systems

All PCR amplifications were performed in the Perkin-Elmer GeneAmp PCR System 9600 using 50-μl reactions that contained 10 mM Tris-HCl (pH 8.3), 50 mM KCl, 200 μM dATP, 200 μM dCTP, 200 μM dGTP, 400 μM dUTP, 0.5 unit of AmpErase uracil N-glycosylase (Perkin-Elmer), and 1.25 unit of AmpliTaq DNA polymerase (Perkin-Elmer). A 295-bp segment from exon 3 of the human β-actin

gene (nucleotides 2141–2435 in the sequence of Nakajima-Iijima et al.)[7] was amplified using primers AFP and ARP (Table 1), which are modified slightly from those of du Breuil et al.[8] Actin amplification reactions contained 4 mM $MgCl_2$, 20 ng of human genomic DNA, 50 nM A1 or A3 probe, and 300 nM each

primer. The thermal regimen was 50°C (2 min), 95°C (10 min), 40 cycles of 95°C (20 sec), 60°C (1 min), and hold at 72°C. A 515-bp segment was amplified from a plasmid that consists of a segment of λ DNA (nucleotides 32,220–32,747) inserted in the *Sma*I site of vector pUC119. These reactions contained 3.5 mM $MgCl_2$, 1 ng of plasmid DNA, 50 nM P2 or P5 probe, 200 nM primer F119, and 200 nM primer R119. The thermal regimen was 50°C (2 min), 95°C (10 min), 25 cycles of 95°C (20 sec), 57°C (1 min), and hold at 72°C.

Fluorescence Detection

For each amplification reaction, a 40-μl aliquot of a sample was transferred to an individual well of a white, 96-well microtiter plate (Perkin-Elmer). Fluorescence was measured on the Perkin-Elmer Taq-Man LS-50B System, which consists of a luminescence spectrometer with plate reader assembly, a 485-nm excitation filter, and a 515-nm emission filter. Excitation was at 488 nm using a 5-nm slit width. Emission was measured at 518 nm for 6-FAM (the reporter or R value) and 582 nm for TAMRA (the quencher or Q value) using a 10-nm slit width. To determine the increase in reporter emission that is caused by cleavage of the probe during PCR, three normalizations are applied to the raw emission data. First, emission intensity of a buffer blank is subtracted for each wavelength. Second, emission intensity of the reporter is

TABLE 1 Sequences of Oligonucleotides

Name	Type	Sequence
F119	primer	ACCCACAGGAACTGATCACCACTC
R119	primer	ATGTCGCGTTCCGGCTGACGTTCTGC
P2	probe	TCGCATTACTGATCGTTGCCAACCAGTp
P2C	complement	GTACTGGTTGGCAACGATCAGTAATGCGATG
P5	probe	CGGATTTGCTGGTATCTATGACAAGGATp
P5C	complement	TTCATCCTTGTCATAGATACCAGCAAATCCG
AFP	primer	TCACCCACACTGTGCCCATCTACGA
ARP	primer	CAGCGGAACCGCTCATTGCCAATGG
A1	probe	ATGCCCTCCCCCATGCCATCCTGCGTp
A1C	complement	AGACGCAGGATGGCATGGGGGAGGGCATAC
A3	probe	CGCCCTGGACTTCGAGCAAGAGATp
A3C	complement	CCATCTCTTGCTCGAAGTCCAGGGCGAC

For each oligonucleotide used in this study, the nucleic acid sequence is given, written in the 5' → 3' direction. There are three types of oligonucleotides: PCR primer, fluorogenic probe used in the 5' nuclease assay, and complement used to hybridize to the corresponding probe. For the probes, the underlined base indicates a position where LAN with TAMRA attached was substituted for a T. (p) The presence of a 3' phosphate on each probe.

358 PCR Methods and Applications

PAGE 3/7 * RCVD AT 10/24/2005 5:55:20 PM [Pacific Daylight Time] * SVR:SVCS01/0 * DNIS:6034 * CSID:(613) 991-5695 * DURATION (mm-ss):05-46

IIIIIResearch

A1-2	RAQGCCCTCCCCCATGCCATCCTGCGTp
A1-7	RATGCCCQCCCCCATGCCATCCTGCGTp
A1-14	RATGCCCTCCCCCAQGCCATCCTGCGTp
A1-19	RATGCCCTCCCCCATGCCAQCCTGCGTp
A1-22	RATGCCCTCCCCCATGCCATCCQGCGTp
A1-26	RATGCCCTCCCCCATGCCATCCTGCGQp

Probe	518 nm		582 nm		RQ⁻	RQ⁺	ΔRQ
	no temp.	+ temp.	no temp.	+ temp.			
A1-2	25.5 ± 2.1	32.7 ± 1.9	38.2 ± 3.0	38.2 ± 2.0	0.67 ± 0.01	0.86 ± 0.06	0.19 ± 0.06
A1-7	53.5 ± 4.3	395.1 ± 21.4	108.5 ± 6.3	110.3 ± 5.3	0.49 ± 0.03	3.58 ± 0.17	3.09 ± 0.18
A1-14	127.0 ± 4.9	403.5 ± 19.1	109.7 ± 5.3	93.1 ± 6.3	1.16 ± 0.02	4.34 ± 0.15	3.18 ± 0.15
A1-19	187.5 ± 17.9	422.7 ± 7.7	70.3 ± 7.4	73.0 ± 2.8	2.67 ± 0.05	5.80 ± 0.15	3.13 ± 0.16
A1-22	224.6 ± 9.4	482.2 ± 43.6	100.0 ± 4.0	96.2 ± 9.6	2.25 ± 0.03	5.02 ± 0.11	2.77 ± 0.12
A1-26	160.2 ± 8.9	454.1 ± 18.4	93.1 ± 5.4	90.7 ± 3.2	1.72 ± 0.02	5.01 ± 0.08	3.29 ± 0.08

FIGURE 2 Results of 5′ nuclease assay comparing β-actin probes with TAMRA at different nucleotide positions. As described in Materials and Methods, PCR amplifications containing the indicated probes were performed, and the fluorescence emission was measured at 518 and 582 nm. Reported values are the average ± 1 s.d. for six reactions run without added template (no temp.) and six reactions run with template (+ temp.). The RQ ratio was calculated for each individual reaction and averaged to give the reported RQ⁻ and RQ⁺ values.

divided by the emission intensity of the quencher to give an RQ ratio for each reaction tube. This normalizes for well-to-well variations in probe concentration and fluorescence measurement. Finally, ΔRQ is calculated by subtracting the RQ value of the no-template control (RQ⁻) from the RQ value for the complete reaction including template (RQ⁺).

RESULTS

A series of probes with increasing distances between the fluorescein reporter and rhodamine quencher were tested to investigate the minimum and maximum spacing that would give an acceptable performance in the 5′ nuclease PCR assay. These probes hybridize to a target sequence in the human β-actin gene. Figure 2 shows the results of an experiment in which these probes were included in PCR that amplified a segment of the β-actin gene containing the target sequence. Performance in the 5′ nuclease PCR assay is monitored by the magnitude of ΔRQ, which is a measure of the increase in reporter fluorescence caused by PCR amplification of the probe target. Probe A1-2 has a ΔRQ value that is close to zero, indicating that the probe was not cleaved appreciably during the amplification reaction. This suggests that with the quencher dye on the second nucleotide from the 5′ end, there is insufficient room for *Taq* polymerase to cleave efficiently between the reporter and quencher. The other five probes exhibited comparable ΔRQ values that are

clearly different from zero. Thus, all five probes are being cleaved during PCR amplification resulting in a similar increase in reporter fluorescence. It should be noted that complete digestion of a probe produces a much larger increase in reporter fluorescence than that observed in Figure 2 (data not shown). Thus, even in reactions where amplification occurs, the majority of probe molecules remain uncleaved. It is mainly for this reason that the fluorescence intensity of the quencher dye TAMRA changes little with amplification of the target. This is what allows us to use the 582-nm fluorescence reading as a normalization factor.

The magnitude of RQ⁻ depends mainly on the quenching efficiency inherent in the specific structure of the probe and the purity of the oligonucleotide. Thus, the larger RQ⁻ values indicate that probes A1-14, A1-19, A1-22, and A1-26 probably have reduced quenching as compared with A1-7. Still, the degree of quenching is sufficient to detect a highly significant increase in reporter fluorescence when each of these probes is cleaved during PCR.

To further investigate the ability of TAMRA on the 3′ end to quench 6-FAM on the 5′ end, three additional pairs of probes were tested in the 5′ nuclease PCR assay. For each pair, one probe has TAMRA attached to an internal nucleotide and the other has TAMRA attached to the 3′ end nucleotide. The results are shown in Table 2. For all three sets, the probe with the 3′ quencher exhibits a ΔRQ value that is considerably higher than for the probe with the internal quencher. The RQ⁻ values suggest that differences in quenching are not as great as those observed with some of the A1 probes. These results demonstrate that a quencher dye on the 3′ end of an oligonucleotide can quench efficiently the

TABLE 2 Results of 5′ Nuclease Assay Comparing Probes with TAMRA Attached to an Internal or 3′-terminal Nucleotide

Probe	518 nm		582 nm		RQ⁻	RQ⁺	ΔRQ
	no temp.	+ temp.	no temp.	+ temp.			
A3-6	54.6 ± 3.2	84.8 ± 3.7	116.2 ± 6.4	115.6 ± 2.5	0.47 ± 0.02	0.73 ± 0.03	0.26 ± 0.04
A3-24	72.1 ± 2.9	236.5 ± 11.1	84.2 ± 4.0	90.2 ± 3.8	0.86 ± 0.02	2.62 ± 0.05	1.76 ± 0.05
P2-7	82.8 ± 4.4	384.0 ± 34.1	105.1 ± 6.4	120.4 ± 10.2	0.79 ± 0.02	3.19 ± 0.16	2.40 ± 0.16
P2-27	113.4 ± 6.6	555.4 ± 14.1	140.7 ± 8.5	118.7 ± 4.8	0.81 ± 0.01	4.68 ± 0.10	3.88 ± 0.10
P5-10	77.5 ± 6.5	244.4 ± 15.9	86.7 ± 4.3	95.8 ± 6.7	0.89 ± 0.05	2.55 ± 0.06	1.66 ± 0.08
P5-28	64.0 ± 5.2	333.6 ± 12.1	100.6 ± 6.1	94.7 ± 6.3	0.63 ± 0.02	3.53 ± 0.12	2.89 ± 0.13

Reactions containing the indicated probes and calculations were performed as described in Material and Methods and in the legend to Fig. 2.

Research

fluorescence of a reporter dye on the 5' end. The degree of quenching is sufficient for this type of oligonucleotide to be used as a probe in the 5' nuclease PCR assay.

To test the hypothesis that quenching by a 3' TAMRA depends on the flexibility of the oligonucleotide, fluorescence was measured for probes in the single-stranded and double-stranded states. Table 3 reports the fluorescence observed at 518 and 582 nm. The relative degree of quenching is assessed by calculating the RQ ratio. For probes with TAMRA 6–10 nucleotides from the 5' end, there is little difference in the RQ values when comparing single-stranded with double-stranded oligonucleotides. The results for probes with TAMRA at the 3' end are much different. For these probes, hybridization to a complementary strand causes a dramatic increase in RQ. We propose that this loss of quenching is caused by the rigid structure of double-stranded DNA, which prevents the 5' and 3' ends from being in proximity.

When TAMRA is placed toward the 3' end, there is a marked Mg^{2+} effect on quenching. Figure 3 shows a plot of observed RQ values for the A1 series of probes as a function of Mg^{2+} concentration. With TAMRA attached near the 5' end (probe A1-2 or A1-7), the RQ value at 0 mM Mg^{2+} is only slightly higher than RQ at 10 mM Mg^{2+}. For probes A1-19, A1-22, and A1-26, the RQ values at 0 mM Mg^{2+} are very high, indicating a much

reduced quenching efficiency. For each of these probes, there is a marked decrease in RQ at 1 mM Mg^{2+} followed by a gradual decline as the Mg^{2+} concentration increases to 10 mM. Probe A1-14 shows an intermediate RQ value at 0 mM Mg^{2+} with a gradual decline at higher Mg^{2+} concentrations. In a low-salt environment with no Mg^{2+} present, a single-stranded oligonucleotide would be expected to adopt an extended conformation because of electrostatic repulsion. The binding of Mg^{2+} ions acts to shield the negative charge of the phosphate backbone so that the oligonucleotide can adopt conformations where the 3' end is close to the 5' end. Therefore, the observed Mg^{2+} effects support the notion that quenching of a 5' reporter dye by TAMRA at or near the 3' end depends on the flexibility of the oligonucleotide.

DISCUSSION

The striking finding of this study is that it seems the rhodamine dye TAMRA, placed at any position in an oligonucleotide, can quench the fluorescent emission of a fluorescein (6-FAM) placed at the 5' end. This implies that a single-stranded, double-labeled oligonucleotide must be able to adopt conformations where the TAMRA is close to the 5' end. It should be noted that the decay of 6-FAM in the excited state requires a certain amount of time. Therefore, what

matters for quenching is not the average distance between 6-FAM and TAMRA but, rather, how close TAMRA can get to 6-FAM during the lifetime of the 6-FAM excited state. As long as the decay time of the excited state is relatively long compared with the molecular motions of the oligonucleotide, quenching can occur. Thus, we propose that TAMRA at the 3' end, or any other position, can quench 6-FAM at the 5' end because TAMRA is in proximity to 6-FAM often enough to be able to accept energy transfer from an excited 6-FAM.

Details of the fluorescence measurements remain puzzling. For example, Table 3 shows that hybridization of probes A1-26, A3-24, and P5-28 to their complementary strands not only causes a large increase in 6-FAM fluorescence at 518 nm but also causes a modest increase in TAMRA fluorescence at 582 nm. If TAMRA is being excited by energy transfer from quenched 6-FAM, then loss of quenching attributable to hybridization should cause a decrease in the fluorescence emission of TAMRA. The fact that the fluorescence emission of TAMRA increases indicates that the situation is more complex. For example, we have anecdotal evidence that the bases of the oligonucleotide, especially G, quench the fluorescence of both 6-FAM and TAMRA to some degree. When double-stranded, base-pairing may reduce the ability of the bases to quench. The primary factor causing the quenching of 6-FAM in an intact probe is the TAMRA dye. Evidence for the importance of TAMRA is that 6-FAM fluorescence remains relatively unchanged when probes labeled only with 6-FAM are used in the 5' nuclease PCR assay (data not shown). Secondary effectors of fluorescence, both before and after cleavage of the probe, need to be explored further.

Regardless of the physical mechanism, the relative independence of position and quenching greatly simplifies the design of probes for the 5' nuclease PCR assay. There are three main factors that determine the performance of a double-labeled fluorescent probe in the 5' nuclease PCR assay. The first factor is the degree of quenching observed in the intact probe. This is characterized by the value of RQ^-, which is the ratio of reporter to quencher fluorescent emissions for a no template control PCR. Influences on the value of RQ^- include the particular reporter and quencher

TABLE 3 Comparison of Fluorescence Emissions of Single-stranded and Double-stranded Fluorogenic Probes

Probe	518 nm		582 nm		RQ	
	ss	ds	ss	ds	ss	ds
A1-7	27.75	68.53	61.08	138.18	0.45	0.50
A1-26	43.31	509.38	53.50	93.86	0.81	5.43
A3-6	16.75	62.88	39.33	165.57	0.43	0.38
A3-24	30.05	578.64	67.72	140.25	0.45	3.21
P2-7	35.02	70.13	54.63	121.09	0.64	0.58
P2-27	39.89	320.47	65.10	61.13	0.61	5.25
P5-10	27.34	144.85	61.95	165.54	0.44	0.87
P5-28	33.65	462.29	72.39	104.61	0.46	4.43

(ss) Single-stranded. The fluorescence emissions at 518 or 582 nm for solutions containing a final concentration of 50 nM indicated probe, 10 mM Tris-HCl (pH 8.3), 50 mM KCl, and 10 mM $MgCl_2$. (ds) Double-stranded. The solutions contained, in addition, 100 nM A1C for probes A1-7 and A1-26, 100 nM A3C for probes A3-6 and A3-24, 100 nM P2C for probes P2-7 and P2-27, or 100 nM P5C for probes P5-10 and P5-28. Before the addition of $MgCl_2$, 120 μl of each sample was heated at 95°C for 5 min. Following the addition of 80 μl of 25 mM $MgCl_2$, each sample was allowed to cool to room temperature and the fluorescence emissions were measured. Reported values are the average of three determinations.
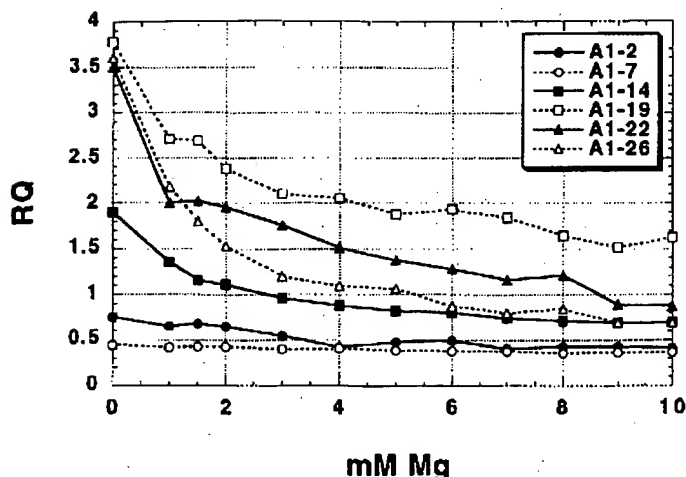
▬▬▬ ▬▬▬ IIIIIIResearch

FIGURE 3 Effect of Mg^{2+} concentration on RQ ratio for the A1 series of probes. The fluorescence emission intensity at 518 and 582 nm was measured for solutions containing 50 nM probe, 10 mM Tris-HCl (pH 8.3), 50 mM KCl, and varying amounts (0–10 mM) of $MgCl_2$. The calculated RQ ratios (518 nm intensity divided by 582 nm intensity) are plotted vs. $MgCl_2$ concentration (mM Mg). The key (*upper right*) shows the probes examined.

dyes used, spacing between reporter and quencher dyes, nucleotide sequence context effects, presence of structure or other factors that reduce flexibility of the oligonucleotide, and purity of the probe. The second factor is the efficiency of hybridization, which depends on probe T_m, presence of secondary structure in probe or template, annealing temperature, and other reaction conditions. The third factor is the efficiency at which *Taq* DNA polymerase cleaves the bound probe between the reporter and quencher dyes. This cleavage is dependent on sequence complementarity between probe and template as shown by the observation that mismatches in the segment between reporter and quencher dyes drastically reduce the cleavage of probe.[1]

The rise in RQ^- values for the A1 series of probes seems to indicate that the degree of quenching is reduced somewhat as the quencher is placed toward the 3′ end. The lowest apparent quenching is observed for probe A1-19 (see Fig. 3) rather than for the probe where the TAMRA is at the 3′ end (A1-26). This is understandable, as the conformation of the 3′ end position would be expected to be less restricted than the conformation of an internal position. In effect, a quencher at the 3′ end is freer to adopt conformations close to the 5′ reporter dye than is an internally placed quencher. For the other three sets of

probes, the interpretation of RQ^- values is less clear-cut. The A3 probes show the same trend as A1, with the 3′ TAMRA probe having a larger RQ^- than the internal TAMRA probe. For the P2 pair, both probes have about the same RQ^- value. For the P5 probes, the RQ^- for the 3′ probe is less than for the internally labeled probe. Another factor that may explain some of the observed variation is that purity affects the RQ^- value. Although all probes are HPLC purified, a small amount of contamination with unquenched reporter can have a large effect on RQ^-.

Although there may be a modest effect on degree of quenching, the position of the quencher apparently can have a large effect on the efficiency of probe cleavage. The most drastic effect is observed with probe A1-2, where placement of the TAMRA on the second nucleotide reduces the efficiency of cleavage to almost zero. For the A3, P2, and P5 probes, ΔRQ is much greater for the 3′ TAMRA probes as compared with the internal TAMRA probes. This is explained most easily by assuming that probes with TAMRA at the 3′ end are more likely to be cleaved between reporter and quencher than are probes with TAMRA attached internally. For the A1 probes, the cleavage efficiency of probe A1-7 must already be quite high, as ΔRQ does not increase when the quencher is placed closer to the 3′ end. This illus-

trates the importance of being able to use probes with a quencher on the 3′ end in the 5′ nuclease PCR assay. In this assay, an increase in the intensity of reporter fluorescence is observed only when the probe is cleaved between the reporter and quencher dyes. By placing the reporter and quencher dyes on the opposite ends of an oligonucleotide probe, any cleavage that occurs will be detected. When the quencher is attached to an internal nucleotide, sometimes the probe works well (A1-7) and other times not so well (A3-6). The relatively poor performance of probe A3-6 presumably means the probe is being cleaved 3′ to the quencher rather than between reporter and quencher. Therefore, the best chance of having a probe that reliably detects accumulation of PCR product in the 5′ nuclease PCR assay is to use a probe with the reporter and quencher dyes on opposite ends.

Placing the quencher dye on the 3′ end may also provide a slight benefit in terms of hybridization efficiency. The presence of a quencher attached to an internal nucleotide might be expected to disrupt base-pairing and reduce the T_m of a probe. In fact, a 2°C–3°C reduction in T_m has been observed for two probes with internally attached TAMRAs.[9] This disruptive effect would be minimized by placing the quencher at the 3′ end. Thus, probes with 3′ quenchers might exhibit slightly higher hybridization efficiencies than probes with internal quenchers.

The combination of increased cleavage and hybridization efficiencies means that probes with 3′ quenchers probably will be more tolerant of mismatches between probe and target as compared with internally labeled probes. This tolerance of mismatches can be advantageous, as when trying to use a single probe to detect PCR-amplified products from samples of different species. Also, it means that cleavage of probe during PCR is less sensitive to alterations in annealing temperature or other reaction conditions. The one application where tolerance of mismatches may be a disadvantage is for allelic discrimination. Lee et al.[1] demonstrated that allele-specific probes were cleaved between reporter and quencher only when hybridized to a perfectly complementary target. This allowed them to distinguish the normal human cystic fibrosis allele from the ΔF508 mutant. Their probes had TAMRA attached to the seventh nucleotide from

Research|||■■■■■■■   ■■■

the 5′ end and were designed so that any mismatches were between the reporter and quencher. Increasing the distance between reporter and quencher would lessen the disruptive effect of mismatches and allow cleavage of the probe on the incorrect target. Thus, probes with a quencher attached to an internal nucleotide may still be useful for allelic discrimination.

In this study loss of quenching upon hybridization was used to show that quenching by a 3′ TAMRA is dependent on the flexibility of a single-stranded oligonucleotide. The increase in reporter fluorescence intensity, though, could also be used to determine whether hybridization has occurred or not. Thus, oligonucleotides with reporter and quencher dyes attached at opposite ends should also be useful as hybridization probes. The ability to detect hybridization in real time means that these probes could be used to measure hybridization kinetics. Also, this type of probe could be used to develop homogeneous hybridization assays for diagnostics or other applications. Bagwell et al.[10] describe just this type of homogeneous assay where hybridization of a probe causes an increase in fluorescence caused by a loss of quenching. However, they utilized a complex probe design that requires adding nucleotides to both ends of the probe sequence to form two imperfect hairpins. The results presented here demonstrate that the simple addition of a reporter dye to one end of an oligonucleotide and a quencher dye to the other end generates a fluorogenic probe that can detect hybridization or PCR amplification.

ACKNOWLEDGMENTS

REFERENCES

1. Lee, L.G., C.R. Connell, and W. Bloch. 1993. Allelic discrimination by nick-translation PCR with fluorogenic probes. *Nucleic Acids Res.* **21**: 3761–3766.
2. Holland, P.M., R.D. Abramson, R. Watson, and D.H. Gelfand. 1991. Detection of specific polymerase chain reaction prod-
uct by utilizing the 5′ to 3′ exonuclease activity of *Thermus aquaticus* DNA polymerase. *Proc. Natl. Acad. Sci.* **88**: 7276–7280.
3. Lyamichev, V., M.A.D. Brow, and J.E. Dahlberg. 1993. Structure-specific endonucleolytic cleavage of nucleic acids by eubacterial DNA polymerases. *Science* **260**: 778–783.
4. Förster, V.Th. 1948. Zwischenmolekulare Energiewanderung und Fluoreszenz. *Ann. Phys. (Leipzig)* **2**: 55–75.
5. Lakowicz, J.R. 1983. Energy transfer. In *Principles of fluorescent spectroscopy*, pp. 303–339. Plenum Press, New York, NY.
6. Stryer, L. and R.P. Haugland. 1967. Energy transfer: A spectroscopic ruler. *Proc. Natl. Acad. Sci.* **58**: 719–726.
7. Nakajima-Iijima, S., H. Hamada, P. Reddy, and T. Kakunaga. 1985. Molecular structure of the human cytoplasmic beta-actin gene: Inter-species homology of sequences in the introns. *Proc. Natl. Acad. Sci.* **82**: 6133–6137.
8. du Breuil, R.M., J.M. Patel, and B.V. Mendelow. 1993. Quantitation of β-actin-specific mRNA transcripts using xeno-competitive PCR. *PCR Methods Applic.* **3**: 57–59.
9. Livak, K.J. (unpubl.).
10. Bagwell, C.B., M.E. Munson, R.L. Christensen, and E.J. Lovett. 1994. A new homogeneous assay system for specific nucleic acid sequences: Poly-dA and poly-A detection. *Nucleic Acids Res.* **22**: 2424–2425.

GENOME METHODS

Real Time Quantitative PCR

Christian A. Heid,[1] Junko Stevens,[2] Kenneth J. Livak,[2] and P. Mickey Williams[1,3]

[1]BioAnalytical Technology Department, Genentech, Inc., South San Francisco, California 94080;
[2]Applied BioSystems Division of Perkin Elmer Corp., Foster City, California 94404

We have developed a novel "real time" quantitative PCR method. The method measures PCR product accumulation through a dual-labeled fluorogenic probe (i.e., TaqMan Probe). This method provides very accurate and reproducible quantitation of gene copies. Unlike other quantitative PCR methods, real-time PCR does not require post-PCR sample handling, preventing potential PCR product carry-over contamination and resulting in much faster and higher throughput assays. The real-time PCR method has a very large dynamic range of starting target molecule determination (at least five orders of magnitude). Real-time quantitative PCR is extremely accurate and less labor-intensive than current quantitative PCR methods.

Quantitative nucleic acid sequence analysis has had an important role in many fields of biological research. Measurement of gene expression (RNA) has been used extensively in monitoring biological responses to various stimuli (Tan et al. 1994; Huang et al. 1995a,b; Prud'homme et al. 1995). Quantitative gene analysis (DNA) has been used to determine the genome quantity of a particular gene, as in the case of the human HER2 gene, which is amplified in ~30% of breast tumors (Slamon et al. 1987). Gene and genome quantitation (DNA and RNA) also have been used for analysis of human immunodeficiency virus (HIV) burden demonstrating changes in the levels of virus throughout the different phases of the disease (Connor et al. 1993; Piatak et al. 1993b; Furtado et al. 1995).

Many methods have been described for the quantitative analysis of nucleic acid sequences (both for RNA and DNA; Southern 1975; Sharp et al. 1980; Thomas 1980). Recently, PCR has proven to be a powerful tool for quantitative nucleic acid analysis. PCR and reverse transcriptase (RT)-PCR have permitted the analysis of minimal starting quantities of nucleic acid (as little as one cell equivalent). This has made possible many experiments that could not have been performed with traditional methods. Although PCR has provided a powerful tool, it is imperative

that it be used properly for quantitation (Raeymaekers 1995). Many early reports of quantitative PCR and RT-PCR described quantitation of the PCR product but did not measure the initial target sequence quantity. It is essential to design proper controls for the quantitation of the initial target sequences (Ferre 1992; Clementi et al. 1993)

Researchers have developed several methods of quantitative PCR and RT-PCR. One approach measures PCR product quantity in the log phase of the reaction before the plateau (Kellogg et al. 1990; Pang et al. 1990). This method requires that each sample has equal input amounts of nucleic acid and that each sample under analysis amplifies with identical efficiency up to the point of quantitative analysis. A gene sequence (contained in all samples at relatively constant quantities, such as β-actin) can be used for sample amplification efficiency normalization. Using conventional methods of PCR detection and quantitation (gel electrophoresis or plate capture hybridization), it is extremely laborious to assure that all samples are analyzed during the log phase of the reaction (for both the target gene and the normalization gene). Another method, quantitative competitive (QC)-PCR, has been developed and is used widely for PCR quantitation. QC-PCR relies on the inclusion of an internal control competitor in each reaction (Becker-Andre 1991; Piatak et al. 1993a,b). The efficiency of each reaction is normalized to the internal competitor. A known amount of internal competitor can be

[3]Corresponding author.

added to each sample. To obtain relative quantitation, the unknown target PCR product is compared with the known competitor PCR product. Success of a quantitative competitive PCR assay relies on developing an internal control that amplifies with the same efficiency as the target molecule. The design of the competitor and the validation of amplification efficiencies require a dedicated effort. However, because QC-PCR does not require that PCR products be analyzed during the log phase of the amplification, it is the easier of the two methods to use.

Several detection systems are used for quantitative PCR and RT-PCR analysis: (1) agarose gels, (2) fluorescent labelling of PCR products and detection with laser-induced fluorescence using capillary electrophoresis (Fasco et al. 1995; Williams et al. 1996) or acrylamide gels, and (3) plate capture and sandwich probe hybridization (Mulder et al. 1994). Although these methods proved successful, each method requires post-PCR manipulations that add time to the analysis and may lead to laboratory contamination. The sample throughput of these methods is limited (with the exception of the plate capture approach), and, therefore, these methods are not well suited for uses demanding high sample throughput (i.e., screening of large numbers of biomolecules or analyzing samples for diagnostics or clinical trials).

Here we report the development of a novel assay for quantitative DNA analysis. The assay is based on the use of the 5' nuclease assay first described by Holland et al. (1991). The method uses the 5' nuclease activity of *Taq* polymerase to cleave a nonextendible hybridization probe during the extension phase of PCR. The approach uses dual-labeled fluorogenic hybridization probes (Lee et al. 1993; Bassler et al. 1995; Livak et al. 1995a,b). One fluorescent dye serves as a reporter [FAM (i.e., 6-carboxyfluorescein)] and its emission spectra is quenched by the second fluorescent dye, TAMRA (i.e., 6-carboxy-tetramethylrhodamine). The nuclease degradation of the hybridization probe releases the quenching of the FAM fluorescent emission, resulting in an increase in peak fluorescent emission at 518 nm. The use of a sequence detector (ABI Prism) allows measurement of fluorescent spectra of all 96 wells of the thermal cycler continuously during the PCR amplification. Therefore, the reactions are monitored in real time. The output data is described and quantitative analysis of input target DNA sequences is discussed below.

RESULTS

PCR Product Detection in Real Time

The goal was to develop a high-throughput, sensitive, and accurate gene quantitation assay for use in monitoring lipid mediated therapeutic gene delivery. A plasmid encoding human factor VIII gene sequence, pF8TM (see Methods), was used as a model therapeutic gene. The assay uses fluorescent Taqman methodology and an instrument capable of measuring fluorescence in real time (ABI Prism 7700 Sequence Detector). The Taqman reaction requires a hybridization probe labeled with two different fluorescent dyes. One dye is a reporter dye (FAM), the other is a quenching dye (TAMRA). When the probe is intact, fluorescent energy transfer occurs and the reporter dye fluorescent emission is absorbed by the quenching dye (TAMRA). During the extension phase of the PCR cycle, the fluorescent hybridization probe is cleaved by the 5'-3' nucleolytic activity of the DNA polymerase. On cleavage of the probe, the reporter dye emission is no longer transferred efficiently to the quenching dye, resulting in an increase of the reporter dye fluorescent emission spectra. PCR primers and probes were designed for the human factor VIII sequence and human β-actin gene (as described in Methods). Optimization reactions were performed to choose the appropriate probe and magnesium concentrations yielding the highest intensity of reporter fluorescent signal without sacrificing specificity. The instrument uses a charge-coupled device (i.e., CCD camera) for measuring the fluorescent emission spectra from 500 to 650 nm. Each PCR tube was monitored sequentially for 25 msec with continuous monitoring throughout the amplification. Each tube was re-examined every 8.5 sec. Computer software was designed to examine the fluorescent intensity of both the reporter dye (FAM) and the quenching dye (TAMRA). The fluorescent intensity of the quenching dye, TAMRA, changes very little over the course of the PCR amplification (data not shown). Therefore, the intensity of TAMRA dye emission serves as an internal standard with which to normalize the reporter dye (FAM) emission variations. The software calculates a value termed ΔRn (or ΔRQ) using the following equation: $\Delta Rn = (Rn^+) - (Rn^-)$, where Rn^+ = emission intensity of reporter/emission intensity of quencher at any given time in a reaction tube, and Rn^- = emission intensity of re-

HUD IT AL.

porter/emission Intensity of quencher measured prior to PCR amplification in that same reaction tube. For the purpose of quantitation, the last three data points (ΔRns) collected during the extension step for each PCR cycle were analyzed. The nucleolytic degradation of the hybridization probe occurs during the extension phase of PCR, and, therefore, reporter fluorescent emission increases during this time. The three data points were averaged for each PCR cycle and the mean value for each was plotted in an "amplification plot" shown in Figure 1A. The ΔRn mean value is plotted on the y-axis, and time, represented by cycle number, is plotted on the x-axis. During the early cycles of the PCR amplification, the ΔRn

value remains at base line When sufficient hybridization probe has been cleaved by the Taq polymerase nuclease activity, the intensity of reporter fluorescent emission increases. Most PCR amplifications reach a plateau phase of reporter fluorescent emission if the reaction is carried out to high cycle numbers. The amplification plot is examined early in the reaction, at a point that represents the log phase of product accumulation. This is done by assigning an arbitrary threshold that is based on the variability of the base-line data. In Figure 1A, the threshold was set at 10 standard deviations above the mean of base line emission calculated from cycles 1 to 15. Once the threshold is chosen, the point at which

A

B

C
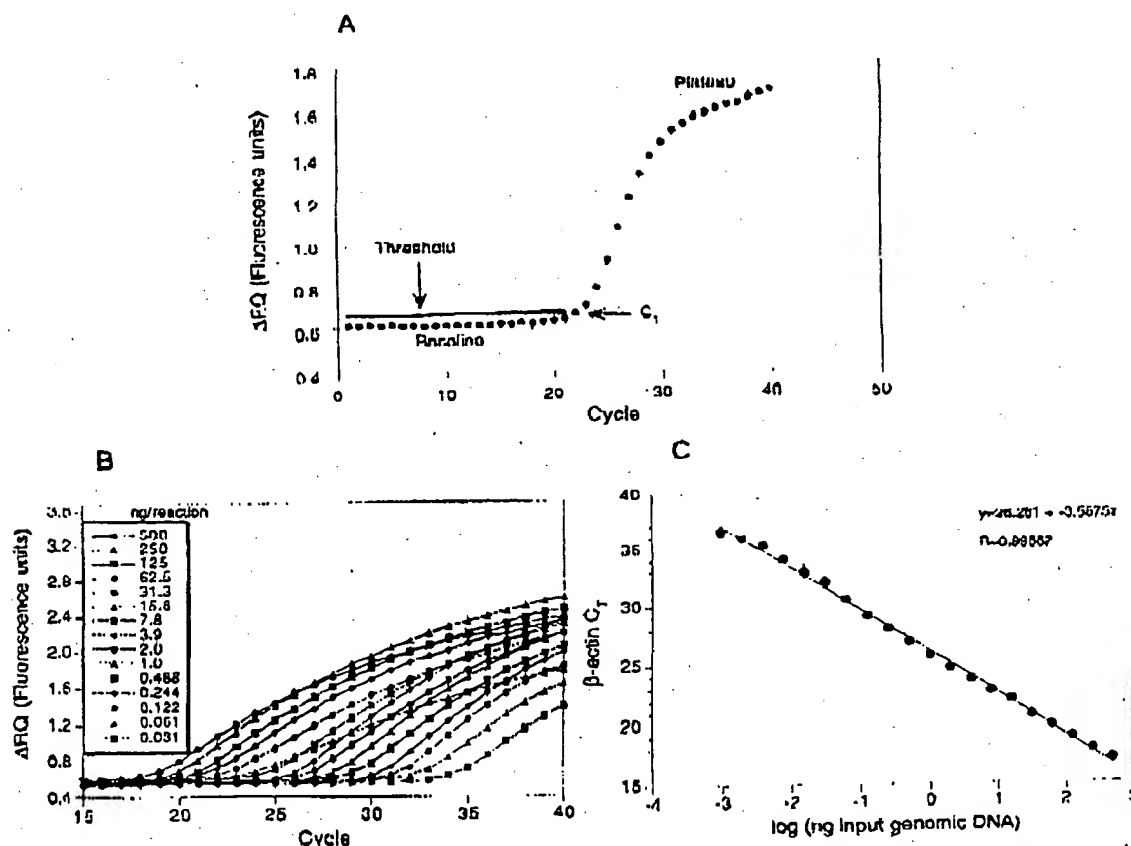
Figure 1 PCR product detection in real time. (A) The Model 7700 software will construct amplification plots from the extension phase fluorescent emission data collected during the PCR amplification. The standard deviation is determined from the data points collected from the base line of the amplification plot. C_T values are calculated by determining the point at which the fluorescence exceeds a threshold limit (usually 10 times the standard deviation of the base line). (B) Overlay of amplification plots of serially (1:2) diluted human genomic DNA samples amplified with β-actin primers. (C) Input DNA concentration of the samples plotted versus C_T. All

the amplification plot crosses the threshold is defined as C_T. C_T is reported as the cycle number at this point. As will be demonstrated, the C_T value is predictive of the quantity of input target.

C_T Values Provide a Quantitative Measurement of Input Target Sequences

Figure 1B shows amplification plots of 15 different PCR amplifications overlaid. The amplifications were performed on a 1:2 serial dilution of human genomic DNA. The amplified target was human β actin. The amplification plots shift to the right (to higher threshold cycles) as the input target quantity is reduced. This is expected because reactions with fewer starting copies of the target molecule require greater amplification to degrade enough probe to attain the threshold fluorescence. An arbitrary threshold of 10 standard deviations above the base line was used to determine the C_T values. Figure 1C represents the C_T values plotted versus the sample dilution value. Each dilution was amplified in triplicate PCR amplifications and plotted as mean values with error bars representing one standard deviation. The C_T values decrease linearly with increasing target quantity. Thus, C_T values can be used as a quantitative measurement of the input target number. It should be noted that the amplification plot for the 15.6-ng sample shown in Figure 1B does not reflect the same fluorescent rate of increase exhibited by most of the other samples. The 15.6-ng sample also achieves endpoint plateau at a lower fluorescent value than would be expected based on the input DNA. This phenomenon has been observed occasionally with other samples (data not shown) and may be attributable to late cycle inhibition; this hypothesis is still under investigation. It is important to note that the flattened slope and early plateau do not impact significantly the calculated C_T value as demonstrated by the fit on the line shown in Figure 1C. All triplicate amplifications resulted in very similar C_T values—the standard deviation did not exceed 0.5 for any dilution. This experiment contains a >100,000-fold range of input target molecules. Using C_T values for quantitation permits a much larger assay range than directly using total fluorescent emission intensity for quantitation. The linear range of fluorescent intensity measurement of the ABI Prism 7700 Se-

ments over a very large range of relative starting target quantities.

Sample Preparation Validation

Several parameters influence the efficiency of PCR amplification: magnesium and salt concentrations, reaction conditions (i.e., time and temperature), PCR target size and composition, primer sequences, and sample purity. All of the above factors are common to a single PCR assay, except sample to sample purity. In an effort to validate the method of sample preparation for the factor VIII assay, PCR amplification reproducibility and efficiency of 10 replicate sample preparations were examined. After genomic DNA was prepared from the 10 replicate samples, the DNA was quantitated by ultraviolet spectroscopy. Amplifications were performed analyzing β-actin gene content in 100 and 25 ng of total genomic DNA. Each PCR amplification was performed in triplicate. Comparison of C_T values for each triplicate sample show minimal variation based on standard deviation and coefficient of variance (Table 1). Therefore, each of the triplicate PCR amplifications was highly reproducible, demonstrating that real time PCR using this instrumentation introduces minimal variation into the quantitative PCR analysis. Comparison of the mean C_T values of the 10 replicate sample preparations also showed minimal variability, indicating that each sample preparation yielded similar results for β-actin gene quantity. The highest C_T difference between any of the samples was 0.85 and 0.71 for the 100 and 25 ng samples, respectively. Additionally, the amplification of each sample exhibited an equivalent rate of fluorescent emission intensity change per amount of DNA target analyzed as indicated by similar slopes derived from the sample dilutions (Fig. 2). Any sample containing an excess of a PCR inhibitor would exhibit a greater measured β-actin C_T value for a given quantity of DNA. In addition, the inhibitor would be diluted along with the sample in the dilution analysis (Fig. 2), altering the expected C_T value change. Each sample amplification yielded a similar result in the analysis, demonstrating that this method of sample preparation is highly reproducible with regard to sample purity.

Quantitative Analysis of a Plasmid After

HHD H AL

Table 1. Reproducibility of Sample Preparation Method							
	100 ng				**25 ng**		
Sample no.	C_T	mean	standard deviation	CV	C_T	mean	standard deviation	CV
1	18.24				20.48			
	18.23				20.55			
	18.33	18.27	0.06	0.32	20.5	20.51	0.03	0.17
2	18.33				20.61			
	18.35				20.59			
	18.44	18.37	0.06	0.32	20.41	20.54	0.11	0.54
3	18.3				20.54			
	18.3				20.6			
	18.42	18.34	0.07	0.36	20.49	20.54	0.06	0.28
4	18.15				20.48			
	18.23				20.44			
	18.32	18.23	0.08	0.46	20.38	20.43	0.05	0.26
5	18.4				20.68			
	18.38				20.87			
	18.46	18.42	0.04	0.23	20.63	20.73	0.13	0.61
6	18.54				21.09			
	18.67				21.04			
	19	18.74	0.24	1.26	21.04	21.06	0.03	0.15
7	18.28				20.67			
	18.36				20.73			
	18.52	18.39	0.12	0.66	20.65	20.68	0.04	0.2
8	18.45				20.98			
	18.7				20.84			
	18.73	18.63	0.16	0.83	20.75	20.86	0.12	0.57
9	18.18				20.46			
	18.34				20.54			
	18.36	18.29	0.1	0.55	20.48	20.51	0.07	0.32
10	18.42				20.79			
	18.57				20.78			
	18.66	18.55	0.12	0.65	20.62	20.73	0.1	0.46
Mean	(1 10)	18.42	0.17	0.90		20.66	0.19	0.94

tor containing a partial cDNA for human factor VIII, pF8TM. A series of transfections was set up using a decreasing amount of the plasmid (40, 4, 0.5, and 0.1 μg). Twenty-four hours post-transfection, total DNA was purified from each flask of cells. β-Actin gene quantity was chosen as a value for normalization of genomic DNA concentration from each sample. In this experiment, β-actin gene content should remain constant relative to total genomic DNA. Figure 3 shows the result of the β-actin DNA measurement (100 ng total DNA determined by ultraviolet spectroscopy) of each sample. Each sample was analyzed in triplicate and the mean β-actin C_T values of the triplicates were plotted (error bars represent one standard deviation). The highest difference

between any two sample means was 0.95 C_T. Ten nanograms of total DNA of each sample were also examined for β-actin. The results again showed that very similar amounts of genomic DNA were present; the maximum mean β actin C_T value difference was 1.0. As Figure 3 shows, the rate of β-actin C_T change between the 100 and 10-ng samples was similar (slope values range between 3.56 and −3.45). This verifies again that the method of sample preparation yields samples of identical PCR integrity (i.e., no sample contained an excessive amount of a PCR inhibitor). However, these results indicate that each sample contained slight differences in the actual amount of genomic DNA analyzed. Determination of actual genomic DNA concentration was accomplished
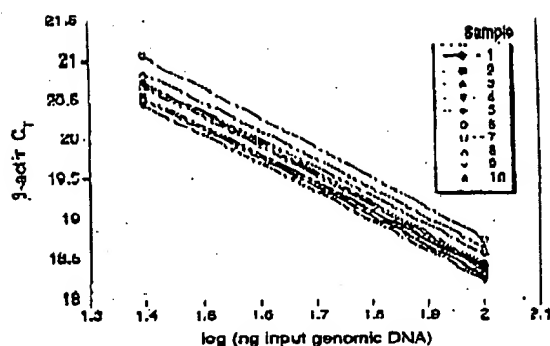
Figure 2 Sample preparation purity. The replicate samples shown in Table 1 were also amplified in tripicate using 25 ng of each DNA sample. The figure shows the input DNA concentration (100 and 25 ng) vs. C_t. In the figure, the 100 and 25 ng points for each sample are connected by a line.

by plotting the mean β-actin C_t value obtained for each 100-ng sample on a β-actin standard curve (shown in Fig. 4C). The actual genomic DNA concentration of each sample, a, was obtained by extrapolation to the x-axis.

Figure 4A shows the measured (i.e., non-normalized) quantities of factor VIII plasmid DNA (pF8TM) from each of the four transient cell transfections. Each reaction contained 100 ng of total sample DNA (as determined by UV spectroscopy). Each sample was analyzed in triplicate
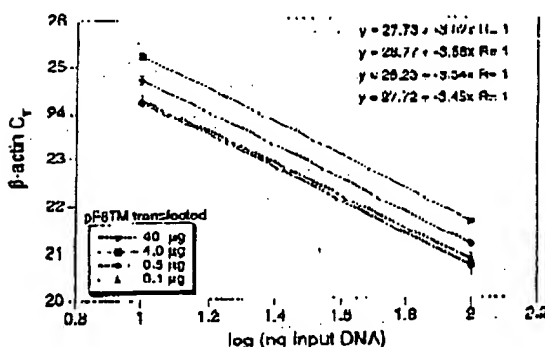
Figure 3 Analysis of transfected cell DNA quantity and purity. The DNA preparations of the four 293 cell transfections (40, 4, 0.5, and 0.1 μg of pF8TM) were analyzed for the β-actin gene. 100 and 10 ng (determined by ultraviolet spectroscopy) of each sample were amplified in triplicate. For each amount of pF8TM that was transfected, the β-actin C_T values are plotted versus the total input DNA concentration.

PCR amplifications. As shown, pF8TM purified from the 293 cells decreases (mean C_t values increase) with decreasing amounts of plasmid transfected. The mean C_t values obtained for pF8TM in Figure 4A were plotted on a standard curve comprised of serially diluted pF8TM, shown in Figure 4B. The quantity of pF8TM, b, found in each of the four transfections was determined by extrapolation to the x axis of the standard curve in Figure 4B. These uncorrected values, b, for pF8TM were normalized to determine the actual amount of pF8TM found per 100 ng of genomic DNA by using the equation:

$$\frac{b \times 100\ ng}{a} = \frac{\text{actual pF8TM copies per}}{100\ ng\ of\ genomic\ DNA}$$

where a = actual genomic DNA in a sample and b = pF8TM copies from the standard curve. The normalized quantity of pF8TM per 100 ng of genomic DNA for each of the four transfections is shown in Figure 4D. These results show that the quantity of factor VIII plasmid associated with the 293 cells, 24 hr after transfection, decreases with decreasing plasmid concentration used in the transfection. The quantity of pF8TM associated with 293 cells, after transfection with 40 μg of plasmid, was 35 pg per 100 ng genomic DNA. This results in ~520 plasmid copies per cell.

DISCUSSION

We have described a new method for quantitating gene copy numbers using real-time analysis of PCR amplifications. Real-time PCR is compatible with either of the two PCR (RT-PCR) approaches: (1) quantitative competitive where an internal competitor for each target sequence is used for normalization (data not shown) or (2) quantitative comparative PCR using a normalization gene contained within the sample (i.e., β-actin) or a "housekeeping" gene for RT-PCR. If equal amounts of nucleic acid are analyzed for each sample and if the amplification efficiency before quantitative analysis is identical for each sample, the internal control (normalization gene or competitor) should give equal signals for all samples.

The real-time PCR method offers several advantages over the other two methods currently employed (see the Introduction). First, the real-time PCR method is performed in a closed-tube system and requires no post-PCR manipulation
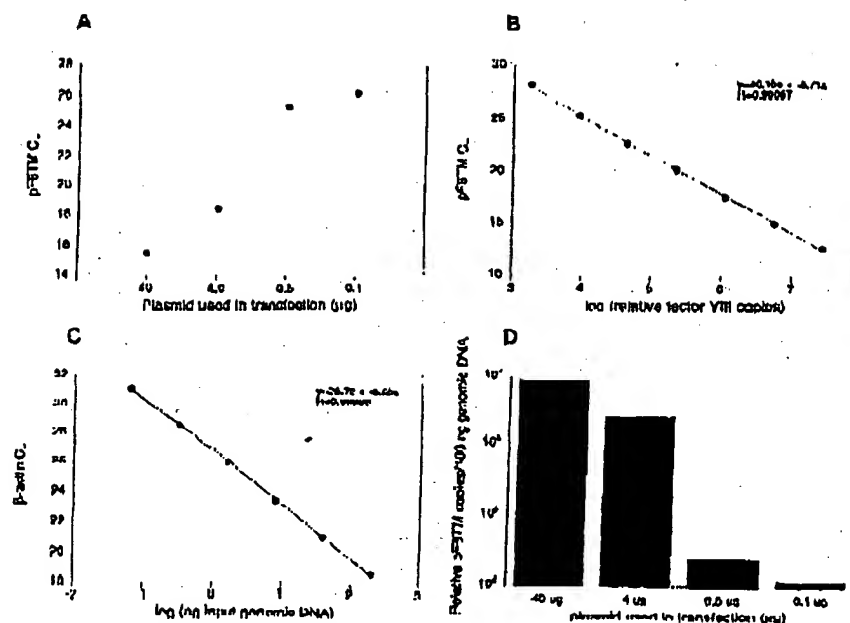
HLIO LI AL.

Figure 4 Quantitative analysis of pF8TM in transfected cells. (A) Amount of plasmid DNA used for the transfection plotted against the mean C_i value determined for pF8TM remaining 24 hr after transfection. (B,C) Standard curves of pF8TM and β-actin, respectively. pF8TM DNA (B) and genomic DNA (C) were diluted serially 1:5 before amplification with the appropriate primers. The β-actin standard curve was used to normalize the results of A to 100 ng of genomic DNA. (D) The amount of pF8TM present per 100 ng of genomic DNA.

of sample. Therefore, the potential for PCR contamination in the laboratory is reduced because amplified products can be analyzed and disposed of without opening the reaction tubes. Second, this method supports the use of a normalization gene (i.e., β-actin) for quantitative PCR or housekeeping genes for quantitative RT-PCR controls. Analysis is performed in real time during the log phase of product accumulation. Analysis during log phase permits many different genes (over a wide input target range) to be analyzed simultaneously, without concern of reaching reaction plateau at different cycles. This will make multigene analysis assays much easier to develop, because individual internal competitors will not be needed for each gene under analysis. Third, sample throughput will increase dramatically with the new method because there is no post-PCR processing time. Additionally, working in a 96-well format is highly compatible with automation technology.

The real-time PCR method is highly reproducible. Replicate amplifications can be analyzed

for each sample minimizing potential error. The system allows for a very large assay dynamic range (approaching 1,000,000-fold starting target). Using a standard curve for the target of interest, relative copy number values can be determined for any unknown sample. Fluorescent threshold values, C_p, correlate linearly with relative DNA copy numbers. Real time quantitative RT-PCR methodology (Gibson et al., this issue) has also been developed. Finally, real time quantitative PCR methodology can be used to develop high-throughput screening assays for a variety of applications [quantitative gene expression (RT-PCR), gene copy assays (Her2, HIV, etc.), genotyping (knockout mouse analysis), and immuno-PCR].

Real-time PCR may also be performed using intercalating dyes (Higuchi et al. 1992) such as ethidium bromide. The fluorogenic probe method offers a major advantage over intercalating dyes—greater specificity (i.e., primer dimers and nonspecific PCR products are not detected).

METHODS

Generation of a Plasmid Containing a Partial cDNA for Human Factor VIII

Total RNA was harvested (RNAsol B from Tel Test, Inc., Friendswood, TX) from cells transfected with a factor VIII expression vector, pCIS2.8c251) (Eaton et al. 1986; Gorman et al. 1990). A factor VIII partial cDNA sequence was generated by RT-PCR [GeneAmp EZ rTth RNA PCR Kit (part N808-0179, PE Applied Biosystems, Foster City, CA)] using the PCR primers F8for and F8rev (primer sequences are shown below). The amplicon was reamplified using modified F8for and F8rev primers (appended with HamHI and HindIII restriction site sequences at the 5' end) and cloned into pKRM-3Z (Promega Corp., Madison, WI). The resulting clone, pF8TM, was used for transient transfection of 293 cells.

Amplification of Target DNA and Detection of Amplicon Factor VIII Plasmid DNA

(pF8TM) was amplified with the primers F8for 5'-CCC-GTCCCAAGAGTGACATGTC-3' and F8rev 5'-AAACCT-CACCCTGGATCGTTACG-3'. The reaction produced a 422-bp PCR product. The forward primer was designed to recognize a unique sequence found in the 5' untranslated region of the parent pCIS2.8c251) plasmid and therefore does not recognize and amplify the human factor VIII gene. Primers were chosen with the assistance of the computer program Oligo 4.0 (National Biosciences, Inc., Plymouth, MN). The human β-actin gene was amplified with the primers β-actin forward primer 5'-TCACCCACACTGT-GCCCATCTACGA-3' and β-actin reverse primer 5'-CAG-CGGAACCGCTCATTGCCAATGG-3'. The reaction produced a 295-bp PCR product.

Amplification reactions (50 μl) contained a DNA sample, 10× PCR Buffer II (5 μl), 200 μM dATP, dCTP, dGTP, and 400 μM dUTP, 4 mM MgCl₂, 1.25 Units AmpliTaq DNA polymerase, 0.5 unit AmpErase uracil N-glycosylase (UNG), 50 pmole of each factor VIII primer, and 15 pmole of each β-actin primer. The reactions also contained one of the following detection probes (100 nM each): F8probe 5'-(FAM)AGCCTCTTCCCACCCTGCTTCTTTCTGT-GCCTT(TAMRA)p 3' and β-actin probe 5' (FAM)ATGCCC-X(TAMRA)CCCCCATGCCATCGp-3' where p indicates phosphorylation and X indicates a linker arm nucleotide. Reaction tubes were MicroAmp Optical Tubes (part number N801 0933, Perkin Elmer) that were frosted (at Perkin Elmer) to prevent light from reflecting. Tube caps were similar to MicroAmp Caps but specially designed to prevent light scattering. All of the PCR consumables were supplied by PE Applied Biosystems (Foster City, CA) except the factor VIII primers, which were synthesized at Genentech, Inc. (South San Francisco, CA). Probes were designed using the Oligo 4.0 software, following guidelines suggested in the Model 7700 Sequence Detector instrument manual. Briefly, probe Tₘ should be at least 5°C higher than the annealing temperature used during thermal cycling; primers should not form stable duplexes with the probe.

The thermal cycling conditions included 2 min at 50°C and 10 min at 95°C. Thermal cycling proceeded with

reactions were performed in the Model 7700 Sequence Detector (PE Applied Biosystems), which contains a Gene-Amp PCR System 9600. Reaction conditions were programmed on a Power Macintosh 7100 (Apple Computer, Santa Clara, CA) linked directly to the Model 7700 Sequence Detector. Analysis of data was also performed on the Macintosh computer. Collection and analysis software was developed at PE Applied Biosystems.

Transfection of Cells with Factor VIII Construct

Four T175 flasks of 293 cells (ATCC CRL 1573), a human fetal kidney suspension cell line, were grown to 80% confluency and transfected pF8TM. Cells were grown in the following media: 50% HAM'S F12 without GHT, 50% low glucose Dulbecco's modified Eagle medium (DMEM) without glycine with sodium bicarbonate, 10% fetal bovine serum, 2 mM L-glutamine, and 1% penicillin–streptomycin. The media was changed 30 min before the transfection. pF8TM DNA amounts of 40, 4, 0.5, and 0.1 μg were added to 1.5 ml of a solution containing 0.125 M CaCl₂ and 1× HEPES. The four mixtures were left at room temperature for 10 min and then added dropwise to the cells. The flasks were incubated at 37°C and 5% CO₂ for 24 hr, washed with PBS, and resuspended in PBS. The resuspended cells were divided into aliquots and DNA was extracted immediately using the QIAamp Blood Kit (Qiagen, Chatsworth, CA). DNA was eluted into 200 μl of 20 mM Tris-HCl at pH 8.0.

REFERENCES

Bassler, H.A., S.J. Flood, K.J. Livak, J. Marmaro, R. Knorr, and C.A. Batt. 1995. Use of a fluorogenic probe in a PCR-based assay for the detection of Listeria monocytogenes. App. Environ. Microbiol. 61: 3724–3728.

Becker-Andre, M. 1991. Quantitative evaluation of mRNA levels. Meth. Mol. Cell. Biol. 2: 189-201.

Clementi, M., S. Menzo, P. Bagnarelli, A. Manzin, A. Valenza, and P.E. Varaldo. 1993. Quantitative PCR and RT-PCR in virology. [Review]. PCR Methods Applic. 2: 191–196.

Connor, R.I., H. Mohri, Y. Cao, and D.D. Ho. 1993. Increased viral burden and cytopathicity correlate temporally with CD4+ T-lymphocyte decline and clinical progression in human immunodeficiency virus type 1-infected individuals. J. Virol. 67: 1772–1777.

Eaton, D.L., W.I. Wood, D. Eaton, P.E. Hass, P.

HFID LI AL.

Venar, and C. Gorman. 1986. Construction and characterization of an active factor VIII variant lacking the central one third of the molecule. *Biochemistry* 25: 8343–8347.

Fasco, M.J., C.P. Treanor, S. Spivack, H.L. Figge, and L.S. Kaminsky. 1995. Quantitative RNA-polymerase chain reaction-DNA analysis by capillary electrophoresis and laser-induced fluorescence. *Anal. Biochem.* 224: 140–147.

Ferre, F. 1992. Quantitative or semi-quantitative PCR: Reality versus myth. *PCR Methods Applic.* 2: 1–9.

Furtado, M.R., L.A. Kingsley, and S.M. Wolinsky. 1995. Changes in the viral mRNA expression pattern correlate with a rapid rate of CD4+ T-cell number decline in human immunodeficiency virus type 1-infected individuals. *J. Virol.* 69: 2092–2100.

Gibson, U.E.M., C.A. Heid, and P.M. Williams. 1996 A novel method for real time quantitative competitive RT-PCR. *Genome Res.* (this issue).

Gorman, C.M., D.R. Gies, and G. McCray. 1990. Transient production of proteins using an adenovirus transformed cell line. *DNA Prot. Engin. Tech.* 2: 3–10.

Higuchi, R., G. Dollinger, P.S. Walsh, and R. Griffith. 1992. Simultaneous amplification and detection of specific DNA sequences. *Biotechnology* 10: 413–417.

Holland, P.M., R.D. Abramson, R. Watson, and D.H. Gelfand. 1991. Detection of specific polymerase chain reaction product by utilizing the 5'→3' exonuclease activity of *Thermus aquaticus* DNA polymerase. *Proc. Natl. Acad. Sci.* 88: 7276–7280.

Huang, S.K., H.Q. Xiao, T.J. Kleine, G. Paciotti, H.G. Marsh, L.M. Lichtenstein, and M.C. Liu. 1995a. IL-13 expression at the sites of allergen challenge in patients with asthma. *J. Immun.* 155: 2688–2694.

Huang, S.K., M. Yi, E. Palmer, and D.G. Marsh. 1995b. A dominant T cell receptor beta-chain in response to a short ragweed allergen, Amb a 5. *J. Immun.* 154: 6157–6162.

Kellogg, D.E., J.J. Sninsky, and S. Kwok. 1990. Quantitation of HIV-1 proviral DNA relative to cellular DNA by the polymerase chain reaction. *Anal. Biochem.* 189: 202–208.

Lee, L.G., C.R. Connell, and W. Bloch. 1993. Allelic discrimination by nick-translation PCR with fluorogenic probes. *Nucleic Acids Res.* 21: 3761–3766.

Livak, K.J., S.J. Flood, J. Marmaro, W. Giusti, and K. Deetz. 1995a. Oligonucleotides with fluorescent dyes at opposite ends provide a quenched probe system useful for detecting PCR product and nucleic acid hybridization. *PCR Methods Applic.* 4: 357–362.

Livak, K.J., J. Marmaro, and J.A. Todd. 1995b. Towards

fully automated genome-wide polymorphism screening. [Letter] *Nature Genet.* 9: 341–342.

Mulder, J., N. McKinney, C. Christopherson, J. Sninsky, L. Greenfield, and S. Kwok. 1994. Rapid and simple PCR assay for quantitation of human immunodeficiency virus type 1 RNA in plasma: Application to acute retroviral infection. *J. Clin. Microbiol.* 32: 292–300.

Pang, S., Y. Koyanagi, S. Miles, C. Wiley, H.V. Vinters, and I.S. Chen. 1990. High levels of unintegrated HIV-1 DNA in brain tissue of AIDS dementia patients. *Nature* 343: 85–89.

Piatak, M.J., K.C. Luk, B. Williams, and J.D. Lifson. 1993a. Quantitative competitive polymerase chain reaction for accurate quantitation of HIV DNA and RNA species. *BioTechniques* 14: 70–81.

Piatak, M.J., M.S Saag, L.C. Yang, S.J. Clark, J.C. Kappes, K.C. Luk, B.H. Hahn, G.M. Shaw, and J.D. Lifson. 1993b. High levels of HIV-1 in plasma during all stages of infection determined by competitive PCR [see comments]. *Science* 259: 1749–1754.

Prud'homme, G.J., D.H. Kono, and A.N. Theofilopoulos. 1995. Quantitative polymerase chain reaction analysis reveals marked overexpression of interleukin-1 beta, interleukin-1 and interferon-gamma mRNA in the lymph nodes of lupus-prone mice. *Mol. Immunol.* 32: 495–503.

Raeymaekers, L. 1995. A commentary on the practical applications of competitive PCR. *Genome Res.* 5: 91–94.

Sharp, P.A., A.J. Berk, and S.M. Berget. 1980. Transcription maps of adenovirus. *Methods Enzymol.* 65: 750–768.

Slamon, D.J., G.M. Clark, S.C. Wong, W.J. Levin, A. Ullrich, and W.L. McGuire. 1987. Human breast cancer: Correlation of relapse and survival with amplification of the HER-2/neu oncogene. *Science* 235: 177–182.

Southern, E.M. 1975. Detection of specific sequences among DNA fragments separated by gel electrophoresis. *J. Mol. Biol.* 98: 503–517.

Tan, X., X. Sun, G.R. Gonzalez, and W. Hsueh. 1994. PAF and TNF increase the precursor of NF-kappa B p50 mRNA in mouse intestine: Quantitative analysis by competitive PCR. *Biochim. Biophys. Acta* 1215: 157–162.

Thomas, P.S. 1980. Hybridization of denatured RNA and small DNA fragments transferred to nitrocellulose. *Proc. Natl. Acad. Sci.* 77: 5201–5205.

Williams, S., C. Schwer, A. Krishnarao, C. Heid, B. Karger, and P.M. Williams. 1996. Quantitative competitive PCR: Analysis of amplified products of the HIV-1 gag gene by capillary electrophoresis with laser induced fluorescence detection. *Anal. Biochem.* (in press).

WISP genes are members of the connective tissue growth factor family that are up-regulated in Wnt-1-transformed cells and aberrantly expressed in human colon tumors

Diane Pennica[*†], Todd A. Swanson[*], James W. Welsh[*], Margaret A. Roy[‡], David A. Lawrence[*],
James Lee[‡], Jennifer Brush[‡], Lisa A. Taneyhill[§], Bethanne Deuel[‡], Michael Lew[¶], Colin Watanabe[‖],
Robert L. Cohen[*], Mona F. Melhem[**], Gene G. Finley[**], Phil Quirke[††], Audrey D. Goddard[‡],
Kenneth J. Hillan[¶], Austin L. Gurney[‡], David Botstein[‡,‡‡], and Arnold J. Levine[§]

Departments of *Molecular Oncology, ‡Molecular Biology, ‖Scientific Computing, and ¶Pathology, Genentech Inc., 1 DNA Way, South San Francisco, CA 94080;
**University of Pittsburgh School of Medicine, Veterans Administration Medical Center, Pittsburgh, PA 15240; ††University of Leeds, Leeds, LS29JT United
Kingdom; ‡‡Department of Genetics, Stanford University, Palo Alto, CA 94305; and §Department of Molecular Biology, Princeton University, Princeton, NJ
08544

Contributed by David Botstein and Arnold J. Levine, October 21, 1998

ABSTRACT Wnt family members are critical to many developmental processes, and components of the Wnt signaling pathway have been linked to tumorigenesis in familial and sporadic colon carcinomas. Here we report the identification of two genes, *WISP-1* and *WISP-2*, that are up-regulated in the mouse mammary epithelial cell line C57MG transformed by Wnt-1, but not by Wnt-4. Together with a third related gene, *WISP-3*, these proteins define a subfamily of the connective tissue growth factor family. Two distinct systems demonstrated *WISP* induction to be associated with the expression of Wnt-1. These included (*i*) C57MG cells infected with a Wnt-1 retroviral vector or expressing Wnt-1 under the control of a tetracyline repressible promoter, and (*ii*) Wnt-1 transgenic mice. The *WISP-1* gene was localized to human chromosome 8q24.1–8q24.3. *WISP-1* genomic DNA was amplified in colon cancer cell lines and in human colon tumors and its RNA overexpressed (2- to >30-fold) in 84% of the tumors examined compared with patient-matched normal mucosa. *WISP-3* mapped to chromosome 6q22–6q23 and also was overexpressed (4- to >40-fold) in 63% of the colon tumors analyzed. In contrast, *WISP-2* mapped to human chromosome 20q12–20q13 and its DNA was amplified, but RNA expression was reduced (2- to >30-fold) in 79% of the tumors. These results suggest that the *WISP* genes may be downstream of Wnt-1 signaling and that aberrant levels of *WISP* expression in colon cancer may play a role in colon tumorigenesis.

Wnt-1 is a member of an expanding family of cysteine-rich, glycosylated signaling proteins that mediate diverse developmental processes such as the control of cell proliferation, adhesion, cell polarity, and the establishment of cell fates (1, 2). Wnt-1 originally was identified as an oncogene activated by the insertion of mouse mammary tumor virus in virus-induced mammary adenocarcinomas (3, 4). Although Wnt-1 is not expressed in the normal mammary gland, expression of Wnt-1 in transgenic mice causes mammary tumors (5).

In mammalian cells, Wnt family members initiate signaling by binding to the seven-transmembrane spanning Frizzled receptors and recruiting the cytoplasmic protein Dishevelled (Dsh) to the cell membrane (1, 2, 6). Dsh then inhibits the kinase activity of the normally constitutively active glycogen synthase kinase-3β (GSK-3β) resulting in an increase in β-catenin levels. Stabilized β-catenin interacts with the transcription factor TCF/Lef1, forming a complex that appears in the nucleus and binds TCF/Lef1 target DNA elements to activate transcription (7, 8). Other experiments suggest that the adenomatous polyposis coli (APC) tumor suppressor gene also plays an important role in Wnt signaling by regulating β-catenin levels (9). APC is phosphorylated by GSK-3β, binds to β-catenin, and facilitates its degradation. Mutations in either APC or β-catenin have been associated with colon carcinomas and melanomas, suggesting these mutations contribute to the development of these types of cancer, implicating the Wnt pathway in tumorigenesis (1).

Although much has been learned about the Wnt signaling pathway over the past several years, only a few of the transcriptionally activated downstream components activated by Wnt have been characterized. Those that have been described cannot account for all of the diverse functions attributed to Wnt signaling. Among the candidate Wnt target genes are those encoding the nodal-related 3 gene, *Xnr3*, a member of the transforming growth factor (TGF)-β superfamily, and the homeobox genes, *engrailed*, *goosecoid*, *twin* (*Xtwn*), and *siamois* (2). A recent report also identifies *c-myc* as a target gene of the Wnt signaling pathway (10).

To identify additional downstream genes in the Wnt signaling pathway that are relevant to the transformed cell phenotype, we used a PCR-based cDNA subtraction strategy, suppression subtractive hybridization (SSH) (11), using RNA isolated from C57MG mouse mammary epithelial cells and C57MG cells stably transformed by a Wnt-1 retrovirus. Overexpression of Wnt-1 in this cell line is sufficient to induce a partially transformed phenotype, characterized by elongated and refractile cells that lose contact inhibition and form a multilayered array (12, 13). We reasoned that genes differentially expressed between these two cell lines might contribute to the transformed phenotype.

In this paper, we describe the cloning and characterization of two genes up-regulated in Wnt-1 transformed cells, *WISP-1* and *WISP-2*, and a third related gene, *WISP-3*. The *WISP* genes are members of the CCN family of growth factors, which includes connective tissue growth factor (CTGF), Cyr61, and *nov*, a family not previously linked to Wnt signaling.

MATERIALS AND METHODS

SSH. SSH was performed by using the PCR-Select cDNA Subtraction Kit (CLONTECH). Tester double-stranded

cDNA was synthesized from 2 μg of poly(A)⁺ RNA isolated from the C57MG/Wnt-1 cell line and driver cDNA from 2 μg of poly(A)⁺ RNA from the parent C57MG cells. The subtracted cDNA library was subcloned into a pGEM-T vector for further analysis.

cDNA Library Screening. Clones encoding full-length mouse *WISP-1* were isolated by screening a λgt10 mouse embryo cDNA library (CLONTECH) with a 70-bp probe from the original partial clone 568 sequence corresponding to amino acids 128–169. Clones encoding full-length human *WISP-1* were isolated by screening λgt10 lung and fetal kidney cDNA libraries with the same probe at low stringency. Clones encoding full-length mouse and human *WISP-2* were isolated by screening a C57MG/Wnt-1 or human fetal lung cDNA library with a probe corresponding to nucleotides 1463–1512. Full-length cDNAs encoding *WISP-3* were cloned from human bone marrow and fetal kidney libraries.

Expression of Human WISP RNA. PCR amplification of first-strand cDNA was performed with human Multiple Tissue cDNA panels (CLONTECH) and 300 μM of each dNTP at 94°C for 1 sec, 62°C for 30 sec, 72°C for 1 min, for 22–32 cycles. *WISP* and glyceraldehyde-3-phosphate dehydrogenase primer sequences are available on request.

In Situ Hybridization. ³³P-labeled sense and antisense riboprobes were transcribed from an 897-bp PCR product corresponding to nucleotides 601–1440 of mouse *WISP-1* or a 294-bp PCR product corresponding to nucleotides 82–375 of mouse *WISP-2*. All tissues were processed as described (40).

Radiation Hybrid Mapping. Genomic DNA from each hybrid in the Stanford G3 and Genebridge4 Radiation Hybrid Panels (Research Genetics, Huntsville, AL) and human and hamster control DNAs were PCR-amplified, and the results were submitted to the Stanford or Massachusetts Institute of Technology web servers.

Cell Lines, Tumors, and Mucosa Specimens. Tissue specimens were obtained from the Department of Pathology (University of Pittsburgh) for patients undergoing colon resection and from the University of Leeds, United Kingdom. Genomic DNA was isolated (Qiagen) from the pooled blood of 10 normal human donors, surgical specimens, and the following ATCC human cell lines: SW480, COLO 320DM, HT-29, WiDr, and SW403 (colon adenocarcinomas), SW620 (lymph node metastasis, colon adenocarcinoma), HCT 116 (colon carcinoma), SK-CO-1 (colon adenocarcinoma, ascites), and HM7 (a variant of ATCC colon adenocarcinoma cell line LS 174T). DNA concentration was determined by using Hoechst dye 33258 intercalation fluorimetry. Total RNA was prepared by homogenization in 7 M GuSCN followed by centrifugation over CsCl cushions or prepared by using RNAzol.

Gene Amplification and RNA Expression Analysis. Relative gene amplification and RNA expression of *WISP*s and c-*myc* in the cell lines, colorectal tumors, and normal mucosa were determined by quantitative PCR. Gene-specific primers and fluorogenic probes (sequences available on request) were designed and used to amplify and quantitate the genes. The relative gene copy number was derived by using the formula $2^{(\Delta ct)}$ where ΔCt represents the difference in amplification cycles required to detect the *WISP* genes in peripheral blood lymphocyte DNA compared with colon tumor DNA or colon tumor RNA compared with normal mucosal RNA. The ∂-method was used for calculation of the SE of the gene copy number or RNA expression level. The *WISP*-specific signal was normalized to that of the glyceraldehyde-3-phosphate dehydrogenase housekeeping gene. All TaqMan assay reagents were obtained from Perkin–Elmer Applied Biosystems.

RESULTS

Isolation of WISP-1 and WISP-2 by SSH. To identify Wnt-1-inducible genes, we used the technique of SSH using the

mouse mammary epithelial cell line C57MG and C57MG cells that stably express Wnt-1 (11). Candidate differentially expressed cDNAs (1,384 total) were sequenced. Thirty-nine percent of the sequences matched known genes or homologues, 32% matched expressed sequence tags, and 29% had no match. To confirm that the transcript was differentially expressed, semiquantitative reverse transcription–PCR and Northern analysis were performed by using mRNA from the C57MG and C57MG/Wnt-1 cells.

Two of the cDNAs, *WISP-1* and *WISP-2*, were differentially expressed, being induced in the C57MG/Wnt-1 cell line, but not in the parent C57MG cells or C57MG cells overexpressing Wnt-4 (Fig. 1 *A* and *B*). Wnt-4, unlike Wnt-1, does not induce the morphological transformation of C57MG cells and has no effect on β-catenin levels (13, 14). Expression of *WISP-1* was up-regulated approximately 3-fold in the C57MG/Wnt-1 cell line and *WISP-2* by approximately 5-fold by both Northern analysis and reverse transcription–PCR.

An independent, but similar, system was used to examine *WISP* expression after Wnt-1 induction. C57MG cells expressing the *Wnt-1* gene under the control of a tetracycline-repressible promoter produce low amounts of Wnt-1 in the repressed state but show a strong induction of *Wnt-1* mRNA and protein within 24 hr after tetracycline removal (8). The levels of Wnt-1 and *WISP* RNA isolated from these cells at various times after tetracycline removal were assessed by quantitative PCR. Strong induction of Wnt-1 mRNA was seen as early as 10 hr after tetracycline removal. Induction of *WISP* mRNA (2- to 6-fold) was seen at 48 and 72 hr (data not shown). These data support our previous observations that show that *WISP* induction is correlated with Wnt-1 expression. Because the induction is slow, occurring after approximately 48 hr, the induction of *WISP*s may be an indirect response to Wnt-1 signaling.

cDNA clones of human *WISP-1* were isolated and the sequence compared with mouse *WISP-1*. The cDNA sequences of mouse and human *WISP-1* were 1,766 and 2,830 bp in length, respectively, and encode proteins of 367 aa, with predicted relative molecular masses of ≈40,000 (M_r 40 K). Both have hydrophobic N-terminal signal sequences, 38 conserved cysteine residues, and four potential N-linked glycosylation sites and are 84% identical (Fig. 2*A*).

Full-length cDNA clones of mouse and human *WISP-2* were 1,734 and 1,293 bp in length, respectively, and encode proteins of 251 and 250 aa, respectively, with predicted relative molecular masses of ≈27,000 (M_r 27 K) (Fig. 2*B*). Mouse and human *WISP-2* are 73% identical. Human *WISP-2* has no potential N-linked glycosylation sites, and mouse *WISP-2* has one at
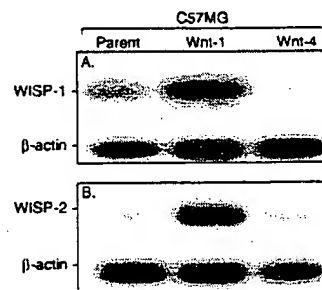

FIG. 1.   *WISP-1* and *WISP-2* are induced by Wnt-1, but not Wnt-4, expression in C57MG cells. Northern analysis of *WISP-1* (*A*) and *WISP-2* (*B*) expression in C57MG, C57MG/Wnt-1, and C57MG/Wnt-4 cells. Poly(A)⁺ RNA (2 μg) was subjected to Northern blot analysis and hybridized with a 70-bp mouse *WISP-1*-specific probe (amino acids 278–300) or a 190-bp *WISP-2*-specific probe (nucleotides 1438–1627) in the 3′ untranslated region. Blots were rehybridized with human β-actin probe.
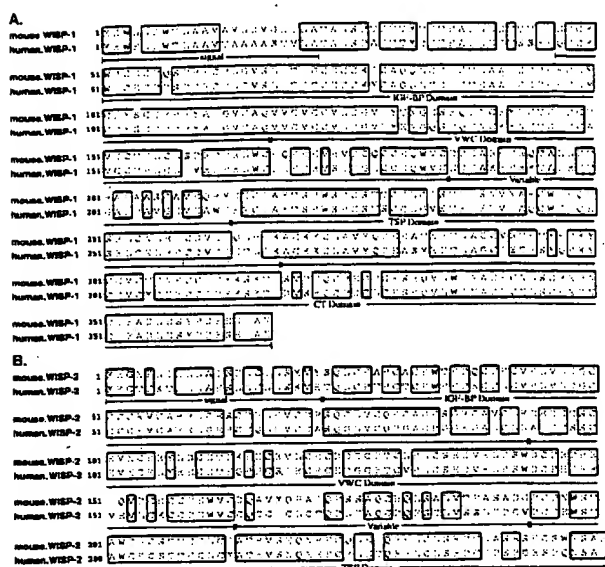
Cell Biology, Medical Sciences: Pennica *et al.*

Proc. Natl. Acad. Sci. USA 95 (1998)   14719

FIG. 2. Encoded amino acid sequence alignment of mouse and human *WISP-1* (*A*) and mouse and human *WISP-2* (*B*). The potential signal sequence, insulin-like growth factor-binding protein (IGF-BP), VWC, thrombospondin (TSP), and C-terminal (CT) domains are underlined.

FIG. 3. (*A*) Encoded amino acid sequence alignment of human WISPs. The cysteine residues of WISP-1 and WISP-2 that are not present in WISP-3 are indicated with a dot. (*B*) Schematic representation of the WISP proteins showing the domain structure and cysteine residues (vertical lines). The four cysteine residues in the VWC domain that are absent in WISP-3 are indicated with a dot. (*C*) Expression of *WISP* mRNA in human tissues. PCR was performed on human multiple-tissue cDNA panels (CLONTECH) from the indicated adult and fetal tissues.

position 197. *WISP-2* has 28 cysteine residues that are conserved among the 38 cysteines found in *WISP-1*.

Identification of *WISP-3*. To search for related proteins, we screened expressed sequence tag (EST) databases with the WISP-1 protein sequence and identified several ESTs as potentially related sequences. We identified a homologous protein that we have called WISP-3. A full-length human *WISP-3* cDNA of 1,371 bp was isolated corresponding to those ESTs that encode a 354-aa protein with a predicted molecular mass of 39,293. WISP-3 has two potential N-linked glycosylation sites and 36 cysteine residues. An alignment of the three human WISP proteins shows that WISP-1 and WISP-3 are the most similar (42% identity), whereas WISP-2 has 37% identity with WISP-1 and 32% identity with WISP-3 (Fig. 3*A*).

WISPs Are Homologous to the CTGF Family of Proteins. Human *WISP-1*, *WISP-2*, and *WISP-3* are novel sequences; however, mouse *WISP-1* is the same as the recently identified *Elm1* gene. *Elm1* is expressed in low, but not high, metastatic mouse melanoma cells, and suppresses the *in vivo* growth and metastatic potential of K-1735 mouse melanoma cells (15). Human and mouse *WISP-2* are homologous to the recently described rat gene, *rCop-1* (16). Significant homology (36–44%) was seen to the CCN family of growth factors. This family includes three members, CTGF, Cyr61, and the protooncogene *nov*. CTGF is a chemotactic and mitogenic factor for fibroblasts that is implicated in wound healing and fibrotic disorders and is induced by TGF-β (17). Cyr61 is an extracellular matrix signaling molecule that promotes cell adhesion, proliferation, migration, angiogenesis, and tumor growth (18, 19). *nov* (nephroblastoma overexpressed) is an immediate early gene associated with quiescence and found altered in Wilms tumors (20). The proteins of the CCN family share functional, but not sequence, similarity to Wnt-1. All are secreted, cysteine-rich heparin binding glycoproteins that associate with the cell surface and extracellular matrix.

WISP proteins exhibit the modular architecture of the CCN family, characterized by four conserved cysteine-rich domains (Fig. 3*B*) (21). The N-terminal domain, which includes the first 12 cysteine residues, contains a consensus sequence (GCGC-CXXC) conserved in most insulin-like growth factor (IGF)-
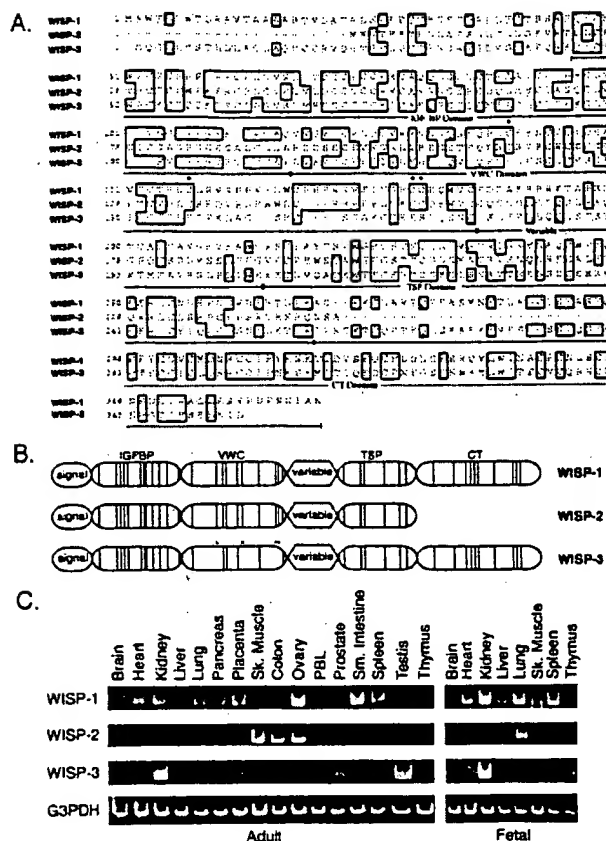
binding proteins (BP). This sequence is conserved in WISP-2 and WISP-3, whereas WISP-1 has a glutamine in the third position instead of a glycine. CTGF recently has been shown to specifically bind IGF (22) and a truncated *nov* protein lacking the IGF-BP domain is oncogenic (23). The von Willebrand factor type C module (VWC), also found in certain collagens and mucins, covers the next 10 cysteine residues, and is thought to participate in protein complex formation and oligomerization (24). The VWC domain of WISP-3 differs from all CCN family members described previously, in that it contains only six of the 10 cysteine residues (Fig. 3 *A* and *B*). A short variable region follows the VWC domain. The third module, the thrombospondin (TSP) domain, is involved in binding to sulfated glycoconjugates and contains six cysteine residues and a conserved WSxCSxxCG motif first identified in thrombospondin (25). The C-terminal (CT) module containing the remaining 10 cysteines is thought to be involved in dimerization and receptor binding (26). The CT domain is present in all CCN family members described to date but is absent in WISP-2 (Fig. 3 *A* and *B*). The existence of a putative signal sequence and the absence of a transmembrane domain suggest that WISPs are secreted proteins, an observation supported by an analysis of their expression and secretion from mammalian cell and baculovirus cultures (data not shown).

Expression of *WISP* mRNA in Human Tissues. Tissue-specific expression of human *WISP*s was characterized by PCR

analysis on adult and fetal multiple tissue cDNA panels. *WISP-1* expression was seen in the adult heart, kidney, lung, pancreas, placenta, ovary, small intestine, and spleen (Fig. 3*C*). Little or no expression was detected in the brain, liver, skeletal muscle, colon, peripheral blood leukocytes, prostate, testis, or thymus. *WISP-2* had a more restricted tissue expression and was detected in adult skeletal muscle, colon, ovary, and fetal lung. Predominant expression of *WISP-3* was seen in adult kidney and testis and fetal kidney. Lower levels of *WISP-3* expression were detected in placenta, ovary, prostate, and small intestine.

In Situ **Localization of *WISP-1* and *WISP-2*.** Expression of *WISP-1* and *WISP-2* was assessed by *in situ* hybridization in mammary tumors from Wnt-1 transgenic mice. Strong expression of *WISP-1* was observed in stromal fibroblasts lying within the fibrovascular tumor stroma (Fig. 4 *A–D*). However, low-level *WISP-1* expression also was observed focally within tumor cells (data not shown). No expression was observed in normal breast. Like *WISP-1*, *WISP-2* expression also was seen in the tumor stroma in breast tumors from Wnt-1 transgenic animals (Fig. 4 *E–H*). However, *WISP-2* expression in the stroma was in spindle-shaped cells adjacent to capillary vessels, whereas

the predominant cell type expressing *WISP-1* was the stromal fibroblasts.

Chromosome Localization of the *WISP* Genes. The chromosomal location of the human *WISP* genes was determined by radiation hybrid mapping panels. *WISP-1* is approximately 3.48 cR from the meiotic marker AFM259xc5 [logarithm of odds (lod) score 16.31] on chromosome 8q24.3, in the same region as the human locus of the *novH* family member (27) and roughly 4 Mbs distal to c-*myc* (28). Preliminary fine mapping indicates that *WISP-1* is located near D8S1712 STS. *WISP-2* is linked to the marker SHGC-33922 (lod = 1,000) on chromosome 20q12–20q13.1. Human *WISP-3* mapped to chromosome 6q22–6q23 and is linked to the marker AFM211ze5 (lod = 1,000). *WISP-3* is approximately 18 Mbs proximal to CTGF and 23 Mbs proximal to the human cellular oncogene *MYB* (27, 29).

Amplification and Aberrant Expression of *WISPs* in Human Colon Tumors. Amplification of protooncogenes is seen in many human tumors and has etiological and prognostic significance. For example, in a variety of tumor types, c-*myc* amplification has been associated with malignant progression and poor prognosis (30). Because *WISP-1* resides in the same general chromosomal location (8q24) as c-*myc*, we asked whether it was a target of gene amplification, and, if so, whether this amplification was independent of the c-*myc* locus. Genomic DNA from human colon cancer cell lines was assessed by quantitative PCR and Southern blot analysis. (Fig. 5 *A* and *B*). Both methods detected similar degrees of *WISP-1* amplification. Most cell lines showed significant (2- to 4-fold) amplification, with the HT-29 and WiDr cell lines demonstrating an 8-fold increase. Significantly, the pattern of amplification observed did not correlate with that observed for c-*myc*, indicating that the c-*myc* gene is not part of the amplicon that involves the *WISP-1* locus.

We next examined whether the *WISP* genes were amplified in a panel of 25 primary human colon adenocarcinomas. The relative *WISP* gene copy number in each colon tumor DNA was compared with pooled normal DNA from 10 donors by quantitative PCR (Fig. 6). The copy number of *WISP-1* and *WISP-2* was significantly greater than one, approximately 2-fold for *WISP-1* in about 60% of the tumors and 2- to 4-fold for *WISP-2* in 92% of the tumors ($P < 0.001$ for each). The copy number for *WISP-3* was indistinguishable from one ($P = 0.166$). In addition, the copy number of *WISP-2* was significantly higher than that of *WISP-1* ($P < 0.001$).

The levels of *WISP* transcripts in RNA isolated from 19 adenocarcinomas and their matched normal mucosa were
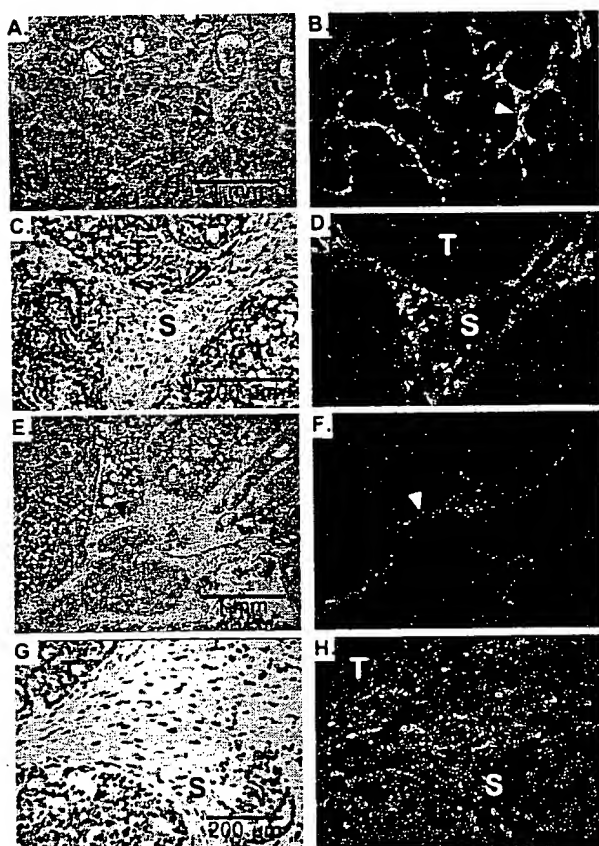
FIG. 4.   (*A*, *C*, *E*, and *G*) Representative hematoxylin/eosin-stained images from breast tumors in Wnt-1 transgenic mice. The corresponding dark-field images showing *WISP-1* expression are shown in *B* and *D*. The tumor is a moderately well-differentiated adenocarcinoma showing evidence of adenoid cystic change. At low power (*A* and *B*), expression of *WISP-1* is seen in the delicate branching fibrovascular tumor stroma (arrowhead). At higher magnification, expression is seen in the stromal(s) fibroblasts (*C* and *D*), and tumor cells are negative. Focal expression of *WISP-1*, however, was observed in tumor cells in some areas. Images of *WISP-2* expression are shown in *E–H*. At low power (*E* and *F*), expression of WISP-2 is seen in cells lying within the fibrovascular tumor stroma. At higher magnification, these cells appeared to be adjacent to capillary vessels whereas tumor cells are negative (*G* and *H*).
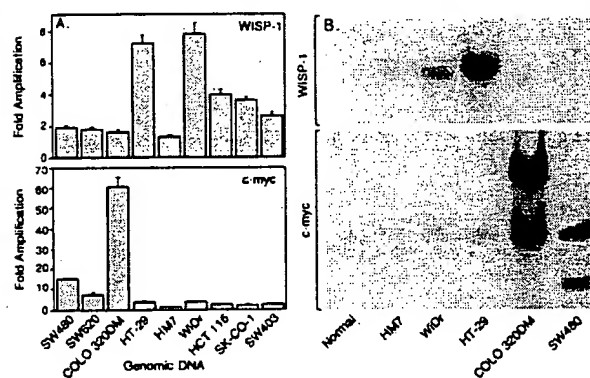
FIG. 5.   Amplification of *WISP-1* genomic DNA in colon cancer cell lines. (*A*) Amplification in cell line DNA was determined by quantitative PCR. (*B*) Southern blots containing genomic DNA (10 μg) digested with *Eco*RI (*WISP-1*) or *Xba*I (c-*myc*) were hybridized with a 100-bp human *WISP-1* probe (amino acids 186–219) or a human c-*myc* probe (located at bp 1901–2000). The *WISP* and *myc* genes are detected in normal human genomic DNA after a longer film exposure.
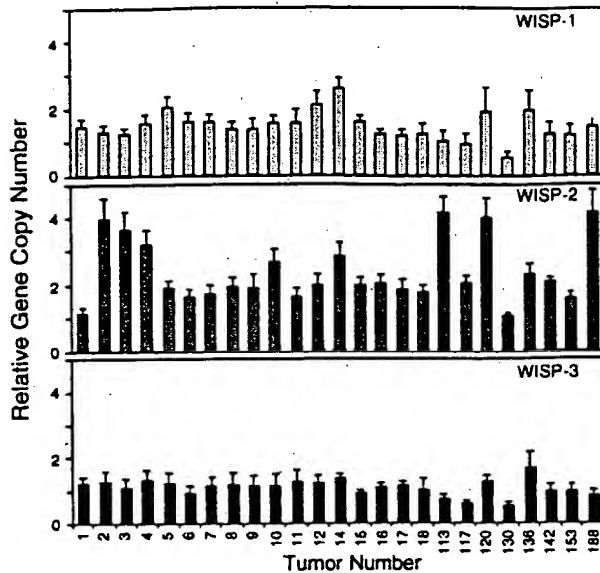
Cell Biology, Medical Sciences: Pennica *et al.*

Proc. Natl. Acad. Sci. USA 95 (1998)   14721

mucosa. The amount of overexpression of *WISP-3* ranged from 4- to >40-fold.

DISCUSSION

One approach to understanding the molecular basis of cancer is to identify differences in gene expression between cancer cells and normal cells. Strategies based on assumptions that steady-state mRNA levels will differ between normal and malignant cells have been used to clone differentially expressed genes (31). We have used a PCR-based selection strategy, SSH, to identify genes selectively expressed in C57MG mouse mammary epithelial cells transformed by Wnt-1.

Three of the genes isolated, *WISP-1*, *WISP-2*, and *WISP-3*, are members of the CCN family of growth factors, which includes CTGF, Cyr61, and *nov*, a family not previously linked to Wnt signaling.

Two independent experimental systems demonstrated that *WISP* induction was associated with the expression of Wnt-1. The first was C57MG cells infected with a Wnt-1 retroviral vector or C57MG cells expressing Wnt-1 under the control of a tetracyline-repressible promoter, and the second was in Wnt-1 transgenic mice, where breast tissue expresses Wnt-1, whereas normal breast tissue does not. No *WISP* RNA expression was detected in mammary tumors induced by polyoma virus middle T antigen (data not shown). These data suggest a link between Wnt-1 and *WISPs* in that in these two situations, *WISP* induction was correlated with Wnt-1 expression.

It is not clear whether the *WISPs* are directly or indirectly induced by the downstream components of the Wnt-1 signaling pathway (i.e., β-catenin-TCF-1/Lef1). The increased levels of *WISP* RNA were measured in Wnt-1-transformed cells, hours or days after Wnt-1 transformation. Thus, *WISP* expression could result from Wnt-1 signaling directly through β-catenin transcription factor regulation or alternatively through Wnt-1 signaling turning on a transcription factor, which in turn regulates *WISPs*.

The *WISPs* define an additional subfamily of the CCN family of growth factors. One striking difference observed in the protein sequence of WISP-2 is the absence of a CT domain, which is present in CTGF, Cyr61, *nov*, WISP-1, and WISP-3. This domain is thought to be involved in receptor binding and dimerization. Growth factors, such as TGF-β, platelet-derived growth factor, and nerve growth factor, which contain a cystine knot motif exist as dimers (32). It is tempting to speculate that WISP-1 and WISP-3 may exist as dimers, whereas WISP-2 exists as a monomer. If the CT domain is also important for receptor binding, WISP-2 may bind its receptor through a different region of the molecule than the other CCN family members. No specific receptors have been identified for CTGF or *nov*. A recent report has shown that integrin $\alpha_v\beta_3$ serves as an adhesion receptor for Cyr61 (33).

The strong expression of *WISP-1* and *WISP-2* in cells lying within the fibrovascular tumor stroma in breast tumors from Wnt-1 transgenic animals is consistent with previous observations that transcripts for the related CTGF gene are primarily expressed in the fibrous stroma of mammary tumors (34). Epithelial cells are thought to control the proliferation of connective tissue stroma in mammary tumors by a cascade of growth factor signals similar to that controlling connective tissue formation during wound repair. It has been proposed that mammary tumor cells or inflammatory cells at the tumor interstitial interface secrete TGF-β1, which is the stimulus for stromal proliferation (34). TGF-β1 is secreted by a large percentage of malignant breast tumors and may be one of the growth factors that stimulates the production of CTGF and WISPs in the stroma.

It was of interest that *WISP-1* and *WISP-2* expression was observed in the stromal cells that surrounded the tumor cells

FIG. 6. Genomic amplification of *WISP* genes in human colon tumors. The relative gene copy number of the *WISP* genes in 25 adenocarcinomas was assayed by quantitative PCR, by comparing DNA from primary human tumors with pooled DNA from 10 healthy donors. The data are means ± SEM from one experiment done in triplicate. The experiment was repeated at least three times.

assessed by quantitative PCR (Fig. 7). The level of *WISP-1* RNA present in tumor tissue varied but was significantly increased (2- to >25-fold) in 84% (16/19) of the human colon tumors examined compared with normal adjacent mucosa. Four of 19 tumors showed greater than 10-fold overexpression. In contrast, in 79% (15/19) of the tumors examined, *WISP-2* RNA expression was significantly lower in the tumor than the mucosa. Similar to *WISP-1*, *WISP-3* RNA was overexpressed in 63% (12/19) of the colon tumors compared with the normal
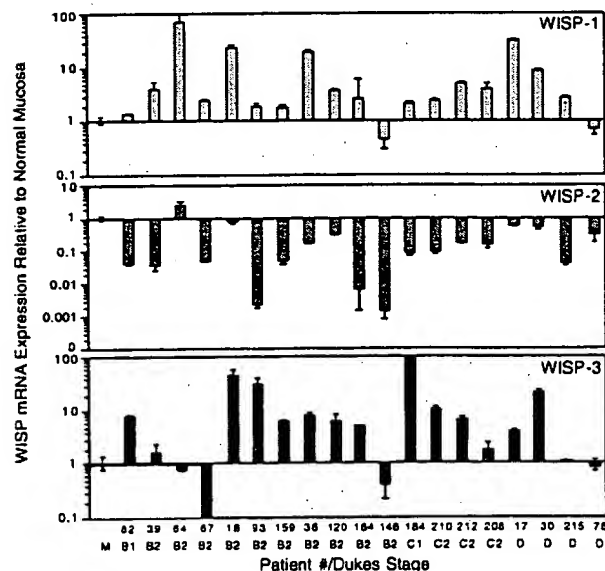
FIG. 7. *WISP* RNA expression in primary human colon tumors relative to expression in normal mucosa from the same patient. Expression of *WISP* mRNA in 19 adenocarcinomas was assayed by quantitative PCR. The Dukes stage of the tumor is listed under the sample number. The data are means ± SEM from one experiment done in triplicate. The experiment was repeated at least twice.

(epithelial cells) in the Wnt-1 transgenic mouse sections of breast tissue. This finding suggests that paracrine signaling could occur in which the stromal cells could supply WISP-1 and WISP-2 to regulate tumor cell growth on the WISP extracellular matrix. Stromal cell-derived factors in the extracellular matrix have been postulated to play a role in tumor cell migration and proliferation (35). The localization of *WISP-1* and *WISP-2* in the stromal cells of breast tumors supports this paracrine model.

An analysis of *WISP-1* gene amplification and expression in human colon tumors showed a correlation between DNA amplification and overexpression, whereas overexpression of *WISP-3* RNA was seen in the absence of DNA amplification. In contrast, *WISP-2* DNA was amplified in the colon tumors, but its mRNA expression was significantly reduced in the majority of tumors compared with the expression in normal colonic mucosa from the same patient. The gene for human *WISP-2* was localized to chromosome 20q12–20q13, at a region frequently amplified and associated with poor prognosis in node negative breast cancer and many colon cancers, suggesting the existence of one or more oncogenes at this locus (36–38). Because the center of the 20q13 amplicon has not yet been identified, it is possible that the apparent amplification observed for *WISP-2* may be caused by another gene in this amplicon.

A recent manuscript on *rCop-1*, the rat orthologue of *WISP-2*, describes the loss of expression of this gene after cell transformation, suggesting it may be a negative regulator of growth in cell lines (16). Although the mechanism by which *WISP-2* RNA expression is down-regulated during malignant transformation is unknown, the reduced expression of *WISP-2* in colon tumors and cell lines suggests that it may function as a tumor suppressor. These results show that the *WISP* genes are aberrantly expressed in colon cancer and suggest that their altered expression may confer selective growth advantage to the tumor.

Members of the Wnt signaling pathway have been implicated in the pathogenesis of colon cancer, breast cancer, and melanoma, including the tumor suppressor gene adenomatous polyposis coli and β-catenin (39). Mutations in specific regions of either gene can cause the stabilization and accumulation of cytoplasmic β-catenin, which presumably contributes to human carcinogenesis through the activation of target genes such as the *WISPs*. Although the mechanism by which Wnt-1 transforms cells and induces tumorigenesis is unknown, the identification of *WISPs* as genes that may be regulated downstream of Wnt-1 in C57MG cells suggests they could be important mediators of Wnt-1 transformation. The amplification and altered expression patterns of the *WISPs* in human colon tumors may indicate an important role for these genes in tumor development.

1. Cadigan, K. M. & Nusse, R. (1997) *Genes Dev.* 11, 3286–3305.
2. Dale, T. C. (1998) *Biochem. J.* 329, 209–223.
3. Nusse, R. & Varmus, H. E. (1982) *Cell* 31, 99–109.
4. van Ooyen, A. & Nusse, R. (1984) *Cell* 39, 233–240.
5. Tsukamoto, A. S., Grosschedl, R., Guzman, R. C., Parslow, T. & Varmus, H. E. (1988) *Cell* 55, 619–625.
6. Brown, J. D. & Moon, R. T. (1998) *Curr. Opin. Cell. Biol.* 10, 182–187.
7. Molenaar, M., van de Wetering, M., Oosterwegel, M., Peterson-Maduro, J., Godsave, S., Korinek, V., Roose, J., Destree, O. & Clevers, H. (1996) *Cell* 86, 391–399.
8. Korinek, V., Barker, N., Willert, K., Molenaar, M., Roose, J., Wagenaar, G., Markman, M., Lamers, W., Destree, O. & Clevers, H. (1998) *Mol. Cell. Biol.* 18, 1248–1256.
9. Munemitsu, S., Albert, I., Souza, B., Rubinfeld, B. & Polakis, P. (1995) *Proc. Natl. Acad. Sci. USA* 92, 3046–3050.
10. He, T. C., Sparks, A. B., Rago, C., Hermeking, H., Zawel, L., da Costa, L. T., Morin, P. J., Vogelstein, B. & Kinzler, K. W. (1998) *Science* 281, 1509–1512.
11. Diatchenko, L., Lau, Y. F., Campbell, A. P., Chenchik, A., Moqadam, F., Huang, B., Lukyanov, S., Lukyanov, K., Gurskaya, N., Sverdlov, E. D. & Siebert, P. D. (1996) *Proc. Natl. Acad. Sci. USA* 93, 6025–6030.
12. Brown, A. M., Wildin, R. S., Prendergast, T. J. & Varmus, H. E. (1986) *Cell* 46, 1001–1009.
13. Wong, G. T., Gavin, B. J. & McMahon, A. P. (1994) *Mol. Cell. Biol.* 14, 6278–6286.
14. Shimizu, H., Julius, M. A., Giarre, M., Zheng, Z., Brown, A. M. & Kitajewski, J. (1997) *Cell Growth Differ.* 8, 1349–1358.
15. Hashimoto, Y., Shindo-Okada, N., Tani, M., Nagamachi, Y., Takeuchi, K., Shiroishi, T., Toma, H. & Yokota, J. (1998) *J. Exp. Med.* 187, 289–296.
16. Zhang, R., Averboukh, L., Zhu, W., Zhang, H., Jo, H., Dempsey, P. J., Coffey, R. J., Pardee, A. B. & Liang, P. (1998) *Mol. Cell. Biol.* 18, 6131–6141.
17. Grotendorst, G. R. (1997) *Cytokine Growth Factor Rev.* 8, 171–179.
18. Kireeva, M. L., Mo, F. E., Yang, G. P. & Lau, L. F. (1996) *Mol. Cell. Biol.* 16, 1326–1334.
19. Babic, A. M., Kireeva, M. L., Kolesnikova, T. V. & Lau, L. F. (1998) *Proc. Natl. Acad. Sci. USA* 95, 6355–6360.
20. Martinerie, C., Huff, V., Joubert, I., Badzioch, M., Saunders, G., Strong, L. & Perbal, B. (1994) *Oncogene* 9, 2729–2732.
21. Bork, P. (1993) *FEBS Lett.* 327, 125–130.
22. Kim, H. S., Nagalla, S. R., Oh, Y., Wilson, E., Roberts, C. T., Jr. & Rosenfeld, R. G. (1997) *Proc. Natl. Acad. Sci. USA* 94, 12981–12986.
23. Joliot, V., Martinerie, C., Dambrine, G., Plassiart, G., Brisac, M., Crochet, J. & Perbal, B. (1992) *Mol. Cell. Biol.* 12, 10–21.
24. Mancuso, D. J., Tuley, E. A., Westfield, L. A., Worrall, N. K., Shelton-Inloes, B. B., Sorace, J. M., Alevy, Y. G. & Sadler, J. E. (1989) *J. Biol. Chem.* 264, 19514–19527.
25. Holt, G. D., Pangburn, M. K. & Ginsburg, V. (1990) *J. Biol. Chem.* 265, 2852–2855.
26. Voorberg, J., Fontijn, R., Calafat, J., Janssen, H., van Mourik, J. A. & Pannekoek, H. (1991) *J. Cell. Biol.* 113, 195–205.
27. Martinerie, C., Viegas-Pequignot, E., Guenard, I., Dutrillaux, B., Nguyen, V. C., Bernheim, A. & Perbal, B. (1992) *Oncogene* 7, 2529–2534.
28. Takahashi, E., Hori, T., O'Connell, P., Leppert, M. & White, R. (1991) *Cytogenet. Cell. Genet.* 57, 109–111.
29. Meese, E., Meltzer, P. S., Witkowski, C. M. & Trent, J. M. (1989) *Genes Chromosomes Cancer* 1, 88–94.
30. Garte, S. J. (1993) *Crit. Rev. Oncog.* 4, 435–449.
31. Zhang, L., Zhou, W., Velculescu, V. E., Kern, S. E., Hruban, R. H., Hamilton, S. R., Vogelstein, B. & Kinzler, K. W. (1997) *Science* 276, 1268–1272.
32. Sun, P. D. & Davies, D. R. (1995) *Annu. Rev. Biophys. Biomol. Struct.* 24, 269–291.
33. Kireeva, M. L., Lam, S. C. T. & Lau, L. F. (1998) *J. Biol. Chem.* 273, 3090–3096.
34. Frazier, K. S. & Grotendorst, G. R. (1997) *Int. J. Biochem. Cell. Biol.* 29, 153–161.
35. Wernert, N. (1997) *Virchows Arch.* 430, 433–443.
36. Tanner, M. M., Tirkkonen, M., Kallioniemi, A., Collins, C., Stokke, T., Karhu, R., Kowbel, D., Shadravan, F., Hintz, M., Kuo, W. L., *et al.* (1994) *Cancer Res.* 54, 4257–4260.
37. Brinkmann, U., Gallo, M., Polymeropoulos, M. H. & Pastan, I. (1996) *Genome Res.* 6, 187–194.
38. Bischoff, J. R., Anderson, L., Zhu, Y., Mossie, K., Ng, L., Souza, B., Schryver, B., Flanagan, P., Clairvoyant, F., Ginther, C., *et al.* (1998) *EMBO J.* 17, 3052–3065.
39. Morin, P. J., Sparks, A. B., Korinek, V., Barker, N., Clevers, H., Vogelstein, B. & Kinzler, K. W. (1997) *Science* 275, 1787–1790.
40. Lu, L. H. & Gillett, N. (1994) *Cell Vision* 1, 169–176.

methods. Peptides AENK or AEQK were dissolved in water, made isotonic with NaCl and diluted into RPMl growth medium. T-cell-proliferation assays were done essentially as described[20,21]. Briefly, after antigen pulsing (30 μg ml^{-1} TTCF) with tetrapeptides (1–2 mg ml^{-1}), PBMCs or EBV-B cells were washed in PBS and fixed for 45 s in 0.05% glutaraldehyde. Glycine was added to a final concentration of 0.1M and the cells were washed five times in RPMI 1640 medium containing 1% FCS before co-culture with T-cell clones in round-bottom 96-well microtitre plates. After 48 h, the cultures were pulsed with 1 μCi of ^{3}H-thymidine and harvested for scintillation counting 16 h later. Predigestion of native TTCF was done by incubating 200 μg TTCF with 0.25 μg pig kidney legumain in 500 μl 50 mM citrate buffer, pH 5.5, for 1 h at 37 °C.

Glycopeptide digestions. The peptides HIDNEEDI, HIDN(N-glucosamine) EEDI and HIDNESDI, which are based on the TTCF sequence, and QQQHLFGSNVTDCSGNFCLFR(KKK), which is based on human transferrin, were obtained by custom synthesis. The three C-terminal lysine residues were added to the natural sequence to aid solubility. The transferrin glycopeptide QQQHLFGSNVTDCSGNFCLFR was prepared by tryptic (Promega) digestion of 5 mg reduced, carboxy-methylated human transferrin followed by concanavalin A chromatography[11]. Glycopeptides corresponding to residues 622–642 and 421–452 were isolated by reverse-phase HPLC and identified by mass spectrometry and N-terminal sequencing. The lyophilized transferrin-derived peptides were redissolved in 50 mM sodium acetate, pH 5.5, 10 mM dithiothreitol, 20% methanol. Digestions were performed for 3 h at 30 °C with 5–50 mU ml^{-1} pig kidney legumain or B-cell AEP. Products were analysed by HPLC or MALDI-TOF mass spectrometry using a matrix of 10 mg ml^{-1} α-cyanocinnamic acid in 50% acetonitrile/0.1% TFA and a PerSeptive Biosystems Elite STR mass spectrometer set to linear or reflector mode. Internal standardization was obtained with a matrix ion of 568.13 mass units.

1. Chen, J. M. et al. Cloning, isolation, and characterisation of mammalian legumain, an asparaginyl endopeptidase. J. Biol. Chem. 272, 8090–8098 (1997).
2. Kembhavi, A. A., Buttle, D. J., Knight, C. G. & Barrett, A. J. The two cysteine endopeptidases of legume seeds: purification and characterization by use of specific fluorometric assays. Arch. Biochem. Biophys. 303, 208–213 (1993).
3. Dalton, J. P., Hola Jamriska, L. & Bridley, P. J. Asparaginyl endopeptidase activity in adult Schistosoma mansoni. Parasitology 111, 575–580 (1995).
4. Bennett, K. et al. Antigen processing for presentation by class II major histocompatibility complex requires cleavage by cathepsin E. Eur. J. Immunol. 22, 1519–1524 (1992).
5. Riese, R. J. et al. Essential role for cathepsin S in MHC class II-associated invariant chain processing and peptide loading. Immunity 4, 357–366 (1996).
6. Rodriguez, G. M. & Diment, S. Role of cathepsin D in antigen presentation of ovalbumin. J. Immunol. 149, 2894–2898 (1992).
7. Hewitt, E. W. et al. Natural processing sites for human cathepsin E and cathepsin D in tetanus toxin: implications for T cell epitope generation. J. Immunol. 159, 4693–4699 (1997).
8. Watts, C. Capture and processing of exogenous antigens for presentation on MHC molecules. Annu. Rev. Immunol. 15, 821–850 (1997).
9. Chapman, H. A. Endosomal proteases and MHC class II function. Curr. Opin. Immunol. 10, 93–102 (1998).
10. Fineschi, B. & Miller, J. Endosomal proteases and antigen processing. Trends Biochem. Sci. 22, 377–382 (1997).
11. Lu, J. & van Halbeek, H. Complete ^{1}H and ^{13}C resonance assignments of a 21-amino acid glycopeptide prepared from human serum transferrin. Carbohydr. Res. 296, 1–21 (1996).
12. Fearon, D. T. & Locksley, R. M. The instructive role of innate immunity in the acquired immune response. Science 272, 50–54 (1996).
13. Medzhitov, R. & Janeway, C. A. J. Innate immunity: the virtues of a nonclonal system of recognition. Cell 91, 295–298 (1997).
14. Wyatt, R. et al. The antigenic structure of the HIV gp120 envelope glycoprotein. Nature 393, 705–711 (1998).
15. Botarelli, P. et al. N-glycosylation of HIV gp120 may constrain recognition by T lymphocytes. J. Immunol. 147, 3128–3132 (1991).
16. Davidson, H. W., West, M. A. & Watts, C. Endocytosis, intracellular trafficking, and processing of membrane IgG and monovalent antigen/membrane IgG complexes in B lymphocytes. J. Immunol. 144, 4101–4109 (1990).
17. Barrett, A. J. & Kirschke, H. Cathepsin B, cathepsin H and cathepsin L. Methods Enzymol. 80, 535–559 (1981).
18. Makoff, A. J., Ballantine, S. P., Smallwood, A. E. & Fairweather, N. F. Expression of tetanus toxin fragment C in E. coli: its purification and potential use as a vaccine. Biotechnology 7, 1043–1046 (1989).
19. Lane, D. P. & Harlow, E. Antibodies: A Laboratory Manual (Cold Spring Harbor Laboratory Press, 1988).
20. Lanzavecchia, A. Antigen-specific interaction between T and B cells. Nature 314, 537–539 (1985).
21. Pond, L. & Watts, C. Characterization of transport of newly assembled, T cell-stimulatory MHC class II-peptide complexes from MHC class II compartments to the cell surface. J. Immunol. 159, 543–553 (1997).

Genomic amplification of a decoy receptor for Fas ligand in lung and colon cancer

Robert M. Pitti*†, Scot A. Marsters*†, David A. Lawrence*†, Margaret Roy*, Frank C. Kischkel*, Patrick Dowd*, Arthur Huang*, Christopher J. Donahue*, Steven W. Sherwood*, Daryl T. Baldwin*, Paul J. Godowski*, William I. Wood*, Austin L. Gurney*, Kenneth J. Hillan*, Robert L. Cohen*, Audrey D. Goddard*, David Botstein‡ & Avi Ashkenazi*

* Departments of Molecular Oncology, Molecular Biology, and Immunology, Genentech Inc., 1 DNA Way, South San Francisco, California 94080, USA
‡ Department of Genetics, Stanford University, Stanford, California 94305, USA
† These authors contributed equally to this work

Fas ligand (FasL) is produced by activated T cells and natural killer cells and it induces apoptosis (programmed cell death) in target cells through the death receptor Fas/Apo1/CD95 (ref. 1). One important role of FasL and Fas is to mediate immune-cytotoxic killing of cells that are potentially harmful to the organism, such as virus-infected or tumour cells[1]. Here we report the discovery of a soluble decoy receptor, termed decoy receptor 3 (DcR3), that binds to FasL and inhibits FasL-induced apoptosis. The DcR3 gene was amplified in about half of 35 primary lung and colon tumours studied, and DcR3 messenger RNA was expressed in malignant tissue. Thus, certain tumours may escape FasL-dependent immune-cytotoxic attack by expressing a decoy receptor that blocks FasL.

By searching expressed sequence tag (EST) databases, we identified a set of related ESTs that showed homology to the tumour necrosis factor (TNF) receptor (TNFR) gene superfamily[2]. Using the overlapping sequence, we isolated a previously unknown full-length complementary DNA from human fetal lung. We named the protein encoded by this cDNA decoy receptor 3 (DcR3). The cDNA encodes a 300-amino-acid polypeptide that resembles members of the TNFR family (Fig. 1a): the amino terminus contains a leader sequence, which is followed by four tandem cysteine-rich domains (CRDs). Like one other TNFR homologue, osteoprotegerin (OPG)[3], DcR3 lacks an apparent transmembrane sequence, which indicates that it may be a secreted, rather than a membrane-asscociated, molecule. We expressed a recombinant, histidine-tagged form of DcR3 in mammalian cells; DcR3 was secreted into the cell culture medium, and migrated on polyacrylamide gels as a protein of relative molecular mass 35,000 (data not shown). DcR3 shares sequence identity in particular with OPG (31%) and TNFR2 (29%), and has relatively less homology with Fas (17%). All of the cysteines in the four CRDs of DcR3 and OPG are conserved; however, the carboxy-terminal portion of DcR3 is 101 residues shorter.

We analysed expression of DcR3 mRNA in human tissues by northern blotting (Fig. 1b). We detected a predominant 1.2-kilobase transcript in fetal lung, brain, and liver, and in adult spleen, colon and lung. In addition, we observed relatively high DcR3 mRNA expression in the human colon carcinoma cell line SW480.

To investigate potential ligand interactions of DcR3, we generated a recombinant, Fc-tagged DcR3 protein. We tested binding of DcR3–Fc to human 293 cells transfected with individual TNF-family ligands, which are expressed as type 2 transmembrane proteins (these transmembrane proteins have their N termini in the cytosol). DcR3–Fc showed a significant increase in binding to cells transfected with FasL[4] (Fig. 2a), but not to cells transfected with TNF[5], Apo2L/TRAIL[6,7], Apo3L/TWEAK[8,9], or OPGL/TRANCE/

RANKL[10-12] (data not shown). DcR3–Fc immunoprecipitated shed FasL from FasL-transfected 293 cells (Fig. 2b) and purified soluble FasL (Fig. 2c), as did the Fc-tagged ectodomain of Fas but not TNFR1. Gel-filtration chromatography showed that DcR3–Fc and soluble FasL formed a stable complex (Fig. 2d). Equilibrium analysis indicated that DcR3–Fc and Fas–Fc bound to soluble FasL with a comparable affinity ($K_d = 0.8 \pm 0.2$ and $1.1 \pm 0.1 \, nM$, respectively; Fig. 2e), and that DcR3–Fc could block nearly all of the binding of soluble FasL to Fas–Fc (Fig. 2e, inset). Thus, DcR3 competes with Fas for binding to FasL.

To determine whether binding of DcR3 inhibits FasL activity, we tested the effect of DcR3–Fc on apoptosis induction by soluble FasL in Jurkat T leukaemia cells, which express Fas (Fig. 3a). DcR3–Fc and Fas–Fc blocked soluble-FasL-induced apoptosis in a similar dose-dependent manner, with half-maximal inhibition at $\sim 0.1 \, \mu g \, ml^{-1}$. Time-course analysis showed that the inhibition did not merely delay cell death, but rather persisted for at least 24 hours (Fig. 3b). We also tested the effect of DcR3–Fc on activation-induced cell death (AICD) of mature T lymphocytes, a FasL-dependent process[1]. Consistent with previous results[13], activation of interleukin-2-stimulated CD4-positive T cells with anti-CD3 antibody increased the level of apoptosis twofold, and Fas–Fc blocked this effect substantially (Fig. 3c); DcR3–Fc blocked the

induction of apoptosis to a similar extent. Thus, DcR3 binding blocks apoptosis induction by FasL.

FasL-induced apoptosis is important in elimination of virus-infected cells and cancer cells by natural killer cells and cytotoxic T lymphocytes; an alternative mechanism involves perforin and granzymes[1,14-16]. Peripheral blood natural killer cells triggered marked cell death in Jurkat T leukaemia cells (Fig. 3d); DcR3–Fc and Fas–Fc each reduced killing of target cells from ~65% to ~30%, with half-maximal inhibition at $\sim 1 \, \mu g \, ml^{-1}$; the residual killing was probably mediated by the perforin/granzyme pathway. Thus, DcR3 binding blocks FasL-dependent natural killer cell activity. Higher DcR3–Fc and Fas–Fc concentrations were required to block natural killer cell activity compared with those required to block soluble FasL activity, which is consistent with the greater potency of membrane-associated FasL compared with soluble FasL[17].

Given the role of immune-cytotoxic cells in elimination of tumour cells and the fact that DcR3 can act as an inhibitor of FasL, we proposed that DcR3 expression might contribute to the ability of some tumours to escape immune-cytotoxic attack. As genomic amplification frequently contributes to tumorigenesis, we investigated whether the DcR3 gene is amplified in cancer. We analysed DcR3 gene-copy number by quantitative polymerase chain
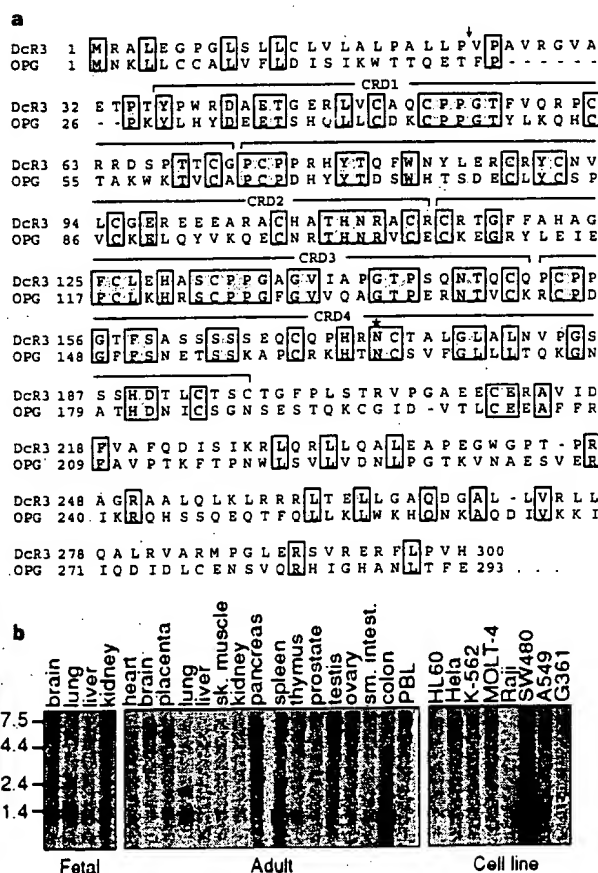

Figure 2 Interaction of DcR3 with FasL. **a**, 293 cells were transfected with pRK5 vector (top) or with pRK5 encoding full-length FasL (bottom), incubated with DcR3-Fc (solid line, shaded area), TNFR1-Fc (dotted line) or buffer control (dashed line) (the dashed and dotted lines overlap), and analysed for binding by FACS. Statistical analysis showed a significant difference ($P < 0.001$) between the binding of DcR3-Fc to cells transfected with FasL or pRK5. PE, phycoerythrin-labelled cells. **b**, 293 cells were transfected as in **a** and metabolically labelled, and cell supernatants were immunoprecipitated with Fc-tagged TNFR1, DcR3 or Fas. **c**, Purified soluble FasL (sFasL) was immunoprecipitated with TNFR1-Fc, DcR3-Fc or Fas-Fc and visualized by immunoblot with anti-FasL antibody. sFasL was loaded directly for comparison in the right-hand lane. **d**, Flag-tagged sFasL was incubated with DcR3-Fc or with buffer and resolved by gel filtration; column fractions were analysed in an assay that detects complexes containing DcR3-Fc and sFasL-Flag. **e**, Equilibrium binding of DcR3-Fc or Fas-Fc to sFasL-Flag. Inset, competition of DcR3-Fc with Fas-Fc for binding to sFasL-Flag.

Figure 1 Primary structure and expression of human DcR3. **a**, Alignment of the amino-acid sequences of DcR3 and of osteoprotegerin (OPG); the C-terminal 101 residues of OPG are not shown. The putative signal cleavage site (arrow), the cysteine-rich domains (CRD 1–4), and the N-linked glycosylation site (asterisk) are shown. **b**, Expression of DcR3 mRNA. Northern hybridization analysis was done using the DcR3 cDNA as a probe and blots of poly(A)⁺ RNA (Clontech) from human fetal and adult tissues or cancer cell lines. PBL, peripheral blood lymphocyte.
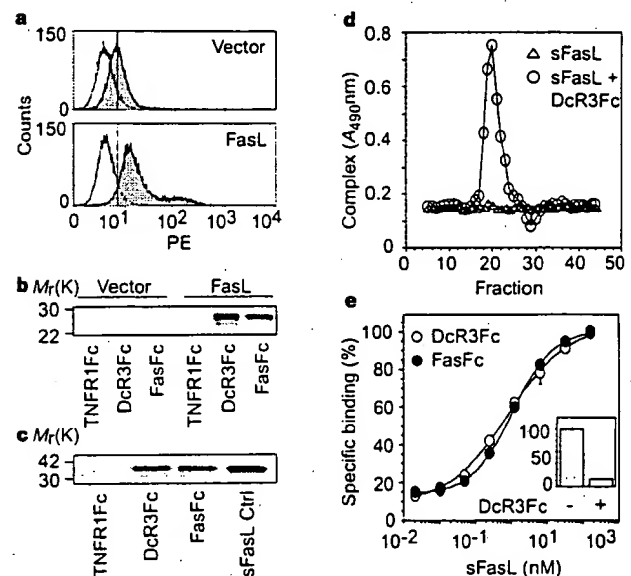
reaction (PCR)[18] in genomic DNA from 35 primary lung and colon tumours, relative to pooled genomic DNA from peripheral blood leukocytes (PBLs) of 10 healthy donors. Eight of 18 lung tumours and 9 of 17 colon tumours showed DcR3 gene amplification, ranging from 2- to 18-fold (Fig. 4a, b). To confirm this result, we analysed the colon tumour DNAs with three more, independent sets of DcR3-based PCR primers and probes; we observed nearly the same amplification (data not shown).

We then analysed DcR3 mRNA expression in primary tumour tissue sections by *in situ* hybridization. We detected DcR3 expression in 6 out of 15 lung tumours, 2 out of 2 colon tumours, 2 out of 5 breast tumours, and 1 out of 1 gastric tumour (data not shown). A section through a squamous-cell carcinoma of the lung is shown in Fig. 4c. DcR3 mRNA was localized to infiltrating malignant epithelium, but was essentially absent from adjacent stroma, indicating tumour-specific expression. Although the individual tumour specimens that we analysed for mRNA expression and gene amplification were different, the *in situ* hybridization results are consistent with the finding that the DcR3 gene is amplified frequently in tumours. SW480 colon carcinoma cells, which showed abundant DcR3 mRNA expression (Fig. 1b), also had marked DcR3 gene amplification, as shown by quantitative PCR (fourfold) and by Southern blot hybridization (fivefold) (data not shown).

If DcR3 amplification in cancer is functionally relevant, then DcR3 should be amplified more than neighbouring genomic regions that are not important for tumour survival. To test this, we mapped the human DcR3 gene by radiation-hybrid analysis; DcR3 showed linkage to marker AFM218xe7 (T160), which maps to chromosome position 20q13. Next, we isolated from a bacterial artificial chromosome (BAC) library a human genomic clone that carries DcR3, and sequenced the ends of the clone's insert. We then determined, from the nine colon tumours that showed twofold or greater amplification of DcR3, the copy number of the DcR3-flanking sequences (reverse and forward) from the BAC, and of seven genomic markers that span chromosome 20 (Fig. 4d). The DcR3-linked reverse marker showed an average amplification of roughly threefold, slightly less than the approximately fourfold amplification of DcR3; the other markers showed little or no amplification. These data indicate that DcR3 may be at the 'epicentre' of a distal chromosome 20 region that is amplified in colon cancer, consistent with the possibility that DcR3 amplification promotes tumour survival.

Our results show that DcR3 binds specifically to FasL and inhibits FasL activity. We did not detect DcR3 binding to several other TNF-ligand-family members; however, this does not rule out the possibility that DcR3 interacts with other ligands, as do some other TNFR family members, including OPG[2,19].

FasL is important in regulating the immune response; however, little is known about how FasL function is controlled. One mechanism involves the molecule cFLIP, which modulates apoptosis signalling downstream of Fas[20]. A second mechanism involves proteolytic shedding of FasL from the cell surface[17]. DcR3 competes with Fas for
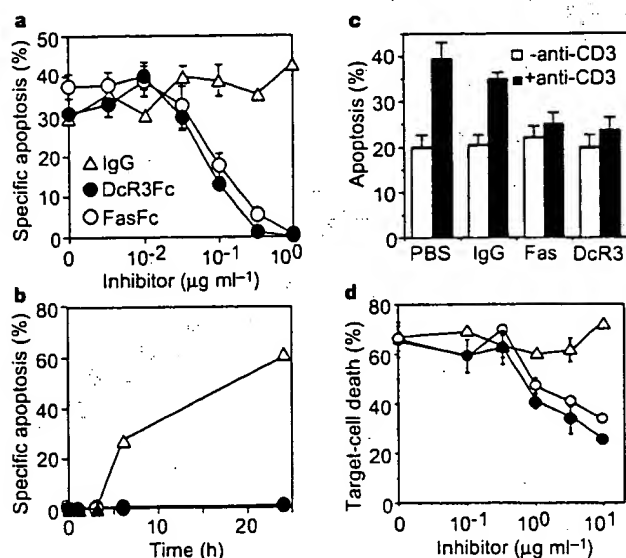

Figure 3 Inhibition of FasL activity by DcR3. **a,** Human Jurkat T leukaemia cells were incubated with Flag-tagged soluble FasL (sFasL; 5 ng ml⁻¹) oligomerized with anti-Flag antibody (0.1 μg ml⁻¹) in the presence of the proposed inhibitors DcR3-Fc, Fas-Fc or human IgG1 and assayed for apoptosis (mean ± s.e.m. of triplicates). **b,** Jurkat cells were incubated with sFasL-Flag plus anti-Flag antibody as in **a,** in presence of 1 μg ml⁻¹ DcR3-Fc (filled circles), Fas-Fc (open circles) or human IgG1 (triangles), and apoptosis was determined at the indicated time points. **c,** Peripheral blood T cells were stimulated with PHA and interleukin-2, followed by control (white bars) or anti-CD3 antibody (filled bars), together with phosphate-buffered saline (PBS), human IgG1, Fas-Fc, or DcR3-Fc (10 μg ml⁻¹). After 16 h, apoptosis of CD4⁺ cells was determined (mean ± s.e.m. of results from five donors). **d,** Peripheral blood natural killer cells were incubated with ⁵¹Cr-labelled Jurkat cells in the presence of DcR3-Fc (filled circles), Fas-Fc (open circles) or human IgG1 (triangles), and target-cell death was determined by release of ⁵¹Cr (mean ± s.d. for two donors, each in triplicate).
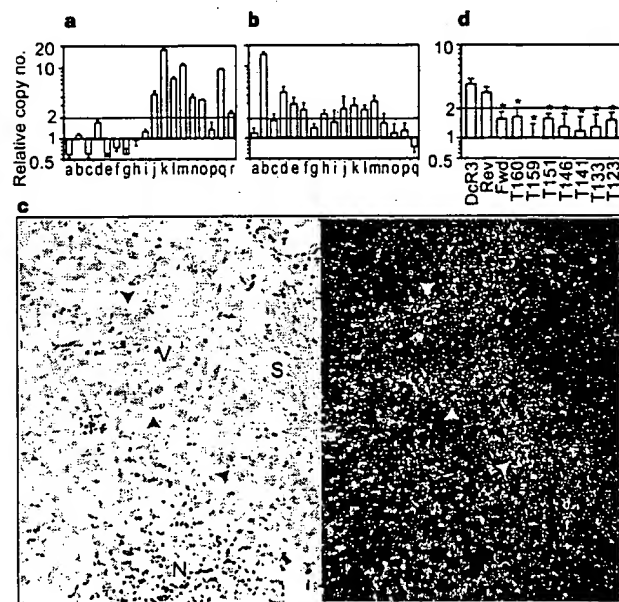
Figure 4 Genomic amplification of DcR3 in tumours. **a,** Lung cancers, comprising eight adenocarcinomas (c, d, f, g, h, j, k, r), seven squamous-cell carcinomas (a, e, m, n, o, p, q), one non-small-cell carcinoma (b), one small-cell carcinoma (i), and one bronchial adenocarcinoma (l). The data are means ± s.d. of 2 experiments done in duplicate. **b,** Colon tumours, comprising 17 adenocarcinomas. Data are means ± s.e.m. of five experiments done in duplicate. **c,** *In situ* hybridization analysis of DcR3 mRNA expression in a squamous-cell carcinoma of the lung. A representative bright-field image (left) and the corresponding dark-field image (right) show DcR3 mRNA over infiltrating malignant epithelium (arrowheads). Adjacent non-malignant stroma (S), blood vessel (V) and necrotic tumour tissue (N) are also shown. **d,** Average amplification of DcR3 compared with amplification of neighbouring genomic regions (reverse and forward, Rev and Fwd), the DcR3-linked marker T160, and other chromosome-20 markers, in the nine colon tumours showing DcR3 amplification of twofold or more (**b**). Data are from two experiments done in duplicate. Asterisk indicates $P < 0.01$ for a Student's *t*-test comparing each marker with DcR3.

FasL binding; hence, it may represent a third mechanism of extracellular regulation of FasL activity. A decoy receptor that modulates the function of the cytokine interleukin-1 has been described[21]. In addition, two decoy receptors that belong to the TNFR family, DcR1 and DcR2, regulate the FasL-related apoptosis-inducing molecule Apo2L[22]. Unlike DcR1 and DcR2, which are membrane-associated proteins, DcR3 is directly secreted into the extracellular space. One other secreted TNFR-family member is OPG[3], which shares greater sequence homology with DcR3 (31%) than do DcR1 (17%) or DcR2 (19%); OPG functions as a third decoy for Apo2L[19]. Thus, DcR3 and OPG define a new subset of TNFR-family members that function as secreted decoys to modulate ligands that induce apoptosis. Pox viruses produce soluble TNFR homologues that neutralize specific TNF-family ligands, thereby modulating the antiviral immune response[2]. Our results indicate that a similar mechanism, namely, production of a soluble decoy receptor for FasL, may contribute to immune evasion by certain tumours. □

....

Methods

Isolation of DcR3 cDNA. Several overlapping ESTs in GenBank (accession numbers AA025672, AA025673 and W67560) and in Lifeseq™ (Incyte Pharmaceuticals; accession numbers 1339238, 1533571, 1533650, 1542861, 1789372 and 2207027) showed similarity to members of the TNFR family. We screened human cDNA libraries by PCR with primers based on the region of EST consensus; fetal lung was positive for a product of the expected size. By hybridization to a PCR-generated probe based on the ESTs, one positive clone (DNA30942) was identified. When searching for potential alternatively spliced forms of DcR3 that might encode a transmembrane protein, we isolated 50 more clones; the coding regions of these clones were identical in size to that of the initial clone (data not shown).

Fc-fusion proteins (immunoadhesins). The entire DcR3 sequence, or the ectodomain of Fas or TNFR1, was fused to the hinge and Fc region of human IgG1, expressed in insect SF9 cells or in human 293 cells, and purified as described[23].

Fluorescence-activated cell sorting (FACS) analysis. We transfected 293 cells using calcium phosphate or Effectene (Qiagen) with pRK5 vector or pRK5 encoding full-length human FasL[4] (2 μg), together with pRK5 encoding CrmA (2 μg) to prevent cell death. After 16 h, the cells were incubated with biotinylated DcR3-Fc or TNFR1-Fc and then with phycoerythrin-conjugated streptavidin (GibcoBRL), and were assayed by FACS. The data were analysed by Kolmogorov-Smirnov statistical analysis. There was some detectable staining of vector-transfected cells by DcR3-Fc; as these cells express little FasL (data not shown), it is possible that DcR3 recognized some other factor that is expressed constitutively on 293 cells.

Immunoprecipitation. Human 293 cells were transfected as above, and metabolically labelled with [35S]cysteine and [35S]methionine (0.5 mCi; Amersham). After 16 h of culture in the presence of z-VAD-fmk (10 μM), the medium was immunoprecipitated with DcR3-Fc, Fas-Fc or TNFR1-Fc (5 μg), followed by protein A-Sepharose (Repligen). The precipitates were resolved by SDS-PAGE and visualized on a phosphorimager (Fuji BAS2000). Alternatively, purified, Flag-tagged soluble FasL (1 μg) (Alexis) was incubated with each Fc-fusion protein (1 μg), precipitated with protein A-Sepharose, resolved by SDS-PAGE and visualized by immunoblotting with rabbit anti-FasL antibody (Oncogene Research).

Analysis of complex formation. Flag-tagged soluble FasL (25 μg) was incubated with buffer or with DcR3-Fc (40 μg) for 1.5 h at 24 °C. The reaction was loaded onto a Superdex 200 HR 10/30 column (Pharmacia) and developed with PBS; 0.6-ml fractions were collected. The presence of DcR3-Fc-FasL complex in each fraction was analysed by placing 100 μl aliquots into microtitre wells precoated with anti-human IgG (Boehringer) to capture DcR3-Fc, followed by detection with biotinylated anti-Flag antibody Bio M2 (Kodak) and streptavidin-horseradish peroxidase (Amersham). Calibration of the column indicated an apparent relative molecular mass of the complex of 420K (data not shown), which is consistent with a stoichiometry of two DcR3-Fc homodimers to two soluble FasL homotrimers.

Equilibrium binding analysis. Microtitre wells were coated with anti-human

IgG, blocked with 2% BSA in PBS. DcR3-Fc or Fas-Fc was added, followed by serially diluted Flag-tagged soluble FasL. Bound ligand was detected with anti-Flag antibody as above. In the competition assay, Fas-Fc was immobilized as above, and the wells were blocked with excess IgG1 before addition of Flag-tagged soluble FasL plus DcR3-Fc.

T-cell AICD. CD3^{+} lymphocytes were isolated from peripheral blood of individual donors using anti-CD3 magnetic beads (Miltenyi Biotech), stimulated with phytohaemagglutinin (PHA; 2 μg ml⁻¹) for 24 h, and cultured in the presence of interleukin-2 (100 U ml⁻¹) for 5 days. The cells were plated in wells coated with anti-CD3 antibody (Pharmingen) and analysed for apoptosis 16 h later by FACS analysis of annexin-V-binding of CD4^{+} cells[24].

Natural killer cell activity. Natural killer cells were isolated from peripheral blood of individual donors using anti-CD56 magnetic beads (Miltenyi Biotech), and incubated for 16 h with 51Cr-loaded Jurkat cells at an effector-to-target ratio of 1:1 in the presence of DcR3-Fc, Fas-Fc or human IgG1. Target-cell death was determined by release of 51Cr in effector-target co-cultures relative to release of 51Cr by detergent lysis of equal numbers of Jurkat cells.

Gene-amplification analysis. Surgical specimens were provided by J. Kern (lung tumours) and P. Quirke (colon tumours). Genomic DNA was extracted (Qiagen) and the concentration was determined using Hoechst dye 33258 intercalation fluorometry. Amplification was determined by quantitative PCR[18] using a TaqMan instrument (ABI). The method was validated by comparison of PCR and Southern hybridization data for the Myc and HER-2 oncogenes (data not shown). Gene-specific primers and fluorogenic probes were designed on the basis of the sequence of DcR3 or of nearby regions identified on a BAC carrying the human DcR3 gene; alternatively, primers and probes were based on Stanford Human Genome Center marker AFM218xe7 (T160), which is linked to DcR3 (likelihood score = 5.4), SHGC-36268 (T159), the nearest available marker which maps to ~500 kilobases from T160, and five extra markers that span chromosome 20. The DcR3-specific primer sequences were 5'-CTTCTTCGCGCACGCTG-3' and 5'-ATCACGCCGGCACCAG-3' and the fluorogenic probe sequence was 5'-(FAM-ACACGATGCGTGCTCCAAGCAG AAp-(TAMARA), where FAM is 5'-fluorescein phosphoramidite. Relative gene-copy numbers were derived using the formula $2^{(\Delta CT)}$, where ΔCT is the difference in amplification cycles required to detect DcR3 in peripheral blood lymphocyte DNA compared to test DNA.

1. Nagata, S. Apoptosis by death factor. Cell 88, 355–365 (1997).
2. Smith, C. A., Farrah, T. & Goodwin, R. G. The TNF receptor superfamily of cellular and viral proteins: activation, costimulation, and death. Cell 76, 959–962 (1994).
3. Simonet, W. S. et al. Osteoprotegerin: a novel secreted protein involved in the regulation of bone density. Cell 89, 309–319 (1997).
4. Suda, T., Takahashi, T., Golstein, P. & Nagata, S. Molecular cloning and expression of Fas ligand, a novel member of the TNF family. Cell 75, 1169–1178 (1993).
5. Pennica, D. et al. Human tumour necrosis factor: precursor structure, expression and homology to lymphotoxin. Nature 312, 724–729 (1984).
6. Pitti, R. M. et al. Induction of apoptosis by Apo-2 ligand, a new member of the tumor necrosis factor receptor family. J. Biol. Chem. 271, 12687–12690 (1996).
7. Wiley, S. R. et al. Identification and characterization of a new member of the TNF family that induces apoptosis. Immunity 3, 673–682 (1995).
8. Marsters, S. A. et al. Identification of a ligand for the death-domain-containing receptor Apo3. Curr. Biol. 8, 525–528 (1998).
9. Chicheportiche, Y. et al. TWEAK, a new secreted ligand in the TNF family that weakly induces apoptosis. J. Biol. Chem. 272, 32401–32410 (1997).
10. Wong, B. R. et al. TRANCE is a novel ligand of the TNFR family that activates c-Jun-N-terminal kinase in T cells. J. Biol. Chem. 272, 25190–25194 (1997).
11. Anderson, D. M. et al. A homolog of the TNF receptor and its ligand enhance T-cell growth and dendritic-cell function. Nature 390, 175–179 (1997).
12. Lacey, D. L. et al. Osteoprotegerin ligand is a cytokine that regulates osteoclast differentiation and activation. Cell 93, 165–176 (1998).
13. Dhein, J., Walczak, H., Baumler, C., Debatin, K. M. & Krammer, P. H. Autocrine T-cell suicide mediated by ApoI/(Fas/CD95). Nature 373, 438–441 (1995).
14. Arase, H., Arase, N. & Saito, T. Fas-mediated cytotoxicity by freshly isolated natural killer cells. J. Exp. Med. 181, 1235–1238 (1995).
15. Medvedev, A. E. et al. Regulation of Fas and Fas ligand expression in NK cells by cytokines and the involvement of Fas ligand in NK/LAK cell-mediated cytotoxicity. Cytokine 9, 394–404 (1997).
16. Moretta, A. Mechanisms in cell-mediated cytotoxicity. Cell 90, 13–18 (1997).
17. Tanaka, M., Itai, T., Adachi, M. & Nagata, S. Downregualtion of Fas ligand by shedding. Nature Med. 4, 31–36 (1998).
18. Gelmini, S. et al. Quantitative PCR-based homogeneous assay with fluorogenic probes to measure c-erbB-2 oncogene amplification. Clin. Chem. 43, 752–758 (1997).
19. Emery, J. G. et al. Osteoprotegerin is a receptor for the cytotoxic ligand TRAIL. J. Biol. Chem. 273, 14363–14367 (1998).
20. Wallach, D. Placing death under control. Nature 388, 123–125 (1997).
21. Collota, F. et al. Interleukin-1 type II receptor: a decoy target for IL-1 that is regulated by IL-4. Science 261, 472–475 (1993).

22. Ashkenazi, A. & Dixit, V. M. Death receptors: signaling and modulation. *Science* 281, 1305–1308 (1998).
23. Ashkenazi, A. & Chamow, S. M. Immunoadhesins as research tools and therapeutic agents. *Curr. Opin. Immunol.* 9, 195–200 (1997).
24. Marsters, S. *et al.* Activation of apoptosis by Apo-2 ligand is independent of FADD but blocked by CrmA. *Curr. Biol.* 6, 750–752 (1996).

Crystal structure of the ATP-binding subunit of an ABC transporter

Li-Wei Hung*, Iris Xiaoyan Wang†, Kishiko Nikaido†, Pei-Qi Liu†, Giovanna Ferro-Luzzi Ames† & Sung-Hou Kim*‡

* E. O. Lawrence Berkeley National Laboratory, † Department of Molecular and Cell Biology, and ‡ Department of Chemistry, University of California at Berkeley, Berkeley, California 94720, USA

ABC transporters (also known as traffic ATPases) form a large family of proteins responsible for the translocation of a variety of compounds across membranes of both prokaryotes and eukaryotes[1]. The recently completed *Escherichia coli* genome sequence revealed that the largest family of paralogous *E. coli* proteins is composed of ABC transporters[2]. Many eukaryotic proteins of medical significance belong to this family, such as the cystic fibrosis transmembrane conductance regulator (CFTR), the P-glycoprotein (or multidrug-resistance protein) and the heterodimeric transporter associated with antigen processing (Tap1–Tap2). Here we report the crystal structure at 1.5 Å resolution of HisP, the ATP-binding subunit of the histidine permease, which is an ABC transporter from *Salmonella typhimurium*. We correlate the details of this structure with the biochemical, genetic and biophysical properties of the wild-type and several mutant HisP proteins. The structure provides a basis for understanding properties of ABC transporters and of defective CFTR proteins.

ABC transporters contain four structural domains: two nucleotide-binding domains (NBDs), which are highly conserved throughout the family, and two transmembrane domains[1]. In prokaryotes these domains are often separate subunits which are assembled into a membrane-bound complex; in eukaryotes the domains are generally fused into a single polypeptide chain. The periplasmic histidine permease of *S. typhimurium* and *E. coli*[1,3–8] is a well-characterized ABC transporter that is a good model for this superfamily. It consists of a membrane-bound complex, HisQMP₂, which comprises integral membrane subunits, HisQ and HisM, and two copies of HisP, the ATP-binding subunit. HisP, which has properties intermediate between those of integral and peripheral membrane proteins[9], is accessible from both sides of the membrane, presumably by its interaction with HisQ and HisM[6]. The two HisP subunits form a dimer, as shown by their cooperativity in ATP hydrolysis[5], the requirement for both subunits to be present for activity[8], and the formation of a HisP dimer upon chemical cross-linking. Soluble HisP also forms a dimer[3]. HisP has been purified and characterized in an active soluble form[3] which can be reconstituted into a fully active membrane-bound complex[8].

The overall shape of the crystal structure of the HisP monomer is that of an 'L' with two thick arms (arm I and arm II); the ATP-binding pocket is near the end of arm I (Fig. 1). A six-stranded β-sheet (β3 and β8–β12) spans both arms of the L, with a domain of a α- plus β-type structure (β1, β2, β4–β7, α1 and α2) on one side (within arm I) and a domain of mostly α-helices (α3–α9) on the
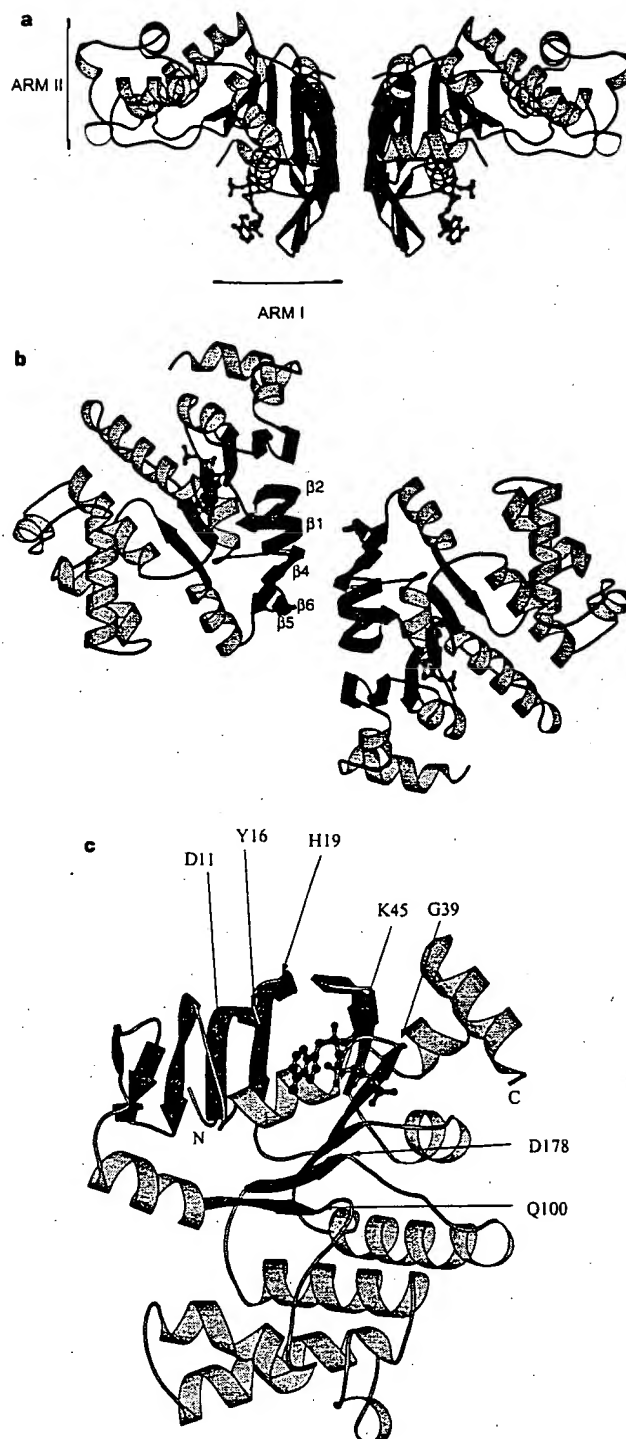

Figure 1 Crystal structure of HisP. **a**, View of the dimer along an axis perpendicular to its two-fold axis. The top and bottom of the dimer are suggested to face towards the periplasmic and cytoplasmic sides, respectively (see text). The thickness of arm II is about 25 Å, comparable to that of membrane. α-Helices are shown in orange and β-sheets in green. **b**, View along the two-fold axis of the HisP dimer, showing the relative displacement of the monomers not apparent in **a**. The β-strands at the dimer interface are labelled. **c**, View of one monomer from the bottom of arm I, as shown in **a**, towards arm II, showing the ATP-binding pocket. **a–c**, The protein and the bound ATP are in 'ribbon' and 'ball-and-stick' representations, respectively. Key residues discussed in the text are indicated in **c**. These figures were prepared with MOLSCRIPT[29]. N, amino terminus; C, C terminus.

NOVEL APPROACH TO QUANTITATIVE POLYMERASE CHAIN REACTION USING REAL-TIME DETECTION: APPLICATION TO THE DETECTION OF GENE AMPLIFICATION IN BREAST CANCER

Ivan Bièche[1,2], Martine Olivi[1], Marie-Hélène Champème[2], Dominique Vidaud[1], Rosette Lidereau[2] and Michel Vidaud[1]*

[1]*Laboratoire de Génétique Moléculaire, Faculté des Sciences Pharmaceutiques et Biologiques de Paris, Paris, France*
[2]*Laboratoire d'Oncogénétique, Centre René Huguenin, St-Cloud, France*

Gene amplification is a common event in the progression of human cancers, and amplified oncogenes have been shown to have diagnostic, prognostic and therapeutic relevance. A kinetic quantitative polymerase-chain-reaction (PCR) method, based on fluorescent TaqMan methodology and a new instrument (ABI Prism 7700 Sequence Detection System) capable of measuring fluorescence in real-time, was used to quantify gene amplification in tumor DNA. Reactions are characterized by the point during cycling when PCR amplification is still in the exponential phase, rather than the amount of PCR product accumulated after a fixed number of cycles. None of the reaction components is limited during the exponential phase, meaning that values are highly reproducible in reactions starting with the same copy number. This greatly improves the precision of DNA quantification. Moreover, real-time PCR does not require post-PCR sample handling, thereby preventing potential PCR-product carry-over contamination; it possesses a wide dynamic range of quantification and results in much faster and higher sample throughput. The real-time PCR method, was used to develop and validate a simple and rapid assay for the detection and quantification of the 3 most frequently amplified genes (*myc, ccnd1* and *erb*B2) in breast tumors. Extra copies of *myc, ccnd1* and *erb*B2 were observed in 10, 23 and 15%, respectively, of 108 breast-tumor DNA; the largest observed numbers of gene copies were 4.6, 18.6 and 15.1, respectively. These results correlated well with those of Southern blotting. The use of this new semi-automated technique will make molecular analysis of human cancers simpler and more reliable, and should find broad applications in clinical and research settings. *Int. J. Cancer* 78:661–666, 1998.
© 1998 Wiley-Liss, Inc.

Gene amplification plays an important role in the pathogenesis of various solid tumors, including breast cancer, probably because over-expression of the amplified target genes confers a selective advantage. The first technique used to detect genomic amplification was cytogenetic analysis. Amplification of several chromosome regions, visualized either as extrachromosomal double minutes (dmins) or as integrated homogeneously staining regions (HSRs), are among the main visible cytogenetic abnormalities in breast tumors. Other techniques such as comparative genomic hybridization (CGH) (Kallioniemi *et al.,* 1994) have also been used in broad searches for regions of increased DNA copy numbers in tumor cells, and have revealed some 20 amplified chromosome regions in breast tumors. Positional cloning efforts are underway to identify the critical gene(s) in each amplified region. To date, genes known to be amplified frequently in breast cancers include *myc* (8q24), *ccnd1* (11q13), and *erb*B2 (17q12-q21) (for review, see Bièche and Lidereau, 1995).

Amplification of the *myc, ccnd1,* and *erb*B2 proto-oncogenes should have clinical relevance in breast cancer, since independent studies have shown that these alterations can be used to identify sub-populations with a worse prognosis (Berns *et al.,* 1992; Schuuring *et al.,* 1992; Slamon *et al.,* 1987). Muss *et al.* (1994) suggested that these gene alterations may also be useful for the prediction and assessment of the efficacy of adjuvant chemotherapy and hormone therapy.

However, published results diverge both in terms of the frequency of these alterations and their clinical value. For instance, over 500 studies in 10 years have failed to resolve the controversy surrounding the link suggested by Slamon *et al.* (1987) between *erb*B2 amplification and disease progression. These discrepancies are partly due to the clinical, histological and ethnic heterogeneity of breast cancer, but technical considerations are also probably involved.

Specific genes (DNA) were initially quantified in tumor cells by means of blotting procedures such as Southern and slot blotting. These batch techniques require large amounts of DNA (5–10 μg/reaction) to yield reliable quantitative results. Furthermore, meticulous care is required at all stages of the procedures to generate blots of sufficient quality for reliable dosage analysis. Recently, PCR has proven to be a powerful tool for quantitative DNA analysis, especially with minimal starting quantities of tumor samples (small, early-stage tumors and formalin-fixed, paraffin-embedded tissues).

Quantitative PCR can be performed by evaluating the amount of product either after a given number of cycles (end-point quantitative PCR) or after a varying number of cycles during the exponential phase (kinetic quantitative PCR). In the first case, an internal standard distinct from the target molecule is required to ascertain PCR efficiency. The method is relatively easy but implies generating, quantifying and storing an internal standard for each gene studied. Nevertheless, it is the most frequently applied method to date.

One of the major advantages of the kinetic method is its rapidity in quantifying a new gene, since no internal standard is required (an external standard curve is sufficient). Moreover, the kinetic method has a wide dynamic range (at least 5 orders of magnitude), giving an accurate value for samples differing in their copy number. Unfortunately, the method is cumbersome and has therefore been rarely used. It involves aliquot sampling of each assay mix at regular intervals and quantifying, for each aliquot, the amplification product. Interest in the kinetic method has been stimulated by a novel approach using fluorescent TaqMan methodology and a new instrument (ABI Prism 7700 Sequence Detection System) capable of measuring fluorescence in real time (Gibson *et al.,* 1996; Heid *et al.,* 1996). The TaqMan reaction is based on the 5' nuclease assay first described by Holland *et al.* (1991). The latter uses the 5' nuclease activity of Taq polymerase to cleave a specific fluorogenic oligonucleotide probe during the extension phase of PCR. The approach uses dual-labeled fluorogenic hybridization probes (Lee *et al.,* 1993). One fluorescent dye, covalently linked to the 5' end of the oligonucleotide, serves as a reporter [FAM (*i.e.,* 6-carboxyfluorescein)] and its emission spectrum is quenched by a second fluorescent dye, TAMRA (*i.e.,* 6-carboxy-tetramethyl-rhodamine) attached to the 3' end. During the extension phase of the PCR

cycle, the fluorescent hybridization probe is hydrolyzed by the 5'-3' nucleolytic activity of DNA polymerase. Nuclease degradation of the probe releases the quenching of FAM fluorescence emission, resulting in an increase in peak fluorescence emission. The fluorescence signal is normalized by dividing the emission intensity of the reporter dye (FAM) by the emission intensity of a reference dye (*i.e.*, ROX, 6-carboxy-X-rhodamine) included in TaqMan buffer, to obtain a ratio defined as the Rn (normalized reporter) for a given reaction tube. The use of a sequence detector enables the fluorescence spectra of all 96 wells of the thermal cycler to be measured continuously during PCR amplification.

The real-time PCR method offers several advantages over other current quantitative PCR methods (Celi *et al.*, 1994): *(i)* the probe-based homogeneous assay provides a real-time method for detecting only specific amplification products, since specific hybridation of both the primers and the probe is necessary to generate a signal; *(ii)* the C_t (threshold cycle) value used for quantification is measured when PCR amplification is still in the log phase of PCR product accumulation. This is the main reason why C_t is a more reliable measure of the starting copy number than are end-point measurements, in which a slight difference in a limiting component can have a drastic effect on the amount of product; *(iii)* use of C_t values gives a wider dynamic range (at least 5 orders of magnitude), reducing the need for serial dilution; *(iv)* The real-time PCR method is run in a closed-tube system and requires no post-PCR sample handling, thus avoiding potential contamination; *(v)* the system is highly automated, since the instrument continuously measures fluorescence in all 96 wells of the thermal cycler during PCR amplification and the corresponding software processes, and analyzes the fluorescence data; *(vi)* the assay is rapid, as results are available just one minute after thermal cycling is complete; *(vii)* the sample throughput of the method is high, since 96 reactions can be analyzed in 2 hr.

Here, we applied this semi-automated procedure to determine the copy numbers of the 3 most frequently amplified genes in breast tumors (*myc, ccnd1* and *erb*B2), as well as 2 genes (*alb* and *app*) located in a chromosome region in which no genetic changes have been observed in breast tumors. The results for 108 breast tumors were compared with previous Southern-blot data for the same samples.

MATERIAL AND METHODS
Tumor and blood samples

Samples were obtained from 108 primary breast tumors removed surgically from patients at the Centre René Huguenin; none of the patients had undergone radiotherapy or chemotherapy. Immediately after surgery, the tumor samples were placed in liquid nitrogen until extraction of high-molecular-weight DNA. Patients were included in this study if the tumor sample used for DNA preparation contained more than 60% of tumor cells (histological analysis). A blood sample was also taken from 18 of the same patients.

DNA was extracted from tumor tissue and blood leukocytes according to standard methods.

Real-time PCR

Theoretical basis. Reactions are characterized by the point during cycling when amplification of the PCR product is first detected, rather than by the amount of PCR product accumulated after a fixed number of cycles. The higher the starting copy number of the genomic DNA target, the earlier a significant increase in fluorescence is observed. The parameter C_t (threshold cycle) is defined as the fractional cycle number at which the fluorescence generated by cleavage of the probe passes a fixed threshold above baseline. The target gene copy number in unknown samples is quantified by measuring C_t and by using a standard curve to determine the starting copy number. The precise amount of genomic DNA (based on optical density) and its quality (*i.e.*, lack

of extensive degradation) are both difficult to assess. We therefore also quantified a control gene *(alb)* mapping to chromosome region 4q11-q13, in which no genetic alterations have been found in breast-tumor DNA by means of CGH (Kallioniemi *et al.*, 1994).

Thus, the ratio of the copy number of the target gene to the copy number of the *alb* gene normalizes the amount and quality of genomic DNA. The ratio defining the level of amplification is termed "N", and is determined as follows:

$$N = \frac{\text{copy number of target gene } (app, myc, ccnd1, erbB2)}{\text{copy number of reference gene } (alb)}.$$

Primers, probes, reference human genomic DNA and PCR consumables. Primers and probes were chosen with the assistance of the computer programs Oligo 4.0 (National Biosciences, Plymouth, MN), EuGene (Daniben Systems, Cincinnati, OH) and Primer Express (Perkin-Elmer Applied Biosystems, Foster City, CA).

Primers were purchased from DNAgency (Malvern, PA) and probes from Perkin-Elmer Applied Biosystems.

Nucleotide sequences for the oligonucleotide hybridization probes and primers are available on request.

The TaqMan PCR Core reagent kit, MicroAmp optical tubes, and MicroAmp caps were from Perkin-Elmer Applied Biosystems.

Standard-curve construction. The kinetic method requires a standard curve. The latter was constructed with serial dilutions of specific PCR products, according to Piatak *et al.* (1993). In practice, each specific PCR product was obtained by amplifying 20 ng of a standard human genomic DNA (Boehringer, Mannheim, Germany) with the same primer pairs as those used later for real-time quantitative PCR. The 5 PCR products were purified using MicroSpin S-400 HR columns (Pharmacia, Uppsala, Sweden) electrophorezed through an acrylamide gel and stained with ethidium bromide to check their quality. The PCR products were then quantified spectrophotometrically and pooled, and serially diluted 10-fold in mouse genomic DNA (Clontech, Palo Alto, CA) at a constant concentration of 2 ng/μl. The standard curve used for real-time quantitative PCR was based on serial dilutions of the pool of PCR products ranging from 10^{-7} (10^5 copies of each gene) to 10^{-10} (10^2 copies). This series of diluted PCR products was aliquoted and stored at −80°C until use.

The standard curve was validated by analyzing 2 known quantities of calibrator human genomic DNA (20 ng and 50 ng).

PCR amplification. Amplification mixes (50 μl) contained the sample DNA (around 20 ng, around 6600 copies of disomic genes), 10× TaqMan buffer (5 μl), 200 μM dATP, dCTP, dGTP, and 400 μM dUTP, 5 mM MgCl$_2$, 1.25 units of AmpliTaq Gold, 0.5 units of AmpErase uracil N-glycosylase (UNG), 200 nM each primer and 100 nM probe. The thermal cycling conditions comprised 2 min at 50°C and 10 min at 95°C. Thermal cycling consisted of 40 cycles at 95°C for 15 s and 65°C for 1 min. Each assay included: a standard curve (from 10^5 to 10^2 copies) in duplicate, a no-template control, 20 ng and 50 ng of calibrator human genomic DNA (Boehringer) in triplicate, and about 20 ng of unknown genomic DNA in triplicate (26 samples can thus be analyzed on a 96-well microplate). All samples with a coefficient of variation (CV) higher than 10% were retested.

All reactions were performed in the ABI Prism 7700 Sequence Detection System (Perkin-Elmer Applied Biosystems), which detects the signal from the fluorogenic probe during PCR.

Equipment for real-time detection. The 7700 system has a built-in thermal cycler and a laser directed via fiber optical cables to each of the 96 sample wells. A charge-coupled-device (CDD) camera collects the emission from each sample and the data are analyzed automatically. The software accompanying the 7700 system calculates C_t and determines the starting copy number in the samples.

Determination of gene amplification. Gene amplification was calculated as described above. Only samples with an N value higher than 2 were considered to be amplified.

RESULTS

To validate the method, real-time PCR was performed on genomic DNA extracted from 108 primary breast tumors, and 18 normal leukocyte DNA samples from some of the same patients. The target genes were the *myc, ccnd1* and *erb*B2 proto-oncogenes, and the β-amyloid precursor protein gene (*app*), which maps to a chromosome region (21q21.2) in which no genetic alterations have been found in breast tumors (Kallioniemi *et al.,* 1994). The reference disomic gene was the albumin gene (*alb,* chromosome 4q11-q13).

Validation of the standard curve and dynamic range of real-time PCR

The standard curve was constructed from PCR products serially diluted in genomic mouse DNA at a constant concentration of 2 ng/μl. It should be noted that the 5 primer pairs chosen to analyze the 5 target genes do not amplify genomic mouse DNA (data not shown). Figure 1 shows the real-time PCR standard curve for the *alb* gene. The dynamic range was wide (at least 4 orders of magnitude), with samples containing as few as 10^2 copies or as many as 10^5 copies.

*Copy-number ratio of the 2 reference genes (*app *and* alb*)*

The *app* to *alb* copy-number ratio was determined in 18 normal leukocyte DNA samples and all 108 primary breast-tumor DNA
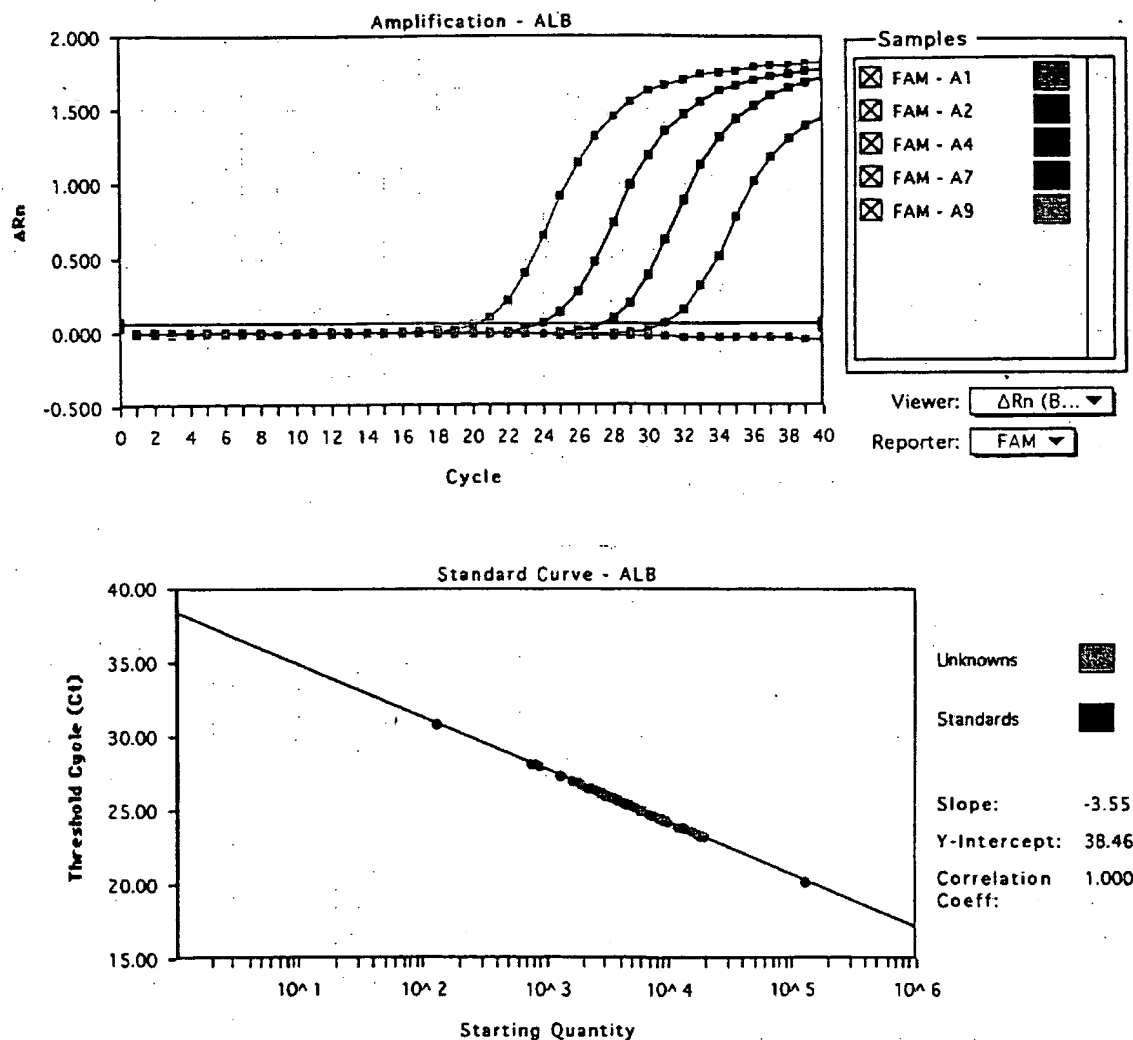

FIGURE 1 – Albumin (*alb*) gene dosage by real-time PCR. Top: Amplification plots for reactions with starting *alb* gene copy number ranging from 10^5 (A9), 10^4 (A7), 10^3 (A4) to 10^2 (A2) and a no-template control (A1). Cycle number is plotted *vs.* change in normalized reporter signal (ΔRn). For each reaction tube, the fluorescence signal of the reporter dye (FAM) is divided by the fluorescence signal of the passive reference dye (ROX), to obtain a ratio defined as the normalized reporter signal (Rn). ΔRn represents the normalized reporter signal (Rn) minus the baseline signal established in the first 15 PCR cycles. ΔRn increases during PCR as *alb* PCR product copy number increases until the reaction reaches a plateau. C_t (threshold cycle) represents the fractional cycle number at which a significant increase in Rn above a baseline signal (horizontal black line) can first be detected. Two replicate plots were performed for each standard sample, but the data for only one are shown here. Bottom: Standard curve plotting log starting copy number *vs.* C_t (threshold cycle). The black dots represent the data for standard samples plotted in duplicate and the red dots the data for unknown genomic DNA samples plotted in triplicate. The standard curve shows 4 orders of linear dynamic range.

samples. We selected these 2 genes because they are located in 2 chromosome regions (app, 21q21.2; alb, 4q11-q13) in which no obvious genetic changes (including gains or losses) have been observed in breast cancers (Kallioniemi et al., 1994). The ratio for the 18 normal leukocyte DNA samples fell between 0.7 and 1.3 (mean 1.02 ± 0.21), and was similar for the 108 primary breast-tumor DNA samples (0.6 to 1.6, mean 1.06 ± 0.25), confirming that alb and app are appropriate reference disomic genes for breast-tumor DNA. The low range of the ratios also confirmed that the nucleotide sequences chosen for the primers and probes were not polymorphic, as mismatches of their primers or probes with the subject's DNA would have resulted in differential amplification.

myc, ccnd1 and erbB2 gene dose in normal leukocyte DNA

To determine the cut-off point for gene amplification in breast-cancer tissue, 18 normal leukocyte DNA samples were tested for the gene dose (N), calculated as described in "Material and Methods". The N value of these samples ranged from 0.5 to 1.3 (mean 0.84 ± 0.22) for myc; 0.7 to 1.6 (mean 1.06 ± 0.23) for ccnd1 and 0.6 to 1.3 (mean 0.91 ± 0.19) for erbB2. Since N values for myc, ccnd1 and erbB2 in normal leukocyte DNA consistently fell between 0.5 and 1.6, values of 2 or more were considered to represent gene amplification in tumor DNA.

myc, ccnd1 and erbB2 gene dose in breast-tumor DNA

myc, ccnd1 and erbB2 gene copy numbers in the 108 primary breast tumors are reported in Table I. Extra copies of ccnd1 were more frequent (23%, 25/108) than extra copies of erbB2 (15%, 16/108) and myc (10%, 11/108), and ranged from 2 to 18.6 for ccnd1, 2 to 15.1 for erbB2, and only 2 to 4.6 for the myc gene. Figure 2 and Table II represent tumors in which the ccnd1 gene was amplified 16-fold (T145), 6-fold (T133) and non-amplified (T118). The 3 genes were never found to be co-amplified in the same tumor. erbB2 and ccnd1 were co-amplified in only 3 cases, myc and ccnd1 in 2 cases and myc and erbB2 in 1 case. This favors the hypothesis that gene amplifications are independent events in breast cancer. Interestingly, 5 tumors showed a decrease of at least 50% in the erbB2 copy number (N < 0.5), suggesting that they bore deletions of the 17q21 region (the site of erbB2). No such decrease in copy number was observed with the other 2 proto-oncogenes.

Comparison of gene dose determined by real-time quantitative PCR and Southern-blot analysis

Southern-blot analysis of myc, ccnd1 and erbB2 amplifications had previously been done on the same 108 primary breast tumors. A perfect correlation between the results of real-time PCR and Southern blot was obtained for tumors with high copy numbers (N ≥ 5). However, there were cases (1 myc, 6 ccnd1 and 4 erbB2) in which real-time PCR showed gene amplification whereas Southern-blot did not, but these were mainly cases with low extra copy numbers (N from 2 to 2.9).

DISCUSSION

The clinical applications of gene amplification assays are currently limited, but would certainly increase if a simple, standardized and rapid method were perfected. Gene amplification status has been studied mainly by means of Southern blotting, but this method is not sensitive enough to detect low-level gene amplification nor accurate enough to quantify the full range of amplification values. Southern blotting is also time-consuming, uses radioactive

TABLE I – DISTRIBUTION OF AMPLIFICATION LEVEL (N) FOR myc, ccnd1 AND erbB2 GENES IN 108 HUMAN BREAST TUMORS

Gene	Amplification level (N)			
	<0.5	0.5–1.9	2–4.9	≥5
myc	0	97 (89.8%)	11 (10.2%)	0
ccnd1	0	83 (76.9%)	17 (15.7%)	8 (7.4%)
erbB2	5 (4.6%)	87 (80.6%)	8 (7.4%)	8 (7.4%)

reagents and requires relatively large amounts of high-quality genomic DNA, which means it cannot be used routinely in many laboratories. An amplification step is therefore required to determine the copy number of a given target gene from minimal quantities of tumor DNA (small early-stage tumors, cytopuncture specimens or formalin-fixed, paraffin-embedded tissues).
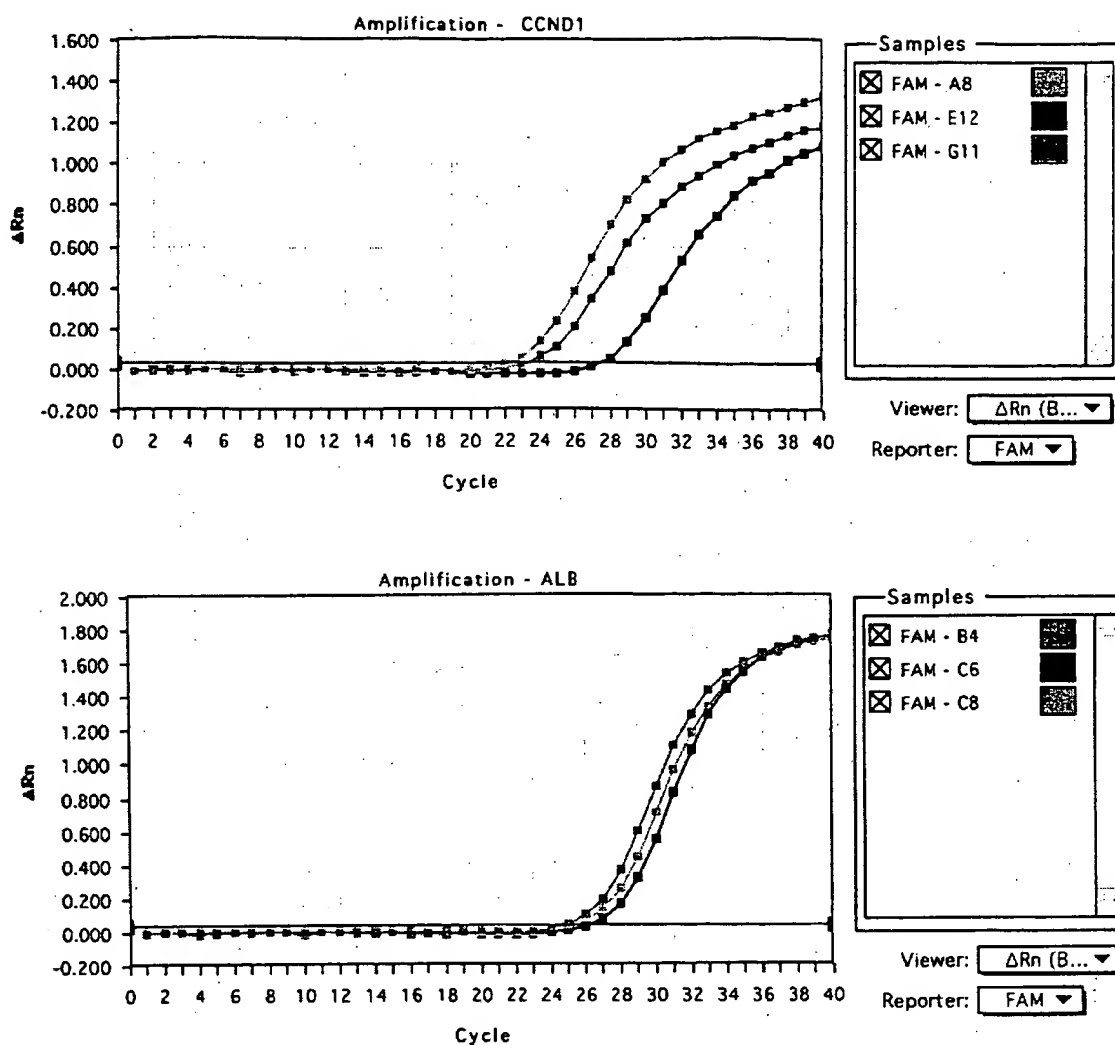
In this study, we validated a PCR method developed for the quantification of gene over-representation in tumors. The method, based on real-time analysis of PCR amplification, has several advantages over other PCR-based quantitative assays such as competitive quantitative PCR (Celi et al., 1994). First, the real-time PCR method is performed in a closed-tube system, avoiding the risk of contamination by amplified products. Re-amplification of carryover PCR products in subsequent experiments can also be prevented by using the enzyme uracil N-glycosylase (UNG) (Longo et al., 1990). The second advantage is the simplicity and rapidity of sample analysis, since no post-PCR manipulations are required. Our results show that the automated method is reliable. We found it possible to determine, in triplicate, the number of copies of a target gene in more than 100 tumors per day. Third, the system has a linear dynamic range of at least 4 orders of magnitude, meaning that samples do not have to contain equal starting amounts of DNA. This technique should therefore be suitable for analyzing formalin-fixed, paraffin-embedded tissues. Fourth, and above all, real-time PCR makes DNA quantification much more precise and reproducible, since it is based on C_t values rather than end-point measurement of the amount of accumulated PCR product. Indeed, the ABI Prism 7700 Sequence Detection System enables C_t to be calculated when PCR amplification is still in the exponential phase and when none of the reaction components is rate-limiting. The within-run CV of the C_t value for calibrator human DNA (5 replicates) was always below 5%, and the between-assay precision in 5 different runs was always below 10% (data not shown). In addition, the use of a standard curve is not absolutely necessary, since the copy number can be determined simply by comparing the C_t ratio of the target gene with that of reference genes. The results obtained by the 2 methods (with and without a standard curve) are similar in our experiments (data not shown). Moreover, unlike competitive quantitative PCR, real-time PCR does not require an internal control (the design and storage of internal controls and the validation of their amplification efficiency is laborious).

The only potential disavantage of real-time PCR, like all other PCR-based methods and solid-matrix blotting techniques (Southern blots and dot blots) is that is cannot avoid dilution artifacts inherent in the extraction of DNA from tumor cells contained in heterogeneous tissue specimens. Only FISH and immunohistochemistry can measure alterations on a cell-by-cell basis (Pauletti et al., 1996; Slamon et al., 1989). However, FISH requires expensive equipment and trained personnel and is also time-consuming. Moreover, FISH does not assess gene expression and therefore cannot detect cases in which the gene product is over-expressed in the absence of gene amplification, which will be possible in the future by real-time quantitative RT-PCR. Immunohistochemistry is subject to considerable variations in the hands of different teams, owing to alterations of target proteins during the procedure, the different primary antibodies and fixation methods used and the criteria used to define positive staining.

The results of this study are in agreement with those reported in the literature. (i) Chromosome regions 4q11-q13 and 21q21.2 (which bear alb and app, respectively) showed no genetic alterations in the breast-cancer samples studied here, in keeping with the results of CGH (Kallioniemi et al., 1994). (ii) We found that amplifications of these 3 oncogenes were independent events, as reported by other teams (Berns et al., 1992; Borg et al., 1992). (iii) The frequency and degree of myc amplification in our breast tumor DNA series were lower than those of ccnd1 and erbB2 amplification, confirming the findings of Borg et al. (1992) and Courjal et al. (1997). (iv) The maxima of ccnd1 and erbB2 over-representation were 18-fold and 15-fold, also in keeping with earlier results (about

Amplification - CCND1

Samples
- ☒ FAM - A8
- ☒ FAM - E12
- ☒ FAM - G11

Viewer: ΔRn (B... ▼)
Reporter: FAM ▼

Amplification - ALB

Samples
- ☒ FAM - B4
- ☒ FAM - C6
- ☒ FAM - C8

Viewer: ΔRn (B... ▼)
Reporter: FAM ▼

Tumor	CCND1 C_t	CCND1 Copy number	ALB C_t	ALB Copy number
■ T118	27.3	4605	26.5	4365
▨ T133	23.2	61659	25.2	10092
▦ T145	22.1	125892	25.6	7762

FIGURE 2 – *ccnd1* and *alb* gene dosage by real-time PCR in 3 breast tumor samples: T118 (E12, C6, black squares), T133 (G11, B4, red squares) and T145 (A8, C8, blue squares). Given the C_t of each sample, the initial copy number is inferred from the standard curve obtained during the same experiment. Triplicate plots were performed for each tumor sample, but the data for only one are shown here. The results are shown in Table II.

30-fold maximum) (Berns *et al.*, 1992; Borg *et al.*, 1992; Courjal *et al.*, 1997). (*v*) The *erb*B2 copy numbers obtained with real-time PCR were in good agreement with data obtained with other quantitative PCR-based assays in terms of the frequency and degree of amplification (An *et al.*, 1995; Deng *et al.*, 1996; Valeron *et al.*, 1996). Our results also correlate well with those recently published by Gelmini *et al.* (1997), who used the TaqMan system to measure *erb*B2 amplification in a small series of breast tumors (n = 25), but with an instrument (LS-50B luminescence spectrometer, Perkin-Elmer Applied Biosystems) which only allows end-

TABLE II – EXAMPLES OF *ccnd1* GENE DOSAGE RESULTS
FROM 3 BREAST TUMORS[1]

Tumor	ccnd1			alb			Nccnd1/alb
	Copy number	Mean	SD	Copy number	Mean	SD	
T118	4525			4223			
	4605	4603	77	4365	4325	89	1.06
	4678			4387			
T133	59821			9787			
	61659	61100	1111	10092	10137	375	6.03
	61821			10533			
T145	128563			7321			
	125892	125392	3448	7762	7672	316	16.34
	121722			7933			

[1]For each sample, 3 replicate experiments were performed and the mean
and the standard deviation (SD) was determined. The level of *ccnd1* gene
amplification (N*ccnd1*/*alb*) is determined by dividing the average *ccnd1*
copy number value by the average *alb* copy number value.

point measurement of fluorescence intensity. Here we report *myc*
and *ccnd1* gene dosage in breast cancer by means of quantitative
PCR. (vi) We found a high degree of concordance between
real-time quantitative PCR and Southern blot analysis in terms of
gene amplification, especially for samples with high copy numbers
(≥5-fold). The slightly higher frequency of gene amplification
(especially *ccnd1* and *erb*B2) observed by means of real-time
quantitative PCR as compared with Southern-blot analysis may be
explained by the higher sensitivity of the former method. However,
we cannot rule out the possibility that some tumors with a few extra

gene copies observed in real-time PCR had additional copies of an
arm or a whole chromosome (trisomy, tetrasomy or polysomy)
rather than true gene amplification. These 2 types of genetic
alteration (polysomy and gene amplification) could be easily
distinguished in the future by using an additional probe located on
the same chromosome arm, but some distance from the target gene.
It is noteworthy that high gene copy numbers have the greatest
prognostic significance in breast carcinoma (Borg *et al.*, 1992;
Slamon *et al.*, 1987).

Finally, this technique can be applied to the detection of gene
deletion as well as gene amplification. Indeed, we found a
decreased copy number of *erb*B2 (but not of the other 2 proto-
oncogenes) in several tumors; *erb*B2 is located in a chromosome
region (17q21) reported to contain both deletions and amplifica-
tions in breast cancer (Bièche and Lidereau, 1995).

In conclusion, gene amplification in various cancers can be used
as a marker of pre-neoplasia, also for early diagnosis of cancer,
staging, prognostication and choice of treatment. Southern blotting
is not sufficiently sensitive, and FISH is lengthy and complex.
Real-time quantitative PCR overcomes both these limitations, and
is a sensitive and accurate method of analyzing large numbers of
samples in a short time. It should find a place in routine clinical
gene dosage.

ACKNOWLEDGEMENTS

REFERENCES

AN, H.X., NIEDERACHER, D., BECKMANN, M.W., GÖHRING, U.J., SCHARL, A., PICARD, F., VAN ROEYEN, C., SCHNÜRCH, H.G. and BENDER, H.G., *erb*B2 gene amplification detected by fluorescent differential polymerase chain reaction in paraffin-embedded breast carcinoma tissues. *Int. J. Cancer (Pred. Oncol.)*, **64**, 291–297 (1995).

BERNS, E.M.J.J., KLIJN, J.G.M., VAN PUTTEN, W.L.J., VAN STAVEREN, I.L., PORTENGEN, H. and FOEKENS, J.A., *c-myc* amplification is a better prognos-tic factor than HER2/*neu* amplification in primary breast cancer. *Cancer Res.*, **52**, 1107–1113 (1992).

BIÈCHE, I. and LIDEREAU, R., Genetic alterations in breast cancer. *Genes Chrom. Cancer*, **14**, 227–251 (1995).

BORG, A., BALDETORP, B., FERNO, M., OLSSON, H. and SIGURDSSON, H., *c-myc* amplification is an independent prognostic factor in post-menopausal breast cancer. *Int. J. Cancer*, **51**, 687–691 (1992).

CELI, F.S., COHEN, M.M., ANTONARAKIS, S.E., WERTHEIMER, E., ROTH, J. and SHULDINER, A.R., Determination of gene dosage by a quantitative adaptation of the polymerase chain reaction (gd-PCR): rapid detection of deletions and duplications of gene sequences. *Genomics*, **21**, 304–310 (1994).

COURJAL, F., CUNY, M., SIMONY-LAFONTAINE, J., LOUASSON, G., SPEISER, P., ZEILLINGER, R., RODRIGUEZ, C. and THEILLET, C., Mapping of DNA amplifications at 15 chromosomal localizations in 1875 breast tumors: definition of phenotypic groups. *Cancer Res.*, **57**, 4360–4367 (1997).

DENG, G., YU, M., CHEN, L.C., MOORE, D., KURISU, W., KALLIONIEMI, A., WALDMAN, F.M., COLLINS, C. and SMITH, H.S., Amplifications of oncogene *erb*B-2 and chromosome 20q in breast cancer determined by differentially competitive polymerase chain reaction. *Breast Cancer Res. Treat.*, **40**, 271–281 (1996).

GELMINI, S., ORLANDO, C., SESTINI, R., VONA, G., PINZANI, P., RUOCCO, L. and PAZZAGLI, M., Quantitative polymerase chain reaction-based homoge-neous assay with fluorogenic probes to measure c-*erb*-2 oncogene amplifi-cation. *Clin. Chem.*, **43**, 752–758 (1997).

GIBSON, U.E.M., HEID, C.A. and WILLIAMS, P.M., A novel method for real-time quantitative RT-PCR. *Genome Res.*, **6**, 995–1001 (1996).

HEID, C.A., STEVENS, J., LIVAK, K.J. and WILLIAMS, P.M., Real-time quantitative PCR. *Genome Res.*, **6**, 986–994 (1996).

HOLLAND, P.M., ABRAMSON, R.D., WATSON, R. and GELFAND, D.H., Detection of specific polymerase chain reaction product by utilizing the 5′ to 3′ exonuclease activity of *Thermus aquaticus* DNA polymerase. *Proc. nat. Acad. Sci. (Wash.)*, **88**, 7276–7280 (1991).

KALLIONIEMI, A., KALLIONIEMI, O.P., PIPER, J., TANNER, M., STOKKES, T., CHEN, L., SMITH, H.S., PINKEL, D., GRAY, J.W. and WALDMAN, F.M., Detection and mapping of amplified DNA sequences in breast cancer by comparative genomic hybridization. *Proc. nat. Acad. Sci. (Wash.)*, **91**, 2156–2160 (1994).

LEE, L.G., CONNELL, C.R. and BIOCH, W., Allelic discrimination by nick-translation PCR with fluorogenic probe. *Nucleic Acids Res.*, **21**, 3761–3766 (1993).

LONGO, N., BERNINGER, N.S. and HARTLEY, J.L., Use of uracil DNA glycosylase to control carry-over contamination in polymerase chain reactions. *Gene*, **93**, 125–128 (1990).

MUSS, H.B., THOR, A.D., BERRY, D.A., KUTE, T., LIU, E.T., KOERNER, F., CIRRINCIONE, C.T., BUDMAN, D.R., WOOD, W.C., BARCOS, M. and HENDER-SON, I.C., c-*erb*B-2 expression and response to adjuvant therapy in women with node-positive early breast cancer. *New Engl. J. Med.*, **330**, 1260–1266 (1994).

PAULETTI, G., GODOLPHIN, W., PRESS, M.F. and SALMON, D.J., Detection and quantification of HER-2/*neu* gene amplification in human breast cancer archival material using fluorescence *in situ* hybridization. *Oncogene*, **13**, 63–72 (1996).

PIATAK, M., LUK, K.C., WILLIAMS, B. and LIFSON, J.D., Quantitative competitive polymerase chain reaction for accurate quantitation of HIV DNA and RNA species. *Biotechniques*, **14**, 70–80 (1993).

SCHUURING, E., VERHOEVEN, E., VAN TINTEREN, H., PETERSE, J.L., NUNNIK, B., THUNNISSEN, F.B.J.M., DEVILEE, P., CORNELISSE, C.J., VAN DE VIJVER, M.J., MOOI, W.J. and MICHALIDES, R.J.A.M., Amplification of genes within the chromosome 11q13 region is indicative of poor prognosis in patients with operable breast cancer. *Cancer Res.*, **52**, 5229–5234 (1992).

SLAMON, D.J., CLARK, G.M., WONG, S.G., LEVIN, W.S., ULLRICH, A. and McGUIRE, W.L., Human breast cancer: correlation of relapse and survival with amplification of the HER-2/*neu* oncogene. *Science*, **235**, 177–182 (1987).

SLAMON, D.J., GODOLPHIN, W., JONES, L.A., HOLT, J.A., WONG, S.G., KEITH, D.E., LEVIN, W.J., STUART, S.G., UDOVE, J., ULLRICH, A. and PRESS, M.F., Studies of the HER-2/*neu* proto-oncogene in human breast and ovarian cancer. *Science*, **244**, 707–712 (1989).

VALERON, P.F., CHIRINO, R., FERNANDEZ, L., TORRES, S., NAVARRO, D., AGUIAR, J., CABRERA, J.J., DIAZ-CHICO, B.N. and DIAZ-CHICO, J.C., Validation of a differential PCR and an ELISA procedure in studying HER-2/*neu* status in breast cancer. *Int. J. Cancer*, **65**, 129–133 (1996).

IN THE UNITED STATES PATENT AND TRADEMARK OFFICE

Applicant	:	Ashkenazi et al.
App. No.	:	09/903,925
Filed	:	July 11, 2001
For	:	SECRETED AND TRANSMEMBRANE POLYPEPTIDES AND NUCLEIC ACIDS ENCODING THE SAME
Examiner	:	Hamud, Fozia M

Commissioner of Patents
P.O. Box 1450
Alexandria, VA 22313-1450

DECLARATION OF AVI ASHKENAZI, Ph.D UNDER 37 C.F.R. § 1.132

I, Avi Ashkenazi, Ph.D. declare and say as follows: -

1.   I am Director and Staff Scientist at the Molecular Oncology Department of Genentech, Inc., South San Francisco, CA 94080.

2.   I joined Genentech in 1988 as a postdoctoral fellow. Since then, I have investigated a variety of cellular signal transduction mechanisms, including apoptosis, and have developed technologies to modulate such mechanisms as a means of therapeutic intervention in cancer and autoimmune disease. I am currently involved in the investigation of a series of secreted proteins over-expressed in tumors, with the aim to identify useful targets for the development of therapeutic antibodies for cancer treatment.

3.   My scientific Curriculum Vitae, including my list of publications, is attached to and forms part of this Declaration (Exhibit A).

4.   Gene amplification is a process in which chromosomes undergo changes to contain multiple copies of certain genes that normally exist as a single copy, and is an important factor in the pathophysiology of cancer. Amplification of certain genes (e.g., Myc or Her2/Neu)

gives cancer cells a growth or survival advantage relative to normal cells, and might also provide a mechanism of tumor cell resistance to chemotherapy or radiotherapy.

5.   If gene amplification results in over-expression of the mRNA and the corresponding gene product, then it identifies that gene product as a promising target for cancer therapy, for example by the therapeutic antibody approach. Even in the absence of over-expression of the gene product, amplification of a cancer marker gene - as detected, for example, by the reverse transcriptase TaqMan® PCR or the fluorescence *in situ* hybridization (FISH) assays -is useful in the diagnosis or classification of cancer, or in predicting or monitoring the efficacy of cancer therapy. An increase in gene copy number can result not only from intrachromosomal changes but also from chromosomal aneuploidy. It is important to understand that detection of gene amplification can be used for cancer diagnosis even if the determination includes measurement of chromosomal aneuploidy. Indeed, as long as a significant difference relative to normal tissue is detected, it is irrelevant if the signal originates from an increase in the number of gene copies per chromosome and/or an abnormal number of chromosomes.

6.   I understand that according to the Patent Office, absent data demonstrating that the increased copy number of a gene in certain types of cancer leads to increased expression of its product, gene amplification data are insufficient to provide substantial utility or well established utility for the gene product (the encoded polypeptide), or an antibody specifically binding the encoded polypeptide. However, even when amplification of a cancer marker gene does not result in significant over-expression of the corresponding gene product, this very absence of gene product over-expression still provides significant information for cancer diagnosis and treatment. Thus, if over-expression of the gene product does not parallel gene amplification in certain tumor types but does so in others, then parallel monitoring of gene amplification and gene product over-expression enables more accurate tumor classification and hence better determination of suitable therapy. In addition, absence of over-expression is crucial information for the practicing clinician. If a gene is amplified but the corresponding gene product is not over-expressed, the clinician accordingly will decide not to treat a patient with agents that target that gene product.

7.   I hereby declare that all statements made herein of my own knowledge are true and that all statements made on information or belief are believed to be true, and further that these statements were made with the knowledge that willful false statements and the like so

made are punishable by fine or imprisonment, or both, under Section 1001 of Title 18 of the United States Code and that such willful statements may jeopardize the validity of the application or any patent issued thereon.

By: _Avi Ashkenazi_   Date: _9/15/03_
Avi Ashkenazi, Ph.D.

CURRICULUM VITAE
Avi Ashkenazi
July 2003

Personal:

Date of birth:	29 November, 1956
Address:	1456 Tarrytown Street, San Mateo, CA 94402
Phone:	(650) 578-9199 (home); (650) 225-1853 (office)
Fax:	(650) 225-6443 (office)
Email:	aa@gene.com

Education:

1983:	B.S. in Biochemistry, with honors, Hebrew University, Israel
1986:	Ph.D. in Biochemistry, Hebrew University, Israel

Employment:

1983-1986:	Teaching assistant, undergraduate level course in Biochemistry
1985-1986:	Teaching assistant, graduate level course on Signal Transduction
1986 - 1988:	Postdoctoral fellow, Hormone Research Dept., UCSF, and Developmental Biology Dept., Genentech, Inc., with J. Ramachandran
1988 - 1989:	Postdoctoral fellow, Molecular Biology Dept., Genentech, Inc., with D. Capon
1989 - 1993:	Scientist, Molecular Biology Dept., Genentech, Inc.
1994 -1996:	Senior Scientist, Molecular Oncology Dept., Genentech, Inc.
1996-1997:	Senior Scientist and Interim director, Molecular Oncology Dept., Genentech, Inc.
1997-1990:	Senior Scientist and preclinical project team leader, Genentech, Inc.
1999 -2002:	Staff Scientist in Molecular Oncology, Genentech, Inc.
2002-present:	Staff Scientist and Director in Molecular Oncology, Genentech, Inc.

Awards:

1988:	First prize, The Boehringer Ingelheim Award

Editorial:

Editorial Board Member: Current Biology

Associate Editor, Clinical Cancer Research.

Associate Editor, Cancer Biology and Therapy.

Refereed papers:

1. Gertler, A., Ashkenazi, A., and Madar, Z. Binding sites for human growth hormone and ovine and bovine prolactins in the mammary gland and liver of the lactating cow. *Mol. Cell. Endocrinol.* **34**, 51-57 (1984).

2. Gertler, A., Shamay, A., Cohen, N., Ashkenazi, A., Friesen, H., Levanon, A., Gorecki, M., Aviv, H., Hadari, D., and Vogel, T. Inhibition of lactogenic activities of ovine prolactin and human growth hormone (hGH) by a novel form of a modified recombinant hGH. *Endocrinology* **118**, 720-726 (1986).

3. Ashkenazi, A., Madar, Z., and Gertler, A. Partial purification and characterization of bovine mammary gland prolactin receptor. *Mol. Cell. Endocrinol.* **50**, 79-87 (1987).

4. Ashkenazi, A., Pines, M., and Gertler, A. Down-regulation of lactogenic hormone receptors in Nb2 lymphoma cells by cholera toxin. *Biochemistry Internatl.* **14**, 1065-1072 (1987).

5. Ashkenazi, A., Cohen, R., and Gertler, A. Characterization of lactogen receptors in lactogenic hormone-dependent and independent Nb2 lymphoma cell lines. *FEBS Lett.* **210**, 51-55 (1987).

6. Ashkenazi, A., Vogel, T., Barash, I., Hadari, D., Levanon, A., Gorecki, M., and Gertler, A. Comparative study on in vitro and in vivo modulation of lactogenic and somatotropic receptors by native human growth hormone and its modified recombinant analog. *Endocrinology* **121**, 414-419 (1987).

7. Peralta, E., Winslow, J., Peterson, G., Smith, D., Ashkenazi, A., Ramachandran, J., Schimerlik, M., and Capon, D. Primary structure and biochemical properties of an M2 muscarinic receptor. *Science* **236**, 600-605 (1987).

8. Peralta, E. Ashkenazi, A., Winslow, J., Smith, D., Ramachandran, J., and Capon, D. J. Distincnt primary structures, ligand-binding properties and tissue-specific expression of four human muscarinic acetylcholine receptors. *EMBO J.* **6**, 3923-3929 (1987).

9. Ashkenazi, A., Winslow, J., Peralta, E., Peterson, G., Schimerlik, M., Capon, D., and Ramachandran, J. An M2 muscarinic receptor subtype coupled to both adenylyl cyclase and phosphoinositide turnover. *Science* **238**, 672-675 (1987).

10. Pines, M., <u>Ashkenazi, A.</u>, Cohen-Chapnik, N., Binder, L., and Gertler, A. Inhibition of the proliferation of Nb2 lymphoma cells by femtomolar concentrations of cholera toxin and partial reversal of the effect by 12-o-tetradecanoyl-phorbol-13-acetate. *J. Cell. Biochem.* **37**, 119-129 (1988).

11. Peralta, E. <u>Ashkenazi, A.</u>, Winslow, J. Ramachandran, J., and Capon, D. Differential regulation of PI hydrolysis and adenylyl cyclase by muscarinic receptor subtypes. *Nature* **334**, 434-437 (1988).

12. <u>Ashkenazi., A.</u> Peralta, E., Winslow, J., Ramachandran, J., and Capon, D. Functionally distinct G proteins couple different receptors to PI hydrolysis in the same cell. *Cell* **56**, 487-493 (1989).

13. <u>Ashkenazi, A.</u>, Ramachandran, J., and Capon, D. Acetylcholine analogue stimulates DNA synthesis in brain-derived cells via specific muscarinic acetylcholine receptor subtypes. *Nature* **340**, 146-150 (1989).

14. Lammare, D., <u>Ashkenazi, A.</u>, Fleury, S., Smith, D., Sekaly, R., and Capon, D. The MHC-binding and gp120-binding domains of CD4 are distinct and separable. *Science* **245**, 743-745 (1989).

15. <u>Ashkenazi., A.</u>, Presta, L., Marsters, S., Camerato, T., Rosenthal, K., Fendly, B., and Capon, D. Mapping the CD4 binding site for human immunodefficiency virus type 1 by alanine-scanning mutagenesis. *Proc. Natl. Acad. Sci. USA.* **87**, 7150-7154 (1990).

16. Chamow, S., Peers, D., Byrn, R., Mulkerrin, M., Harris, R., Wang, W., Bjorkman, P., Capon, D., and <u>Ashkenazi, A.</u> Enzymatic cleavage of a CD4 immunoadhesin generates crystallizable, biologically active Fd-like fragments. *Biochemistry* **29**, 9885-9891 (1990).

17. <u>Ashkenazi, A.</u>, Smith, D., Marsters, S., Riddle, L., Gregory, T., Ho, D., and Capon, D. Resistance of primary isolates of human immunodefficiency virus type 1 to soluble CD4 is independent of CD4-rgp120 binding affinity. *Proc. Natl. Acad. Sci. USA.* **88**, 7056-7060 (1991).

18. <u>Ashkenazi, A.</u>, Marsters, S., Capon, D., Chamow, S., Figari., I., Pennica, D., Goeddel., D., Palladino, M., and Smith, D. Protection against endotoxic shock by a tumor necrosis factor receptor immunoadhesin. *Proc. Natl. Acad. Sci. USA.* **88**, 10535-10539 (1991).

19. Moore, J., McKeating, J., Huang, Y., <u>Ashkenazi, A.</u>, and Ho, D. Virions of primary HIV-1 isolates resistant to sCD4 neutralization differ in sCD4 affinity and glycoprotein gp120 retention from sCD4-sensitive isolates. *J. Virol.* **66**, 235-243 (1992).

20. Jin, H., Oksenberg, D., Ashkenazi, A., Peroutka, S., Duncan, A., Rozmahel., R., Yang, Y., Mengod, G., Palacios, J., and O'Dowd, B. Characterization of the human 5-hydroxytryptamine$_{1B}$ receptor. *J. Biol. Chem.* **267**, 5735-5738 (1992).

21. Marsters, A., Frutkin, A., Simpson, N., Fendly, B. and Ashkenazi, A. Identification of cysteine-rich domains of the type 1 tumor necrosis receptor involved in ligand binding. *J. Biol. Chem.* **267**, 5747-5750 (1992).

22. Chamow, S., Kogan, T., Peers, D., Hastings, R., Byrn, R., and Ashkenazi, A. Conjugation of sCD4 without loss of biological activity via a novel carbohydrate-directed cross-linking reagent. *J. Biol. Chem.* **267**, 15916-15922 (1992).

23. Oksenberg, D., Marsters, A., O'Dowd, B., Jin, H., Havlik, S., Peroutka, S., and Ashkenazi, A. A single amino-acid difference confers major pharmacologic variation between human and rodent 5-HT$_{1B}$ receptors. *Nature* **360**, 161-163 (1992).

24. Haak-Frendscho, M., Marsters, S., Chamow, S., Peers, D., Simpson, N., and Ashkenazi, A. Inhibition of interferon γ by an interferon γ receptor immunoadhesin. *Immunology* **79**, 594-599 (1993).

25. Penica, D., Lam, V., Weber, R., Kohr, W., Basa, L., Spellman, M., Ashkenazi, Shire, S., and Goeddel, D. Biochemical characterization of the extracellular domain of the 75-kd tumor necrosis factor receptor. *Biochemistry* **32**, 3131-3138. (1993).

26. Barfod, L., Zheng, Y., Kuang, W., Hart, M., Evans, T., Cerione, R., and Ashkenazi, A. Cloning and expression of a human CDC42 GTPase Activating Protein reveals a functional SH3-binding domain. *J. Biol. Chem.* **268**, 26059-26062 (1993).

27. Chamow, S., Zhang, D., Tan, X., Mhtre, S., Marsters, S., Peers, D., Byrn, R., Ashkenazi, A., and Yunghans, R. A humanized bispecific immunoadhesin-antibody that retargets CD3+ effectors to kill HIV-1-infected cells. *J. Immunol.* **153**, 4268-4280 (1994).

28. Means, R., Krantz, S., Luna, J., Marsters, S., and Ashkenazi, A. Inhibition of murine erythroid colony formation in vitro by iterferon γ and correction by interferon γ receptor immunoadhesin. *Blood* **83**, 911-915 (1994).

29. Haak-Frendscho, M., Marsters, S., Mordenti, J., Gillet, N., Chen, S., andAshkenazi, A. Inhibition of TNF by a TNF receptor immunoadhesin: comparison with an anti-TNF mAb. *J. Immunol.* **152**, 1347-1353 (1994).

30.   Chamow, S., Kogan, T., Venuti, M., Gadek, T., Peers, D., Mordenti, J., Shak, S., and Ashkenazi, A. Modification of CD4 immunoadhesin with monomethoxy-PEG aldehyde via reductive alkilation. *Bioconj. Chem.* **5**, 133-140 (1994).

31.   Jin, H., Yang, R., Marsters, S., Bunting, S., Wurm, F., Chamow, S., and Ashkenazi, A. Protection against rat endotoxic shock by p55 tumor necrosis factor (TNF) receptor immunoadhesin: comparison to anti-TNF monoclonal antibody. *J. Infect. Diseases* **170**, 1323-1326 (1994).

32.   Beck, J., Marsters, S., Harris, R., Ashkenazi, A., and Chamow, S. Generation of soluble interleukin-1 receptor from an immunoadhesin by specific cleavage. *Mol. Immunol.* **31**, 1335-1344 (1994).

33.   Pitti, B., Marsters, M., Haak-Frendscho, M., Osaka, G., Mordenti, J., Chamow, S., and Ashkenazi, A. Molecular and biological properties of an interleukin-1 receptor immunoadhesin. *Mol. Immunol.* **31**, 1345-1351 (1994).

34.   Oksenberg, D., Havlik, S., Peroutka, S., and Ashkenazi, A. The third intracellular loop of the 5-HT2 receptor specifies effector coupling. *J. Neurochem.* **64**, 1440-1447 (1995).

35.   Bach, E., Szabo, S., Dighe, A., Ashkenazi, A., Aguet, M., Murphy, K., and Schreiber, R. Ligand-induced autoregulation of IFN-γ receptor β chain expression in T helper cell subsets. *Science* **270**, 1215-1218 (1995).

36.   Jin, H., Yang, R., Marsters, S., Ashkenazi, A., Bunting, S., Marra, M., Scott, R., and Baker, J. Protection against endotoxic shock by bactericidal/permeability-increasing protein in rats. *J. Clin. Invest.* **95**, 1947-1952 (1995).

37.   Marsters, S., Penica, D., Bach, E., Schreiber, R., and Ashkenazi, A. Interferon γ signals via a high-affinity multisubunit receptor complex that contains two types of polypeptide chain. *Proc. Natl. Acad. Sci. USA.* **92**, 5401-5405 (1995).

38.   Van Zee, K., Moldawer, L., Oldenburg, H., Thompson, W., Stackpole, S., Montegut, W., Rogy, M., Meschter, C., Gallati, H., Schiller, C., Richter, W., Loetcher, H., Ashkenazi, A., Chamow, S., Wurm, F., Calvano, S., Lowry, S., and Lesslauer, W. Protection against lethal E. coli bacteremia in baboons by pretreatment with a 55-kDa TNF receptor-Ig fusion protein, Ro45-2081. *J. Immunol.* **156**, 2221-2230 (1996).

39.   Pitti, R., Marsters, S., Ruppert, S., Donahue, C., Moore, A., and Ashkenazi, A. Induction of apoptosis by Apo-2 Ligand, a new member of the tumor necrosis factor cytokine family. *J. Biol. Chem.* **271**, 12687-12690 (1996).

40. Marsters, S., Pitti, R., Donahue, C., Rupert, S., Bauer, K., and Ashkenazi, A. Activation of apoptosis by Apo-2 ligand is independent of FADD but blocked by CrmA. *Curr. Biol.* **6**, 1669-1676 (1996).

41. Marsters, S., Skubatch, M., Gray, C., and Ashkenazi, A. Herpesvirus entry mediator, a novel member of the tumor necrosis factor receptor family, activates the NF-κB and AP-1 transcription factors. *J. Biol. Chem.* **272**, 14029-14032 (1997).

42. Sheridan, J., Marsters, S., Pitti, R., Gurney, A., Skubatch, M., Baldwin, D., Ramakrishnan, L., Gray, C., Baker, K., Wood, W.I., Goddard, A., Godowski, P., and Ashkenazi, A. Control of TRAIL-induced apoptosis by a family of signaling and decoy receptors. *Science* **277**, 818-821 (1997).

43. Marsters, S., Sheridan, J., Pitti, R., Gurney, A., Skubatch, M., Balswin, D., Huang, A., Yuan, J., Goddard, A., Godowski, P., and Ashkenazi, A. A novel receptor for Apo2L/TRAIL contains a truncated death domain. *Curr. Biol.* **7**, 1003-1006 (1997).

44. Marsters, A., Sheridan, J., Pitti, R., Brush, J., Goddard, A., and Ashkenazi, A. Identification of a ligand for the death-domain-containing receptor Apo3. *Curr. Biol.* **8**, 525-528 (1998).

45. Rieger, J., Naumann, U., Glaser, T., Ashkenazi, A., and Weller, M. Apo2 ligand: a novel weapon against malignant glioma? *FEBS Lett.* **427**, 124-128 (1998).

46. Pender, S., Fell, J., Chamow, S., Ashkenazi, A., and MacDonald, T. A p55 TNF receptor immunoadhesin prevents T cell mediated intestinal injury by inhibiting matrix metalloproteinase production. *J. Immunol.* **160**, 4098-4103 (1998).

47. Pitti, R., Marsters, S., Lawrence, D., Roy, Kischkel, F., M., Dowd, P., Huang, A., Donahue, C., Sherwood, S., Baldwin, D., Godowski, P., Wood, W., Gurney, A., Hillan, K., Cohen, R., Goddard, A., Botstein, D., and Ashkenazi, A. Genomic amplification of a decoy receptor for Fas ligand in lung and colon cancer. *Nature* **396**, 699-703 (1998).

48. Mori, S., Marakami-Mori, K., Nakamura, S., Ashkenazi, A., and Bonavida, B. Sensitization of AIDS Kaposi's sarcoma cells to Apo-2 ligand-induced apoptosis by actinomycin D. *J. Immunol.* **162**, 5616-5623 (1999).

49. Gurney, A. Marsters, S., Huang, A., Pitti, R., Mark, M., Baldwin, D., Gray, A., Dowd, P., Brush, J., Heldens, S., Schow, P., Goddard, A., Wood, W., Baker, K., Godowski, P., and Ashkenazi, A. Identification of a new member of the tumor necrosis factor family and its receptor, a human ortholog of mouse GITR. *Curr. Biol.* **9**, 215-218 (1999).

50. Ashkenazi, A., Pai, R., Fong, s., Leung, S., Lawrence, D., Marsters, S., Blackie, C., Chang, L., McMurtrey, A., Hebert, A., DeForge, L., Khoumenis, I., Lewis, D., Harris, L., Bussiere, J., Koeppen, H., Shahrokh, Z., and Schwall, R. Safety and anti-tumor activity of recombinant soluble Apo2 ligand. *J. Clin. Invest.* **104**, 155-162 (1999).

51. Chuntharapai, A., Gibbs, V., Lu, J., Ow, A., Marsters, S., Ashkenazi, A., De Vos, A., Kim, K.J. Determination of residues involved in ligand binding and signal transmissiion in the human IFN-α receptor 2. *J. Immunol.* **163**, 766-773 (1999).

52. Johnsen, A.-C., Haux, J., Steinkjer, B., Nonstad, U., Egeberg, K., Sundan, A., Ashkenazi, A., and Espevik, T. Regulation of Apo2L/TRAIL expression in NK cells – involvement in NK cell-mediated cytotoxicity. *Cytokine* **11**, 664-672 (1999).

53. Roth, W., Isenmann, S., Naumann, U., Kugler, S., Bahr, M., Dichgans, J., Ashkenazi, A., and Weller, M. Eradication of intracranial human malignant glioma xenografts by Apo2L/TRAIL. *Biochem. Biophys. Res. Commun.* **265**, 479-483 (1999).

54. Hymowitz, S.G., Christinger, H.W., Fuh, G., Ultsch, M., O'Connell, M., Kelley, R.F., Ashkenazi, A. and de Vos, A.M. Triggering Cell Death: The Crystal Structure of Apo2L/TRAIL in a Complex with Death Receptor 5. *Molec. Cell* **4**, 563–571 (1999).

55. Hymowitz, S.G., O'Connel, M.P., Utsch, M.H., Hurst, A., Totpal, K., Ashkenazi, A., de Vos, A.M., Kelley, R.F. A unique zinc-binding site revealed by a high-resolution X-ray structure of homotrimeric Apo2L/TRAIL. *Biochemistry* **39**, 633-640 (2000).

56. Zhou, Q., Fukushima, P., DeGraff, W., Mitchell, J.B., Stetler-Stevenson, M., Ashkenazi, A., and Steeg, P.S. Radiation and the Apo2L/TRAIL apoptotic pathway preferentially inhibit the colonization of premalignant human breast cancer cells overexpressing cyclin D1. *Cancer Res.* **60**, 2611-2615 (2000).

57. Kischkel, F.C., Lawrence, D. A., Chuntharapai, A., Schow, P., Kim, J., and Ashkenazi, A. Apo2L/TRAIL-dependent recruitment of endogenous FADD and Caspase-8 to death receptors 4 and 5. *Immunity* **12**, 611-620 (2000).

58. Yan, M., Marsters, S.A., Grewal, I.S., Wang, H., *Ashkenazi, A., and *Dixit, V.M. Identification of a receptor for BlyS demonstrates a crucial role in humoral immunity. *Nature Immunol.* **1**, 37-41 (2000).

59. Marsters, S.A., Yan, M., Pitti, R.M., Haas, P.E., Dixit, V.M., and <u>Ashkenazi, A.</u> Interaction of the TNF homologues BLyS and APRIL with the TNF receptor homologues BCMA and TACI. *Curr. Biol.* **10**, 785-788 (2000).

60. Kischkel, F.C., and <u>Ashkenazi, A</u>. Combining enhanced metabolic labeling with immunoblotting to detect interactions of endogenous cellular proteins. *Biotechniques* **29**, 506-512 (2000).

61. Lawrence, D., Shahrokh, Z., Marsters, S., Achilles, K., Shih, D. Mounho, B., Hillan, K., Totpal, K. DeForge, L., Schow, P., Hooley, J., Sherwood, S., Pai, R., Leung, S., Khan, L., Gliniak, B., Bussiere, J., Smith, C., Strom, S., Kelley, S., Fox, J., Thomas, D., and <u>Ashkenazi, A.</u> Differential hepatocyte toxicity of recombinant Apo2L/TRAIL versions. *Nature Med.* **7**, 383-385 (2001).

62. Chuntharapai, A., Dodge, K., Grimmer, K., Schroeder, K., Martsters, S.A., Koeppen, H., <u>Ashkenazi, A.</u>, and Kim, K.J. Isotype-dependent inhibition of tumor growth in vivo by monoclonal antibodies to death receptor 4. *J. Immunol.* **166**, 4891-4898 (2001).

63. Pollack, I.F., Erff, M., and <u>Ashkenazi, A</u>. Direct stimulation of apoptotic signaling by soluble Apo2L/tumor necrosis factor-related apoptosis-inducing ligand leads to selective killing of glioma cells. *Clin. Cancer Res.* **7**, 1362-1369 (2001).

64. Wang, H., Marsters, S.A., Baker, T., Chan, B., Lee, W.P., Fu, L., Tumas, D., Yan, M., Dixit, V.M., *<u>Ashkenazi, A.</u>, and *Grewal, I.S. TACI-ligand interactions are required for T cell activation and collagen-induced arthritis in mice. *Nature Immunol.* **2**, 632-637 (2001).

65. Kischkel, F.C., Lawrence, D. A., Tinel, A., Virmani, A., Schow, P., Gazdar, A., Blenis, J., Arnott, D., and <u>Ashkenazi, A</u>. Death receptor recruitment of endogenous caspase-10 and apoptosis initiation in the absence of caspase-8. *J. Biol. Chem.* **276**, 46639-46646 (2001).

66. LeBlanc, H., Lawrence, D.A., Varfolomeev, E., Totpal, K., Morlan, J., Schow, P., Fong, S., Schwall, R., Sinicropi, D., and <u>Ashkenazi, A</u> Tumor cell resistance to death receptor induced apoptosis through mutational inactivation of the proapoptotitc Bcl-2 homolog Bax. *Nature Med.* **8**, 274-281 (2002).

67. Miller, K., Meng, G., Liu, J., Hurst, A., Hsei, V., Wong, W-L., Ekert, R., Lawrence, D., Sherwood, S., DeForge, L., Gaudreault., Keller, G., Sliwkowski, M., <u>Ashkenazi, A.</u>, and Presta, L. Design, Construction, and analyses of multivalent antibodies. *J. Immunol.* **170**, 4854-4861 (2003).

68.   Varfolomeev, E., Kischkel, F., Martin, F., Wanh, H., Lawrence, D., Olsson, C.,
        Tom, L., Erickson, S., French, D., Schow, P., Grewal, I. and Ashkenazi, A.
        Immune system development in APRIL knockout mice. Submitted.

Review articles:

1.   Ashkenazi, A., Peralta, E., Winslow, J., Ramachandran, J., and Capon, D., J.
        Functional role of muscarinic acetylcholine receptor subtype diversity. *Cold
        Spring Harbor Symposium on Quantitative Biology.* LIII, 263-272 (1988).

2.   Ashkenazi, A., Peralta, E., Winslow, J., Ramachandran, J., and Capon, D.
        Functional diversity of muscarinic receptor subtypes in cellular signal
        transduction and growth. *Trends Pharmacol. Sci.* Dec Supplement, 12-21 (1989).

3.   Chamow, S., Duliege, A., Ammann, A., Kahn, J., Allen, D., Eichberg, J., Byrn,
        R., Capon, D., Ward, R., and Ashkenazi, A. CD4 immunoadhesins in anti-HIV
        therapy: new developments. *Int. J. Cancer* Supplement 7, 69-72 (1992).

4.   Ashkenazi, A., Capon, and D. Ward, R. Immunoadhesins. *Int. Rev. Immunol.* 10,
        217-225 (1993).

5.   Ashkenazi, A., and Peralta, E. Muscarinic Receptors. In *Handbook of Receptors
        and Channels.* (S. Peroutka, ed.), CRC Press, Boca Raton, Vol. I, p. 1-27, (1994).

6.   Krantz, S. B., Means, R. T., Jr., Lina, J., Marsters, S. A., and Ashkenazi, A.
        Inhibition of erythroid colony formation in vitro by gamma interferon. In
        Molecular Biology of Hematopoiesis (N. Abraham, R. Shadduck, A. Levine F.
        Takaku, eds.) Intercept Ltd. Paris, Vol. 3, p. 135-147 (1994).

7.   Ashkenazi, A. Cytokine neutralization as a potential therapeutic approach for
        SIRS and shock. *J. Biotechnology in Healthcare* 1, 197-206 (1994).

8.   Ashkenazi, A., and Chamow, S. M. Immunoadhesins: an alternative to human
        monoclonal antibodies. *Immunomethods: A companion to Methods in
        Enzimology* 8, 104-115 (1995).

9.   Chamow, S., and Ashkenazi, A. Immunoadhesins: Principles and Applications.
        Trends Biotech. 14, 52-60 (1996).

10.   Ashkenazi, A., and Chamow, S. M. Immunoadhesins as research tools and
        therapeutic agents. *Curr. Opin. Immunol.* 9, 195-200 (1997).

11.   Ashkenazi, A., and Dixit, V. Death receptors: signaling and modulation. *Science*
        281, 1305-1308 (1998).

12.   Ashkenazi, A., and Dixit, V. Apoptosis control by death and decoy receptors.
        Curr. Opin. Cell. Biol. 11, 255-260 (1999).

13. <u>Ashkenazi, A</u>. Chapters on Apo2L/TRAIL; DR4, DR5, DcR1, DcR2; and DcR3. Online Cytokine Handbook (www.apnet.com/cytokinereference/).

14. <u>Ashkenazi, A</u>. Targeting death and decoy receptors of the tumor necrosis factor superfamily. *Nature Rev. Cancer* 2, 420-430 (2002).

15. LeBlanc, H. and <u>Ashkenazi, A</u>. Apoptosis signaling by Apo2L/TRAIL. *Cell Death and Differentiation* 10, 66-75 (2003).

16. Almasan, A. and <u>Ashkenazi, A</u>. Apo2L/TRAIL: apoptosis signaling, biology, and potential for cancer therapy. Cytokine and Growth Factor Reviews 14, 337-348 (2003).

Book:

Antibody Fusion Proteins (Chamow, S., and <u>Ashkenazi, A</u>., eds., John Wiley and Sons Inc.) (1999).

Talks:

1. Resistance of primary HIV isolates to CD4 is independent of CD4-gp120 binding affinity. UCSD Symposium, HIV Disease: Pathogenesis and Therapy. Greenelefe, FL, March 1991.

2. Use of immuno-hybrids to extend the half-life of receptors. IBC conference on Biopharmaceutical Halflife Extension. New Orleans, LA, June 1992.

3. Results with TNF receptor Immunoadhesins for the Treatment of Sepsis. IBC conference on Endotoxemia and Sepsis. Philadelphia, PA, June 1992.

4. Immunoadhesins: an alternative to human antibodies. IBC conference on Antibody Engineering. San Diego, CA, December 1993.

5. Tumor necrosis factor receptor: a potential therapeutic for human septic shock. American Society for Microbiology Meeting, Atlanta, GA, May 1993.

6. Protective efficiacy of TNF receptor immunoadhesin vs anti-TNF monoclonal antibody in a rat model for endotoxic shock. 5th International Congress on TNF. Asilomar, CA, May 1994.

7. Interferon-γ signals via a multisubunit receptor complex that contains two types of polypeptide chain. American Association of Immunologists Conference. San Franciso, CA, July 1995.

8. Immunoadhesins: Principles and Applications. Gordon Research Conference on Drug Delivery in Biology and Medicine. Ventura, CA, February 1996.

9. Apo-2 Ligand, a new member of the TNF family that induces apoptosis in tumor cells. Cambridge Symposium on TNF and Related Cytokines in Treatment of Cancer. Hilton-Head, NC, March 1996.

10. Induction of apoptosis by Apo2 Ligand. American Society for Biochemistry and Molecular Biology, Symposium on Growth Factors and Cytokine Receptors. New Orleans, LA, June, 1996.

11. Apo2 ligand, an extracellular trigger of apoptosis. 2nd Clontech Symposium, Palo Alto, CA, October 1996.

12. Regulation of apoptosis by members of the TNF ligand and receptor families. Stanford University School of Medicine, Palo Alto, CA, December 1996.

13. Apo-3: anovel receptor that regulates cell death and inflammation. 4th International Congress on Immune Consequences of Trauma, Shock, and Sepsis. Munich, Germany, March 1997.

14. New members of the TNF ligand and receptor families that regulate apoptosis, inflammation, and immunity. UCLA School of Medicine, LA, CA, March 1997.

15. Immunoadhesins: an alternative to monoclonal antibodies. 5th World Conference on Bispecific Antibodies. Volendam, Holland, June 1997.

16. Control of Apo2L signaling. Cold Spring Harbor Laboratory Symposium on Programmed Cell Death. Cold Spring Harbor, New York. September, 1997.

17. Chairman and speaker, Apoptosis Signaling session. IBC's 4th Annual Conference on Apoptosis. San Diego, CA., October 1997.

18. Control of Apo2L signaling by death and decoy receptors. American Association for the Advancement of Science. Philladelphia, PA, February 1998.

19. Apo2 ligand and its receptors. American Society of Immunologists. San Francisco, CA, April 1998.

20. Death receptors and ligands. 7th International TNF Congress. Cape Cod, MA, May 1998.

21. Apo2L as a potential therapeutic for cancer. UCLA School of Medicine. LA, CA, June 1998.

22. Apo2L as a potential therapeutic for cancer. Gordon Research Conference on Cancer Chemotherapy. New London, NH, July 1998.

23. Control of apoptosis by Apo2L. Endocrine Society Conference, Stevenson, WA, August 1998.

24. Control of apoptosis by Apo2L. International Cytokine Society Conference, Jerusalem, Israel, October 1998.

25. Apoptosis control by death and decoy receptors. American Association for Cancer Research Conference, Whistler, BC, Canada, March 1999.

26. Apoptosis control by death and decoy receptors. American Society for Biochemistry and Molecular Biology Conference, San Francisco, CA, May 1999.

27. Apoptosis control by death and decoy receptors. Gordon Research Conference on Apoptosis, New London, NH, June 1999.

28. Apoptosis control by death and decoy receptors. Arthritis Foundation Research Conference, Alexandria GA, Aug 1999.

29. Safety and anti-tumor activity of recombinant soluble Apo2L/TRAIL. Cold Spring Harbor Laboratory Symposium on Programmed Cell Death. . Cold Spring Harbor, NY, September 1999.

30. The Apo2L/TRAIL system: therapeutic potential. American Association for Cancer Research, Lake Tahoe, NV, Feb 2000.

31. Apoptosis and cancer therapy. Stanford University School of Medicine, Stanford, CA, Mar 2000.

32. Apoptosis and cancer therapy. University of Pennsylvania School of Medicine, Philladelphia, PA, Apr 2000.

33. Apoptosis signaling by Apo2L/TRAIL. International Congress on TNF. Trondheim, Norway, May 2000.

34. The Apo2L/TRAIL system: therapeutic potential. Cap-CURE summit meeting. Santa Monica, CA, June 2000.

35. The Apo2L/TRAIL system: therapeutic potential. MD Anderson Cancer Center. Houston, TX, June 2000.

36. Apoptosis signaling by Apo2L/TRAIL. The Protein Society, 14th Symposium. San Diego, CA, August 2000.

37. Anti-tumor activity of Apo2L/TRAIL. AAPS annual meeting. Indianapolis, IN Aug 2000.

38. Apoptosis signaling and anti-cancer potential of Apo2L/TRAIL. Cancer Research Institute, UC San Francisco, CA, September 2000.

39. Apoptosis signaling by Apo2L/TRAIL. Kenote address, TNF family Minisymposium, NIH. Bethesda, MD, September 2000.

40. Death receptors: signaling and modulation. Keystone symposium on the Molecular basis of cancer. Taos, NM, Jan 2001.

41. Preclinical studies of Apo2L/TRAIL in cancer. Symposium on Targeted therapies in the treatment of lung cancer. Aspen, CO, Jan 2001.

42. Apoptosis signaling by Apo2L/TRAIL. Wiezmann Institute of Science, Rehovot, Israel, March 2001.

43. Apo2L/TRAIL: Apoptosis signaling and potential for cancer therapy. Weizmann Institute of Science, Rehovot, Israel, March 2001.

44. Targeting death receptors in cancer with Apo2L/TRAIL. Cell Death and Disease conference, North Falmouth, MA, Jun 2001.

45. Targeting death receptors in cancer with Apo2L/TRAIL. Biotechnology Organization conference, San Diego, CA, Jun 2001.

46. Apo2L/TRAIL signaling and apoptosis resistance mechanisms. Gordon Research Conference on Apoptosis, Oxford, UK, July 2001.

47. Apo2L/TRAIL signaling and apoptosis resistance mechanisms. Cleveland Clinic Foundation, Cleveland, OH, Oct 2001.

48. Apoptosis signaling by death receptors: overview. International Society for Interferon and Cytokine Research conference, Cleveland, OH, Oct 2001.

49. Apoptosis signaling by death receptors. American Society of Nephrology Conference. San Francisco, CA, Oct 2001.

50. Targeting death receptors in cancer. Apoptosis: commercial opportunities. San Diego, CA, Apr 2002.

51. Apo2L/TRAIL signaling and apoptosis resistance mechanisms. Kimmel Cancer Research Center, Johns Hopkins University, Baltimore MD. May 2002.

52. Apoptosis control by Apo2L/TRAIL. (Keynote Address) University of Alabama Cancer Center Retreat, Birmingham, Ab. October 2002.

53. Apoptosis signaling by Apo2L/TRAIL. (Session co-chair) TNF international conference. San Diego, CA. October 2002.

54. Apoptosis signaling by Apo2L/TRAIL. Swiss Institute for Cancer Research (ISREC). Lausanne, Swizerland. Jan 2003.

55. Apoptosis induction with Apo2L/TRAIL. Conference on New Targets and Innovative Strategies in Cancer Treatment. Monte Carlo. February 2003.

56. Apoptosis signaling by Apo2L/TRAIL. Hermelin Brain Tumor Center Symposium on Apoptosis. Detroit, MI. April 2003.

57. Targeting apoptosis through death receptors. Sixth Annual Conference on Targeted Therapies in the Treatment of Breast Cancer. Kona, Hawaii. July 2003.

58. Targeting apoptosis through death receptors. Second International Conference on Targeted Cancer Therapy. Washington, DC. Aug 2003.

Issued Patents:

1. Ashkenazi, A., Chamow, S. and Kogan, T. Carbohydrate-directed crosslinking reagents. US patent 5,329,028 (Jul 12, 1994).

2. Ashkenazi, A., Chamow, S. and Kogan, T. Carbohydrate-directed crosslinking reagents. US patent 5,605,791 (Feb 25, 1997).

3. Ashkenazi, A., Chamow, S. and Kogan, T. Carbohydrate-directed crosslinking reagents. US patent 5,889,155 (Jul 27, 1999).

4. Ashkenazi, A., APO-2 Ligand. US patent 6,030,945 (Feb 29, 2000).

5. Ashkenazi, A., Chuntharapai, A., Kim, J., APO-2 ligand antibodies. US patent 6, 046, 048 (Apr 4, 2000).

6. Ashkenazi, A., Chamow, S. and Kogan, T. Carbohydrate-directed crosslinking reagents. US patent 6,124,435 (Sep 26, 2000).

7. Ashkenazi, A., Chuntharapai, A., Kim, J., Method for making monoclonal and cross-reactive antibodies. US patent 6,252,050 (Jun 26, 2001).

8. Ashkenazi, A. APO-2 Receptor. US patent 6,342,369 (Jan 29, 2002).

9. Ashkenazi, A. Fong, S., Goddard, A., Gurney, A., Napier, M., Tumas, D., Wood, W. A-33 polypeptides. US patent 6,410,708 (Jun 25, 2002).

10. Ashkenazi, A. APO-3 Receptor. US patent 6,462,176 B1 (Oct 8, 2002).

11. Ashkenazi, A. APO-2LI and APO-3 polypeptide antibodies. US patent 6,469,144 B1 (Oct 22, 2002).

12. Ashkenazi, A., Chamow, S. and Kogan, T. Carbohydrate-directed crosslinking reagents. US patent 6,582,928B1 (Jun 24, 2003).

DECLARATION OF PAUL POLAKIS, Ph.D.

I, Paul Polakis, Ph.D., declare and say as follows:

1.   I was awarded a Ph.D. by the Department of Biochemistry of the Michigan State University in 1984. My scientific Curriculum Vitae is attached to and forms part of this Declaration (Exhibit A).

2.   I am currently employed by Genentech, Inc. where my job title is Staff Scientist. Since joining Genentech in 1999, one of my primary responsibilities has been leading Genentech's Tumor Antigen Project, which is a large research project with a primary focus on identifying tumor cell markers that find use as targets for both the diagnosis and treatment of cancer in humans.

3.   As part of the Tumor Antigen Project, my laboratory has been analyzing differential expression of various genes in tumor cells relative to normal cells. The purpose of this research is to identify proteins that are abundantly expressed on certain tumor cells and that are either (i) not expressed, or (ii) expressed at lower levels, on corresponding normal cells. We call such differentially expressed proteins "tumor antigen proteins". When such a tumor antigen protein is identified, one can produce an antibody that recognizes and binds to that protein. Such an antibody finds use in the diagnosis of human cancer and may ultimately serve as an effective therapeutic in the treatment of human cancer.

4.   In the course of the research conducted by Genentech's Tumor Antigen Project, we have employed a variety of scientific techniques for detecting and studying differential gene expression in human tumor cells relative to normal cells, at genomic DNA, mRNA and protein levels. An important example of one such technique is the well known and widely used technique of microarray analysis which has proven to be extremely useful for the identification of mRNA molecules that are differentially expressed in one tissue or cell type relative to another. In the course of our research using microarray analysis, we have identified approximately 200 gene transcripts that are present in human tumor cells at significantly higher levels than in corresponding normal human cells. To date, we have generated antibodies that bind to about 30 of the tumor antigen proteins expressed from these differentially expressed gene transcripts and have used these antibodies to quantitatively determine the level of production of these tumor antigen proteins in both human cancer cells and corresponding normal cells. We have then compared the levels of mRNA and protein in both the tumor and normal cells analyzed.

5.   From the mRNA and protein expression analyses described in paragraph 4 above, we have observed that there is a strong correlation between changes in the level of mRNA present in any particular cell type and the level of protein

expressed from that mRNA in that cell type. In approximately 80% of our observations we have found that increases in the level of a particular mRNA correlates with changes in the level of protein expressed from that mRNA when human tumor cells are compared with their corresponding normal cells.

6. Based upon my own experience accumulated in more than 20 years of research, including the data discussed in paragraphs 4 and 5 above and my knowledge of the relevant scientific literature, it is my considered scientific opinion that for human genes, an increased level of mRNA in a tumor cell relative to a normal cell typically correlates to a similar increase in abundance of the encoded protein in the tumor cell relative to the normal cell. In fact, it remains a central dogma in molecular biology that increased mRNA levels are predictive of corresponding increased levels of the encoded protein. While there have been published reports of genes for which such a correlation does not exist, it is my opinion that such reports are exceptions to the commonly understood general rule that increased mRNA levels are predictive of corresponding increased levels of the encoded protein.

7. I hereby declare that all statements made herein of my own knowledge are true and that all statements made on information or belief are believed to be true, and further that these statements were made with the knowledge that willful false statements and the like so made are punishable by fine or imprisonment, or both, under Section 1001 of Title 18 of the United States Code and that such willful statements may jeopardize the validity of the application or any patent issued thereon.

Dated: _5/07/04_   By:_____

                                          Paul Polakis, Ph.D.

SV 2031808 v1

2

CURRICULUM VITAE

PAUL G. POLAKIS
Staff Scientist
Genentech, Inc
1 DNA Way, MS#40
S. San Francisco, CA 94080

EDUCATION:

Ph.D., Biochemistry, Department of Biochemistry,
Michigan State University (1984)

B.S., Biology. College of Natural Science, Michigan State University (1977)

PROFESSIONAL EXPERIENCE:

2002-present	Staff Scientist, Genentech, Inc S. San Francisco, CA
1999- 2002	Senior Scientist, Genentech, Inc., S. San Francisco, CA
1997 -1999	Research Director Onyx Pharmaceuticals, Richmond, CA
1992- 1996	Senior Scientist, Project Leader, Onyx Pharmaceuticals, Richmond, CA
1991-1992	Senior Scientist, Chiron Corporation, Emeryville, CA.
1989-1991	Scientist, Cetus Corporation, Emeryville CA.
1987-1989	Postdoctoral Research Associate, Genentech, Inc., South SanFrancisco, CA.
1985-1987	Postdoctoral Research Associate, Department of Medicine, Duke University Medical Center, Durham, NC

1984-1985   Assistant Professor, Department of Chemistry, Oberlin College, Oberlin, Ohio

1980-1984   Graduate Research Assistant, Department of Biochemistry, Michigan State University East Lansing, Michigan

PUBLICATIONS:

1. **Polakis, P G.** and Wilson, J. E. 1982 Purification of a Highly Bindable Rat Brain Hexokinase by High Performance Liquid Chromatography. **Biochem. Biophys. Res. Commun**. 107, 937-943.

2. **Polakis, P.G**. and Wilson, J. E. 1984 Proteolytic Dissection of Rat Brain Hexokinase: Determination of the Cleavage Pattern during Limited Digestion with Trypsin. **Arch. Biochem. Biophys**. 234, 341-352.

3. **Polakis, P. G**. and Wilson, J. E. 1985 An Intact Hydrophobic N-Terminal Sequence is Required for the Binding Rat Brain Hexokinase to Mitochondria. **Arch. Biochem. Biophys**. 236, 328-337.

4. Uhing, R.J., **Polakis,P.G**. and Snyderman, R. 1987 Isolaton of GTP-binding Proteins from Myeloid HL60 Cells. **J. Biol. Chem**. 262, 15575-15579.

5. **Polakis, P.G**., Uhing, R.J. and Snyderman, R. 1988 The Formylpeptide Chemoattractant Receptor Copurifies with a GTP-binding Protein Containing a Distinct 40 kDa Pertussis Toxin Substrate. **J. Biol. Chem**. 263, 4969-4979.

6. Uhing, R. J., Dillon, S., **Polakis, P. G**., Truett, A. P. and Snyderman, R. 1988 Chemoattractant Receptors and Signal Transduction Processes in Cellular and Molecular Aspects of Inflammation (Poste, G. and Crooke, S. T. eds.) pp 335-379.

7. **Polakis, P.G**., Evans, T. and Snyderman 1989 Multiple Chromatographic Forms of the Formylpeptide Chemoattractant Receptor and their Relationship to GTP-binding Proteins. **Biochem. Biophys. Res. Commun**. 161, 276-283.

8. **Polakis, P. G**., Snyderman, R. and Evans, T. 1989 Characterization of G25K, a GTP-binding Protein Containing a Novel Putative Nucleotide Binding Domain. **Biochem. Biophys. Res. Comun**. 160, 25-32.

9. **Polakis, P**., Weber,R.F., Nevins,B., Didsbury, J. Evans,T. and Snyderman, R. 1989 Identification of the ral and rac1 Gene Products, Low Molecular Mass GTP-binding Proteins from Human Platelets. **J. Biol. Chem**. 264, 16383-16389.

10. Snyderman, R., Perianin, A., Evans, T., **Polakis, P**. and Didsbury, J. 1989 G Proteins and Neutrophil Function. In ADP-Ribosylating Toxins and G Proteins: Insights into Signal Transduction. (J. Moss and M. Vaughn, eds.) Amer. Soc. Microbiol. pp. 295-323.

11. Hart, M.J., **Polakis, P.G.**, Evans, T. and Cerrione, R.A. 1990 The Identification and Charaterization of an Epidermal Growth Factor-Stimulated Phosphorylation of a Specific Low Molecular Mass GTP-binding Protein in a Reconstituted Phospholipid Vesicle System. **J. Biol. Chem**. 265, 5990-6001.

12. Yatani, A., Okabe, K., **Polakis, P.** Halenbeck, R. McCormick, F. and Brown, A. M. 1990 ras p21 and GAP Inhibit Coupling of Muscarinic Receptors to Atrial K$^+$ Channels. **Cell**. 61, 769-776.

13. Munemitsu, S., Innis, M.A., Clark, R., McCormick, F., Ullrich, A. and **Polakis, P.G.** 1990 Molecular Cloning and Expression of a G25K cDNA, the Human Homolog of the Yeast Cell Cycle Gene CDC42. **Mol. Cell. Biol**. 10, 5977-5982.

14. Polakis, P.G. Rubinfeld, B. Evans, T. and McCormick, F. 1991 Purification of Plasma Membrane-Associated GTPase Activating Protein (GAP) Specific for rap-1/krev-1 from HL60 Cells. **Proc. Natl. Acad. Sci. USA** 88, 239-243.

15. Moran, M. F., **Polakis, P.**, McCormick, F., Pawson, T. and Ellis, C. 1991 Protein Tyrosine Kinases Regulate the Phosphorylation, Protein Interactions, Subcellular Distribution, and Activity of p21ras GTPase Activating Protein. **Mol. Cell. Biol**. 11, 1804-1812

16. Rubinfeld, B., Wong, G., Bekesi, E. Wood, A. McCormick, F. and **Polakis, P. G.** 1991 A Synthetic Peptide Corresponding to a Sequence in the GTPase Activating Protein Inhibits p21^{ras} Stimulation and Promotes Guanine Nucleotide Exchange. **Internatl. J. Peptide and Prot. Res**. 38, 47-53.

17. Rubinfeld, B., Munemitsu, S., Clark, R., Conroy, L., Watt, K., Crosier, W., McCormick, F., and **Polakis, P.** 1991 Molecular Cloning of a GTPase Activating Protein Specific for the Krev-1 Protein p21^{rap1}. **Cell** 65, 1033-1042.

18. Zhang, K. Papageorge, A., G., Martin, P., Vass, W. C., Olah, Z., **Polakis, P.**, McCormick, F. and Lowy, D, R. 1991 Heterogenous Amino Acids in RAS and Rap1A Specifying Sensitivity to GAP Proteins. **Science** 254, 1630-1634.

19. Martin, G., Yatani, A., Clark, R., **Polakis, P.**, Brown, A. M. and McCormick, F. 1992 GAP Domains Responsible for p21^{ras}-dependent Inhibition of Muscarinic Atrial K$^+$ Channel Currents. **Science** 255, 192-194.

20. McCormick, F., Martin, G. A., Clark, R., Bollag, G. and **Polakis, P** . 1992 Regulation of p21ras by GTPase Activating Proteins. Cold Spring Harbor **Symposia on Quantitative Biology**. Vol. 56, 237-241.

21. Pronk, G. B., **Polakis, P.**, Wong, G., deVries-Smits, A. M., Bos J. L. and McCormick, F. 1992 p60^{v-src} Can Associate with and Phosphorylate the p21^{ras} GTPase Activating Protein. **Oncogene** 7,389-394.

22. Polakis P. and McCormick, F. 1992 Interactions Between p21^{ras} Proteins and Their GTPase Activating Proteins. In <u>**Cancer Surveys**</u> (Franks, L. M., ed.) 12, 25-42.

23. Wong, G., Muller, O., Clark, R., Conroy, L., Moran, M., **Polakis,P.** and McCormick, F. 1992 Molecular coloning and nucleic acid binding properties of the GAP-associated tyrosine phosphoprotein p62. **Cell** 69, 551-558.

24. **Polakis, P.**, Rubinfeld, B. and McCormick, F. 1992 Phosphorylation of rap1GAP in vivo and by cAMP-dependent Kinase and the Cell Cycle p34^{cdc2} Kinase in vitro. **J. Biol. Chem**. 267, 10780-10785.

25. McCabe, P.C., Haubrauck, H., **Polakis, P.**, McCormick, F., and Innis, M. A. 1992 Functional Interactions Between p21^{rap1A} and Components of the Budding pathway of *Saccharomyces cerevisiae*. **Mol. Cell. Biol.** 12, 4084-4092.

26. Rubinfeld, B., Crosier, W.J., Albert, I., Conroy,L., Clark, R., McCormick, F. and **Polakis, P**. 1992 Localization of the rap1GAP Catalytic Domain and Sites of Phosphorylation by Mutational Analysis. **Mol. Cell . Biol**. 12, 4634-4642.

27. Ando, S., Kaibuchi, K., Sasaki, K., Hiraoka, T., Nishiyama, T., Mizuno, T., Asada, M., Nunoi, H., Matsuda, I., Matsuura, Y., **Polakis, P.**, McCormick, F. and Takai, Y. 1992 Post-translational processing of rac p21s is important both for their interaction with the GDP/GTP exchange proteins and for their activation of NADPH oxidase. **J. Biol. Chem**. 267, 25709-25713.

28. Janoueix-Lerosey, I., **Polakis, P.**, Tavitian, A. and deGunzberg, J. 1992 Regulation of the GTPase activity of the ras-related rap2 protein. **Biochem. Biophys. Res. Commun**. 189, 455-464.

29. **Polakis, P**. 1993 GAPs Specific for the rap1/Krev-1 Protein. in <u>GTP-binding Proteins: the *ras*-superfamily.</u> (J.C. LaCale and F. McCormick, eds.) 445-452.

30. **Polakis, P.** and McCormick, F. 1993 Structural requirements for the interaction of p21^{ras} with GAP, exchange factors, and its bological effector target. **J. Biol Chem**. 268, 9157-9160.

31. Rubinfeld, B., Souza, B. Albert, I., Muller, O., Chamberlain, S., Masiarz, F., Munemitsu, S. and **Polakis, P**. 1993 Association of the APC gene product with beta- catenin. **Science** 262, 1731-1734.

32. Weiss, J., Rubinfeld, B., **Polakis, P.**, McCormick, F. Cavenee, W. A. and Arden, K. 1993 The gene for human rap1-GTPase activating protein (rap1GAP) maps to chromosome 1p35-1p36.1. **Cytogenet. Cell Genet**. 66, 18-21.

33. Sato, K. Y., **Polakis, P.**, Haubruck, H., Fasching, C. L., McCormick, F. and Stanbridge, E. J. 1994 Analysis of the tumor suppressor acitvity of the K-rev gene in human tumor cell lines. **Cancer Res**. 54, 552-559.

34. Janoueix-Lerosey, I., Fontenay, M., Tobelem, G., Tavitian, A., **Polakis, P.** and DeGunzburg, J. 1994 Phosphorylation of rap1GAP during the cell cycle. **Biochem. Biophys. Res. Commun**. 202, 967-975

35. Munemitsu, S., Souza, B., Mueller, O., Albert, I., Rubinfeld, B., and **Polakis, P.** 1994 The APC gene product associates with microtubules in vivo and affects their assembly in vitro. **Cancer Res**. 54, 3676-3681.

36. Rubinfeld, B. and **Polakis, P.** 1995 Purification of baculovirus produced rap1GAP. **Methods Enz.** 255,31

37. **Polakis, P.** 1995 Mutations in the APC gene and their implications for protein structure and function. **Current Opinions in Genetics and Development** 5, 66-71

38. Rubinfeld, B., Souza, B., Albert, I., Munemitsu, S. and **Polakis P.** 1995 The APC protein and E-cadherin form similar but independent complexes with α-catenin, β-catenin and Plakoglobin. **J. Biol. Chem.** 270, 5549-5555

39. Munemitsu, S., Albert, I., Souza, B., Rubinfeld, B., and **Polakis, P.** 1995 Regulation of intracellular β-catenin levels by the APC tumor suppressor gene. **Proc. Natl. Acad. Sci.** 92, 3046-3050.

40. Lock, P., Fumagalli, S., **Polakis, P.** McCormick, F. and Courtneidge, S. A. 1996 The human p62 cDNA encodes Sam68 and not the rasGAP-associated p62 protein. **Cell** 84, 23-24.

41. Papkoff, J., Rubinfeld, B., Schryver, B. and **Polakis, P.** 1996 Wnt-1 regulates free pools of catenins and stabilizes APC-catenin complexes. **Mol. Cell. Biol.** 16, 2128-2134.

42. Rubinfeld, B., Albert, I., Porfiri, E., Fiol, C., Munemitsu, S. and **Polakis, P.** 1996 Binding of GSK3β to the APC-β-catenin complex and regulation of complex assembly. **Science** 272, 1023-1026.

43. Munemitsu, S., Albert, I., Rubinfeld, B. and **Polakis, P.** 1996 Deletion of amino-terminal structure stabilizes β-catenin in vivo and promotes the hyperphosphorylation of the APC tumor suppressor protein. **Mol. Cell. Biol.**16, 4088-4094.

44. Hart, M. J., Callow, M. G., Sousa, B. and **Polakis P.** 1996 IQGAP1, a calmodulin binding protein witha rasGAP related domain, is a potential effector for cdc42Hs. **EMBO J.** 15, 2997-3005.

45. Nathke, I. S., Adams, C. L., **Polakis, P.**, Sellin, J. and Nelson, W. J. 1996 The adenomatous polyposis coli (APC) tumor suppressor protein is localized to plasma membrane sites involved in active epithelial cell migration. **J. Cell. Biol.** 134, 165-180.

46. Hart, M. J., Sharma, S., elMasry, N., Qui, R-G., McCabe, P., **Polakis, P.** and Bollag, G. 1996 Identification of a novel guanine nucleotide exchange factor for the rho GTPase. **J. Biol. Chem.** 271, 25452.

47. Thomas JE, Smith M, Rubinfeld B, Gutowski M, Beckmann RP, and **Polakis P.** 1996 Subcellular localization and analysis of apparent 180-kDa and 220-kDa proteins of the breast cancer susceptibility gene, BRCA1. **J. Biol. Chem.** 1996 271, 28630-28635

48. Hayashi, S., Rubinfeld, B., Souza, B., **Polakis, P.**, Wieschaus, E., and Levine, A. 1997 A Drosophila homolog of the tumor suppressor adenomatous polyposis coli

down-regulates β -catenin but its zygotic expression is not essential for the regulation of armadillo. **Proc. Natl. Acad. Sci.** 94, 242-247.

49. Vleminckx, K., Rubinfeld, B., **Polakis, P.** and Gumbiner, B. 1997 The APC tumor suppressor protein induces a new axis in Xenopus embryos. **J. Cell. Biol.** 136, 411-420.

50. Rubinfeld, B., Robbins, P., El-Gamil, M., Albert, I., Porfiri, P. and **Polakis, P.** 1997 Stabilization of β-catenin by genetic defects in melanoma cell lines. **Science** 275, 1790-1792.

51. **Polakis, P.** The adenomatous polyposis coli (APC) tumor suppressor. 1997 **Biochem. Biophys. Acta,** 1332, F127-F147.

52. Rubinfeld, B., Albert, I., Porfiri, E., Munemitsu, S., and **Polakis, P** 1997 Loss of β-catenin regulation by the APC tumor suppressor protein correlates with loss of structure due to common somatic mutations of the gene. **Cancer Res.** 57, 4624-4630.

53. Porfiri, E., Rubinfeld, B., Albert, I., Hovanes. K., Waterman, M., and **Polakis, P.** 1997 Induction of a β-catenin-LEF-1 complex by wnt-1 and transforming mutants of β-catenin. **Oncogene** 15, 2833-2839.

54. Thomas JE, Smith M, Tonkinson JL, Rubinfeld B, and **Polakis P.,** 1997 Induction of phosphorylation on BRCA1 during the cell cycle and after DNA damage. **Cell Growth Differ.** 8, 801-809.

55. Hart, M., de los Santos, R., Albert, I., Rubinfeld, B., and **Polakis P.,** 1998 Down regulation of β-catenin by human Axin and its association with the adenomatous polyposis coli (APC) tumor suppressor, β-catenin and glycogen synthase kinase 3β. **Current Biology 8,** 573-581.

56. **Polakis, P.** 1998 The oncogenic activation of β-catenin. **Current Opinions in Genetics and Development** 9, 15-21

57. Matt Hart, Jean-Paul Concordet, Irina Lassot, Iris Albert, Rico del los Santos, Herve Durand, Christine Perret, Bonnee Rubinfled, Florence Margottin, Richard Benarous and **Paul Polakis.** 1999 The F-box protein β–TrCP associates with phosphorylated β–catenin and regulates its activity in the cell. **Current Biology** 9, 207-10.

58. Howard C. Crawford, Barbara M. Fingleton, Bonnee Rubinfeld, **Paul Polakis** and Lynn M. Matrisian 1999 The metalloproteinase matrilysin is a target of β–catenin transactivation in intestinal tumours. **Oncogene** 18, 2883-91.

59. Meng J, Glick JL, **Polakis P,** Casey PJ. 1999 Functional interaction between Galpha(z) and Rap1GAP suggests a novel form of cellular cross-talk. **J Biol Chem.** 17, 36663-9

60. Vijayasurian Easwaran, Virginia Song, **Paul Polakis** and Steve Byers 1999 The ubiquitin-proteosome pathway and serine kinase activity modulate APC mediated regulation of β-catenin-LEF signaling. **J. Biol. Chem.** 274(23):16641-5.

61 **Polakis P**, Hart M and Rubinfeld B. 1999 Defects in the regulation of beta-catenin
in colorectal cancer. **Adv Exp Med Biol.** 470, 23-32

62 Shen Z, Batzer A, Koehler JA, **Polakis P**, Schlessinger J, Lydon NB, Moran MF. 1999 Evidence for SH3 domain directed binding and phosphorylation of Sam68 by Src. **Oncogene.** 18, 4647-53

64. Thomas GM, Frame S, Goedert M, Nathke I, **Polakis P**, Cohen P. 1999 A GSK3- binding peptide from FRAT1 selectively inhibits the GSK3-catalysed phosphorylation of axin and beta-catenin. **FEBS Lett.** 458, 247-51.

65. Peifer M, **Polakis P**. 2000 Wnt signaling in oncogenesis and embryogenesis--a look outside the nucleus. **Science** 287,1606-9.

66. **Polakis P.** 2000 Wnt signaling and cancer. **Genes Dev;**14, 1837-1851.

67. Spink KE, **Polakis P**, Weis WI 2000 Structural basis of the Axin-adenomatous polyposis coli interaction. **EMBO J** 19, 2270-2279.

68. Szeto, W., Jiang, W., Tice, D.A., Rubinfeld, B., Hollingshead, P.G., Fong, S.E., Dugger, D.L., Pham, T., Yansura, D.E., Wong, T.A., Grimaldi, J.C., Corpuz, R.T., Singh J.S., Frantz, G.D., Devaux, B., Crowley, C.W., Schwall, R.H., Eberhard, D.A., Rastelli, L., **Polakis, P.** and Pennica, D. 2001 Overexpression of the Retinoic Acid-Responsive Gene Stra6 in Human Cancers and its Synergistic Induction by Wnt-1 and Retinoic Acid. **Cancer Res** 61, 4197-4204.

69. Rubinfeld B, Tice DA, **Polakis P**. 2001 Axin dependent phosphorylation of the adenomatous polyposis coli protein mediated by casein kinase 1 epsilon. **J Biol Chem** 276, 39037-39045.

70. **Polakis P**. 2001 More than one way to skin a catenin. **Cell** 2001 105, 563-566.

71. Tice DA, Soloviev I, **Polakis P**. 2002 Activation of the Wnt Pathway Interferes withSerum Response Element-driven Transcription of Immediate Early Genes. **J Biol.** **Chem.** 277, 6118-6123.

72. Tice DA, Szeto W, Soloviev I, Rubinfeld B, Fong SE, Dugger DL, Winer J,

Williams PM, Wieand D, Smith V, Schwall RH, Pennnica D, **Polakis P**. 2002 Synergistic activation of tumor antigens by wnt-1 signaling and retinoic acid revealed by gene expression profiling. **J Biol Chem**. 277,14329-14335.

73. **Polakis, P**. 2002 Casein kinase I: A wnt'er of disconnect. **Curr. Biol**. 12, R499.

74. Mao,W. , Luis, E., Ross, S., Silva, J., Tan, C., Crowley, C., Chui, C., Franz, G., Senter, P., Koeppen, H., **Polakis, P.** 2004 EphB2 as a therapeutic antibody drug target for the treatment of colorectal cancer. **Cancer Res**. 64, 781-788.

75. Shibamoto, S., Winer, J., Williams, M., Polakis, P. 2003 A Blockade in Wnt signaling is activated following the differentiation of F9 teratocarcinoma cells. **Exp. Cell Res**. 29211-20.

76. Zhang Y, Eberhard DA, Frantz GD, Dowd P, Wu TD, Zhou Y, Watanabe C, Luoh SM, **Polakis P,** Hillan KJ, Wood WI, Zhang Z. 2004 GEPIS--quantitative gene expression profiling in normal and cancer tissues. **Bioinformatics**, April 8

■■■■ TECHNICAL UPDATE

FROM YOUR LABORATORY SERVICES PROVIDER

HER-2/neu Breast Cancer Predictive Testing

Julie Sanford Hanna, Ph.D. and Dan Mornin, M.D.

EACH YEAR, OVER 182,000 WOMEN in the United States are diagnosed with breast cancer, and approximately 45,000 die of the disease.[1] Incidence appears to be increasing in the United States at a rate of roughly 2% per year. The reasons for the increase are unclear, but non-genetic risk factors appear to play a large role.[2]

Five-year survival rates range from approximately 65%-85%, depending on demographic group, with a significant percentage of women experiencing recurrence of their cancer within 10 years of diagnosis. One of the factors most predictive for recurrence once a diagnosis of breast cancer has been made is the number of axillary lymph nodes to which tumor has metastasized. Most node-positive women are given adjuvant therapy, which increases their survival. However, 20%-30% of patients without axillary node involvement also develop recurrent disease, and the difficulty lies in how to identify this high-risk subset of patients. These patients could benefit from increased surveillance, early intervention, and treatment.

Prognostic markers currently used in breast cancer recurrence prediction include tumor size, histological grade, steroid hormone receptor status, DNA ploidy, proliferative index, and cathepsin D status. Expression of growth factor receptors and over-expression of the HER-2/neu oncogene have also been identified as having value regarding treatment regimen and prognosis.

HER-2/neu (also known as c-erbB2) is an oncogene that encodes a transmembrane glycoprotein that is homologous to, but distinct from, the epidermal growth factor receptor. Numerous studies have indicated that high levels of expression of this protein are associated with rapid tumor growth, certain forms of therapy resistance, and shorter disease-free survival. The gene has been shown to be amplified and/or overexpressed in 10%-30% of invasive breast cancers and in 40%-60% of intraductal breast carcinoma.[3]

There are two distinct FDA-approved methods by which HER-2/neu status can be evaluated: immunohistochemistry (IHC, HercepTest™) and FISH (fluorescent in situ hybridization, PathVysion™ Kit). Both methods can be performed on archived and current specimens. The first method allows visual assessment of the amount of HER-2/neu protein present on the cell membrane. The latter method allows direct quantification of the level of gene amplification present in the tumor, enabling differentiation between low- versus high-amplification. At least one study has demonstrated a difference in

recurrence risk in women younger than 40 years of age for low- versus high-amplified tumors (54.5% compared to 85.7%); this is compared to a recurrence rate of 16.7% for patients with no HER-2/neu gene amplification.[4] HER-2/neu status may be particularly important to establish in women with small (≤1 cm) tumor size.

The choice of methodology for determination of HER-2/neu status depends in part on the clinical setting. FDA approval for the Vysis FISH test was granted based on clinical trials involving 1549 node-positive patients. Patients received one of three different treatments consisting of different doses of cyclophosphamide, Adriamycin, and 5-fluorouracil (CAF). The study showed that patients with amplified HER-2/neu benefited from treatment with higher doses of adriamycin-based therapy, while those with normal HER-2/neu levels did not. The study therefore identified a sub-set of women, who because they did not benefit from more aggressive treatment, did not need to be exposed to the associated side effects. In addition, other evidence indicates that HER-2/neu amplification in node-negative patients can be used as an independent prognostic indicator for early recurrence, recurrent disease at any time and disease-related death.[5] Demonstration of HER-2/neu gene amplification by FISH has also been shown to be of value in predicting response to chemotherapy in stage-2 breast cancer patients.

Selection of patients for Herceptin© (Trastuzumab) monoclonal antibody therapy, however, is based upon demonstration of HER-2/neu protein overexpression using HercepTest™. Studies using Herceptin© in patients with metastatic breast cancer show an increase in time to disease progression, increased response rate to chemotherapeutic agents and a small increase in overall survival rate. The FISH assays have not yet been approved for this purpose, and studies looking at response to Herceptin© in patients with or without gene amplification status determined by FISH are in progress.

In general, FISH and IHC results correlate well. However, subsets of tumors are found which show discordant results; i.e., protein overexpression without gene amplification or lack of protein overexpression with gene amplification. The clinical significance of such results is unclear. Based on the above considerations, HER-2/neu testing at SHMC/PAML will utilize immunohistochemistry (HercepTest©) as a screen, followed by FISH in IHC-negative cases. Alternatively, either method may be ordered individually depending on the clinical setting or clinician preference.

CPT code information

HER-2/neu via IHC

88342   (including interpretive report)

HER-2/neu via FISH

88271×2   Molecular cytogenetics, DNA probe, each

88274   Molecular cytogenetics, interphase in situ hybrid-
ization, analyze 25-99 cells

88291   Cytogenetics and molecular cytogenetics, interpre-
tation and report

Procedural Information

Immunohistochemistry is performed using the FDA-approved DAKO antibody kit, Herceptest©. The DAKO kit contains reagents required to complete a two-step immunohisto-chemical staining procedure for routinely processed, paraffin-embedded specimens. Following incubation with the primary rabbit antibody to human HER-2/neu protein, the kit employs a ready-to-use dextran-based visualization reagent. This reagent consists of both secondary goat anti-rabbit antibody molecules with horseradish peroxidase molecules linked to a common dextran polymer backbone, thus eliminating the need for sequential application of link antibody and peroxidase conjugated antibody. Enzymatic conversion of the subsequently added chromogen results in formation of visible reaction product at the antigen site. The specimen is then counterstained; a pathologist using light-microscopy interprets results.

FISH analysis at SHMC/PAML is performed using the FDA-approved PathVysion™ HER-2/neu DNA probe kit, produced by Vysis, Inc. Formalin fixed, paraffin-embedded breast tissue is processed using routine histological methods, and then slides are treated to allow hybridization of DNA probes to the nuclei present in the tissue section. The Pathvysion™ kit contains two direct-labeled DNA probes, one specific for the alphoid repetitive DNA (CEP 17, spectrum orange) present at the chromosome 17 centromere and the second for the HER-2/neu oncogene located at 17q11.2-12 (spectrum green). Enumeration of the probes allows a ratio of the number of copies of chromosome 17 to the number of copies of HER-2/neu to be obtained; this enables quantification of low versus high amplification levels, and allows an estimate of the percentage of cells with HER-2/neu gene amplification. The clinically relevant distinction is whether the gene amplification is due to increased gene copy number on the two chromosome 17 homologues normally present or an increase in the number of chromosome 17s in the cells. In the majority of cases, ratio equivalents less than 2.0 are indicative of a normal/negative result, ratios of 2.1 and over indicate that amplification is present and to what degree. Interpretation of this data will be performed and reported from the Vysis-certified Cytogenetics laboratory at SHMC.

References

1. Wingo, P.A., Tong, T., Bolden, S., "Cancer Statistics", 1995;45:1:8-31.

2. "Cancer Rates and Risks", 4th ed., National Institutes of Health, National Cancer Institute, 1996, p. 120.

3. Slamon, D.J., Clark, G.M., Song, S.G., Levin, W.J., Ullrich, A., McGuire, W.L. "Human breast Cancer: Correlation of relapse and survival with amplification of the her-2/neu oncogene". Science, 235:177-182, 1987.

4. Xing, W.R., Gilchrist, K.W., Harris, C.P., Samson, W., Meisner, L.F. "FISH detection of HER-s/neu oncogene amplification in early onset breast cancer". Breast Cancer Res. And Treatment 39(2):203-212, 1996.

5. Press, M.F. Bernstein, L., Thomas, P.A., Meisner, L.F., Zhou, J.Y., Ma, Y., Hung, G., Robinson, R.A., Harris, C., El-Naggar, A., Slamon, D.J., Phillips, R.N., Ross, J.S., Wolman, S.R., Flom, K.J., "Her-2/neu gene amplification characterized by fluorescence in situ hybridization: poor prognosis in node-negative breast carcinomas", J. Clinical Oncology 15(8):2894-2904, 1997.

Impact of DNA Amplification on Gene Expression Patterns in Breast Cancer[1,2]

Elizabeth Hyman,[3] Päivikki Kauraniemi,[3] Sampsa Hautaniemi, Maija Wolf, Spyro Mousses, Ester Rozenblum, Markus Ringnér, Guido Sauter, Outi Monni, Abdel Elkahloun, Olli-P. Kallioniemi, and Anne Kallioniemi[4]

Howard Hughes Medical Institute-NIH Research Scholar, Bethesda, Maryland 20892 [E. H.]; Cancer Genetics Branch, National Human Genome Research Institute, NIH, Bethesda, Maryland 20892 [E. H., P. K., S. H., M. W., S. M., E. R., M. R., A. E., O. K., A. K.]; Laboratory of Cancer Genetics, Institute of Medical Technology, University of Tampere and Tampere University Hospital, FIN-33520 Tampere, Finland [P. K., A. K.]; Signal Processing Laboratory, Tampere University of Technology, FIN-33101 Tampere, Finland [S. H.]; Institute of Pathology, University of Basel, CH-4003 Basel, Switzerland [G. S.]; and Biomedicum Biochip Center, Helsinki University Hospital, Biomedicum Helsinki, FIN-00014 Helsinki, Finland [O. M.]

ABSTRACT

Genetic changes underlie tumor progression and may lead to cancer-specific expression of critical genes. Over 1100 publications have described the use of comparative genomic hybridization (CGH) to analyze the pattern of copy number alterations in cancer, but very few of the genes affected are known. Here, we performed high-resolution CGH analysis on cDNA microarrays in breast cancer and directly compared copy number and mRNA expression levels of 13,824 genes to quantitate the impact of genomic changes on gene expression. We identified and mapped the boundaries of 24 independent amplicons, ranging in size from 0.2 to 12 Mb. Throughout the genome, both high- and low-level copy number changes had a substantial impact on gene expression, with 44% of the highly amplified genes showing overexpression and 10.5% of the highly overexpressed genes being amplified. Statistical analysis with random permutation tests identified 270 genes whose expression levels across 14 samples were systematically attributable to gene amplification. These included most previously described amplified genes in breast cancer and many novel targets for genomic alterations, including the *HOXB7* gene, the presence of which in a novel amplicon at 17q21.3 was validated in 10.2% of primary breast cancers and associated with poor patient prognosis. In conclusion, CGH on cDNA microarrays revealed hundreds of novel genes whose overexpression is attributable to gene amplification. These genes may provide insights to the clonal evolution and progression of breast cancer and highlight promising therapeutic targets.

INTRODUCTION

Gene expression patterns revealed by cDNA microarrays have facilitated classification of cancers into biologically distinct categories, some of which may explain the clinical behavior of the tumors (1–6). Despite this progress in diagnostic classification, the molecular mechanisms underlying gene expression patterns in cancer have remained elusive, and the utility of gene expression profiling in the identification of specific therapeutic targets remains limited.

Accumulation of genetic defects is thought to underlie the clonal evolution of cancer. Identification of the genes that mediate the effects of genetic changes may be important by highlighting transcripts that are actively involved in tumor progression. Such transcripts and their encoded proteins would be ideal targets for anticancer therapies, as demonstrated by the clinical success of new therapies against amplified oncogenes, such as *ERBB2* and *EGFR* (7, 8), in breast cancer and other solid tumors. Besides amplifications of known oncogenes, over
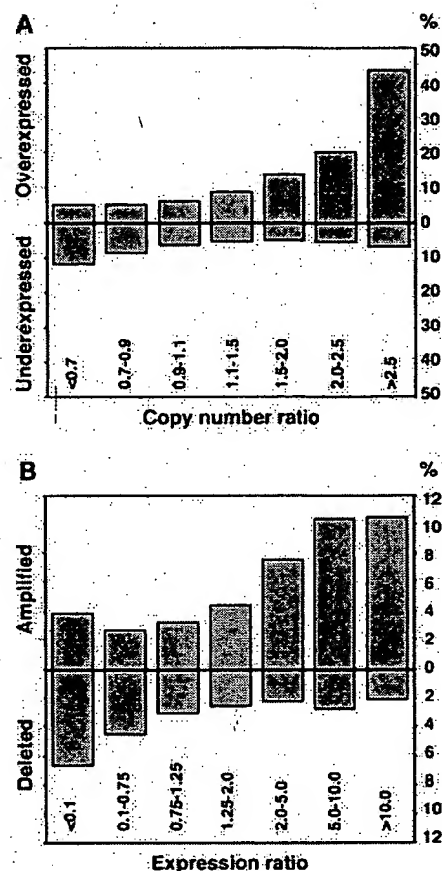

Fig. 1. Impact of gene copy number on global gene expression levels. *A*, percentage of over- and underexpressed genes (*Y axis*) according to copy number ratios (*X axis*). Threshold values used for over- and underexpression were >2.184 (global upper 7% of the cDNA ratios) and <0.4826 (global lower 7% of the expression ratios). *B*, percentage of amplified and deleted genes according to expression ratios. Threshold values for amplification and deletion were >1.5 and <0.7.

20 recurrent regions of DNA amplification have been mapped in breast cancer by CGH[5] (9, 10). However, these amplicons are often large and poorly defined, and their impact on gene expression remains unknown.

We hypothesized that genome-wide identification of those gene expression changes that are attributable to underlying gene copy number alterations would highlight transcripts that are actively involved in the causation or maintenance of the malignant phenotype. To identify such transcripts, we applied a combination of cDNA and CGH microarrays to: (*a*) determine the global impact that gene copy number variation plays in breast cancer development and progression; and (*b*) identify and characterize those genes whose mRNA expres-
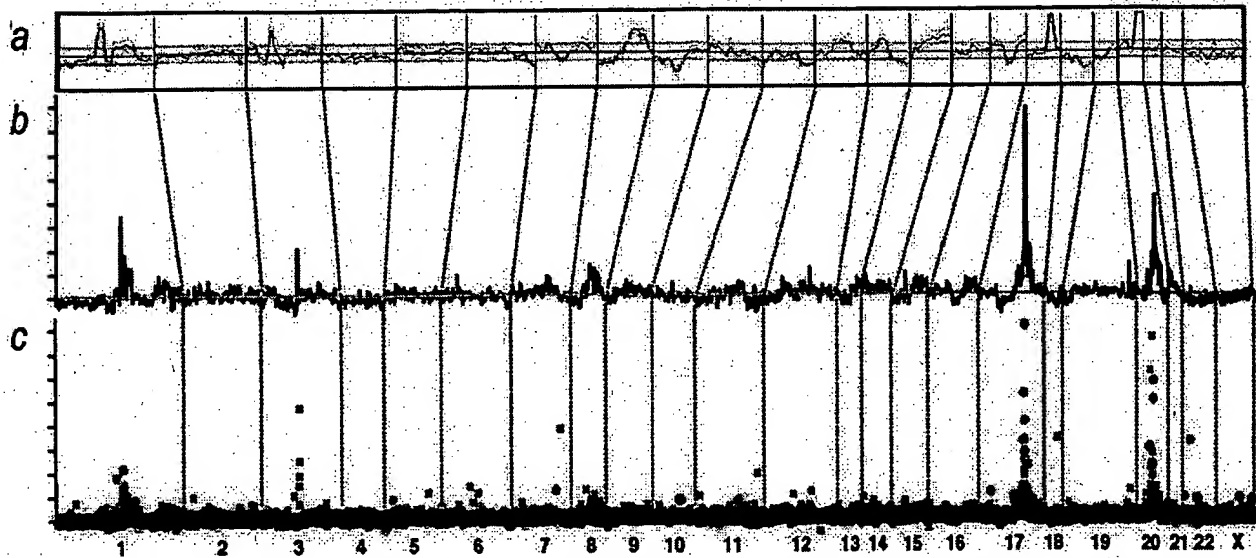
Fig. 2. Genome-wide copy number and expression analysis in the MCF-7 breast cancer cell line. *A*, chromosomal CGH analysis of MCF-7. The copy number ratio profile (*blue line*) across the entire genome from 1p telomere to Xq telomere is shown along with ±1 SD (*orange lines*). The *black horizontal line* indicates a ratio of 1.0; *red line*, a ratio of 0.8; and *green line*, a ratio of 1.2. *B–C*, genome-wide copy number analysis in MCF-7 by CGH on cDNA microarray. The copy number ratios were plotted as a function of the position of the cDNA clones along the human genome. In *B*, individual data points are connected with a line, and a moving median of 10 adjacent clones is shown. *Red horizontal line*, the copy number ratio of 1.0. In *C*, individual data points are labeled by color coding according to cDNA expression ratios. The *bright red dots* indicate the upper 2%, and *dark red dots*, the next 5% of the expression ratios in MCF-7 cells (overexpressed genes); *bright green dots* indicate the lowest 2%, and *dark green dots*, the next 5% of the expression ratios (underexpressed genes); the rest of the observations are shown with *black crosses*. The chromosome numbers are shown at the *bottom* of the figure, and chromosome boundaries are indicated with a *dashed line*.

sion is most significantly associated with amplification of the corresponding genomic template.

MATERIALS AND METHODS

Breast Cancer Cell Lines. Fourteen breast cancer cell lines (BT-20, BT-474, HCC1428, Hs578t, MCF7, MDA-361, MDA-436, MDA-453, MDA-468, SKBR-3, T-47D, UACC812, ZR-75-1, and ZR-75-30) were obtained from the American Type Culture Collection (Manassas, VA). Cells were grown under recommended culture conditions. Genomic DNA and mRNA were isolated using standard protocols.

Copy Number and Expression Analyses by cDNA Microarrays. The preparation and printing of the 13,824 cDNA clones on glass slides were performed as described (11–13). Of these clones, 244 represented uncharacterized expressed sequence tags, and the remainder corresponded to known genes. CGH experiments on cDNA microarrays were done as described (14, 15). Briefly, 20 μg of genomic DNA from breast cancer cell lines and normal human WBCs were digested for 14–18 h with *AluI* and *RsaI* (Life Technologies, Inc., Rockville, MD) and purified by phenol/chloroform extraction. Six μg of digested cell line DNAs were labeled with Cy3-dUTP (Amersham Pharmacia) and normal DNA with Cy5-dUTP (Amersham Pharmacia) using the Bioprime Labeling kit (Life Technologies, Inc.). Hybridization (14, 15) and posthybridization washes (13) were done as described. For the expression analyses, a standard reference (Universal Human Reference RNA; Stratagene, La Jolla, CA) was used in all experiments. Forty μg of reference RNA were labeled with Cy3-dUTP and 3.5 μg of test mRNA with Cy5-dUTP, and the labeled cDNAs were hybridized on microarrays as described (13, 15). For both microarray analyses, a laser confocal scanner (Agilent Technologies, Palo Alto, CA) was used to measure the fluorescence intensities at the target locations using the DEARRAY software (16). After background subtraction, average intensities at each clone in the test hybridization were divided by the average intensity of the corresponding clone in the control hybridization. For the copy number analysis, the ratios were normalized on the basis of the distribution of ratios of all targets on the array and for the expression analysis on the basis of 88 housekeeping genes, which were spotted four times onto the array. Low quality measurements (*i.e.*, copy number data with mean reference intensity <100 fluorescent units, and expression data with both test and reference intensity <100 fluorescent units and/or with spot size <50 units)

were excluded from the analysis and were treated as missing values. The distributions of fluorescence ratios were used to define cutpoints for increased/decreased copy number. Genes with CGH ratio >1.43 (representing the upper 5% of the CGH ratios across all experiments) were considered to be amplified, and genes with ratio <0.73 (representing the lower 5%) were considered to be deleted.

Statistical Analysis of CGH and cDNA Microarray Data. To evaluate the influence of copy number alterations on gene expression, we applied the following statistical approach. CGH and cDNA calibrated intensity ratios were log-transformed and normalized using median centering of the values in each cell line. Furthermore, cDNA ratios for each gene across all 14 cell lines were median centered. For each gene, the CGH data were represented by a vector that was labeled 1 for amplification (ratio, >1.43) and 0 for no amplification. Amplification was correlated with gene expression using the signal-to-noise statistics (1). We calculated a weight, w_g, for each gene as follows:

$$w_g = \frac{m_{g1} - m_{g0}}{\sigma_{g1} + \sigma_{g0}}$$

where m_{g1}, σ_{g1} and m_{g0}, σ_{g0} denote the means and SDs for the expression levels for amplified and nonamplified cell lines, respectively. To assess the statistical significance of each weight, we performed 10,000 random permutations of the label vector. The probability that a gene had a larger or equal weight by random permutation than the original weight was denoted by α. A low α (<0.05) indicates a strong association between gene expression and amplification.

Genomic Localization of cDNA Clones and Amplicon Mapping. Each cDNA clone on the microarray was assigned to a Unigene cluster using the Unigene Build 141.[6] A database of genomic sequence alignment information for mRNA sequences was created from the August 2001 freeze of the University of California Santa Cruz's GoldenPath database.[7] The chromosome and bp positions for each cDNA clone were then retrieved by relating these data sets. Amplicons were defined as a CGH copy number ratio >2.0 in at least two adjacent clones in two or more cell lines or a CGH ratio >2.0 in at least three adjacent clones in a single cell line. The amplicon start and end positions were

---

[6] Internet address: http://research.nhgri.nih.gov/microarray/downloadable_cdna.html.
[7] Internet address: www.genome.ucsc.edu.

Table 1 *Summary of independent amplicons in 14 breast cancer cell lines by CGH microarray*

Location	Start (Mb)	End (Mb)	Size (Mb)
1p13	132.79	132.94	0.2
1q21	173.92	177.25	3.3
1q22	179.28	179.57	0.3
3p14	71.94	74.66	2.7
7p12.1–7p11.2	55.62	60.95	5.3
7q31	125.73	130.96	5.2
7q32	140.01	140.68	0.7
8q21.11–8q21.13	86.45	92.46	6.0
8q21.3	98.45	103.05	4.6
8q23.3–8q24.14	129.88	142.15	12.3
8q24.22	151.21	152.16	1.0
9p13	38.65	39.25	0.6
13q22–q31	77.15	81.38	4.2
16q22	86.70	87.62	0.9
17q11	29.30	30.85	1.6
17q12–q21.2	39.79	42.80	3.0
17q21.32–q21.33	52.47	55.80	3.3
17q22–q23.3	63.81	69.70	5.9
17q23.3–q24.3	69.93	74.99	5.1
19q13	40.63	41.40	0.8
20q11.22	34.59	35.85	1.3
20q13.12	44.00	45.62	1.6
20q13.12–q13.13	46.45	49.43	3.0
20q13.2–q13.32	51.32	59.12	7.8

extended to include neighboring nonamplified clones (ratio, <1.5). The amplicon size determination was partially dependent on local clone density.

FISH. Dual-color interphase FISH to breast cancer cell lines was done as described (17). Bacterial artificial chromosome clone RP11-361K8 was labeled with SpectrumOrange (Vysis, Downers Grove, IL), and SpectrumOrange-labeled probe for EGFR was obtained from Vysis. SpectrumGreen-labeled chromosome 7 and 17 centromere probes (Vysis) were used as a reference. A tissue microarray containing 612 formalin-fixed, paraffin-embedded primary breast cancers (17) was applied in FISH analyses as described (18). The use of these specimens was approved by the Ethics Committee of the University of Basel and by the NIH. Specimens containing a 2-fold or higher increase in the number of test probe signals, as compared with corresponding centromere signals, in at least 10% of the tumor cells were considered to be amplified. Survival analysis was performed using the Kaplan-Meier method and the log-rank test.

RT-PCR. The HOXB7 expression level was determined relative to GAPDH. Reverse transcription and PCR amplification were performed using Access RT-PCR System (Promega Corp., Madison, WI) with 10 ng of mRNA as a template. HOXB7 primers were 5'-GAGCAGAGGGACTCGGACTT-3' and 5'-GCGTCAGGTAGCGATTGTAG-3'.

RESULTS

Global Effect of Copy Number on Gene Expression. 13,824 arrayed cDNA clones were applied for analysis of gene expression and gene copy number (CGH microarrays) in 14 breast cancer cell lines. The results illustrate a considerable influence of copy number on gene expression patterns. Up to 44% of the highly amplified transcripts (CGH ratio, >2.5) were overexpressed (*i.e.*, belonged to the global upper 7% of expression ratios), compared with only 6% for genes with normal copy number levels (Fig. 1A). Conversely, 10.5% of the transcripts with high-level expression (cDNA ratio, >10) showed increased copy number (Fig. 1B). Low-level copy number increases and decreases were also associated with similar, although less dramatic, outcomes on gene expression (Fig. 1).

Identification of Distinct Breast Cancer Amplicons. Base-pair locations obtained for 11,994 cDNAs (86.8%) were used to plot copy number changes as a function of genomic position (Fig. 2, Supplement Fig. A). The average spacing of clones throughout the genome was 267 kb. This high-resolution mapping identified 24 independent breast cancer amplicons, spanning from 0.2 to 12 Mb of DNA (Table 1). Several amplification sites detected previously by chromosomal

CGH were validated, with 1q21, 17q12–q21.2, 17q22–q23, 20q13.1, and 20q13.2 regions being most commonly amplified. Furthermore, the boundaries of these amplicons were precisely delineated. In addition, novel amplicons were identified at 9p13 (38.65–39.25 Mb), and 17q21.3 (52.47–55.80 Mb).

Direct Identification of Putative Amplification Target Genes. The cDNA/CGH microarray technique enables the direct correlation of copy number and expression data on a gene-by-gene basis throughout the genome. We directly annotated high-resolution CGH plots with gene expression data using color coding. Fig. 2C shows that most of the amplified genes in the MCF-7 breast cancer cell line at 1p13, 17q22–q23, and 20q13 were highly overexpressed. A view of chromosome 7 in the MDA-468 cell line implicates EGFR as the most highly overexpressed and amplified gene at 7p11–p12 (Fig. 3A). In BT-474, the two known amplicons at 17q12 and 17q22–q23 contained numerous highly overexpressed genes (Fig. 3B). In addition, several genes, including the homeobox genes HOXB2 and HOXB7, were highly amplified in a previously undescribed independent amplicon at 17q21.3. HOXB7 was systematically amplified (as validated by FISH, Fig. 3B, inset) as well as overexpressed (as verified by RT-PCR, data not shown) in BT-474, UACC812, and ZR-75-30 cells. Furthermore, this novel
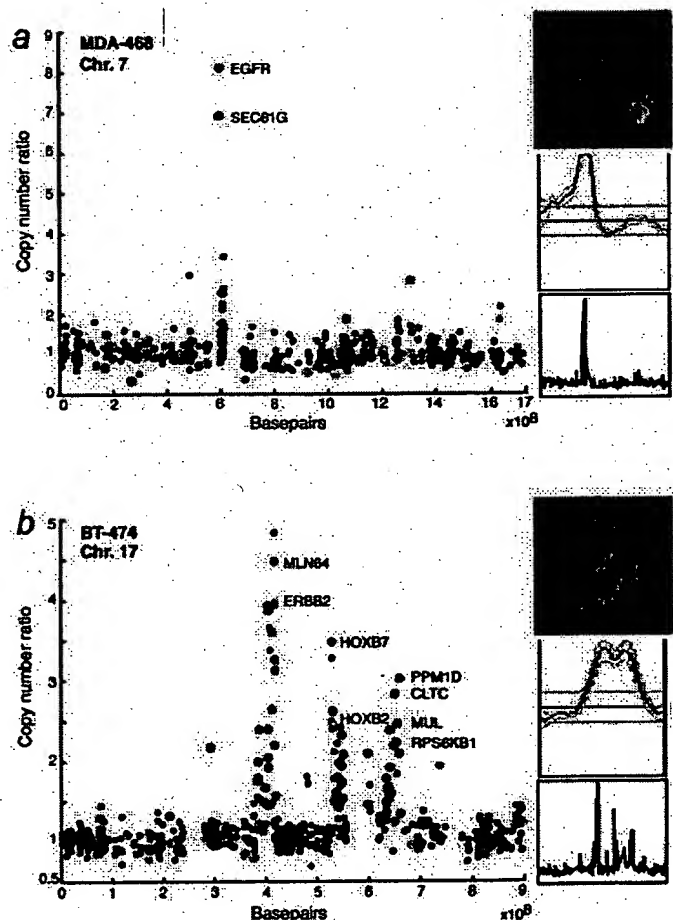
Fig. 3. Annotation of gene expression data on CGH microarray profiles. A, genes in the 7p11-p12 amplicon in the MDA-468 cell line are highly expressed (red dots) and include the EGFR oncogene. B, several genes in the 17q12, 17q21.3, and 17q23 amplicons in the BT-474 breast cancer cell line are highly overexpressed (red) and include the HOXB7 gene. The data labels and color coding are as indicated for Fig. 2C. Insets show chromosomal CGH profiles for the corresponding chromosomes and validation of the increased copy number by interphase FISH using EGFR (red) and chromosome 7 centromere probe (green) to MDA-468 (A) and HOXB7-specific probe (red) and chromosome 17 centromere (green) to BT-474 cells (B).

Gene name	Locus	Alpha
adaptor-related protein complex 4, beta 1 subunit	1p13	0.014
tripartite motif-containing 33	1p13	0.014
breast carcinoma amplified sequence 2	1p13	0.011
NRAS-related gene	1p13	0.010
renin	1q32	0.046
KIAA0456 protein	1q32	0.022
rab3 GTPase-activating protein	1q41	0.011
eukaryotic translation initiation factor 3, subunit 5	2p16	0.010
replication factor C	3q27	0.005
retinoic acid induced 14	5p13	0.010
mitogen-activated protein kinase kinase kinase 1	5q11	0.023
epidermal growth factor receptor	7p11	0.011
glioblastoma amplified sequence	7p11	0.012
CGI-82 protein	8q21	0.014
zinc finger protein RINZF	8q21	0.019
syndecan 2	8q22	0.011
eukaryotic translation initiation factor 3, subunit 6	8q23	0.039
v-myc	8q24	0.020
stomatin-like 2	9p13	0.010
protein phosphatase 1	11q13	0.046
NADH dehydrogenase	11q13	0.008
alanyl-tRNA synthetase	16q22	0.005
breast cancer anti-estrogen resistance 1	16q23	0.022
zinc finger protein 144 (Mel-18)	17q12	0.002
LIM and SH3 protein 1	17q12	0.012
hypothetical protein FLJ20940	17q21	0.007
steroidogenic acute regulatory protein related	17q21	0.001
phenylethanolamine N-methyltransferase	17q21	0.003
v-erb-b2	17q21	0.003
MLN51 protein	17q21	0.011
homeo box B2	17q21	0.030
homeo box B7	17q21	0.021
RAD51 (S. cerevisiae) homolog C	17q22	0.015
Mulibrey nanism	17q22	0.003
clathrin, heavy polypeptide (Hc)	17q23	0.002
ribosomal protein S6 kinase	17q23	0.003
amyloid beta precursor protein-binding protein 2	17q23	0.001
protein phosphatase 1D magnesium-dependent	17q23	0.022
angiopoietin-like 4	19p13	0.022
nuclear receptor coactivator RAP250	20q11	0.001
acetyl-CoA synthetase	20q11	0.026
topoisomerase (DNA) I	20q12	0.011
MYBL2	20q13	0.010
serine/threonine kinase 4	20q13	0.021
nuclear receptor coactivator 3	20q13	0.010
prefoldin 4	20q13	0.019
transcription factor AP-2 gamma	20q13	0.003
bone morphogenetic protein 7	20q13	0.001
zinc finger protein 278	22q12	0.002
KIAA0443 gene product	Xq22	0.007

Copy number ratios: top 2%, top 3-5%, middle 90%, bottom 3-5%, bottom 2%

Expression ratios: top 2%, top 3-7%, middle 86%, bottom 3-7%, bottom 2%

Fig. 4. List of 50 genes with a statistically significant correlation (α value <0.05) between gene copy number and gene expression. Name, chromosomal location, and the α value for each gene are indicated. The genes have been ordered according to their position in the genome. The color maps on the *right* illustrate the copy number and expression ratio patterns in the 14 cell lines. The key to the color code is shown at the *bottom* of the graph. *Gray squares,* missing values. The complete list of 270 genes is shown in supplemental Fig. B.
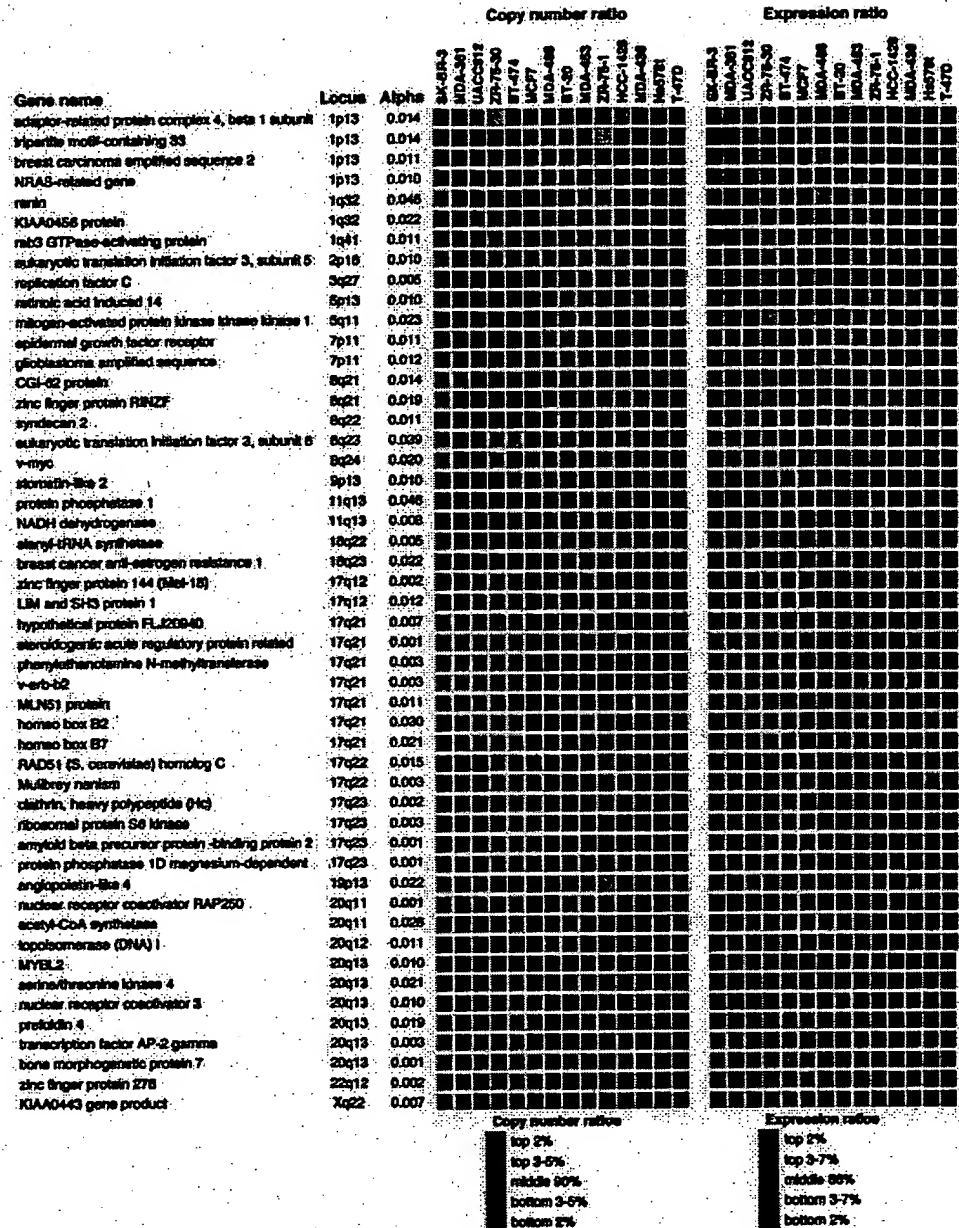
amplification was validated to be present in 10.2% of 363 primary breast cancers by FISH to a tissue microarray and was associated with poor prognosis of the patients ($P = 0.001$).

Statistical Identification and Characterization of 270 Highly Expressed Genes in Amplicons. Statistical comparison of expression levels of all genes as a function of gene amplification identified 270 genes whose expression was significantly influenced by copy number across all 14 cell lines (Fig. 4, Supplemental Fig. B). According to the gene ontology data,[8] 91 of the 270 genes represented hypothetical proteins or genes with no functional annotation, whereas 179 had associated functional information available. Of these, 151 (84%) are implicated in apoptosis, cell proliferation, signal transduction, and transcription, whereas 28 (16%) had functional annotations that could not be directly linked with cancer.

DISCUSSION

The importance of recurrent gene and chromosome copy number changes in the development and progression of solid tumors has been characterized in >1000 publications applying CGH[9] (9, 10), as well as in a large number of other molecular cytogenetic, cytogenetic, and molecular genetic studies. The effects of these somatic genetic changes on gene expression levels have remained largely unknown, although a few studies have explored gene expression changes occurring in specific amplicons (15, 19–21). Here, we applied genome-wide cDNA microarrays to identify transcripts whose expression changes were attributable to underlying gene copy number alterations in breast cancer.

The overall impact of copy number on gene expression patterns was substantial with the most dramatic effects seen in the case of high-

[8] Internet address: http://www.geneontology.org/.

[9] Internet address: http://www.ncbi.nlm.nih.gov/entrez.

level copy number increase. Low-level copy number gains and losses also had a significant influence on expression levels of genes in the regions affected, but these effects were more subtle on a gene-by-gene basis than those of high-level amplifications. However, the impact of low-level gains on the dysregulation of gene expression patterns in cancer may be equally important if not more important than that of high-level amplifications. Aneuploidy and low-level gains and losses of chromosomal arms represent the most common types of genetic alterations in breast and other cancers and, therefore, have an influence on many genes. Our results in breast cancer extend the recent studies on the impact of aneuploidy on global gene expression patterns in yeast cells, acute myeloid leukemia, and a prostate cancer model system (22–24).

The CGH microarray analysis identified 24 independent breast cancer amplicons. We defined the precise boundaries for many amplicons detected previously by chromosomal CGH (9, 10, 25, 26) and also discovered novel amplicons that had not been detected previously, presumably because of their small size (only 1–2 Mb) or close proximity to other larger amplicons. One of these novel amplicons involved the homeobox gene region at 17q21.3 and led to the overexpression of the *HOXB7* and *HOXB2* genes. The homeodomain transcription factors are known to be key regulators of embryonic development and have been occasionally reported to undergo aberrant expression in cancer (27, 28). *HOXB7* transfection induced cell proliferation in melanoma, breast, and ovarian cancer cells and increased tumorigenicity and angiogenesis in breast cancer (29–32). The present results imply that gene amplification may be a prominent mechanism for overexpressing *HOXB7* in breast cancer and suggest that *HOXB7* contributes to tumor progression and confers an aggressive disease phenotype in breast cancer. This view is supported by our finding of amplification of *HOXB7* in 10% of 363 primary breast cancers, as well as an association of amplification with poor prognosis of the patients.

We carried out a systematic search to identify genes whose expression levels across all 14 cell lines were attributable to amplification status. Statistical analysis revealed 270 such genes (representing ~2% of all genes on the array), including not only previously described amplified genes, such as *HER-2*, *MYC*, *EGFR*, ribosomal protein s6 kinase, and *AIB3*, but also numerous novel genes such as *NRAS-related gene* (1p13), *syndecan-2* (8q22), and *bone morphogenic protein* (20q13.1), whose activation by amplification may similarly promote breast cancer progression. Most of the 270 genes have not been implicated previously in breast cancer development and suggest novel pathogenetic mechanisms. Although we would not expect all of them to be causally involved, it is intriguing that 84% of the genes with associated functional information were implicated in apoptosis, cell proliferation, signal transduction, transcription, or other cellular processes that could directly imply a possible role in cancer progression. Therefore, a detailed characterization of these genes may provide biological insights to breast cancer progression and might lead to the development of novel therapeutic strategies.

In summary, we demonstrate application of cDNA microarrays to the analysis of both copy number and expression levels of over 12,000 transcripts throughout the breast cancer genome, roughly once every 267 kb. This analysis provided: (a) evidence of a prominent global influence of copy number changes on gene expression levels; (b) a high-resolution map of 24 independent amplicons in breast cancer; and (c) identification of a set of 270 genes, the overexpression of which was statistically attributable to gene amplification. Characterization of a novel amplicon at 17q21.3 implicated amplification and overexpression of the *HOXB7* gene in breast cancer, including a clinical association

between *HOXB7* amplification and poor patient prognosis. Overall, our results illustrate how the identification of genes activated by gene amplification provides a powerful approach to highlight genes with an important role in cancer as well as to prioritize and validate putative targets for therapy development.

REFERENCES

1. Golub, T. R., Slonim, D. K., Tamayo, P., Huard, C., Gaasenbeek, M., Mesirov, J. P., Coller, H., Loh, M. L., Downing, J. R., Caligiuri, M. A., Bloomfield, C. D., and Lander, E. S. Molecular classification of cancer: class discovery and class prediction by gene expression monitoring. Science (Wash. DC), *286:* 531–537, 1999.
2. Alizadeh, A. A., Eisen, M. B., Davis, R. E., Ma, C., Lossos, I. S., Rosenwald, A., Boldrick, J. C., Sabet, H., Tran, T., Yu, X., *et al.* Distinct types of diffuse large B-cell lymphoma identified by gene expression profiling. Nature (Lond.), *403:* 503–511, 2000.
3. Bittner, M., Meltzer, P., Chen, Y., Jiang, Y., Seftor, E., Hendrix, M., Radmacher, M., Simon, R., Yakhini, Z., Ben-Dor, A., *et al.* Molecular classification of cutaneous malignant melanoma by gene expression profiling. Nature (Lond.), *406:* 536–540, 2000.
4. Perou, C. M., Sorlie, T., Eisen, M. B., van de Rijn, M., Jeffrey, S. S., Rees, C. A., Pollack, J. R., Ross, D. T., Johnsen, H., Akslen, L. A., *et al.* Molecular portraits of human breast tumours. Nature (Lond.), *406:* 747–752, 2000.
5. Dhanasekaran, S. M., Barrette, T. R., Ghosh, D., Shah, R., Varambally, S., Kurachi, K., Pienta, K. J., Rubin, M. A., and Chinnaiyan, A. M. Delineation of prognostic biomarkers in prostate cancer. Nature (Lond.), *412:* 822–826, 2001.
6. Sorlie, T., Perou, C. M., Tibshirani, R., Aas, T., Geisler, S., Johnsen, H., Hastie, T., Eisen, M. B., van de Rijn, M., Jeffrey, S. S., *et al.* Gene expression patterns of breast carcinomas distinguish tumor subclasses with clinical implications. Proc. Natl. Acad. Sci. USA, *98:* 10869–10874, 2001.
7. Ross, J. S., and Fletcher, J. A. The *HER-2/neu* oncogene: prognostic factor, predictive factor and target for therapy. Semin. Cancer Biol., *9:* 125–138, 1999.
8. Arteaga, C. L. The epidermal growth factor receptor: from mutant oncogene in nonhuman cancers to therapeutic target in human neoplasia. J. Clin. Oncol., *19:* 32–40, 2001.
9. Knuutila, S., Bjorkqvist, A. M., Autio, K., Tarkkanen, M., Wolf, M., Monni, O., Szymanska, J., Larramendy, M. L., Tapper, J., Pere, H., El-Rifai, W., *et al.* DNA copy number amplifications in human neoplasms: review of comparative genomic hybridization studies. Am. J. Pathol., *152:* 1107–1123, 1998.
10. Knuutila S., Autio K., and Aalto Y. Online access to CGH data of DNA sequence copy number changes. Am. J. Pathol., *157:* 689, 2000.
11. DeRisi, J., Penland, L., Brown, P. O., Bittner, M. L., Meltzer, P. S., Ray, M., Chen, Y., Su, Y. A., and Trent, J. M. Use of a cDNA microarray to analyse gene expression patterns in human cancer. Nat. Genet., *14:* 457–460, 1996.
12. Shalon, D., Smith, S. J., and Brown, P. O. A DNA microarray system for analyzing complex DNA samples using two-color fluorescent probe hybridization. Genome Res., *6:* 639–645, 1996.
13. Mousses, S., Bittner, M. L., Chen, Y., Dougherty, E. R., Baxevanis, A., Meltzer, P. S., and Trent, J. M. Gene expression analysis by cDNA microarrays. In: F. J. Livesey and S. P. Hunt (eds.), Functional Genomics, pp. 113–137. Oxford: Oxford University Press, 2000.
14. Pollack, J. R., Perou, C. M., Alizadeh, A. A., Eisen, M. B., Pergamenschikov, A., Williams, C. F., Jeffrey, S. S., Botstein, D., and Brown, P. O. Genome-wide analysis of DNA copy-number changes using cDNA microarrays. Nat. Genet., *23:* 41–46, 1999.
15. Monni, O., Bärlund, M., Mousses, S., Kononen, J., Sauter, G., Heiskanen, M., Paavola, P., Avela, K., Chen, Y., Bittner, M. L., and Kallioniemi, A. Comprehensive copy number and gene expression profiling of the 17q23 amplicon in human breast cancer. Proc. Natl. Acad. Sci. USA, *98:* 5711–5716, 2001.
16. Chen, Y., Dougherty, E. R., and Bittner, M. L. Ratio-based decisions and the quantitative analysis of cDNA microarray images. J. Biomed. Optics, *2:* 364–374, 1997.
17. Bärlund, M., Forozan, F., Kononen, J., Bubendorf, L., Chen, Y., Bittner, M. L., Torhorst, J., Haas, P., Bucher, C., Sauter, G., *et al.* Detecting activation of ribosomal protein S6 kinase by complementary DNA and tissue microarray analysis. J. Natl. Cancer Inst., *92:* 1252–1259, 2000.
18. Andersen, C. L., Hostetter, G., Grigoryan, A., Sauter, G., and Kallioniemi, A. Improved procedure for fluorescence *in situ* hybridization on tissue microarrays. Cytometry, *45:* 83–86, 2001.
19. Kauraniemi, P., Bärlund, M., Monni, O., and Kallioniemi, A. New amplified and highly expressed genes discovered in the ERBB2 amplicon in breast cancer by cDNA microarrays. Cancer Res., *61:* 8235–8240, 2001.
20. Clark, J., Edwards, S., John, M., Flohr, P., Gordon, T., Maillard, K., Giddings, I., Brown, C., Bagherzadeh, A., Campbell, C., Shipley, J., Wooster, R., and Cooper, C. S. Identification of amplified and expressed genes in breast cancer by comparative hybridization onto microarrays of randomly selected cDNA clones. Genes Chromosomes Cancer, *34:* 104–114, 2002.
21. Varis, A., Wolf, M., Monni, O., Vakkari, M. L., Kokkola, A., Moskaluk, C., Frierson, H., Powell, S. M., Knuutila, S., Kallioniemi, A., and El-Rifai, W. Targets of gene amplification and overexpression at 17q in gastric cancer. Cancer Res., *62:* 2625–2629, 2002.
22. Hughes, T. R., Roberts, C. J., Dai, H., Jones, A. R., Meyer, M. R., Slade, D., Burchard, J., Dow, S., Ward, T. R., Kidd, M. J., Friend, S. H., and Marton M. J.

Widespread aneuploidy revealed by DNA microarray expression profiling. Nat. Genet., *25:* 333–337, 2000.

23. Virtaneva, K., Wright, F. A., Tanner, S. M., Yuan, B., Lemon, W. J., Caligiuri, M. A., Bloomfield, C. D., de La Chapelle, A., and Krahe, R. Expression profiling reveals fundamental biological differences in acute myeloid leukemia with isolated trisomy 8 and normal cytogenetics. Proc. Natl. Acad. Sci. USA, *98:* 1124–1129, 2001.

24. Phillips, J. L., Hayward, S. W., Wang, Y., Vasselli, J., Pavlovich, C., Padilla-Nash, H., Pezullo, J. R., Ghadimi, B. M., Grossfeld, G. D., Rivera, A., Linehan, W. M., Cunha, G. R., and Ried, T. The consequences of chromosomal aneuploidy on gene expression profiles in a cell line model for prostate carcinogenesis. Cancer Res., *61:* 8143–8149, 2001.

25. Bärlund, M., Tirkkonen, M., Forozan, F., Tanner, M. M., Kallioniemi, O. P., and Kallioniemi, A. Increased copy number at 17q22–q24 by CGH in breast cancer is due to high-level amplification of two separate regions. Genes Chromosomes Cancer, *20:* 372–376, 1997.

26. Tanner, M. M., Tirkkonen, M., Kallioniemi, A., Isola, J., Kuukasjärvi, T., Collins, C., Kowbel, D., Guan, X. Y., Trent, J., Gray, J. W., Meltzer, P., and Kallioniemi O. P. Independent amplification and frequent co-amplification of three nonsyntenic regions on the long arm of chromosome 20 in human breast cancer. Cancer Res., *56:* 3441–3445, 1996.

27. Cillo, C., Faiella, A., Cantile, M., and Boncinelli, E. Homeobox genes and cancer. Exp. Cell Res., *248:* 1–9, 1999.

28. Cillo, C., Cantile, M., Faiella, A., and Boncinelli, E. Homeobox genes in normal and malignant cells. J. Cell. Physiol., *188:* 161–169, 2001.

29. Care, A., Silvani, A., Meccia, E., Mattia, G., Stoppacciaro, A., Parmiani, G., Peschle, C., and Colombo, M. P. HOXB7 constitutively activates basic fibroblast growth factor in melanomas. Mol. Cell. Biol., *16:* 4842–4851, 1996.

30. Care, A., Silvani, A., Meccia, E., Mattia, G., Peschle, C., and Colombo, M. P. Transduction of the SkBr3 breast carcinoma cell line with the *HOXB7* gene induces bFGF expression, increases cell proliferation and reduces growth factor dependence. Oncogene, *16:* 3285–3289, 1998.

31. Care, A., Felicetti, F., Meccia, E., Bottero, L., Parenza, M., Stoppacciaro, A., Peschle, C., and Colombo, M. P. HOXB7: a key factor for tumor-associated angiogenic switch. Cancer Res., *61:* 6532–6539, 2001.

32. Naora, H., Yang, Y. Q., Montz, F. J., Seidman, J. D., Kurman, R. J., and Roden, R. B. A serologically identified tumor antigen encoded by a homeobox gene promotes growth of ovarian epithelial cells. Proc. Natl. Acad. Sci. USA, *98:* 4060–4065, 2001.

Genome-wide Study of Gene Copy Numbers, Transcripts, and Protein Levels in Pairs of Non-invasive and Invasive Human Transitional Cell Carcinomas*

Torben F. Ørntoft‡§, Thomas Thykjaer¶, Frederic M. Waldman||, Hans Wolf**, and Julio E. Celis‡‡

Gain and loss of chromosomal material is characteristic of bladder cancer, as well as malignant transformation in general. The consequences of these changes at both the transcription and translation levels is at present unknown partly because of technical limitations. Here we have attempted to address this question in pairs of non-invasive and invasive human bladder tumors using a combination of technology that included comparative genomic hybridization, high density oligonucleotide array-based monitoring of transcript levels (5600 genes), and high resolution two-dimensional gel electrophoresis. The results showed that there is a gene dosage effect that in some cases superimposes on other regulatory mechanisms. This effect depended ($p < 0.015$) on the magnitude of the comparative genomic hybridization change. In general (18 of 23 cases), chromosomal areas with more than 2-fold gain of DNA showed a corresponding increase in mRNA transcripts. Areas with loss of DNA, on the other hand, showed either reduced or unaltered transcript levels. Because most proteins resolved by two-dimensional gels are unknown it was only possible to compare mRNA and protein alterations in relatively few cases of well focused abundant proteins. With few exceptions we found a good correlation ($p < 0.005$) between transcript alterations and protein levels. The implications, as well as limitations, of the approach are discussed. *Molecular & Cellular Proteomics 1:37–45, 2002.*

Aneuploidy is a common feature of most human cancers (1), but little is known about the genome-wide effect of this phenomenon at both the transcription and translation levels. High throughput array studies of the breast cancer cell line BT474 has suggested that there is a correlation between DNA copy numbers and gene expression in highly amplified areas (2), and studies of individual genes in solid tumors have revealed a good correlation between gene dose and mRNA or protein levels in the case of c-erb-B2, cyclin d1, ems1, and N-myc (3–5). However, a high cyclin D1 protein expression has been observed without simultaneous amplification (4), and a low level of c-myc copy number increase was observed without concomitant c-myc protein overexpression (6).

In human bladder tumors, karyotyping, fluorescent *in situ* hybridization, and comparative genomic hybridization (CGH)[1] have revealed chromosomal aberrations that seem to be characteristic of certain stages of disease progression. In the case of non-invasive pTa transitional cell carcinomas (TCCs), this includes loss of chromosome 9 or parts of it, as well as loss of Y in males. In minimally invasive pT1 TCCs, the following alterations have been reported: 2q−, 11p−, 1q+, 11q13+, 17q+, and 20q+ (7–12). It has been suggested that these regions harbor tumor suppressor genes and oncogenes; however, the large chromosomal areas involved often contain many genes, making meaningful predictions of the functional consequences of losses and gains very difficult.

In this investigation we have combined genome-wide technology for detecting genomic gains and losses (CGH) with gene expression profiling techniques (microarrays and proteomics) to determine the effect of gene copy number on transcript and protein levels in pairs of non-invasive and invasive human bladder TCCs.

EXPERIMENTAL PROCEDURES

Material—Bladder tumor biopsies were sampled after informed consent was obtained and after removal of tissue for routine pathology examination. By light microscopy tumors 335 and 532 were staged by an experienced pathologist as pTa (superficial papillary),

[1] The abbreviations used are: CGH, comparative genomic hybridization; TCC, transitional cell carcinoma; LOH, loss of heterozygosity; PA-FABP, psoriasis-associated fatty acid-binding protein; 2D, two-dimensional.
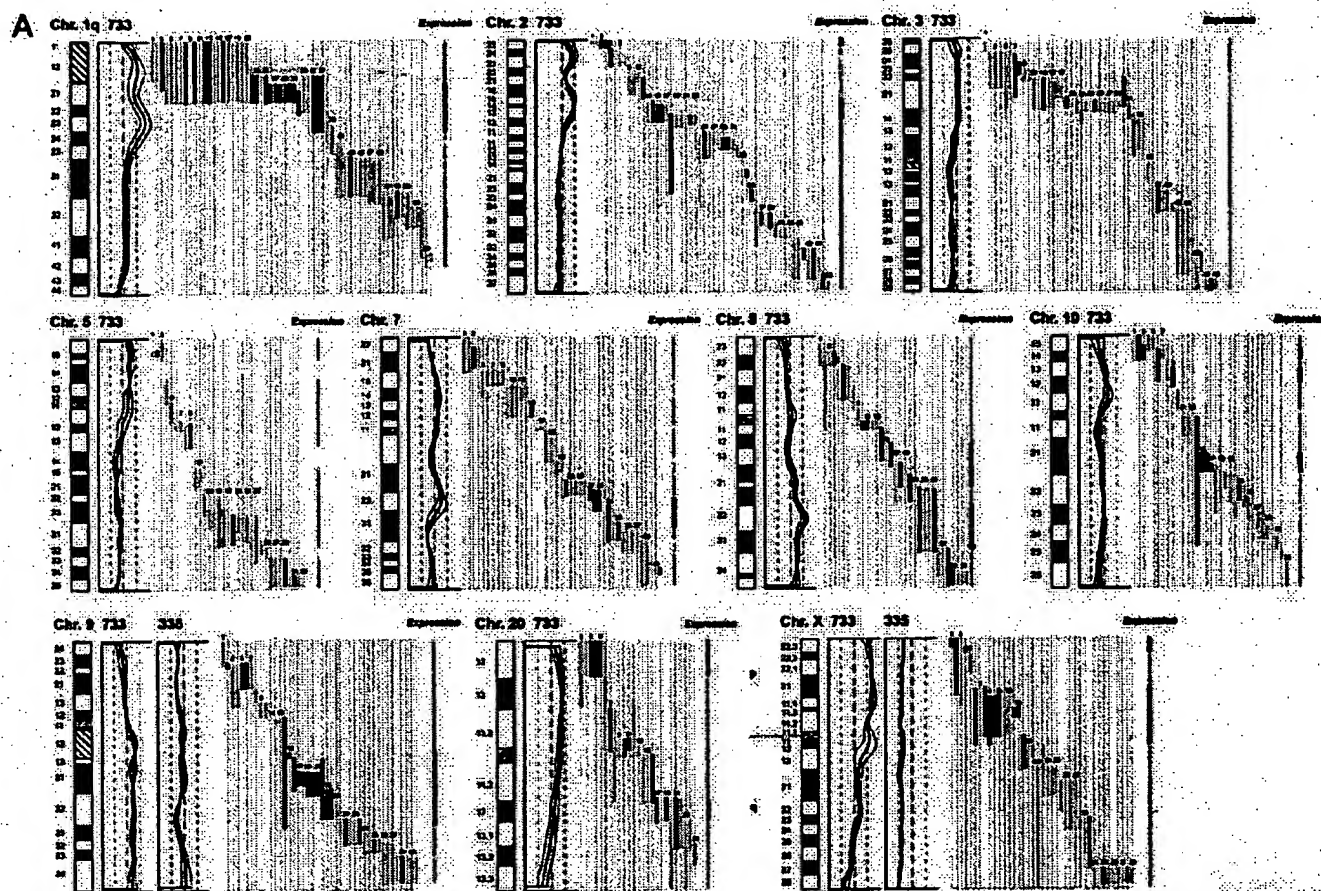
FIG. 1. **DNA copy number and mRNA expression level.** Shown from *left* to *right* are chromosome (*Chr.*), CGH profiles, gene location and expression level of specific genes, and overall expression level along the chromosome. *A*, expression of mRNA in invasive tumor 733 as compared with the non-invasive counterpart tumor 335. *B*, expression of mRNA in invasive tumor 827 compared with the non-invasive counterpart tumor 532. The average fluorescent signal ratio between tumor DNA and normal DNA is shown along the length of the chromosome (*left*). The *bold curve* in the ratio profile represents a mean of four chromosomes and is surrounded by *thin curves* indicating one standard deviation. The *central vertical line* (*broken*) indicates a ratio value of 1 (no change), and the *vertical lines* next to it (*dotted*) indicate a ratio of 0.5 (*left*) and 2.0 (*right*). In chromosomes where the non-invasive tumor 335 used for comparison showed alterations in DNA content, the ratio profile of that chromosome is shown to the *right* of the invasive tumor profile. The *colored bars* represents one gene each, identified by the running *numbers above* the *bars* (the name of the gene can be seen at www.MDL.DK/sdata.html). The *bars* indicate the purported location of the gene, and the *colors* indicate the expression level of the gene in the invasive tumor compared with the non-invasive counterpart; >2-fold increase (*black*), >2-fold decrease (*blue*), no significant change (*orange*). The *bar* to the *far right*, entitled *Expression* shows the resulting change in expression along the chromosome; the *colors* indicate that at least half of the genes were up-regulated (*black*), at least half of the genes down-regulated (*blue*), or more than half of the genes are unchanged (*orange*). If a gene was absent in one of the samples and present in another, it was regarded as more than a 2-fold change. A 2-fold level was chosen as this corresponded to one standard deviation in a double determination of ~1800 genes. Centromeres and heterochromatic regions were excluded from data analysis.

grade I and II, respectively, tumors 733 and 827 were staged as pT1 (invasive into submucosa), 733 was staged as solid, and 827 was staged as papillary, both grade III.

mRNA Preparation—Tissue biopsies, obtained fresh from surgery, were embedded immediately in a sodium-guanidinium thiocyanate solution and stored at −80 °C. Total RNA was isolated using the RNAzol B RNA isolation method (WAK-Chemie Medical GMBH). poly(A)$^+$ RNA was isolated by an oligo(dT) selection step (Oligotex mRNA kit; Qiagen).

cRNA Preparation—1 µg of mRNA was used as starting material. The first and second strand cDNA synthesis was performed using the SuperScript® choice system (Invitrogen) according to the manufacturer's instructions but using an oligo(dT) primer containing a T7 RNA polymerase binding site. Labeled cRNA was prepared using the ME-GAscrip® *in vitro* transcription kit (Ambion). Biotin-labeled CTP and

UTP (Enzo) was used, together with unlabeled NTPs in the reaction. Following the *in vitro* transcription reaction, the unincorporated nucleotides were removed using RNeasy columns (Qiagen).

Array Hybridization and Scanning—Array hybridization and scanning was modified from a previous method (13). 10 µg of cRNA was fragmented at 94 °C for 35 min in buffer containing 40 mm Tris acetate, pH 8.1, 100 mm KOAc, 30 mm MgOAc. Prior to hybridization, the fragmented cRNA in a 6× SSPE-T hybridization buffer (1 m NaCl, 10 mm Tris, pH 7.6, 0.005% Triton), was heated to 95 °C for 5 min, subsequently cooled to 40 °C, and loaded onto the Affymetrix probe array cartridge. The probe array was then incubated for 16 h at 40 °C at constant rotation (60 rpm). The probe array was exposed to 10 washes in 6× SSPE-T at 25 °C followed by 4 washes in 0.5× SSPE-T at 50 °C. The biotinylated cRNA was stained with a streptavidin-phycoerythrin conjugate, 10 µg/ml (Molecular Probes) in 6× SSPE-T
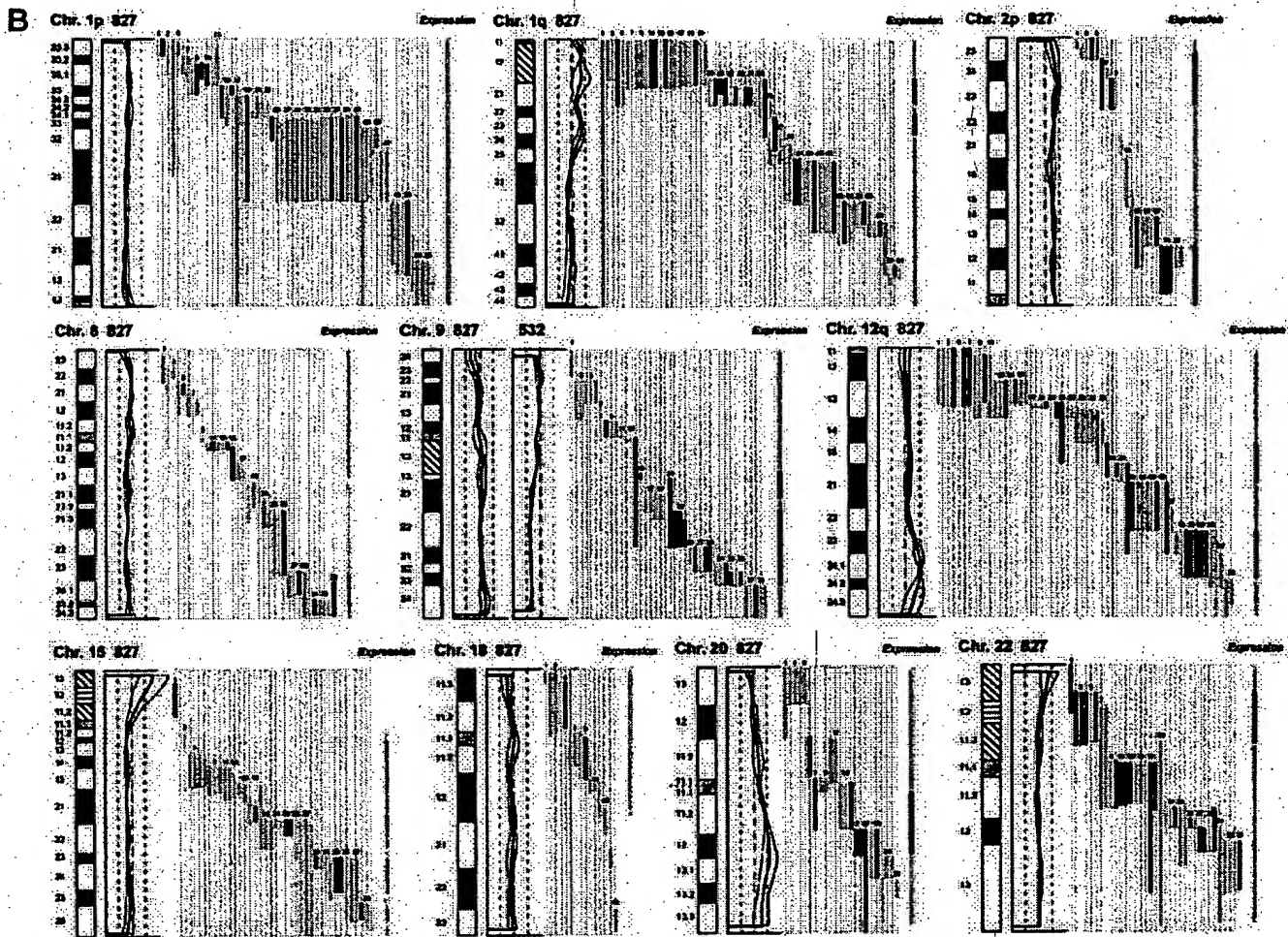
FIG. 1—continued

for 30 min at 25 °C followed by 10 washes in 6× SSPE-T at 25 °C. The probe arrays were scanned at 560 nm using a confocal laser scanning microscope (made for Affymetrix by Hewlett-Packard). The readings from the quantitative scanning were analyzed by Affymetrix gene expression analysis software.

Microsatellite Analysis—Microsatellite Analysis was performed as described previously (14). Microsatellites were selected by use of www.ncbi.nlm.nih.gov/genemap98, and primer sequences were obtained from the genome data base at www.gdb.org. DNA was extracted from tumor and blood and amplified by PCR in a volume of 20 μl for 35 cycles. The amplicons were denatured and electrophoresed for 3 h in an ABI Prism 377. Data were collected in the Gene Scan program for fragment analysis. Loss of heterozygosity was defined as less than 33% of one allele detected in tumor amplicons compared with blood.

Proteomic Analysis—TCCs were minced into small pieces and homogenized in a small glass homogenizer in 0.5 ml of lysis solution. Samples were stored at −20 °C until use. The procedure for 2D gel electrophoresis has been described in detail elsewhere (15; 16). Gels were stained with silver nitrate and/or Coomassie Brilliant Blue. Proteins were identified by a combination of procedures that included microsequencing, mass spectrometry, two-dimensional gel Western immunoblotting, and comparison with the master two-dimensional gel image of human keratinocyte proteins; see biobase.dk/cgi-bin/celis.

CGH—Hybridization of differentially labeled tumor and normal DNA to normal metaphase chromosomes was performed as described previously (10). Fluorescein-labeled tumor DNA (200 ng), Texas Red-

labeled reference DNA (200 ng), and human Cot-1 DNA (20 μg) were denatured at 37 °C for 5 min and applied to denatured normal metaphase slides. Hybridization was at 37 °C for 2 days. After washing, the slides were counterstained with 0.15 μg/ml 4,6-diamidino-2-phenylindole in an anti-fade solution. A second hybridization was performed for all tumor samples using fluorescein-labeled reference DNA and Texas Red-labeled tumor DNA (inverse labeling) to confirm the aberrations detected during the initial hybridization. Each CGH experiment also included a normal control hybridization using fluorescein- and Texas Red-labeled normal DNA. Digital image analysis was used to identify chromosomal regions with abnormal fluorescence ratios, indicating regions of DNA gains and losses. The average green:red fluorescence intensity ratio profiles were calculated using four images of each chromosome (eight chromosomes total) with normalization of the green:red fluorescence intensity ratio for the entire metaphase and background correction. Chromosome identification was performed based on 4,6-diamidino-2-phenylindole banding patterns. Only images showing uniform high intensity fluorescence with minimal background staining were analyzed. All centromeres, p arms of acrocentric chromosomes, and heterochromatic regions were excluded from the analysis.

RESULTS

Comparative Genomic Hybridization—The CGH analysis identified a number of chromosomal gains and losses in the

TABLE I

Correlation between alterations detected by CGH and by expression monitoring

Top, CGH used as independent variable (if CGH alteration − what expression ratio was found); bottom, altered expression used as independent variable (if expression alteration − what CGH deviation was found).

| CGH alterations | Tumor 733 vs. 335 | Concordance | CGH alterations | Tumor 827 vs. 532 | Concordance |
	Expression change clusters			Expression change clusters	
13 Gain	10 Up-regulation 0 Down-regulation 3 No change	77%	10 Gain	8 Up-regulation 0 Down-regulation 2 No change	80%
10 Loss	1 Up-regulation 5 Down-regulation 4 No change	50%	12 Loss	3 Up-regulation 2 Down regulation 7 No change	17%

| Expression change clusters | Tumor 733 vs. 335 | Concordance | Expression change clusters | Tumor 827 vs. 532 | Concordance |
	CGH alterations			CGH alterations	
16 Up-regulation	11 Gain 2 Loss 3 No change	69%	17 Up-regulation	10 Gain 5 Loss 2 No change	59%
21 Down-regulation	1 Gain 8 Loss 12 No change	38%	9 Down-regulation	0 Gain 3 Loss 6 No change	33%
15 No change	3 Gain 3 Loss 9 No change	60%	21 No change	1 Gain 3 Loss 17 No change	81%

two invasive tumors (stage pT1, TCCs 733 and 827), whereas the two non-invasive papillomas (stage pTa, TCCs 335 and 532) showed only 9p−, 9q22-q33−, and X−, and 7+, 9q−, and Y−, respectively. Both invasive tumors showed changes (1q22-24+, 2q14.1-qter−, 3q12-q13.3−, 6q12-q22−, 9q34+, 11q12-q13+, 17+, and 20q11.2-q12+) that are typical for their disease stage, as well as additional alterations, some of which are shown in Fig. 1. Areas with gains and losses deviated from the normal copy number to some extent, and the average numerical deviation from normal was 0.4-fold in the case of TCC 733 and 0.3-fold for TCC 827. The largest changes, amounting to at least a doubling of chromosomal content, were observed at 1q23 in TCC 733 (Fig. 1A) and 20q12 in TCC 827 (Fig. 1B).

mRNA Expression in Relation to DNA Copy Number—The mRNA levels from the two invasive tumors (TCCs 827 and 733) were compared with the two non-invasive counterparts (TCCs 532 and 335). This was done in two separate experiments in which we compared TCCs 733 to 335 and 827 to 532, respectively, using two different scaling settings for the arrays to rule out scaling as a confounding parameter. Approximately 1,800 genes that yielded a signal on the arrays were searched in the Unigene and Genemap data bases for chromosomal location, and those with a known location (1096) were plotted as bars covering their purported locus. In that way it was possible to construct a graphic presentation of DNA copy number and relative mRNA levels along the individual chromosomes (Fig. 1).

For each mRNA a ratio was calculated between the level in the invasive versus the non-invasive counterpart. Bars, which represent chromosomal location of a gene, were color-coded according to the expression ratio, and only differences larger

than 2-fold were regarded as informative (Fig. 1). The density of genes along the chromosomes varied, and areas containing only one gene were excluded from the calculations. The resolution of the CGH method is very low, and some of the outlier data may be because of the fact that the boundaries of the chromosomal aberrations are not known at high resolution.

Two sets of calculations were made from the data. For the first set we used CGH alterations as the independent variable and estimated the frequency of expression alterations in these chromosomal areas. In general, areas with a strong gain of chromosomal material contained a cluster of genes having increased mRNA expression. For example, both chromosomes 1q21-q25, 2p and 9q, showed a relative gain of more than 100% in DNA copy number that was accompanied by increased mRNA expression levels in the two tumor pairs (Fig. 1). In most cases, chromosomal gains detected by CGH were accompanied by an increased level of transcripts in both TCCs 733 (77%) and 827 (80%) (Table I, top). Chromosomal losses, on the other hand, were not accompanied by decreased expression in several cases, and were often registered as having unaltered RNA levels (Table I, top). The inability to detect RNA expression changes in these cases was not because of fewer genes mapping to the lost regions (data not shown).

In the second set of calculations we selected expression alterations above 2-fold as the independent variable and estimated the frequency of CGH alterations in these areas. As above, we found that increased transcript expression correlated with gain of chromosomal material (TCC 733, 69% and TCC 827, 59%), whereas reduced expression was often detected in areas with unaltered CGH ratios (Table I, bottom). Furthermore, as a control we looked at areas with no alter-
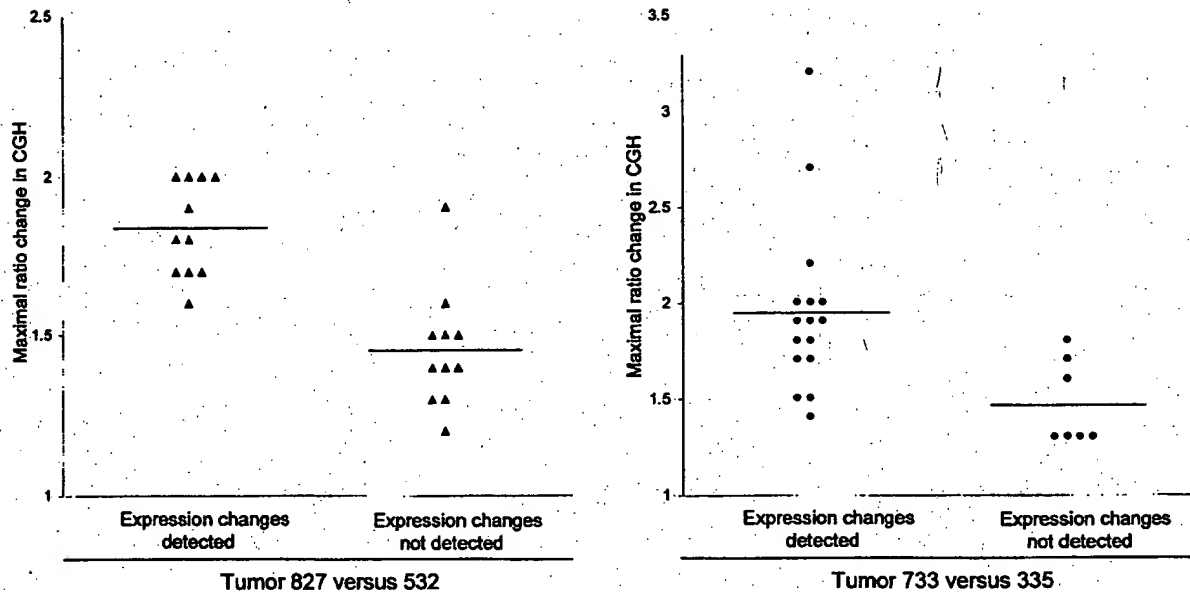
FIG. 2. Correlation between maximum CGH aberration and the ability to detect expression change by oligonucleotide array monitoring. The aberration is shown as a numerical -fold change in ratio between invasive tumors 827 (▲) and 733 (♦) and their non-invasive counterparts 532 and 335. The expression change was taken from the *Expression* line to the *right* in Fig. 1, which depicts the resulting expression change for a given chromosomal region. At least half of the mRNAs from a given region have to be either up- or down-regulated to be scored as an expression change. All chromosomal arms in which the CGH ratio plus or minus one standard deviation was outside the ratio value of one were included.

ation in expression. No alteration was detected by CGH in most of these areas (TCC 733, 60% and TCC 827, 81%; see Table I, *bottom*). Because the ability to observe reduced or increased mRNA expression clustering to a certain chromosomal area clearly reflected the extent of copy number changes, we plotted the maximum CGH aberrations in the regions showing CGH changes against the ability to detect a change in mRNA expression as monitored by the oligonucleotide arrays (Fig. 2). For both tumors TCC 733 ($p < 0.015$) and TCC 827 ($p < 0.00003$) a highly significant correlation was observed between the level of CGH ratio change (reflecting the DNA copy number) and alterations detected by the array based technology (Fig. 2). Similar data were obtained when areas with altered expression were used as independent variables. These areas correlated best with CGH when the CGH ratio deviated 1.6- to 2.0-fold (Table I, *bottom*) but mostly did not at lower CGH deviations. These data probably reflect that loss of an allele may only lead to a 50% reduction in expression level, which is at the cut-off point for detection of expression alterations. Gain of chromosomal material can occur to a much larger extent.

Microsatellite-based Detection of Minor Areas of Losses—In TCC 733, several chromosomal areas exhibiting DNA amplification were preceded or followed by areas with a normal CGH but reduced mRNA expression (see Fig. 1, TCC 733 chromosome 1q32, 2p21, and 7q21 and q32, 9q34, and 10q22). To determine whether these results were because of undetected loss of chromosomal material in these regions or

because of other non-structural mechanisms regulating transcription, we examined two microsatellites positioned at chromosome 1q25-32 and two at chromosome 2p22. Loss of heterozygosity (LOH) was found at both 1q25 and at 2p22 indicating that minor deleted areas were not detected with the resolution of CGH (Fig. 3). Additionally, chromosome 2p in TCC 733 showed a CGH pattern of gain/no change/gain of DNA that correlated with transcript increase/decrease/increase. Thus, for the areas showing increased expression there was a correlation with the DNA copy number alterations (Fig. 1A). As indicated above, the mRNA decrease observed in the middle of the chromosomal gain was because of LOH, implying that one of the mechanisms for mRNA down-regulation may be regions that have undergone smaller losses of chromosomal material. However, this cannot be detected with the resolution of the CGH method.

In both TCC 733 and TCC 827, the telomeric end of chromosome 11p showed a normal ratio in the CGH analysis; however, clusters of five and three genes, respectively, lost their expression. Two microsatellites (D11S1760, D11S922) positioned close to MUC2, IGF2, and cathepsin D indicated LOH as the most likely mechanism behind the loss of expression (data not shown).

A reduced expression of mRNA observed in TCC 733 at chromosomes 3q24, 11p11, 12p12.2, 12q21.1, and 16q24 and in TCC 827 at chromosome 11p15.5, 12p11, 15q11.2, and 18q12 was also examined for chromosomal losses using microsatellites positioned as close as possible to the gene loci
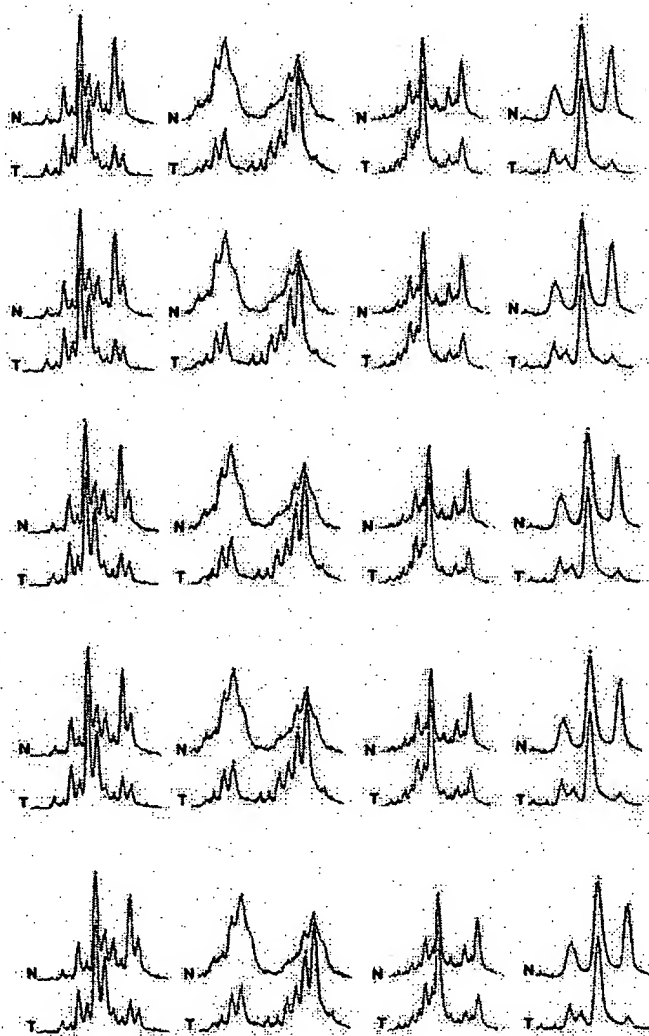
FIG. 3. Microsatellite analysis of loss of heterozygosity. Tumor 733 showing loss of heterozygosity at chromosome 1q25, detected (a) by D1S215 close to Hu class I histocompatibility antigen (gene number 38 in Fig. 1), (b) by D1S2735 close to cathepsin E (gene number 41 in Fig. 1), and (c) at chromosome 2p23 by D2S2251 close to general β-spectrin (gene number 11 on Fig. 1) and of (d) tumor 827 showing loss of heterozygosity at chromosome 18q12 by S18S1118 close to mitochondrial 3-oxoacyl-coenzyme A thiolase (gene number 12 in Fig. 1). The *upper curves* show the electropherogram obtained from normal DNA from leukocytes (*N*), and the *lower curves* show the electropherogram from tumor DNA (*T*). In all cases one allele is partially lost in the tumor amplicon.

FIG. 4. **Correlation between protein levels as judged by 2D-PAGE and transcript ratio.** For comparison proteins were divided in three groups, unaltered in level or up- or down-regulated (*horizontal axis*). The mRNA ratio as determined by oligonucleotide arrays was plotted for each gene (*vertical axis*). ▲, mRNAs that were scored as present in both tumors used for the ratio calculation; △, mRNAs that were scored as absent in the invasive tumors (along *horizontal axis*) or as absent in non-invasive reference (*top* of figure). Two different scalings were used to exclude scaling as a confounder, TCCs 827 and 532 (▲△) were scaled with background suppression, and TCCs 733 and 335 (●○) were scaled without suppression. Both comparisons showed highly significant (p < 0.005) differences in mRNA ratios between the groups. Proteins shown were as follows: Group A (from *left*), phosphoglucomutase 1, glutathione transferase class μ number 4, fatty acid-binding protein homologue, cytokeratin 15, and cytokeratin 13; B (from *left*), fatty acid-binding protein homologue, 28-kDa heat shock protein, cytokeratin 13, and calcyclin; C (from *left*), α-enolase, hnRNP B1, 28-kDa heat shock protein, 14-3-3-ε, and pre-mRNA splicing factor; D, mesothelial keratin K7 (type II); E (from *top*), glutathione S-transferase-π and mesothelial keratin K7 (type II); F (from *top* and *left*), adenylyl cyclase-associated protein, E-cadherin, keratin 19, calgizzarin, phosphoglycerate mutase, annexin IV, cytoskeletal γ-actin, hnRNP A1, integral membrane protein calnexin (IP90), hnRNP H, brain-type clathrin light chain-a, hnRNP F, 70-kDa heat shock protein, heterogeneous nuclear ribonucleoprotein A/B, translationally controlled tumor protein, liver glyceraldehyde-3-phosphate dehydrogenase, keratin 8, aldehyde reductase, and Na,K-ATPase β-1 subunit; G, (from *top* and *left*), TCP20, calgizzarin, 70-kDa heat shock protein, calnexin, hnRNP H, cytokeratin 15, ATP synthase, keratin 19, triosephosphate isomerase, hnRNP F, liver glyceraldehyde-3-phosphatase dehydrogenase, glutathione S-transferase-π, and keratin 8; H (from *left*), plasma gelsolin, autoantigen calreticulin, thioredoxin, and NAD+-dependent 15 hydroxyprostaglandin dehydrogenase; I (from *top*), prolyl 4-hydroxylase β-subunit, cytokeratin 20, cytokeratin 17, prohibition, and fructose 1,6-biphosphatase; J annexin II; K, annexin IV; L (from *top* and *left*), 90-kDa heat shock protein, prolyl 4-hydroxylase β-subunit, α-enolase, GRP 78, cyclophilin, and cofilin.

showing reduced mRNA transcripts. Only the microsatellite positioned at 18q12 showed LOH (Fig. 3), suggesting that transcriptional down-regulation of genes in the other regions may be controlled by other mechanisms.

Relation between Changes in mRNA and Protein Levels— 2D-PAGE analysis, in combination with Coomassie Brilliant Blue and/or silver staining, was carried out on all four tumors using fresh biopsy material. 40 well resolved abundant known proteins migrating in areas away from the edges of the pH

gradient, and having a known chromosomal location, were selected for analysis in the TCC pair 827/532. Proteins were identified by a combination of methods (see "Experimental Procedures"). In general there was a highly significant correlation (p < 0.005) between mRNA and protein alterations (Fig. 4). Only one gene showed disagreement between transcript alteration and protein alteration. Except for a group of cyto-
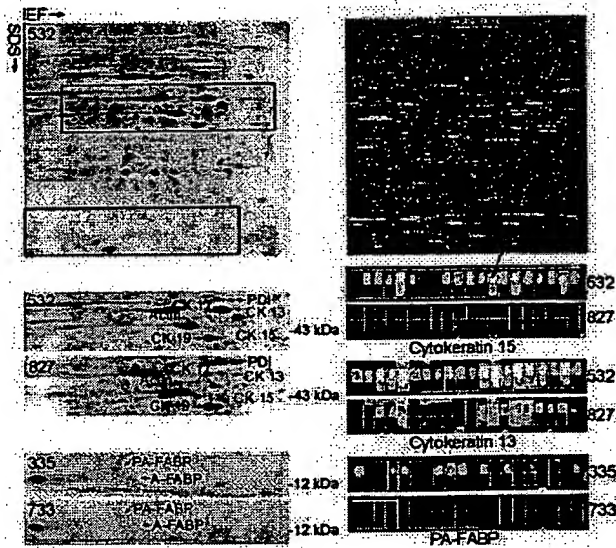
FIG. 5. Comparison of protein and transcript levels in invasive and non-invasive TCCs. The upper part of the figure shows a 2D gel (left) and the oligonucleotide array (right) of TCC 532. The red rectangles on the upper gel highlight the areas that are compared below. Identical areas of 2D gels of TCCs 532 and 827 are shown below. Clearly, cytokeratins 13 and 15 are strongly down-regulated in TCC 827 (red annotation). The tile on the array containing probes for cytokeratin 15 is enlarged below the array (red arrow) from TCC 532 and is compared with TCC 827. The upper row of squares in each tile corresponds to perfect match probes; the lower row corresponds to mismatch probes containing a mutation (used for correction for un-specific binding). Absence of signal is depicted as black, and the higher the signal the lighter the color. A high transcript level was detected in TCC 532 (6151 units) whereas a much lower level was detected in TCC 827 (absence of signals). For cytokeratin 13, a high transcript level was also present in TCC 532 (15659 units), and a much lower level was present in TCC 827 (623 units). The 2D gels at the bottom of the figure (left) show levels of PA-FABP and adipocyte-FABP in TCCs 335 and 733 (invasive), respectively. Both proteins are down-regulated in the invasive tumor. To the right we show the array tiles for the PA-FABP transcript. A medium transcript level was detected in the case of TCC 335 (1277 units) whereas very low levels were detected in TCC 733 (166 units). IEF, isoelectric focusing.

keratins encoded by genes on chromosome 17 (Fig. 5) the analyzed proteins did not belong to a particular family. 26 well focused proteins whose genes had a know chromosomal location were detected in TCCs 733 and 335, and of these 19 correlated ($p < 0.005$) with the mRNA changes detected using the arrays (Fig. 4). For example, PA-FABP was highly expressed in the non-invasive TCC 335 but lost in the invasive counterpart (TCC 733; see Fig. 5). The smaller number of proteins detected in both 733 and 335 was because of the smaller size of the biopsies that were available.

11 chromosomal regions where CGH showed aberrations that corresponded to the changes in transcript levels also showed corresponding changes in the protein level (Table II). These regions included genes that encode proteins that are found to be frequently altered in bladder cancer, namely cytokeratins 17 and 20, annexins II and IV, and the fatty acid-binding proteins PA-FABP and FBP1. Four of these proteins were encoded by genes in chromosome 17q, a frequently amplified chromosomal area in invasive bladder cancers.

DISCUSSION

Most human cancers have abnormal DNA content, having lost some chromosomal parts and gained others. The present study provides some evidence as to the effect of these gains and losses on gene expression in two pairs of non-invasive and invasive TCCs using high throughput expression arrays and proteomics, in combination with CGH. In general, the results showed that there is a clear individual regulation of the mRNA expression of single genes, which in some cases was superimposed by a DNA copy number effect. In most cases, genes located in chromosomal areas with gains often exhibited increased mRNA expression, whereas areas showing losses showed either no change or a reduced mRNA expression. The latter might be because of the fact that losses most often are restricted to loss of one allele, and the cut-off point for detection of expression alterations was a 2-fold change, thus being at the border of detection. In several cases, how-

TABLE II

Proteins whose expression level correlates with both mRNA and gene dose changes

Protein	Chromosomal location	Tumor TCC	CGH alteration	Transcript alteration[a]	Protein alteration
Annexin II	1q21	733	Gain	Abs to Pres[e]	Increase
Annexin IV	2p13	733	Gain	3.9-Fold up	Increase
Cytokeratin 17	17q12-q21	827	Gain	3.8-Fold up	Increase
Cytokeratin 20	17q21.1	827	Gain	5.6-Fold up	Increase
(PA-)FABP	8q21.2	827	Loss	10-Fold down	Decrease
FBP1	9q22	827	Gain	2.3-Fold up	Increase
Plasma gelsolin	9q31	827	Gain	Abs to Pres	Increase
Heat shock protein 28	15q12-q13	827	Loss	2.5-Fold up	Decrease
Prohibitin	17q21	827/733	Gain	3.7-/2.5-Fold up[b]	Increase
Prolyl-4-hydroxyl	17q25	827/733	Gain	5.7-/1.6-Fold up	Increase
hnRNPB1	7p15	827	Loss	2.5-Fold down	Decrease

[a] Abs, absent; Pres, present.
[b] In cases where the corresponding alterations were found in both TCCs 827 and 733 these are shown as 827/733.

ever, an increase or decrease in DNA copy number was associated with *de novo* occurrence or complete loss of transcript, respectively. Some of these transcripts could not be detected in the non-invasive tumor but were present at relatively high levels in areas with DNA amplifications in the invasive tumors (*e.g.* in TCC 733 transcript from cellular ligand of annexin II gene (chromosome 1q21) from absent to 2670 arbitrary units; in TCC 827 transcript from small proline-rich protein 1 gene (chromosome 1q12-q21.1) from absent to 1326 arbitrary units). It may be anticipated from these data that significant clustering of genes with an increased expression to a certain chromosomal area indicates an increased likelihood of gain of chromosomal material in this area.

Considering the many possible regulatory mechanisms acting at the level of transcription, it seems striking that the gene dose effects were so clearly detectable in gained areas. One hypothetical explanation may lie in the loss of controlled methylation in tumor cells (17–19). Thus, it may be possible that in chromosomes with increased DNA copy numbers two or more alleles could be demethylated simultaneously leading to a higher transcription level, whereas in chromosomes with losses the remaining allele could be partly methylated, turning off the process (20, 21). A recent report has documented a ploidy regulation of gene expression in yeast, but in this case all the genes were present in the same ratio (22), a situation that is not analogous to that of cancer cells, which show marked chromosomal aberrations, as well as gene dosage effects.

Several CGH studies of bladder cancer have shown that some chromosomal aberrations are common at certain stages of disease progression, often occurring in more than 1 of 3 tumors. In pTa tumors, these include 9p−, 9q−, 1q+, Y− (2, 6), and in pT1 tumors, 2q−,11p−, 11q−, 1q+, 5p+, 8q+, 17q+, and 20q+ (2–4, 6, 7). The pTa tumors studied here showed similar aberrations such as 9p− and 9q22-q33− and 9q− and Y−, respectively. Likewise, the two minimal invasive pT1 tumors showed aberrations that are commonly seen at that stage, and TCC 827 had a remarkable resemblance to the commonly seen pattern of losses and gains, such as 1q22–24 amplification (seen in both tumors), 11q14-q22 loss, the latter often linked to 17 q+ (both tumors), and 1q+ and 9p−, often linked to 20q+ and 11 q13+ (both tumors) (7–9). These observations indicate that the pairs of tumors used in this study exhibit chromosomal changes observed in many tumors, and therefore the findings could be of general importance for bladder cancer.

Considering that the mapping resolution of CGH is of about 20 megabases it is only possible to get a crude picture of chromosomal instability using this technique. Occasionally, we observed reduced transcript levels close to or inside regions with increased copy numbers. Analysis of these regions by positioning heterozygous microsatellites as close as possible to the locus showing reduced gene expression revealed loss of heterozygosity in several cases. It seems likely that multiple and different events occur along each chromosomal

arm and that the use of cDNA microarrays for analysis of DNA copy number changes will reach a resolution that can resolve these changes, as has recently been proposed (2). The outlier data were not more frequent at the boundaries of the CGH aberrations. At present we do not know the mechanism behind chromosomal aneuploidy and cannot predict whether chromosomal gains will be transcribed to a larger extent than the two native alleles. A mechanism as genetic imprinting has an impact on the expression level in normal cells and is often reduced in tumors. However, the relation between imprinting and gain of chromosomal material is not known.

We regard it as a strength of this investigation that we were able to compare invasive tumors to benign tumors rather than to normal urothelium, as the tumors studied were biologically very close and probably may represent successive steps in the progression of bladder cancer. Despite the limited amount of fresh tissue available it was possible to apply three different state of the art methods. The observed correlation between DNA copy number and mRNA expression is remarkable when one considers that different pieces of the tumor biopsies were used for the different sets of experiments. This indicate that bladder tumors are relatively homogenous, a notion recently supported by CGH and LOH data that showed a remarkable similarity even between tumors and distant metastasis (10, 23).

In the few cases analyzed, mRNA and protein levels showed a striking correspondence although in some cases we found discrepancies that may be attributed to translational regulation, post-translational processing, protein degradation, or a combination of these. Some transcripts belong to undertranslated mRNA pools, which are associated with few translationally inactive ribosomes; these pools, however, seem to be rare (24). Protein degradation, for example, may be very important in the case of polypeptides with a short half-life (*e.g.* signaling proteins). A poor correlation between mRNA and protein levels was found in liver cells as determined by arrays and 2D-PAGE (25), and a moderate correlation was recently reported by Ideker *et al.* (26) in yeast. Interestingly, our study revealed a much better correlation between gained chromosomal areas and increased mRNA levels than between loss of chromosomal areas and reduced mRNA levels. In general, the level of CGH change determined the ability to detect a change in transcript. One possible explanation could be that by losing one allele the change in mRNA level is not so dramatic as compared with gain of material, which can be rather unlimited and may lead to a severalfold increase in gene copy number resulting in a much higher impact on transcript level. The latter would be much easier to detect on the expression arrays as the cut-off point was placed at a 2-fold level so as not to be biased by noise on the array. Construction of arrays with a better signal to noise ratio may in the future allow detection of lesser than 2-fold alterations in transcript levels, a feature that may facilitate the analysis of the effect of loss of chromosomal areas on transcript levels.

In eleven cases we found a significant correlation between DNA copy number, mRNA expression, and protein level. Four of these proteins were encoded by genes located at a frequently amplified area in chromosome 17q. Whether DNA copy number is one of the mechanisms behind alteration of these eleven proteins is at present unknown and will have to be proved by other methods using a larger number of samples. One factor making such studies complicated is the large extent of protein modification that occurs after translation, requiring immunoidentification and/or mass spectrometry to correctly identify the proteins in the gels.

In conclusion, the results presented in this study exemplify the large body of knowledge that may be possible to gather in the future by combining state of the art techniques that follow the pathway from DNA to protein (26). Here, we used a traditional chromosomal CGH method, but in the future high resolution CGH based on microarrays with many thousand radiation hybrid-mapped genes will increase the resolution and information derived from these types of experiments (2). Combined with expression arrays analyzing transcripts derived from genes with known locations, and 2D gel analysis to obtain information at the post-translational level, a clearer and more developed understanding of the tumor genome will be forthcoming.

REFERENCES

1. Lengauer, C., Kinzler, K. W., and Vogelstein, B. (1998) Genetic instabilities in human cancers. *Nature* **17,** 643–649
2. Pollack, J. R., Perou, C. M., Alizadeh, A. A., Eisen, M. B., Pergamenschikov, A., Williams, C. F., Jeffrey, S. S., Botstein, D., and Brown, P. O. (1999) Genome-wide analysis of DNA copy-number changes using cDNA microarrays. *Nat. Genet.* **23,** 41–46
3. de Cremoux, P., Martin, E. C., Vincent-Salomon, A., Dieras, V., Barbaroux, C., Liva, S., Pouillart, P., Sastre-Garau, X., and Magdelenat, H. (1999) Quantitative PCR analysis of c-erb B-2 (HER2/neu) gene amplification and comparison with p185(HER2/neu) protein expression in breast cancer drill biopsies. *Int. J. Cancer* **83,** 157–161
4. Brungier, P. P., Tamimi, Y., Shuuring, E., and Schalken, J. (1996) Expression of cyclin D1 and EMS1 in bladder tumors; relationship with chromosome 11q13 amplifications. *Oncogene* **12,** 1747–1753
5. Slavc, I., Ellenbogen, R., Jung, W. H., Vawter, G. F., Kretschmar, C., Grier, H., and Korf, B. R. (1990) *myc* gene amplification and expression in primary human neuroblastoma. *Cancer Res.* **50,** 1459–1463
6. Sauter, G., Carroll, P., Moch, H., Kallioniemi, A., Kerschmann, R., Narayan,

7. P., Mihatsch, M. J., and Waldman, F. M. (1995) c-*myc* copy number gains in bladder cancer detected by fluorescence *in situ* hybridization. *Am J. Pathol.* **146,** 1131–1139
7. Richter, J., Jiang, F., Gorog, J. P., Sartorious, G., Egenter, C., Gasser, T. C., Moch, H., Mihatsch, M. J., and Sauter, G. (1997) Marked genetic differences between stage pTa and stage pT1 papillary bladder cancer detected by comparative genomic hybridization. *Cancer Res.* **57,** 2860–2864
8. Richter, J., Beffa, L., Wagner, U., Schraml, P., Gasser, T. C., Moch, H., Mihatsch, M. J., and Sauter, G. (1998) Patterns of chromosomal imbalances in advanced urinary bladder cancer detected by comparative genomic hybridization. *Am. J. Pathol.* **153,** 1615–1621
9. Bruch, J., Wohr, G., Hautmann, R., Mattfeldt, T., Bruderlein, S., Moller, P., Sauter, S., Hameister, H., Vogel, W., and Paiss, T. (1998) Chromosomal changes during progression of transitional cell carcinoma of the bladder and delineation of the amplified interval on chromosome arm 8q. *Genes Chromosomes Cancer* **23,** 167–174
10. Hovey, R. M., Chu, L., Balazs, M., De Vries, S., Moore, D., Sauter, G., Carroll, P. R., and Waldman, F. M. (1998) Genetic alterations in primary bladder cancers and their metastases. *Cancer Res.* **15,** 3555–3560
11. Simon, R., Burger, H., Brinkschmidt, C., Bocker, W., Hertle, L., and Terpe, H. J. (1998) Chromosomal aberrations associated with invasion in papillary superficial bladder cancer. *J. Pathol.* **185,** 345–351
12. Koo, S. H., Kwon, K. C., Ihm, C. H., Jeon, Y. M., Park, J. W., and Sul, C. K. (1999) Detection of genetic alterations in bladder tumors by comparative genomic hybridization and cytogenetic analysis. *Cancer Genet. Cytogenet.* **110,** 87–93
13. Wodicka, L., Dong, H., Mittmann, M., Ho, M. H., and Lockhart, D. J. (1997) Genome-wide expression monitoring in *Saccharomyces cerevisiae. Nat. Biotechnol.* **15,** 1359–1367
14. Christensen, M., Sunde, L., Bolund, L., and Orntoft, T. F. (1999) Comparison of three methods of microsatellite detection. *Scand. J. Clin. Lab. Invest.* **59,** 167–177
15. Celis, J. E., Ostergaard, M., Basse, B., Celis, A., Lauridsen, J. B., Ratz, G. P., Andersen, I., Hein, B., Wolf, H., Orntoft, T. F., and Rasmussen, H. H. (1996) Loss of adipocyte-type fatty acid binding protein and other protein biomarkers is associated with progression of human bladder transitional cell carcinomas. *Cancer Res.* **56,** 4782–4790
16. Celis, J. E., Ratz, G., Basse, B., Lauridsen, J. B., and Celis, A. (1994) in *Cell Biology: A Laboratory Handbook* (Celis, J. E., ed) Vol. 3, pp. 222–230, Academic Press, Orlando, FL
17. Ohlsson, R., Tycko, B., and Sapienza, C. (1998) Monoallelic expression: 'there can only be one'. *Trends Genet.* **14,** 435–438
18. Hollander, G. A., Zuklys, S., Morel, C., Mizoguchi, E., Mobisson, K., Simpson, S., Terhorst, C., Wishart, W., Golan, D. E., Bhan, A. K., and Burakoff, S. J. (1998) Monoallelic expression of the interleukin-2 locus. *Science* **279,** 2118–2121
19. Brannan, C. I., and Bartolomei, M. S. (1999) Mechanisms of genomic imprinting. *Curr. Opin. Genet. Dev.* **9,** 164–170
20. Ohlsson, R., Cui, H., He, L., Pfeifer, S., Malmikumpa, H., Jiang, S., Feinberg, A. P., and Hedborg, F. (1999) Mosaic allelic insulin-like growth factor 2 expression patterns reveal a link between Wilms' tumorigenesis and epigenetic heterogeneity. *Cancer Res.* **59,** 3889–3892
21. Cui, H., Hedborg, F., He, L., Nordenskjold, A., Sandstedt, B., Pfeifer-Ohlsson, S., and Ohlsson, R. (1997) Inactivation of H19, an imprinted and putative tumor repressor gene, is a preneoplastic event during Wilms' tumorigenesis. *Cancer Res.* **57,** 4469–4473
22. Galitski, T., Saldanha, A. J., Styles, C. A., Lander, E. S., and Fink, G. R. (1999) Ploidy regulation of gene expression. *Science* **285,** 251–254
23. Tsao, J., Yatabe, Y., Markl, I. D., Hajyan, K., Jones, P. A., and Shibata, D. (2000) Bladder cancer genotype stability during clinical progression. *Genes Chromosomes Cancer* **29,** 26–32
24. Zong, Q., Schummer, M., Hood, L., and Morris, D. R. (1999) Messenger RNA translation state: the second dimension of high-throughput expression screening. *Proc. Natl. Acad. Sci. U. S. A.* **96,** 10632–10636
25. Anderson, L., and Seilhamer, J. (1997) Comparison of selected mRNA and protein abundances in human liver. *Electrophoresis* **18,** 533–537
26. Ideker, T., Thorsson, V., Ranish, J. A., Christmas, R., Buhler, J., Eng, J. K., Bumgarner, R., Goodlett, D. R., Aebersold, R., and Hood, L. (2001) Integrated genomic and proteomic analyses of a systematically perturbed metabolic network. *Science* **292,** 929–934

Microarray analysis reveals a major direct role of DNA copy number alteration in the transcriptional program of human breast tumors

Jonathan R. Pollack[*][†][‡], Therese Sørlie[§], Charles M. Perou[¶], Christian A. Rees[∥][**], Stefanie S. Jeffrey[††], Per E. Lonning[‡‡], Robert Tibshirani[§§], David Botstein[∥], Anne-Lise Børresen-Dale[§], and Patrick O. Brown[†¶¶]

Departments of *Pathology, ∥Genetics, ††Surgery, §§Health Research and Policy, and ¶¶Biochemistry, and †Howard Hughes Medical Institute, Stanford University School of Medicine, Stanford, CA 94305; §Department of Genetics, Norwegian Radium Hospital, Montebello, N-0310 Oslo, Norway; ‡‡Department of Medicine (Oncology), Haukeland University Hospital, N-5021 Bergen, Norway; and ¶Department of Genetics and Lineberger Comprehensive Cancer Center, University of North Carolina, Chapel Hill, NC 27599

Contributed by Patrick O. Brown, August 6, 2002

Genomic DNA copy number alterations are key genetic events in the development and progression of human cancers. Here we report a genome-wide microarray comparative genomic hybridization (array CGH) analysis of DNA copy number variation in a series of primary human breast tumors. We have profiled DNA copy number alteration across 6,691 mapped human genes, in 44 predominantly advanced, primary breast tumors and 10 breast cancer cell lines. While the overall patterns of DNA amplification and deletion corroborate previous cytogenetic studies, the high-resolution (gene-by-gene) mapping of amplicon boundaries and the quantitative analysis of amplicon shape provide significant improvement in the localization of candidate oncogenes. Parallel microarray measurements of mRNA levels reveal the remarkable degree to which variation in gene copy number contributes to variation in gene expression in tumor cells. Specifically, we find that 62% of highly amplified genes show moderately or highly elevated expression, that DNA copy number influences gene expression across a wide range of DNA copy number alterations (deletion, low-, mid- and high-level amplification), that on average, a 2-fold change in DNA copy number is associated with a corresponding 1.5-fold change in mRNA levels, and that overall, at least 12% of all the variation in gene expression among the breast tumors is directly attributable to underlying variation in gene copy number. These findings provide evidence that widespread DNA copy number alteration can lead directly to global deregulation of gene expression, which may contribute to the development or progression of cancer.

C onventional cytogenetic techniques, including comparative genomic hybridization (CGH) (1), have led to the identification of a number of recurrent regions of DNA copy number alteration in breast cancer cell lines and tumors (2–4). While some of these regions contain known or candidate oncogenes [e.g., FGFR1 (8p11), MYC (8q24), CCND1 (11q13), ERBB2 (17q12), and ZNF217 (20q13)] and tumor suppressor genes [RB1 (13q14) and TP53 (17p13)], the relevant gene(s) within other regions (e.g., gain of 1q, 8q22, and 17q22–24, and loss of 8p) remain to be identified. A high-resolution genome-wide map, delineating the boundaries of DNA copy number alterations in tumors, should facilitate the localization and identification of oncogenes and tumor suppressor genes in breast cancer. In this study, we have created such a map, using array-based CGH (5–7) to profile DNA copy number alteration in a series of breast cancer cell lines and primary tumors.

An unresolved question is the extent to which the widespread DNA copy number changes that we and others have identified in breast tumors alter expression of genes within involved regions. Because we had measured mRNA levels in parallel in the same samples (8), using the same DNA microarrays, we had an opportunity to explore on a genomic scale the relationship between DNA copy number changes and gene expression. From this analysis, we have identified a significant impact of widespread DNA copy number alteration on the transcriptional programs of breast tumors.

Materials and Methods

Tumors and Cell Lines. Primary breast tumors were predominantly large (>3 cm), intermediate-grade, infiltrating ductal carcinomas, with more than 50% being lymph node positive. The fraction of tumor cells within specimens averaged at least 50%. Details of individual tumors have been published (8, 9), and are summarized in Table 1, which is published as supporting information on the PNAS web site, www.pnas.org. Breast cancer cell lines were obtained from the American Type Culture Collection. Genomic DNA was isolated either using Qiagen genomic DNA columns, or by phenol/chloroform extraction followed by ethanol precipitation.

DNA Labeling and Microarray Hybridizations. Genomic DNA labeling and hybridizations were performed essentially as described in Pollack et al. (7), with slight modifications. Two micrograms of DNA was labeled in a total volume of 50 microliters and the volumes of all reagents were adjusted accordingly. "Test" DNA (from tumors and cell lines) was fluorescently labeled (Cy5) and hybridized to a human cDNA microarray containing 6,691 different mapped human genes (i.e., UniGene clusters). The "reference" (labeled with Cy3) for each hybridization was normal female leukocyte DNA from a single donor. The fabrication of cDNA microarrays and the labeling and hybridization of mRNA samples have been described (8).

Data Analysis and Map Positions. Hybridized arrays were scanned on a GenePix scanner (Axon Instruments, Foster City, CA), and fluorescence ratios (test/reference) calculated using SCANALYZE software (available at http://rana.lbl.gov). Fluorescence ratios were normalized for each array by setting the average log fluorescence ratio for all array elements equal to 0. Measurements with fluorescence intensities more than 20% above background were considered reliable. DNA copy number profiles that deviated significantly from background ratios measured in normal genomic DNA control hybridizations were interpreted as evidence of real DNA copy number alteration (see Estimating Significance of Altered Fluorescence Ratios in the supporting information). When indicated, DNA copy number profiles are displayed as a moving average (symmetric 5-nearest neighbors). Map positions for arrayed human cDNAs were assigned by
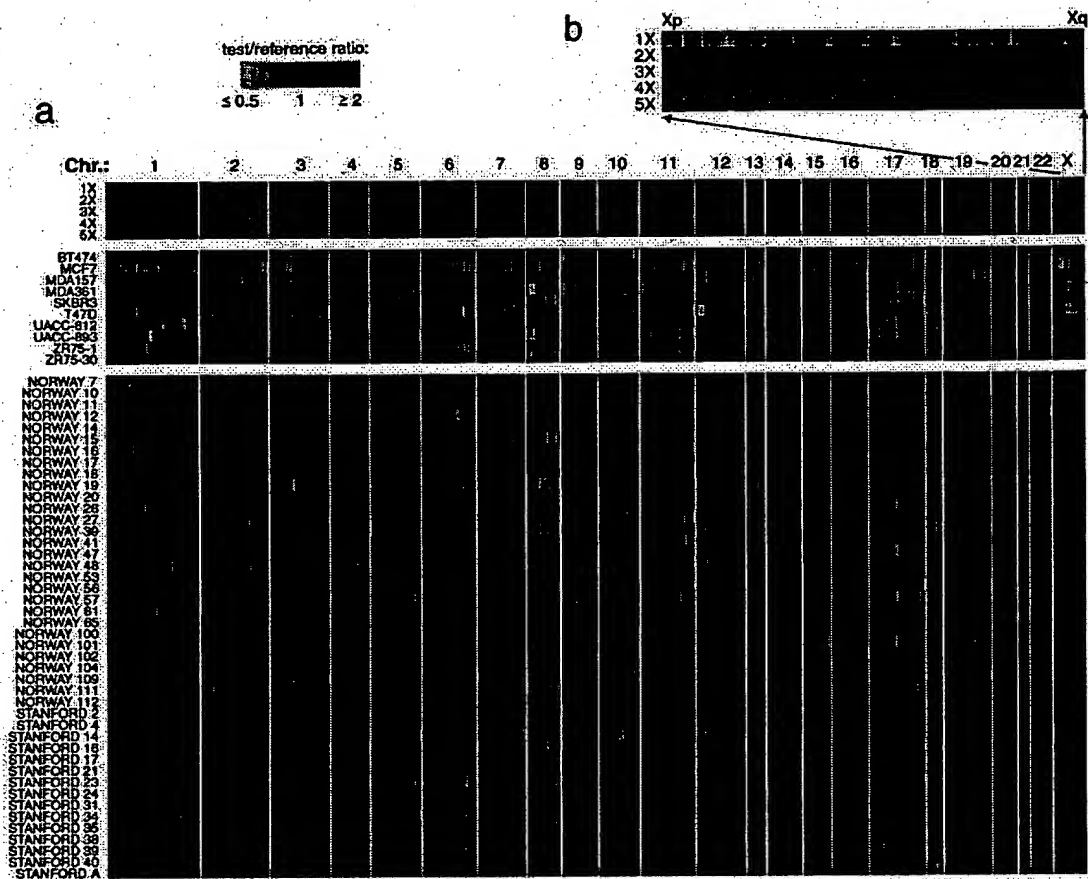
GENETICS

Fig. 1. Genome-wide measurement of DNA copy number alteration by array CGH. (a) DNA copy number profiles are illustrated for cell lines containing different numbers of X chromosomes, for breast cancer cell lines, and for breast tumors. Each row represents a different cell line or tumor, and each column represents one of 6,691 different mapped human genes present on the microarray, ordered by genome map position from 1pter through Xqter. Moving average (symmetric 5-nearest neighbors) fluorescence ratios (test/reference) are depicted using a $\log_2$-based pseudocolor scale (indicated), such that red luminescence reflects fold-amplification, green luminescence reflects fold-deletion, and black indicates no change (gray indicates poorly measured data). (b) Enlarged view of DNA copy number profiles across the X chromosome, shown for cell lines containing different numbers of X chromosomes.

identifying the starting position of the best and longest match of any DNA sequence represented in the corresponding UniGene cluster (10) against the "Golden Path" genome assembly (http://genome.ucsc.edu/; Oct 7, 2000 Freeze). For UniGene clusters represented by multiple arrayed elements, mean fluorescence ratios (for all elements representing the same UniGene cluster) are reported. For mRNA measurements, fluorescence ratios are "mean-centered" (i.e., reported relative to the mean ratio across the 44 tumor samples). The data set described here can be accessed in its entirety in the supporting information.

Results

We performed CGH on 44 predominantly locally advanced, primary breast tumors and 10 breast cancer cell lines, using cDNA microarrays containing 6,691 different mapped human genes (Fig. 1a; also see *Materials and Methods* for details of microarray hybridizations). To take full advantage of the improved spatial resolution of array CGH, we ordered (fluorescence ratios for) the 6,691 cDNAs according to the "Golden Path" (http://genome.ucsc.edu/) genome assembly of the draft human genome sequences (11). In so doing, arrayed cDNAs not only themselves represent genes of potential interest (e.g., candidate oncogenes within amplicons), but also provide precise genetic landmarks for chromosomal regions of amplification and

deletion. Parallel analysis of DNA from cell lines containing different numbers of X chromosomes (Fig. 1b), as we did before (7), demonstrated the sensitivity of our method to detect single-copy loss (45, XO), and 1.5- (47,XXX), 2- (48,XXXX), or 2.5-fold (49,XXXXX) gains (also see Fig. 5, which is published as supporting information on the PNAS web site). Fluorescence ratios were linearly proportional to copy number ratios, which were slightly underestimated, in agreement with previous observations (7). Numerous DNA copy number alterations were evident in both the breast cancer cell lines and primary tumors (Fig. 1a), detected in the tumors despite the presence of euploid non-tumor cell types; the magnitudes of the observed changes were generally lower in the tumor samples. DNA copy-number alterations were found in every cancer cell line and tumor, and on every human chromosome in at least one sample. Recurrent regions of DNA copy number gain and loss were readily identifiable. For example, gains within 1q, 8q, 17q, and 20q were observed in a high proportion of breast cancer cell lines/tumors (90%/69%, 100%/47%, 100%/60%, and 90%/44%, respectively), as were losses within 1p, 3p, 8p, and 13q (80%/24%, 80%/22%, 80%/22%, and 70%/18%, respectively), consistent with published cytogenetic studies (refs. 2–4; a complete listing of gains/losses is provided in Tables 2 and 3, which are published as supporting information on the PNAS web site). The total
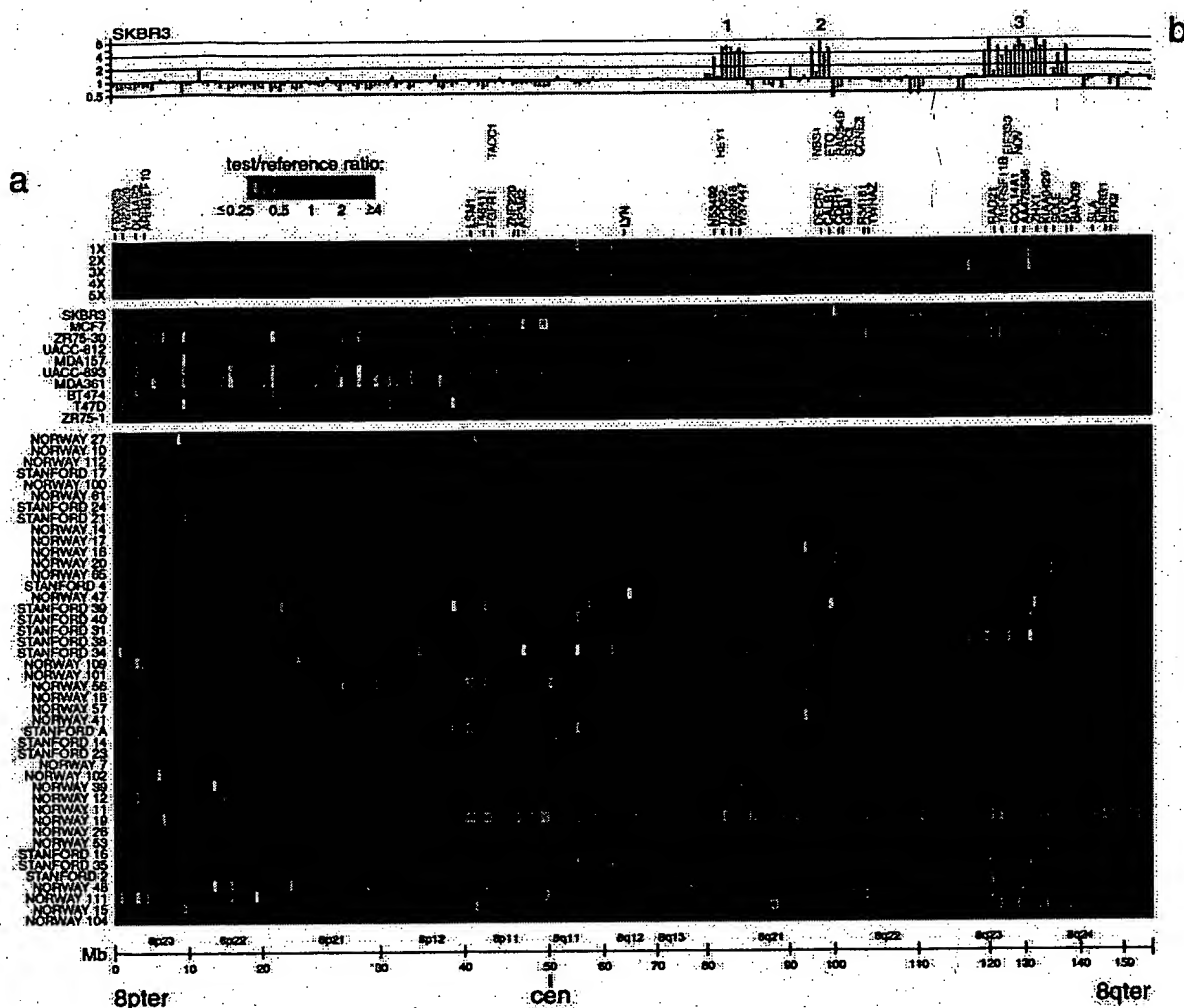
Fig. 2. DNA copy number alteration across chromosome 8 by array CGH. (a) DNA copy number profiles are illustrated for cell lines containing different numbers of X chromosomes, for breast cancer cell lines, and for breast tumors. Breast cancer cell lines and tumors are separately ordered by hierarchical clustering to highlight recurrent copy number changes. The 241 genes present on the microarrays and mapping to chromosome 8 are ordered by position along the chromosome. Fluorescence ratios (test/reference) are depicted by a $\log_2$ pseudocolor scale (indicated). Selected genes are indicated with color-coded text (red, increased; green, decreased; black, no change; gray, not well measured) to reflect correspondingly altered mRNA levels (observed in the majority of the subset of samples displaying the DNA copy number change). The map positions for genes of interest that are not represented on the microarray are indicated in the row above those genes represented on the array. (b) Graphical display of DNA copy number profile for breast cancer cell line SKBR3. Fluorescence ratios (tumor/normal) are plotted on a $\log_2$ scale for chromosome 8 genes, ordered along the chromosome.

number of genomic alterations (gains and losses) was found to be significantly higher in breast tumors that were high grade ($P = 0.008$), consistent with published CGH data (3), estrogen receptor negative ($P = 0.04$), and harboring TP53 mutations ($P = 0.0006$) (see Table 4, which is published as supporting information on the PNAS web site).

The improved spatial resolution of our array CGH analysis is illustrated for chromosome 8, which displayed extensive DNA copy number alteration in our series. A detailed view of the variation in the copy number of 241 genes mapping to chromosome 8 revealed multiple regions of recurrent amplification; each of these potentially harbors a different known or previously uncharacterized oncogene (Fig. 2a). The complexity of amplicon structure is most easily appreciated in the breast cancer cell line SKBR3. Although a conventional CGH analysis of 8q in SKBR3 identified only two distinct regions of amplification (12), we observed three distinct regions of high-level amplification (labeled 1–3 in Fig. 2b). For each of these regions we can define the

boundaries of the interval recurrently amplified in the tumors we examined; in each case, known or plausible candidate oncogenes can be identified (a description of these regions, as well as the recurrently amplified regions on chromosomes 17 and 20, can be found in Figs. 6 and 7, which are published as supporting information on the PNAS web site).

For a subset of breast cancer cell lines and tumors (4 and 37, respectively), and a subset of arrayed genes (6,095), mRNA levels were quantitatively measured in parallel by using cDNA microarrays (8). The parallel assessment of mRNA levels is useful in the interpretation of DNA copy number changes. For example, the highly amplified genes that are also highly expressed are the strongest candidate oncogenes within an amplicon. Perhaps more significantly, our parallel analysis of DNA copy number changes and mRNA levels provides us the opportunity to assess the global impact of widespread DNA copy number alteration on gene expression in tumor cells.

A strong influence of DNA copy number on gene expression is evident in an examination of the pseudocolor representations
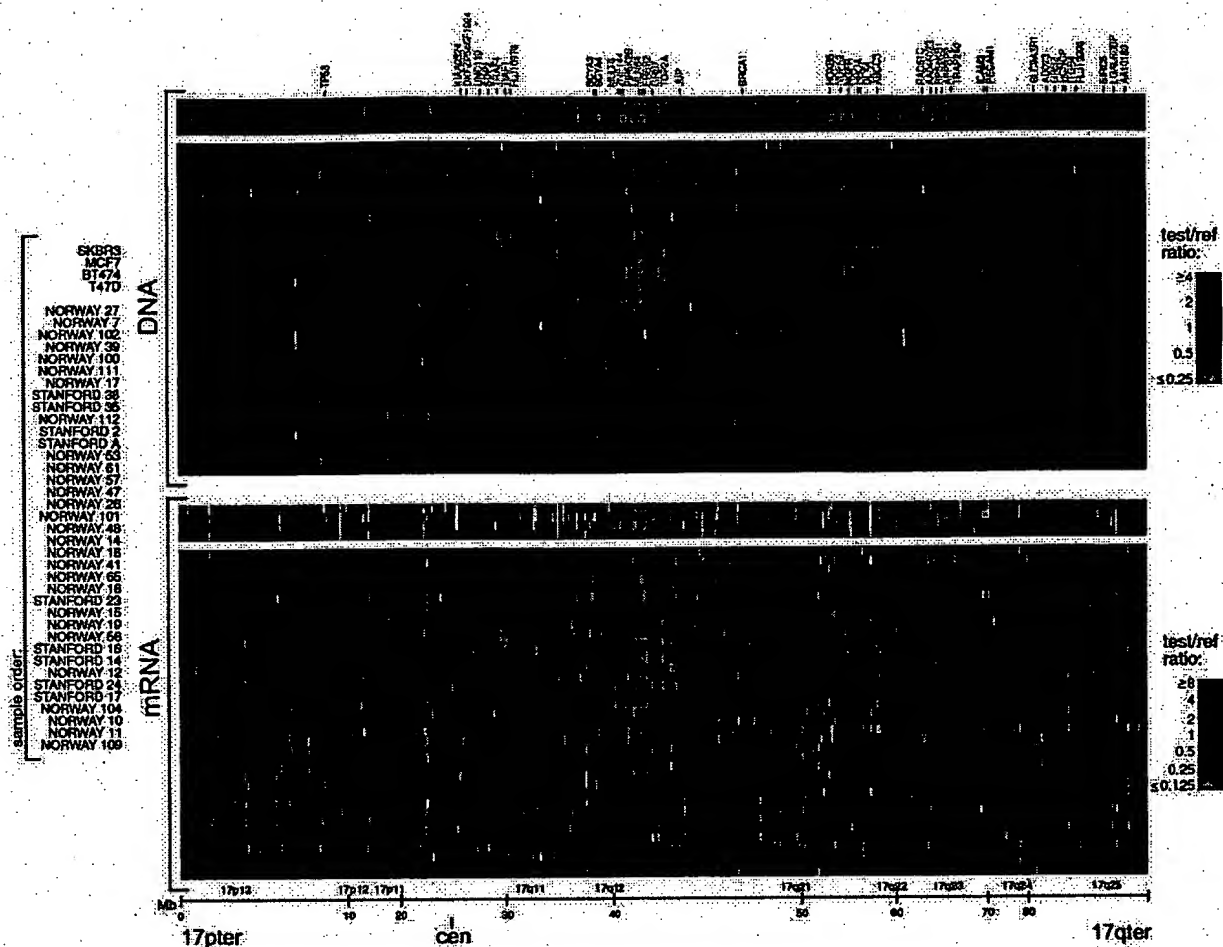
Pollack et al.

Fig. 3. Concordance between DNA copy number and gene expression across chromosome 17. DNA copy number alteration (*Upper*) and mRNA levels (*Lower*) are illustrated for breast cancer cell lines and tumors. Breast cancer cell lines and tumors are separately ordered by hierarchical clustering (*Upper*), and the identical sample order is maintained (*Lower*). The 354 genes present on the microarrays and mapping to chromosome 17, and for which both DNA copy number and mRNA levels were determined, are ordered by position along the chromosome; selected genes are indicated in color-coded text (see Fig. 2 legend). Fluorescence ratios (test/reference) are depicted by separate $\log_2$ pseudocolor scales (indicated).

of DNA copy number and mRNA levels for genes on chromosome 17 (Fig. 3). The overall patterns of gene amplification and elevated gene expression are quite concordant; i.e., a significant fraction of highly amplified genes appear to be correspondingly highly expressed. The concordance between high-level amplification and increased gene expression is not restricted to chromosome 17. Genome-wide, of 117 high-level DNA amplifications (fluorescence ratios >4, and representing 91 different genes), 62% (representing 54 different genes; see Table 5, which is published as supporting information on the PNAS web site) are found associated with at least moderately elevated mRNA levels (mean-centered fluorescence ratios >2), and 42% (representing 36 different genes) are found associated with comparably highly elevated mRNA levels (mean-centered fluorescence ratios >4).

To determine the extent to which DNA deletion and lower-level amplification (in addition to high-level amplification) are also associated with corresponding alterations in mRNA levels, we performed three separate analyses on the complete data set (4 cell lines and 37 tumors, across 6,095 genes). First, we determined the average mRNA levels for each of five classes of genes, representing DNA deletion, no change, and low-, medium-, and high-level amplification (Fig. 4a). For both the

breast cancer cell lines and tumors, average mRNA levels tracked with DNA copy number across all five classes, in a statistically significant fashion (*P* values for pair-wise Student's *t* tests comparing adjacent classes: cell lines, 4×10^{-49}, 1×10^{-49}, 5×10^{-5}, 1×10^{-2}; tumors, 1×10^{-43}, 1×10^{-214}, 5×10^{-41}, 1×10^{-4}). A linear regression of the average log(DNA copy number), for each class, against average log(mRNA level) demonstrated that on average, a 2-fold change in DNA copy number was accompanied by 1.4- and 1.5-fold changes in mRNA level for the breast cancer cell lines and tumors, respectively (Fig. 4a, regression line not shown). Second, we characterized the distribution of the 6,095 correlations between DNA copy number and mRNA level, each across the 37 tumor samples (Fig. 4b). The distribution of correlations forms a normal-shaped curve, but with the peak markedly shifted in the positive direction from zero. This shift is statistically significant, as evidenced in a plot of observed vs. expected correlations (Fig. 4c), and reflects a pervasive global influence of DNA copy number alterations on gene expression. Notably, the highest correlations between DNA copy number and mRNA level (the right tail of the distribution in Fig. 4b) comprise both amplified and deleted genes (data not shown). Third, we used a linear regression model to estimate the fraction of all variation measured in mRNA levels among the 37
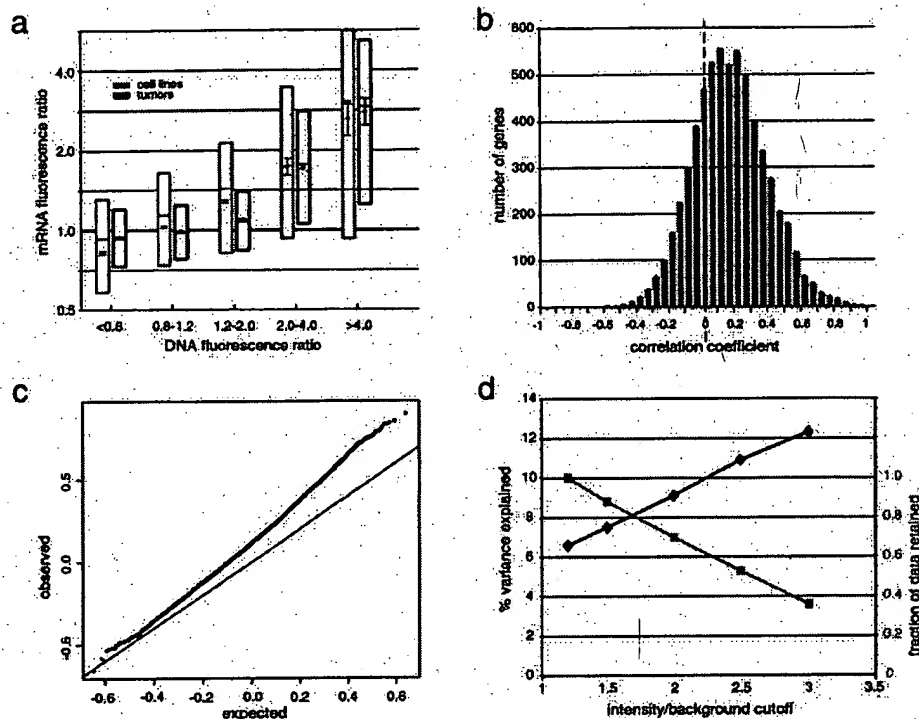
a

mRNA fluorescence ratio

- cell lines
- tumors

4.0
2.0
1.0
0.5

<0.8   0.8-1.2   1.2-2.0   2.0-4.0   >4.0

DNA fluorescence ratio

b

number of genes

800
500
400
300
200
100
0

-1 -0.8 -0.6 -0.4 -0.2 0 0.2 0.4 0.6 0.8 1

correlation coefficient

c

observed

0.5
0.0
-0.5

-0.6 -0.4 -0.2 0.0 0.2 0.4 0.6

expected

d

% variance explained

.14
.12
10
8
6
4
2
0

fraction of data retained

1.0
0.8
0.6
0.4
0.2
0

1 1.5 2 2.5 3 3.5

intensity/background cutoff

Fig. 4. Genome-wide influence of DNA copy number alterations on mRNA levels. (a) For breast cancer cell lines (gray) and tumor samples (black), both mean-centered mRNA fluorescence ratio ($\log_2$ scale) quartiles (box plots indicate 25th, 50th, and 75th percentile) and averages (diamonds; Y-value error bars indicate standard errors of the mean) are plotted for each of five classes of genes, representing DNA deletion (tumor/normal ratio < 0.8), no change (0.8–1.2), low- (1.2–2), medium- (2–4), and high-level (>4) amplification. P values for pair-wise Student's t tests, comparing averages between adjacent classes (moving left to right), are 4×10^{-49}, 1×10^{-49}, 5×10^{-5}, 1×10^{-2} (cell lines), and 1×10^{-43}, 1×10^{-214}, 5×10^{-41}, 1×10^{-4} (tumors). (b) Distribution of correlations between DNA copy number and mRNA levels, for 6,095 different human genes across 37 breast tumor samples. (c) Plot of observed versus expected correlation coefficients. The expected values were obtained by randomization of the sample labels in the DNA copy number data set. The line of unity is indicated. (d) Percent variance in gene expression (among tumors) directly explained by variation in gene copy number. Percent variance explained (black line) and fraction of data retained (gray line) are plotted for different fluorescence intensity/background (a rough surrogate for signal/noise) cutoff values. Fraction of data retained is relative to the 1.2 intensity/background cutoff. Details of the linear regression model used to estimate the fraction of variation in gene expression attributable to underlying DNA copy number alteration can be found in the supporting information (see *Estimating the Fraction of Variation in Gene Expression Attributable to Underlying DNA Copy Number Alteration*).

tumors that could be attributed to underlying variation in DNA copy number. From this analysis, we estimate that, overall, about 7% of all of the observed variation in mRNA levels can be explained directly by variation in copy number of the altered genes (Fig. 4d). We can reduce the effects of experimental measurement error on this estimate by using only that fraction of the data most reliably measured (fluorescence intensity/ background >3); using that data, our estimate of the percent variation in mRNA levels directly attributed to variation in gene copy number increases to 12% (Fig. 4d). This still undoubtedly represents a significant underestimate, as the observed variation in global gene expression is affected not only by true variation in the expression programs of the tumor cells themselves, but also by the variable presence of non-tumor cell types within clinical samples.

Discussion

This genome-wide, array CGH analysis of DNA copy number alteration in a series of human breast tumors demonstrates the usefulness of defining amplicon boundaries at high resolution (gene-by-gene), and quantitatively measuring amplicon shape, to assist in locating and identifying candidate oncogenes. By analyzing mRNA levels in parallel, we have also discovered that changes in DNA copy number have a large, pervasive, direct effect on global gene expression patterns in both breast cancer

cell lines and tumors. Although the DNA microarrays used in our analysis may display a bias toward characterized and/or highly expressed genes, because we are examining such a large fraction of the genome (approximately 20% of all human genes), and because, as detailed above, we are likely underestimating the contribution of DNA copy number changes to altered gene expression, we believe our findings are likely to be generalizable (but would nevertheless still be remarkable if only applicable to this set of ~6,100 genes).

In budding yeast, aneuploidy has been shown to result in chromosome-wide gene expression biases (13). Two recent studies have begun to examine the global relationship between DNA copy number and gene expression in cancer cells. In agreement with our findings, Phillips et al. (14) have shown that with the acquisition of tumorigenicity in an immortalized prostate epithelial cell line, new chromosomal gains and losses resulted in a statistically significant respective increase and decrease in the average expression level of involved genes. In contrast, Platzer et al. (15) recently reported that in metastatic colon tumors only ~4% of genes within amplified regions were found more highly (>2-fold) expressed, when compared with normal colonic epithelium. This report differs substantially from our finding that 62% of highly amplified genes in breast cancer exhibit at least 2-fold increased expression. These contrasting findings may reflect methodological differences between the

studies. For example, the study of Platzer et al. (15) may have systematically under-measured gene expression changes. In this regard it is remarkable that only 14 transcripts of many thousand residing within unamplified chromosomal regions were found to exhibit at least 4-fold altered expression in metastatic colon cancer. Additionally, their reliance on lower-resolution chromosomal CGH may have resulted in poorly delimiting the boundaries of high-complexity amplicons, effectively overcalling regions with amplification. Alternatively, the contrasting findings for amplified genes may represent real biological differences between breast and metastatic colon tumors; resolution of this issue will require further studies.

Our finding that widespread DNA copy number alteration has a large, pervasive and direct effect on global gene expression patterns in breast cancer has several important implications. First, this finding supports a high degree of copy number-dependent gene expression in tumors. Second, it suggests that most genes are not subject to specific autoregulation or dosage compensation. Third, this finding cautions that elevated expression of an amplified gene cannot alone be considered strong independent evidence of a candidate oncogene's role in tumorigenesis. In our study, fully 62% of highly amplified genes demonstrated moderately or highly elevated expression. This highlights the importance of high-resolution mapping of amplicon boundaries and shape [to identify the "driving" gene(s) within amplicons (16)], on a large number of samples, in addition to functional studies. Fourth, this finding suggests that analyzing the genomic distribution of expressed genes, even within existing microarray gene expression data sets, may permit the inference of DNA copy number aberration, particularly aneuploidy (where gene expression can be averaged across large chromosomal regions; see Fig. 3 and supporting information). Fifth, this finding implies that a substantial portion of the phenotypic uniqueness (and by extension, the heterogeneity in clinical behavior) among patients' tumors may be traceable to underlying variation in DNA copy number. Sixth, this finding supports a possible role for widespread DNA copy number alteration in tumorigenesis (17, 18), beyond the amplification of specific oncogenes and deletion of specific tumor suppressor genes. Widespread DNA copy number alteration, and the concomitant widespread imbalance in gene expression, might disrupt critical stochiometric relationships in cell metabolism and physiology (e.g., proteosome, mitotic spindle), possibly promoting further chromosomal instability and directly contributing to tumor development or progression. Finally, our findings suggest the possibility of cancer therapies that exploit specific or global imbalances in gene expression in cancer.

1. Kallioniemi, A., Kallioniemi, O. P., Sudar, D., Rutovitz, D., Gray, J. W., Waldman, F. & Pinkel, D. (1992) Science 258, 818–821.
2. Kallioniemi, A., Kallioniemi, O. P., Piper, J., Tanner, M., Stokke, T., Chen, L., Smith, H. S., Pinkel, D., Gray, J. W. & Waldman, F. M. (1994) Proc. Natl. Acad. Sci. USA 91, 2156–2160.
3. Tirkkonen, M., Tanner, M., Karhu, R., Kallioniemi, A., Isola, J. & Kallioniemi, O. P. (1998) Genes Chromosomes Cancer 21, 177–184.
4. Forozan, F., Mahlamaki, E. H., Monni, O., Chen, Y., Veldman, R., Jiang, Y., Gooden, G. C., Ethier, S. P., Kallioniemi, A. & Kallioniemi, O. P. (2000) Cancer Res. 60, 4519–4525.
5. Solinas-Toldo, S., Lampel, S., Stilgenbauer, S., Nickolenko, J., Benner, A., Dohner, H., Cremer, T. & Lichter, P. (1997) Genes Chromosomes Cancer 20, 399–407.
6. Pinkel, D., Segraves, R., Sudar, D., Clark, S., Poole, I., Kowbel, D., Collins, C., Kuo, W. L., Chen, C., Zhai, Y., et al. (1998) Nat. Genet. 20, 207–211.
7. Pollack, J. R., Perou, C. M., Alizadeh, A. A., Eisen, M. B., Pergamenschikov, A., Williams, C. F., Jeffrey, S. S., Botstein, D. & Brown, P. O. (1999) Nat. Genet. 23, 41–46.
8. Perou, C. M., Sorlie, T., Eisen, M. B., van de Rijn, M., Jeffrey, S. S., Rees, C. A., Pollack, J. R., Ross, D. T., Johnsen, H., Akslen, L. A., et al. (2000) Nature (London) 406, 747–752.
9. Sorlie, T., Perou, C. M., Tibshirani, R., Aas, T., Geisler, S., Johnsen, H., Hastie, T., Eisen, M. B., van de Rijn, M., Jeffrey, S. S., et al. (2001) Proc. Natl. Acad. Sci. USA 98, 10869–10874.
10. Schuler, G. D. (1997) J. Mol. Med. 75, 694–698.
11. Lander, E. S., Linton, L. M., Birren, B., Nusbaum, C., Zody, M. C., Baldwin, J., Devon, K., Dewar, K., Doyle, M., FitzHugh, W., et al. (2001) Nature (London) 409, 860–921.
12. Fejzo, M. S., Godfrey, T., Chen, C., Waldman, F. & Gray, J. W. (1998) Genes Chromosomes Cancer 22, 105–113.
13. Hughes, T. R., Roberts, C. J., Dai, H., Jones, A. R., Meyer, M. R., Slade, D., Burchard, J., Dow, S., Ward, T. R., Kidd, M. J., et al. (2000) Nat. Genet. 25, 333–337.
14. Phillips, J. L., Hayward, S. W., Wang, Y., Vasselli, J., Pavlovich, C., Padilla-Nash, H., Pezullo, J. R., Ghadimi, B. M., Grossfeld, G. D., Rivera, A., et al. (2001) Cancer Res. 61, 8143–8149.
15. Platzer, P., Upender, M. B., Wilson, K., Willis, J., Lutterbaugh, J., Nosrati, A., Willson, J. K., Mack, D., Ried, T. & Markowitz, S. (2002) Cancer Res. 62, 1134–1138.
16. Albertson, D. G., Ylstra, B., Segraves, R., Collins, C., Dairkee, S. H., Kowbel, D., Kuo, W. L., Gray, J. W. & Pinkel, D. (2000) Nat. Genet. 25, 144–146.
17. Li, R., Yerganian, G., Duesberg, P., Kraemer, A., Willer, A., Rausch, C. & Hehlmann, R. (1997) Proc. Natl. Acad. Sci. USA 94, 14506–14511.
18. Rasnick, D. & Duesberg, P. H. (1999) Biochem. J. 340, 621–630.